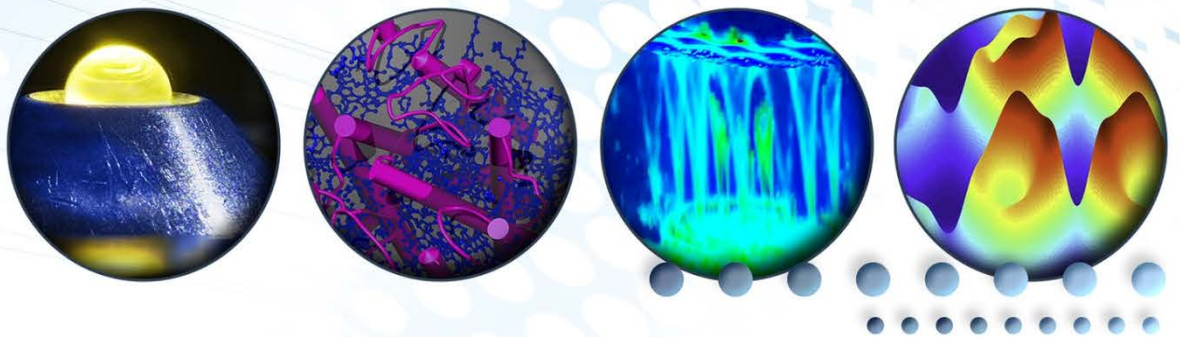


Instruments for Emerging Science: A Science Case for the Second Target Station

Limited distribution.
Preliminary.



This report was prepared as an account of work sponsored by an agency of the United States Government. Neither the United States Government nor any agency thereof, nor any of their employees, makes any warranty, express or implied, or assumes any legal liability or responsibility for the accuracy, completeness, or usefulness of any information, apparatus, product, or process disclosed, or represents that its use would not infringe privately owned rights. Reference herein to any specific commercial product, process, or service by trade name, trademark, manufacturer, or otherwise, does not necessarily constitute or imply its endorsement, recommendation, or favoring by the United States Government or any agency thereof. The views and opinions of authors expressed herein do not necessarily state or reflect those of the United States Government or any agency thereof.

CONTENTS

LIST OF FIGURES.....	v
LIST OF TABLES.....	xi
ACRONYMS	xiii
1. INTRODUCTION	1-1
1.1 FUTURE SCIENCE NEEDS FOR NEUTRONS AND THEIR ROLE.....	1-2
1.1.1 Quantum Materials.....	1-2
1.1.2 Soft Matter.....	1-4
1.1.3 Biology.....	1-4
1.1.4 Materials Discovery, Characterization, and Application.....	1-5
1.2 ADDRESSING FUTURE SCIENCE CHALLENGES WITH SECOND TARGET STATION.....	1-6
1.3 PERFORMANCE AND CAPABILITIES OF SECOND TARGET STATION: A FOURTH GENERATION NEUTRON FACILITY.....	1-7
1.4 SCIENCE IMPACT OF SECOND TARGET STATION	1-8
1.5 THREE SOURCE STRATEGY	1-10
1.6 FUTURE STEPS.....	1-11
1.7 CURRENT AND PROPOSED NEUTRON SOURCES AT ORNL.....	1-11
1.7.1 Introduction	1-11
1.7.2 Source Characteristics and Strengths	1-12
1.7.3 Optimizing Instruments at Three ORNL Neutron Sources.....	1-14
1.7.4 STS Instrument Strategies.....	1-16
1.7.5 References	1-17
2. CHALLENGES IN QUANTUM CONDENSED MATTER.....	2-1
2.1 COLD SPECTROSCOPY	2-4
2.2 CHESS—CHOPPER SPECTROMETER FOR SMALL SAMPLES.....	2-6
2.3 HERTZ—HIGH ENERGY RESOLUTION TERAHERTZ SPECTROMETER	2-12
2.4 MANTA (MULTIPLE ANALYZER TRIPLE-AXIS) FOR HFIR.....	2-17
2.5 ULTRA-HIGH RESOLUTION SPECTROSCOPY WITH NEUTRON SPIN ECHO OPTION FOR TAS AT HFIR.....	2-23
2.6 MAGNETIC STRUCTURE.....	2-27
2.7 M-STAR (MAGNETISM—SECOND TARGET ADVANCED REFLECTOMETER)	2-28
2.8 M-WASABI (MAGNETISM—WIDE AND SMALL ANGLES WITH BIG INTENSITY)	2-34
2.9 NESCRY (NEUTRON SINGLE CRYSTAL DIFFRACTOMETER) FOR STS	2-39
2.10 VERDI (VERSATILE DIFFRACTOMETER FOR COMPLEX MAGNETIC STRUCTURES) FOR STS.....	2-44
2.11 ZEEMANS: A HIGH MAGNETIC FIELD BEAM LINE.....	2-49
3. GRAND CHALLENGES IN BIOLOGY.....	3-1
3.1 10 GRAND CHALLENGES.....	3-2
3.2 RECOMMENDATIONS	3-3
3.3 DYNAMICALLY POLARIZED CRYSTALLOGRAPHY (DYPOL) FOR STS	3-4
3.4 EWALD: ENHANCED WIDE ANGLE LAUE DIFFRACTOMETER FOR STS	3-8
3.5 COLD NEUTRON DIFFRACTOMETER WITH POLARIZATION FOR QUASI- CRYSTALLINE MATERIALS (ALIGN)	3-13
3.6 NEUTRON RADIOGRAPHY AND TOMOGRAPHY STATION (NEURATOM).....	3-17
3.7 BARNs (BROAD ANGULAR RANGE NEUTRON SCATTERING)	3-19
3.8 FLUX-OPTIMIZED ORDER/DISORDER SANS (FLOODS) FOR STS	3-25
4. GRAND CHALLENGES IN SOFT MATTER	4-1

4.1	AREAS OF SOFT MATTER WHERE MORE RESEARCH IS REQUIRED TO DEVELOP FUNDAMENTAL UNDERSTANDING	4-1
4.2	RECOMMENDATIONS TO HELP ADDRESS THESE AREAS OF NEED	4-3
4.3	HIRES-SWANS (HIGH RESOLUTION SMALL/WIDE ANGLE NEUTRON SCATTERING) FOR STS	4-4
4.4	KINETICS REFLECTOMETER	4-13
4.5	VBPR (VARIABLE BEAM PROFILE REFLECTOMETER)	4-19
4.6	MBARS (MICA BACKSCATTERING SPECTROMETER) FOR STS	4-23
4.7	BWAVES (BROAD-RANGE WIDE ANGLE VELOCITY SELECTOR) FOR STS	4-28
4.8	MICROSECOND NEUTRON SPIN ECHO (MICROSE) FOR HFIR	4-31
5.	CHEMISTRY AND ENGINEERING MATERIALS	5-1
5.1	CHALLENGES IN MATERIALS DISCOVERY, CHARACTERIZATION, AND APPLICATION	5-1
5.2	JANUS: INS INSTRUMENT FOR CATALYSIS	5-3
5.3	EXTREME ENVIRONMENT MULTI-ENERGY SPECTROMETER WITH XTAL ANALYZERS (XTREME-X)	5-8
5.4	SPHERICAL INDIRECT INELASTIC XTAL SPECTROMETER (SPHIINXS)	5-15
5.5	MATERIALS PERFORMANCE AND PROCESSING	5-19
5.6	VENUS (VERSATILE NEUTRON IMAGING INSTRUMENT AT THE SNS)	5-21
5.7	GRATING INTERFEROMETRY NEUTRON IMAGING (GINI)	5-25
5.8	MATERIALS ENGINEERING BY NEUTRON SCATTERING (MENUS)	5-28
5.9	HIGHRESPD (HIGH RESOLUTION POWDER DIFFRACTION) FOR STS	5-33
5.10	RAPID (RAPID ACQUISITION PARAMETRIC AND IN-SITU DIFFRACTION) FOR FTS	5-36
6.	ENABLING TECHNOLOGIES AND REQUIREMENTS	6-1
6.1	MODERATORS AND TARGET OPTIMIZATION	6-2
6.2	NEUTRON OPTICS AND POLARIZATION	6-4
6.3	NEW GUIDE CONCEPT HFIR HB-4 COLD SOURCE.....	6-10
6.4	LARMOR LABELING TECHNIQUES	6-12
6.5	DETECTOR REQUIREMENTS	6-15
6.6	INVENT (INSTRUMENT WITH VERSATILE ENVIRONMENT FOR NOVEL TECHNOLOGIES).....	6-22
APPENDIX A. DISCUSSION ON THE RELATIVE MERITS OF A SHORT- OR LONG-PROTON PULSE SECOND TARGET STATION AT THE SPALLATION NEUTRON SOURCE		A-1

LIST OF FIGURES

Fig. 1.1. Converging source and instrumentation technologies have defined completely new scientific capabilities with each generation of neutron facility.	1-1
Fig. 1.2. Neutrons are either unique or play a vital role in combination with other experimental techniques over an enormous range of next generation science challenges.	1-3
Fig. 1.3. The working groups were charge to explore transformational performance changes that would access new science.	1-7
Fig. 1.4. The convergence of technologies in source and moderators, high performance computing, spin manipulation, and optics allows new levels of performance.	1-8
Fig. 1.5. The 22 neutron scattering instrument concepts explored for the Second Target Station span a range of science capabilities and science areas.	1-9
Fig. 1.6. The second target station and instrumentation in this report provide transformative science capabilities impacting materials challenges and the new ways in which research is undertaken.	1-10
Fig. 1.7. The ORNL three source strategy.	1-11
Fig. 1.8. Comparison of ORNL neutron source characteristics.	1-13
Fig. 1.9. Moderator pulse shapes for coupled moderators at FTS and STS at $\lambda = 5 \text{ \AA}$, 2 \AA , and 1 \AA in (a), (b), and (c) respectively.	1-14
Fig. 1.10. Optimal performance map of elastic scattering instruments across the ORNL neutron sources.	1-15
Fig. 1.11. Performance map of the inelastic spectrometers.	1-16
Fig. 1.12. Compact small angle neutron scattering instrument developed at MIT and tested at HFIR. [2]	1-17
Fig. 2.1. Phase diagram of κ -(BEDT-TTF) ₂ X as a function of pressure with arrows indicating the location of different compounds at ambient pressure [Müller].	2-7
Fig. 2.2. Photos of single crystal samples of κ -(ET) ₂ Cu[N(CN) ₂]Br (Photo: J. A. Schlueter).	2-7
Fig. 2.3. Suppression of antiferromagnetic order and appearance of superconductivity in the heavy fermion compound CePd ₂ Si ₂ [6].	2-8
Fig. 2.4. Powder inelastic scattering from Na ₂ IrO ₃ [11].	2-8
Fig. 2.5. Schematic phase diagram as a function of a tuning parameter, p.	2-9
Fig. 2.6. Multiferroic materials exhibit at least two coexisting orders.	2-13
Fig. 2.7. (a) Elastic modulus for four dry proteins, myoglobin (MYO), bovine serum albumin (BSA), lysozyme (LYS), and green fluorescent protein (GFP), as a function of the boson peak frequency ν_{BP}	2-14
Fig. 2.8. (a) Inelastic neutron scattering spectra of Cr ₇ Ni molecular magnet at T = 2 K (circles) and T = 12 K (triangles) [11]. (b) T ₁ (spin lattice relaxation times) and T ₂ (phase-coherence relaxation times) as a function of temperature for Cr ₇ Ni (blue open circles), Cr ₇ Mn (red open squares), and perdeuterated Cr ₇ Ni (blue filled squares). At low temperatures, T ₂ for perdeuterated Cr ₇ Ni approaches 4 μ s [12].	2-15
Fig. 2.9. Inelastic scattering from finite length spin-1 chains within Y ₂ Ba(Ni _{0.96} Mg _{0.04})O ₅ in zero and applied field reveals the presence of topologically protected edge states [2].	2-19
Fig. 2.10. (A) Measured and (B) calculated elastic neutron diffraction from classical spin ice in Dy ₂ Ti ₂ O ₇	2-20
Fig. 2.11. Inelastic neutron scattering from the topological Kondo insulator SmB ₆ measured on SEQUOIA.	2-20
Fig. 2.12. Precise measurements of phonon dispersions and lifetimes will provide new insights on the thermal conductivity in thermoelectric materials (After [7]).	2-23

Fig. 2.13. Ultra-high-resolution spectroscopy enables the measurements of the phonon line widths with micro electron volt resolution (After [8]).	2-24
Fig. 2.14. The intercalation of Cu in TiSe ₂ leads to the suppression of the CDW state and the appearance of superconductivity Cu _x TiSe ₂ (After [10]).	2-24
Fig. 2.15. Schematics of the Neutron Resonance Spin Echo instrument.	2-25
Fig. 2.16. Schematics of a neutron spin echo instrument based on the newly developed superconducting magnetic Wollaston prisms (4,5) instead of the RF coils of the NRSE instrument.	2-26
Fig. 2.17. Domain in uniaxial thin films [1].	2-29
Fig. 2.18. Schematic structure showing the layer stacking sequence deposited on a silicon substrate. FIF (ferromagnet-insulator-ferromagnet) magnetic tunnel junctions with (a) interface doping layers and (b) δ -doping layers of copper and gold.	2-30
Fig. 2.19. Example of a magnetic tunnel junction (MTJ) device, which can be studied with polarized neutron reflectometry. The lateral size of the sample can be 1–2 mm in diameter.	2-30
Fig. 2.20. A heterostructure device with a TI quantum well [3].	2-31
Fig. 2.21. Ferroelectric (FE) tunnel junctions for information storage and processing.	2-32
Fig. 2.22. Schematic view of the focusing optics scheme proposed for M-STAR.	2-34
Fig. 2.23. Schematic drawing of VAI nanocomposite architecture.	2-35
Fig. 2.24. Lattice parameters of the proposed starting model materials.	2-36
Fig. 2.25. SEM images of 30 nm pitch dots before (a,b) and after (c,d) cobalt or palladium multilayer deposition.	2-37
Fig. 2.26. Nanorings. (a) A nanoring MTJ with (b) onion/onion and (c) vortex/vortex states.	2-37
Fig. 2.27. Schematic view of the focusing optics for M-WASABI.	2-39
Fig. 2.28. Skyrmion lattice in the MnSi chiral magnet [1].	2-41
Fig. 2.29. Crystal structure of Fe ₂ [Nb(CN) ₈](4-pyridinealdoxime) ₈ ·2H ₂ O (left). Magnetization change caused by photo-induced spin-crossover (right). [3]	2-42
Fig. 2.30. Polyhedral view of an example acentric polar crystal structure of boracite, Mn ₃ B ₇ O ₁₃ Cl (left) and its Mn cluster (right).	2-43
Fig. 2.31. Pressure–temperature phase diagram of oxygen.	2-46
Fig. 2.32. Proposed model of the incommensurate helical structure induced by magnetic fields in Sul-Cu ₂ Cl ₄ [3].	2-47
Fig. 2.33. Diffuse scattering maps from spin ice, Ho ₂ Ti ₂ O ₇ . Experimental SF, non-spin flip scattering at T = 1.7 K with pinch points at (0, 0, 2), (1, 1, 1), (2, 2, 2) [(A) to (C)] versus theory [(D) to (F)] (see Ref [1]).	2-48
Fig. 2.34. Comparison of flux on a sample between ZEEMANS in the spectrometry configuration and HYSPEC.	2-52
Fig. 2.35. The flux on sample per pulse for white beam ZEEMANS configurations with TOPAZ for comparison.	2-53
Fig. 2.36. Detector vessel, magnet, and differentially pumped rotation seal.	2-53
Fig. 3.1. Proton scattering cross-section from polarized neutrons as a function of proton polarization.	3-5
Fig. 3.2. Structure of a bacteriochlorophyll (BCL) pigment from the <i>P. aestuarii</i> FMO.	3-6
Fig. 3.3. Overall structure of a G-protein coupled receptor (gray).	3-6
Fig. 3.4. Overall structure of the hammerhead ribozyme.	3-7
Fig. 3.5. Schematic of the DNP sample environment.	3-8
Fig. 3.6. The DNA polymerase active site.	3-9
Fig. 3.7. Overall structure of the HIV-1 RT.	3-10

Fig. 3.8. Overall structure of protein kinase A (surface representation) bound to a substrate analog peptide (magenta).....	3-11
Fig. 3.9. Schematic diagram of a raft-containing lipid bilayer.....	3-14
Fig. 3.10. Seed Coat Lignin Compositions of Euphorbiaceae and Cleomaceae Plants.....	3-15
Fig. 3.11. Schematic representations of different amyloid/lipid association scenarios.....	3-15
Fig. 3.12. Thykoid membranes in cyanobacteria mutants and their response to light.....	3-21
Fig. 3.13. Complex structure of cell-wall biomass during the pretreatment process in a computational model.....	3-22
Fig. 3.14. SANS data obtained over a larger Q-range allow the NtQ ₄₂ P ₁₀ fibril structure to be carefully probed.....	3-22
Fig. 3.15. Atomic layer deposition (ALD).....	3-23
Fig. 3.16 Structure of the p27/Cdk2/cyclin A complex.....	3-27
Fig. 3.17. TEM image of the fibrils formed by NtQ ₄₂ P ₁₀ with a calculated fibril radius, $R = 40 \pm 8$ Å.....	3-28
Fig. 3.18. SANS resolves shapes of membrane protein reconstituted in liposome.....	3-28
Fig. 3.19. A cellulase enzyme (orange) hydrolyzing a cellulose (green) strand despite the presence of lignin aggregates (brown) on the cellulose surface.....	3-29
Fig. 3.20. Concept of a SANS instrument with the sample at the focal length and the detector at the imaging length.....	3-30
Fig. 4.1. Polymer-grafted nanoparticles in a polymer nanocomposite self-assemble in a polymer chain length- and grafting density-dependent manner [1].....	4-7
Fig. 4.2. The geometry of grazing-incidence scattering with a simulated 2D scattering pattern showing in-plane and off-plane structure of a protein-membrane assembly.....	4-9
Fig. 4.3. Formation of a DNA Origami box from the DNA framework, to the assembled sides of the box, and ultimately to the final 3D structure.....	4-10
Fig. 4.4. Plasmonic nanostructures formed through DNA templating.....	4-10
Fig. 4.5. (a) Colloidal crystal of CdSe NCs.....	4-12
[1] Akcora, et al. <i>Nature Materials</i> 8, 354–359 (2009).....	4-13
[2] Andersen, et al. <i>Nature</i> 459, 73–77 (2009).....	4-13
Fig. 4.6. Neutron reflectivity (left) and fitted scattering length density profiles (right) of PCBM/P3HT bilayer.....	4-15
Fig. 4.7. Dissolution of lipid monolayer on water surface upon exposure to ozone tracked in 750 s time shots [3].....	4-15
Fig. 4.8. Neutron reflectivity of DSPC/DMPC bilayer against D ₂ O collected in 2.5 min shots [4].....	4-16
Fig. 4.9. (a) Contact angle as a function of the contact line velocity of a water droplet spontaneously spreading on a 2.7 μm thick layer of maltodextrin.....	4-16
Fig. 4.10. Schematic representation of (A) a lamellar crystal, (B) a crystal with a nonparallel backbone structure, and (C) a quadrite, an epitaxial arrangement of two lamellae across the ac plane.....	4-18
Fig. 4.11. Schematic representation of surface forces experiment on a biomimetic bottlebrush polymer.....	4-21
Fig. 4.12. Plasmonic nanoparticles built with hard core nanoparticles and soft linking materials at the interfaces. [4].....	4-22
Fig. 4.13. The protein-solvent dynamic processes in hydrated/solvated proteins (left figure [1]) have been studied using neutron spectrometers of variable energy resolution (right figure [2]).....	4-25
Fig. 4.14. Schematic of lithium transport in a solid state battery.....	4-26

Fig. 4.15. Schematic presentation of the microscopic dynamic processes in complex glass-forming systems spanning many orders of magnitude in relaxation time.	4-26
Fig. 4.16. Instead of commonly performed to date model system studies of proteins as hydrated powders (left figure, adapted from [1]), we aim at studies of proteins in real-life biological solvents (right figure), with simultaneous characterization of the microscopic dynamics of both the solute and solvent.	4-29
Fig. 4.17. Possible reorientational motions of the Emim cation (top) and contour plots (bottom) of the spatial distribution of the C ₅ carbon atom relative to the N ₁ carbon atom in the solid (right) and liquid (left) phases in a room temperature ionic liquid 1-ethyl-3-methylimidazolium bromide [2].	4-30
Fig. 4.18. A schematic representation of the topological change in the nearest neighbor configuration when one bond between colloid A and colloid B is broken and a new bond between colloid C and colloid D is formed in the immediate neighborhood.	4-33
Fig. 4.19. Left panels: SANS absolute intensity of silica solutions projected in the velocity (<i>v</i>) – velocity gradient (∇v) plane at shear rate 0 and 500 1/s.	4-34
Fig. 4.20. Molecular model illustrating the associating and caging effect of a lithium ion by water at it moves through a hydrated poly(ethylene oxide) matrix.	4-34
Fig. 5.1. Calculated angular dependency for polyethylene at 300K at (a) $E_{incident} = 2,300 \text{ cm}^{-1}$ and (b) $E = 1,150 \text{ cm}^{-1}$	5-3
Fig. 5.2. Structure of the zeolite model system and zeolite chabasite.	5-5
Fig. 5.3. Deuterated bridging hydroxyl before and after adsorption of ethylene in UHV.	5-6
Fig. 5.4. Calculated reaction pathways for the ODH of isobutane on dicarbonyls at zigzag edges (upper) and quinones (lower) at armchair edges.	5-6
Fig. 5.5. INS of solid hydrogen dosed at 1 bar (black trace) and parahydrogen at 1.5 kbar (red trace) measured at $\sim 5 \text{ K}$	5-10
Fig. 5.6. Visual representation of the ortho hydrogen molecule in the solid at 1 bar (left) and 20 GPa (right).	5-10
Fig. 5.7. The temperature and pressure regimes associated with most of the 13 known crystalline phases are indicated here [21].	5-11
Fig. 5.8. Optical absorption α for Si-XII and Si forms used in solar cells compared with the solar spectrum irradiance under standard conditions (AM 1.5) taken from [3].	5-12
Fig. 5.9. In situ study of CO ₂ hydrogenation on CeO _x /Cu(111) catalysts.	5-16
Fig. 5.10. Reduction of Cu ₂ O by CO.	5-16
Fig. 5.11. Excitation spectra of liquid ⁴ He confined in silica FSM-16 (28 Å mean pore diameter) at various temperatures measured on CNCS (2).	5-16
Fig. 5.12. The VENUS instrument.	5-24
Fig. 5.13. Measurement of the superlattice peak P100 of beta prime precipitates occurring at large <i>d</i> and the resolved misfit in the Fe based super alloys.	5-30
Fig. 5.14. (a) The phase evolutions of anode and cathode in a fresh large format battery.	5-31
Fig. 5.15. Structure of the low-temperature Mg(BH ₄) ₂ phase in space group P6 ₁ viewed along the hexagonal <i>a</i> axis, showing two unit cells.	5-33
Fig. 5.16. Structure of polymer phase of alkali doped fullerene RbC ₆₀	5-34
Fig. 5.17. Magnetic structure of BiFeO ₃ as measured on POWGEN (right and with Mn substitution in the Fe site) and the ISIS HRPD instrument (left) [5].	5-35
Fig. 5.18. Shown at left is a coin cell where the amount of active cathode material is 0.01 g.	5-37
Fig. 5.19. Diffraction pattern collected at different states of cycling to establish the voltage fade mechanism in cathodes that are Li and Mn rich layered compounds.	5-38
Fig. 5.20. Powder diffraction data from ZrRhBi.	5-38

Fig. 5.21. Stroboscopic measurement done at the ILL D20 powder diffractometer to study ultrasound excited single crystals as switchable neutron mirrors.....	5-39
Fig. 6.1. Preliminary moderator/target geometry for STS.	6-2
Fig. 6.2. Schematic diagram of the IMAGINE instrument.	6-6
Fig. 6.3. Spin dependent reflectivity and polarization from an Fe/Si polarizing supermirror $m = 4$	6-9
Fig. 6.4. Entrance configuration of the new guide design proposed for the HFIR cold source.	6-10
Fig. 6.5. Configuration of the new guide design proposed for the HFIR cold source at 5.2 m from the source.....	6-11
Fig. 6.6. Overall layout of the proposed new guide system with possible instrument selections indicated.	6-12
Fig. 6.7. ^3He detector arrays; (a) is a standard 8-pack showing the associated electronics package, and (b) is an assembled array of 8-pack modules.....	6-17
Fig. 6.8. Multi-wire ^3He gas detector.	6-17
Fig. 6.9. Anger camera.	6-18
Fig. 6.10. Wavelength shifting fiber detector.	6-18

LIST OF TABLES

Table 2.1. Key instrument parameters for CHESS.....	2-11
Table 2.2. Key instrument parameters for HERTZ	2-16
Table 2.3. Key instrument parameters for MANTA	2-22
Table 2.4. Key instrument parameters for M-STAR.....	2-33
Table 2.5. Key instrument parameters for M-WASABI	2-39
Table 2.6. Key instrument parameters for NeSCry	2-44
Table 2.7. Key instrument parameters for VERDI	2-49
Table 2.8. Key instrument parameters for ZEEMANS.....	2-54
Table 3.1. First target station source parameters	3-12
Table 3.2. Key instrument parameters for EWALD	3-12
Table 3.3. Key instrument parameters for ALIGN.....	3-17
Table 3.4. Key instrument parameters for NEURATOM	3-19
Table 3.5. Key instrument parameters for BARNs.....	3-25
Table 3.6. Key instrument parameters for FLOODS.....	3-31
Table 4.1. Key instrument parameters for HiRes-SWANS	4-13
Table 4.2. Key instrument parameters for Kinetics Reflectometer	4-19
Table 4.3. Key instrument parameters for VBPR	4-23
Table 4.4. Key instrument parameters for MBARS.....	4-27
Table 4.5. Key instrument parameters for BWAVES.....	4-31
Table 4.6. Key instrument parameters for MICROSE.....	4-36
Table 5.1. Key instrument parameters for JANUS	5-7
Table 5.2. Key instrument parameters for XTREME-X.....	5-13
Table 5.3. Key instrument parameters for SPHIINXS	5-18
Table 5.4. VENUS specific parameters	5-24
Table 5.5. Key instrument parameters for VENUS.....	5-25
Table 5.6. GINI instrument specifications	5-27
Table 5.7. Key instrument parameters for MENUS.....	5-33
Table 5.8. Key instrument parameters for HighResPD	5-36
Table 5.9. Data collection rate of RAPID relative to POWGEN	5-39
Table 5.10. Key instrument parameters for RAPID.....	5-40
Table 6.1. FTS detector parameters.....	6-16
Table 6.2. New technology detector parameters	6-18
Table 6.3. Detector requirements for proposed instruments	6-20
Table 6.4. Key instrument parameters for INVENT.....	6-24

ACRONYMS

1D	one-dimensional
2D	two-dimensional
3D	three-dimensional
ac	alternating current
AFM	atomic force microscopy
ALARA	as low as reasonably achievable
ALD	atomic layer deposition
AND/R	advanced neutron diffractometer/reflectometer
ANL	Argonne National Laboratory
ANSTO	Australian Nuclear Science and Technology Organisation
BARNS	Broad Angular Range Neutron Scattering
BASIS	Backscattering Silicon Spectrometer
BER	Biological and Environmental Research
BES	Basic Energy Sciences
BESAC	BES Advisory Committee
BPM	bit-patterned media
BSMD	Biology and Soft Matter Division
BWAVES	Broad-range Wide-Angle Velocity Selector
CBM	cellulose binding module
CBPM	capped bit-patterned media
CCR	closed cycle refrigerator
CDW	charge density wave
CEMD	Chemical and Engineering Materials Division
CHESS	chopper spectrometer for small samples
CNCS	cold neutron chopper spectrometer
CTW	Cryogenic Tube West
CW	continuous wave
D	deuterium
DARPA	Defense Advanced Research Projects Agency
dc	direct current
DMPC	1,2-dimyristoyl-sn-glycero-3-phosphorylcholine
DNA	deoxyribonucleic acid
DNP	Dynamic Nuclear Polarization
DOE	Department of Energy
dsDNA	double-stranded DNA
DSPC	1,2-distearoyl-sn-glycero-3-phosphocholine
DyPol	Dynamically Polarized Crystallography
EERE	Office of Energy Efficiency and Renewable Energy
ESS	European Spallation Source
EWALD	Enhanced Wide Angle Laue Diffractometer
FI	ferromagnetic insulator
FIF	ferromagnet–insulator–ferromagnet
FLOODS	Flux-Optimized Order/Disorder SANS
FM	ferromagnetic
FOV	field-of-view
FTS	first target station

FWHM	full width at half maximum
GI-SANS	grazing-incidence small-angle neutron scattering
GP-SANS	general purpose small-angle neutron scattering
GINS	grazing-incidence neutron scattering
GPCR	G protein-coupled receptor
H	hydrogen
HERTZ	high energy resolution terahertz spectrometer
HFIR	High Flux Isotope Reactor
HIV	human immunodeficiency virus
HTS	high temperature superconducting
HYSPEC	Hybrid-Spectrometer
IDP	intrinsically disordered protein
IDR	intrinsically disordered region
ILL	Institut Laue-Langevin
INS	inelastic neutron scattering
INVENT	Instrument with Versatile Environment for Novel Technologies
IR	infrared
ISD	Instrument and Source Division
JCNS	Jülich Center for Neutron Science
J-PARC	Japan Proton Accelerator Research Complex
LANL	Los Alamos National Laboratory
LAO	LaAlO ₃
LLB	Laboratoire Léon Brillouin
LPSD	linear position sensitive detector
LSMO	La _x Sr _{1-x} MnO ₃
M-STAR	Magnetism–Second Target Advanced Reflectometer
M-WASABI	Magnetism—Wide And Small Angles with Big Intensity
MaNDI	Macromolecular Neutron Diffractometer
MANTA	multiple analyzer triple-axis spectrometer
MCP	microchannel plate
McStas	Monte Carlo simulation of triple axis spectrometers
MBARS	Mica Backscattering Spectrometer
MICROSE	Microsecond Neutron Spin Echo
MIEZE	modulation of intensity emerging with zero-effort
MTG	methanol to gasoline
MTJ	magnetic tunnel junctions
NAE	National Academy of Engineering
NAS	National Academy of Sciences
NC	nanocrystal
NDAV	Neutron Data Analysis and Visualization Division
NeSCry	neutron single crystal diffractometer
NHMFL	National High Magnetic Field Laboratory
NI	neutron imaging
NIH	National Institutes of Health
NIST	National Institute of Standards and Technology
nmr	nuclear magnetic resonance
NR	neutron reflectometry
NRC	National Research Council

NRSE	neutron resonance spin echo
NS	neutron scattering
NScD	Neutron Sciences Directorate
NSE	neutron spin echo
NSSAC	Neutron Scattering Sciences Advisory Committee
ODH	oxidative dehydrogenation
ORNL	Oak Ridge National Laboratory
P3HT	poly(3-hexylthiophene)
PCBM	phenyl-C61-butyric acid methyl ester
PDF	pair distribution function
PKA	protein kinase A
PMT	photomultiplier tube
PNR	polarized neutron reflectometry
PSD	position sensitive detector
QCMD	Quantum Condensed Matter Division
QCP	quantum critical point
QENS	quasielastic neutron scattering
R&D	research and development
RF	radio frequency
Rheo-SANS	rheology combined with small angle neutron scattering
RIXS	resonant inelastic x-ray scattering
RNA	ribonucleic acid
RRM	repetition rate multiplication
RT	reverse transcriptase
RTIL	room-temperature ionic liquid
SANS	small-angle neutron scattering
SAS	small-angle scattering
SAXS	small-angle x-ray scattering
SC	superconductor
sCMOS	scientific complementary metal–oxide–semiconductor
SDD	sample-to-detector distance
SEI	solid-electrolyte interphase
SEM	scanning electron microscopy
SERGIS	spin echo resolved grazing incidence scattering
SESANS	spin echo small-angle neutron scattering
SF	spin flip
SFA	Surface Forces Apparatus
SFD	switching field distribution
SIF	superconductor–insulator–ferromagnet
SNAP	Spallation Neutrons and Pressure
SNS	Spallation Neutron Source
ssDNA	single-stranded DNA
STS	second target station
SWANS	small/wide angle neutron scattering
T-REX	Time-of-flight Reciprocal space Explorer
TAS	triple axis spectrometer
TDR	Technical Design Report
TEM	transmission electron microscopy

THEL	Temperature–Magnetic Field–Electric Field–Light
TI	topological insulator
TISANE	Time-dependent SANS Experiments
TOF	time-of-flight
TR	time reversal
UCSB	University of California, Santa Barbara
UCSD	University of California, San Diego
USANS	ultra-small-angle neutron scattering
VAI	vertically aligned interfacial
VBPR	Variable Beam Profile Reflectometer
VERDI	versatile diffractometer
VCN	Very-Cold Neutron
VOR	Versatile Optimum Resolution chopper spectrometer
VSANS	very-high resolution small-angle neutron scattering
WHO	World Health Organization
WUSTL	Washington University in St. Louis

1. INTRODUCTION

Oak Ridge National Laboratory (ORNL) is a leading center for neutron sciences worldwide with the mission to ensure that the nation is served with cutting-edge capabilities for undertaking research that addresses the needs of the Department of Energy as well as the broader community. As part of this mission, the Neutron Sciences Directorate (NScD) has undertaken, in consultation with the sponsors and science community, an in-depth look at the major needs for neutron sciences and areas of significant impact spanning the next decade and beyond. A central part of this process has been the formation of four high level science-themed workshops to delineate emerging and future challenges and identify priority areas where developments in neutron sciences are most needed. This effort has been complemented by the formation of a series of working groups charged with exploring how these challenges could be addressed. A key component is the proposed Second Target Station (STS) at the Spallation Neutron Source (SNS), which will create new opportunities for neutron sciences as the first Fourth Generation Neutron Source (see Fig. 1.1).

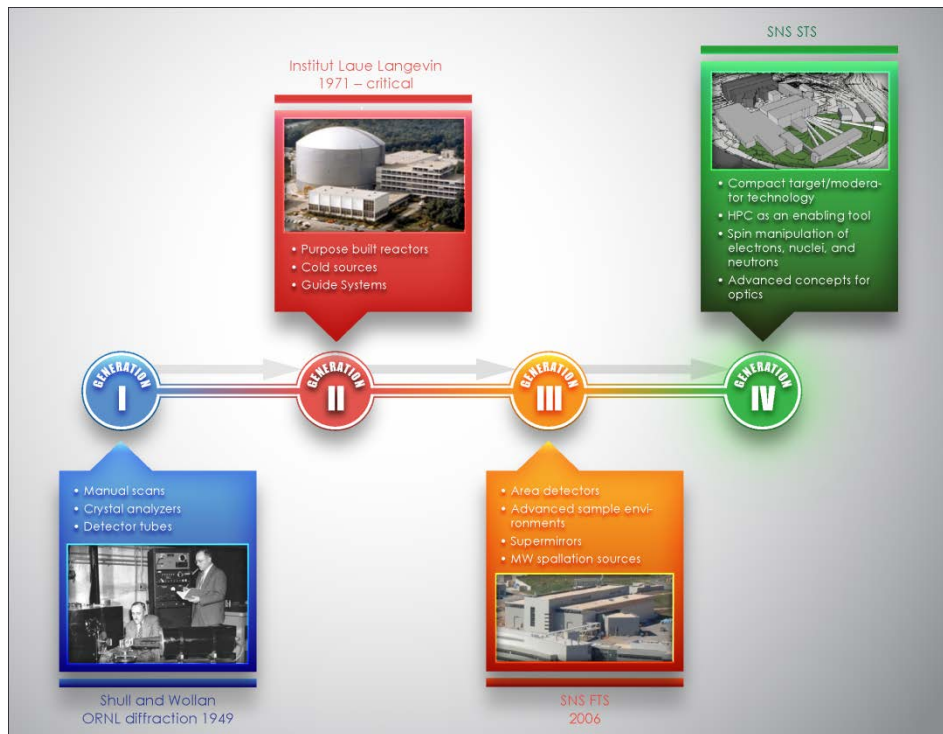


Fig. 1.1. Converging source and instrumentation technologies have defined completely new scientific capabilities with each generation of neutron facility. The Institut Laue-Langevin (ILL) in France integrated the technologies of the day into a class defining facility. Over the years, many of the advances of the technologies of Generation III have been integrated into this facility, especially with the Millennium project, and ILL remains one of the leading neutron facilities worldwide. In the United States, the construction of SNS brought a new level of capabilities in the form of a mega-Watt pulsed spallation source that re-established ORNL as a leading center. Second Target Station will, along with the planned European Spallation Source, be among the first fourth generation neutron facilities worldwide and will open up new areas of science.

STS was recognized as being “absolutely central” to US science in the Office of Science Facilities Prioritization Round 2013. However, there were “science/engineering challenges to resolve before initiating construction.” The engineering challenges are largely assessed in the accompanying Technical Design Report (TDR) documentation, while the following scientific challenges are addressed here:

- (1) What are the expected needs for neutrons and requirements for instrumentation?
- (2) Where do neutrons fit in with other developments in photons, electrons, etc., and where will they remain irreplaceable?
- (3) What new scientific capabilities can STS deliver?
- (4) How would a Second Target Station complement the capabilities of the First Target Station at SNS and the High Flux Isotope Reactor (HFIR)?

1.1 FUTURE SCIENCE NEEDS FOR NEUTRONS AND THEIR ROLE

To identify emerging science where neutrons are an essential tool as well as the needs of the community, four workshops addressed the future of quantum condensed matter, soft matter, biology, and the frontiers in materials discovery. These workshops provided a host of compelling scientific and technological challenges for the decade ahead that are inaccessible to other techniques or where the contribution of neutrons in combination with other techniques is vital. They also identified areas where a step change in capabilities is needed. In nearly all cases, the primary capability gaps that need to be addressed require more intense beams in the long wavelength (“cold”) regime and for instrumentation using a large bandwidth. STS, as proposed in the accompanying TDR¹, will provide exactly these capabilities and will be the most advanced source of its kind. Indeed, the capabilities envisaged will make this a truly next generation facility, and together with the first target station and HFIR reactor source, the STS facility will ensure US capabilities that go beyond any existing or planned sources worldwide for the next generation.

1.1.1 Quantum Materials²

Although normally associated with physics at the atomic scale, quantum coherence can give rise to spectacular properties when it transcends the atomic scale through collective behavior in so-called quantum materials. Neutrons provide access to the spatial and temporal electronic correlations and have played a pivotal role in our rapidly developing understanding of these materials.

The workshop on Quantum Condensed Matter examined the current state of research on quantum materials, how the field might evolve over the next decade, and the role of neutron scattering in these developments. It also covered the synthesis of new materials, the complementary use of neutrons and x-rays, and included discussion of the roles of muons and high magnetic fields. Overall, the scientific field of quantum condensed matter is found to be uncovering a rich variety of collective phenomena, some of which present exciting opportunities for technological impacts, and neutron scattering was determined to be an absolutely central technique for progress in the field.

¹ “Second Target Station at the Spallation Neutron Source” Technical Design Review, October 2014.

² Based on the report of the Quantum Condensed Matter Workshop, December 5–6, 2013, LBNL, Bob Birgeneau, UC Berkeley.

The workshop highlighted a number of crucial problems in quantum materials research where neutrons are indispensable. These problems range from understanding the exotic ground states that emerge in quantum spin systems, quantum critical phenomena, topological states of matter, and quantum materials out of equilibrium, to the physics underlying unconventional superconductors and itinerant magnets.

Increasingly, quantum materials are poised to make a major technological impact both in information technologies and energy. Progress in new devices and spintronics in particular require advances in neutron capabilities for probing structure and dynamics in thin films/heterostructures/nanomaterials. The importance of the special properties of strongly correlated states in energy storage and conversion are now being recognized and open up new needs for diffraction and inelastic neutron scattering.

A major trend in the coming years is the increasing importance of mesoscale phenomena for controlling properties. These techniques will require spatially-resolved probes of (especially magnetic) structure of materials on the sub-micron scale, as well as determination of the structure of partially ordered materials including defect structures (Fig. 1.2).

Next Generation

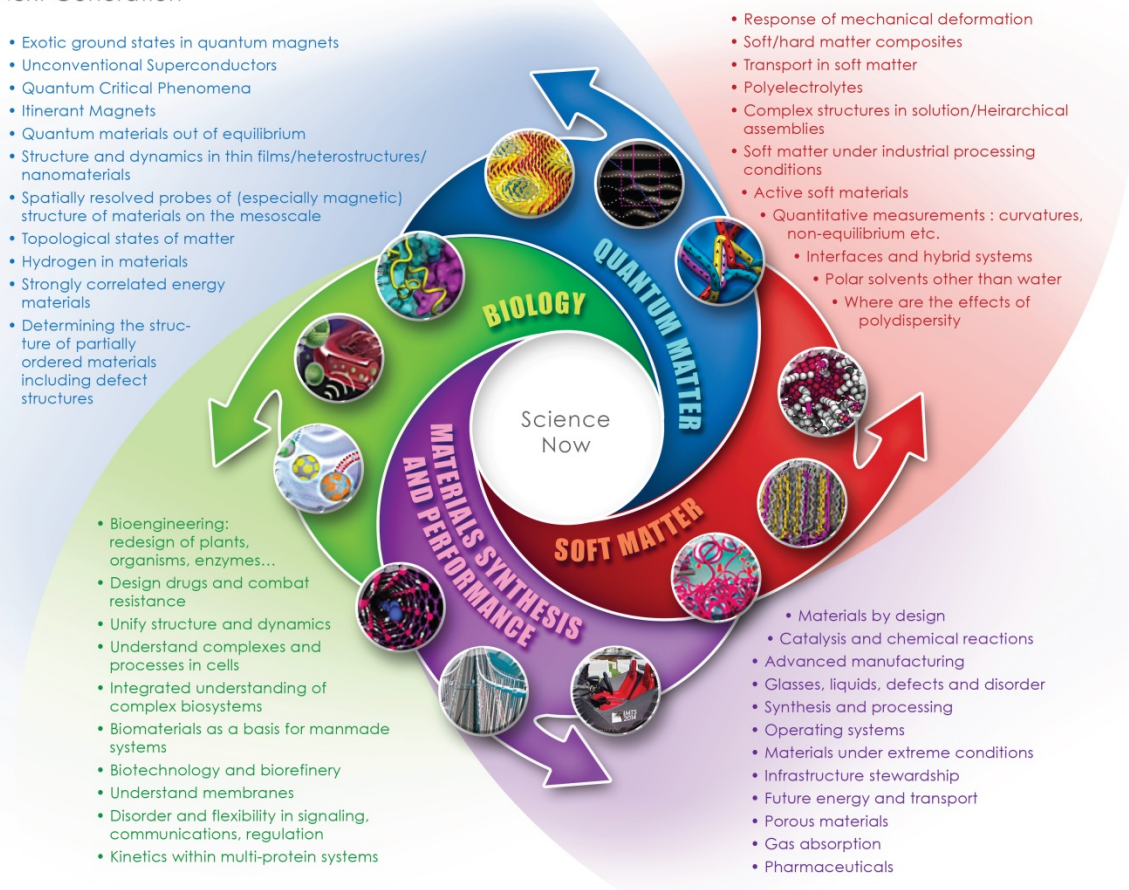


Fig. 1.2. Neutrons are either unique or play a vital role in combination with other experimental techniques over an enormous range of next generation science challenges. Shown above are key areas identified in the workshops where neutrons are needed but also require new capabilities. What these capabilities could look like is developed in this document.

The new challenges identified here need the much more advanced capabilities in cold neutrons offered by STS. Focused beams will be required to measure smaller samples, and the technology to fully exploit polarized beams is necessary to separate the component parts of complex states in materials. Coupling neutrons with materials exploration requires more versatile measurement capabilities, including application of multiple characterization techniques. Furthermore, the manipulation of states in situ means enhanced sample environments are crucial. Neutrons are unparalleled in their direct relevance to theory, and the most advanced data analysis and simulation capabilities are needed to address this potential.

1.1.2 Soft Matter³

One of the goals of modern science is to create materials by design with specific functionalities. Soft matter composed of covalently bound molecular building blocks (including polymers, surfactants, nanoparticles, gels, etc.) provides almost endless complexity and tunability for making new materials to achieve this goal. As the complexity of these systems grows, so do the challenges for developing our fundamental understanding of the materials' properties with the ultimate goal of controlling static and dynamic function.

Areas of compelling scientific need where neutrons will play a key role have been established. These extend into the response of soft matter to mechanical deformation, soft/hard composite materials, interfaces, and transport in soft matter. Also of fundamental need are capabilities to understand polar solvents other than water, polyelectrolytes, and complex structures in solution such as hierarchical assemblies. The widespread impact of soft matter technologies will require looking at soft matter under industrial processing conditions, understanding active soft materials, expanding our ability to make quantitative measurements, and gaining insight into the effects of poly-dispersity on physical properties.

While neutrons are an essential tool for studying soft matter today, in the future, new techniques and new sources will provide even more information on these complex systems. The proposed Second Target Station at SNS will be optimized to provide a high flux of long wavelength neutrons over a wide bandwidth. It will be ideally suited to simultaneously studying multiple temporal and spatial scales, which are crucial to understanding complexity in soft systems. To exploit and fully interpret the data, a closer coupling between modeling and experiment will be essential. Significantly increased facilities for selective isotopic labeling (primarily deuteration) will be needed. Soft matter has a growing synergistic relationship with molecular and cellular biology in the area of synthetically reproducing and enhancing the functionality found in living systems. Achieving these goals may involve the marriage of synthetic and biological moieties.

1.1.3 Biology⁴

Gaining a predictive understanding of the behavior of complex biological systems is one of the greatest scientific challenges that we will face over the next decade. This understanding will guide us in protecting and repairing physiological systems; it will allow us to mimic the architectures and processes of living systems to create new biomaterials and bio-inspired technologies; and it will provide the information necessary to manipulate micro-organisms and their ecosystems to create new biotechnology and biorefinery solutions to emerging energy and environmental challenges.

³ Report from "Grand Challenges in Soft Matter" workshop May 17–18, 2014, University of California Santa Barbara, Fyl Pincus (UCSB) and Matt Tirrell (University of Chicago).

⁴ Report from "Grand Challenges in Biological Neutron Scattering" workshop January 17–18, 2014, University of California San Diego, Susan Taylor (UCSD) and Heidi Hamm (Vanderbilt University).

Neutrons provide several types of unique information that will be important in addressing future problems and are poised to have major potential impacts, including influence on membrane associated biological processes and the dynamic assembly and regulation of large biological complexes. Their high sensitivity to hydrogen, which drives the chemistry and physics of living systems, in conjunction with deuterium labeling, which enhances the visibility of specific parts of complex biological systems through isotopic substitution, give neutrons direct access to crucial processes. The application of neutrons is being opened up by high performance computing simulations, which allow for prediction and interpretation of data from systems that are too complex for analytical theory. Neutrons are also complementary to techniques using photons and electrons. Photons and electrons interact with the atomic electric field and are most sensitive to heavy atoms; but with just one electron, hydrogen is all but invisible. Neutrons interact with nuclei; light atoms such as H are highly visible. In addition, because they cause little radiation damage and are highly penetrating, neutrons enable the use of complex sample environments.

Despite the advantages in using neutron scattering, significant technical gaps must be bridged not only in neutron scattering instrumentation but also in molecular biology, deuterium labeling, and computational technologies. They include the need for more advanced deuterium labeling techniques, better access to neutron beam lines, increased neutron flux on available beam lines, neutron beam lines optimized for membrane diffraction, the development of innovative techniques for polarizing neutron beams and hydrogen atoms in samples to enhance scattering power and to dynamically control scattering contrast, the development of new instrumentation that allows simultaneous access to broad regions of time and space, better integration of high performance computing techniques with neutron scattering experiments, and the development of computational tools that allow the combination of experimental data from multiple complementary techniques to generate more complete models of complex biological systems.

The Second Target Station is able to bridge these gaps and will allow neutrons to be used in a transformative way to unify the structural and dynamical description of biological systems across length and time scales. This advancement will transition the concept of a predictive understanding of biological systems to a reality.

1.1.4 Materials Discovery, Characterization, and Application⁵

Materials are at the heart of technologies that will define the future economy and provide solutions to the challenges in energy, security, and transportation. Predictive modeling of materials holds the promise of accelerating the development of new solutions; however, as a prerequisite, this development requires an understanding of materials' structure and dynamics from the atomic scale to real world components and systems. In addition, understanding and modeling synthesis and processing are vital to achieving transformative impact.

The unique physical properties of neutrons make high intensity beams indispensable to materials discovery, characterization, and application where they complement the capabilities of electrons and photons. Among these characteristics, their nondestructive nature, ability to penetrate real components and materials under working condition, sensitivity to light elements, ability to observe modes and dynamics over virtually all length and time scales, absence of selection rules, and the ability to highlight

⁵ Report from "Frontiers in Materials Discover, Characterization, and Application" workshop August 2–3, 2014, Schaumburg, IL, George Crabtree (Argonne National Laboratory) and John Parise (University of Stony Brook).

components using isotope substitution make their contribution unique. Areas where neutrons will be essential for future materials science and engineering include infrastructure stewardship, advanced propulsion systems, advanced materials processing, nuclear fuels and radiation tolerant materials, energy storage and energy conversion integrated systems, materials by design (integrated computational materials engineering), and materials under extreme environments.

To meet future challenges, new developments are needed in the following:

1. Monitoring and understanding chemical reactions and catalysis including gas adsorption and separation
2. Using analytical chemical spectroscopy where neutrons could provide a high throughput technique, providing information not accessible to photons
3. Understanding the role of disorder and defects and manipulating these
4. Addressing the fundamental challenges of glasses and liquids as well as fluid flow and reactivity
5. Conducting in situ studies including under pumping conditions, kinetics studies, materials growth and synthesis, and materials under extreme conditions
6. Understanding how components and integrated materials in devices function under realistic conditions using instruments that can combine multiple techniques such as imaging, diffraction and spectroscopy

The combination of intensity, dynamic range, and beam focusing at STS is crucial to provide transformative capabilities to enable these developments.

Overall, the outstanding scope of the science and technological challenges where neutrons play an irreplaceable role ensure they will be needed as a central part of a national facilities strategy for decades to come and show the compelling need for forefront facilities to ensure scientific and technological competitiveness.

1.2 ADDRESSING FUTURE SCIENCE CHALLENGES WITH SECOND TARGET STATION

To connect these science challenges with the source capabilities provided by STS and determine how this would be complemented by the First Target Station and HFIR, we convened a series of 14 working groups involving 70 of our scientists (Fig. 1.3). They were charged with exploring new concepts and instrumentation. In this report we present a series of instrument concepts that demonstrate new levels of performance as well as proposed science these instruments would allow that we cannot do now. Together, these new concepts provide a case for the impact of neutrons for the coming decade and beyond and demonstrate the compelling need for a Second Target Station at the Spallation Neutron Source.

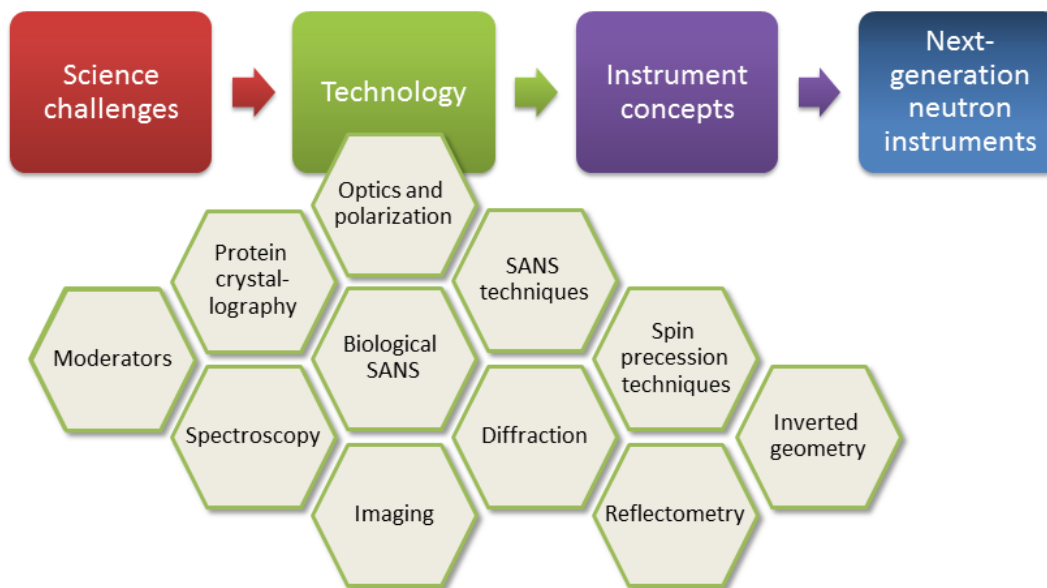


Fig. 1.3. The working groups were charge to explore transformational performance changes that would access new science.

The groups were formed from experts in science, technologies, and instrumentation. By exploring fundamental physical limits, new ideas for instrument types were generated.

1.3 PERFORMANCE AND CAPABILITIES OF SECOND TARGET STATION: A FOURTH GENERATION NEUTRON FACILITY

As outlined in this document, the performance and capabilities of the instrumentation enabled by STS make it truly a next generation facility (Fig. 1.4). Gains in performance of two orders of magnitude and beyond over existing capabilities make it transformative for many of the compelling research areas identified. At the heart of this dramatic step forward in capabilities are a series of advances that, when combined, create new classes of instrumentation. The major drivers for this advancement include, of course, the advances in target and moderator technology (see TDR), as well as high performance computing that enables reconstruction and analysis of multimodal data and simulation of systems gluing together disparate data sets and open complex scenarios to analysis and interpretation. In addition, the big advances in manipulation of the spin of electrons, nuclei, and neutrons allow control of scattering cross sections and contrast in situ and revolutionize what we can measure in magnetic and hydrogenous materials. Another area of great advance is in neutron optics where lensing, guiding, and wavelength analysis are all taking major steps forward. Taken together these define STS as a new generation of neutron facility of far reaching science impact.

STS instrumentation can address the science challenges

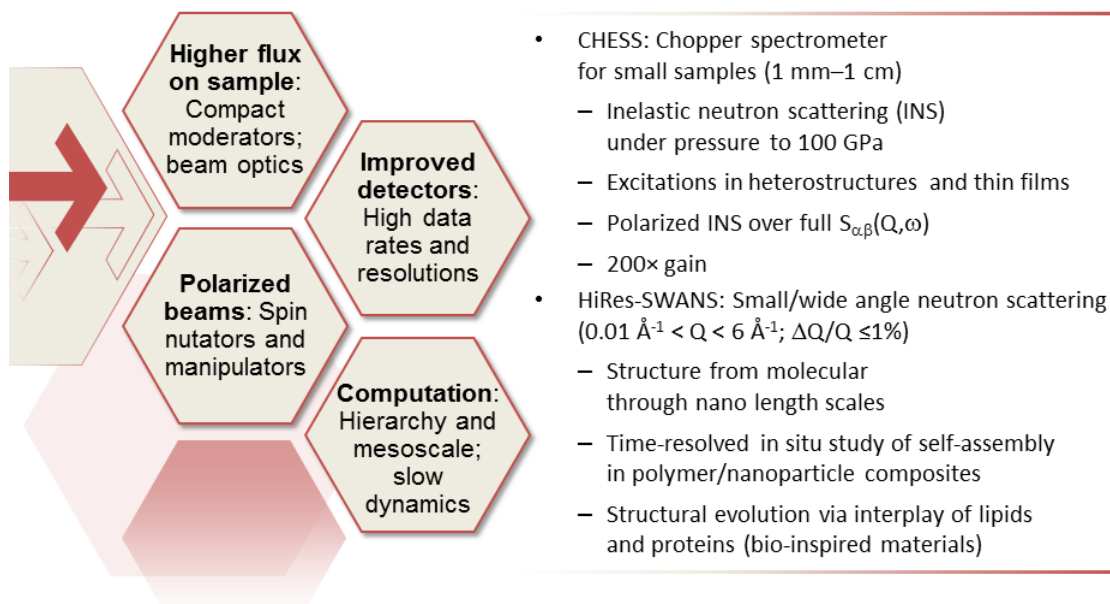


Fig. 1.4. The convergence of technologies in source and moderators, high performance computing, spin manipulation, and optics allows new levels of performance.

These include transformational advances in spectroscopy. An example is the CHES instrument, which will achieve gains of 200 over the current world leader CNCS at SNS. This advancement opens up the ability to look at dynamics in artificial crystals grown by epitaxy as well as heterostructures bringing neutrons to new realms of quantum materials and devices. Hierarchical materials present challenges beyond anything available currently. The HiRes-SWANS concept combines small and wide angle scattering to span length scales, giving access to structure from chemical bonding to mesoscale organization. This new class of instrumentation enabled by source and optics will be crucial for understanding the functional materials of tomorrow.

1.4 SCIENCE IMPACT OF SECOND TARGET STATION

We have explored 22 instrument concepts for the Second Target Station, which provide unprecedented levels of performance (See Fig. 1.5). These offer multimodal measurements both in terms of using advanced optics and computing to allow measurement and integration of multiple types of neutron measurement simultaneously but also enabling orthogonal, complementary techniques to monitor the system in parallel. In addition, the flexibility of design offered by new manufacturing technologies and complex data handling will allow the concept of a laboratory on a beam line to be realized where steering of complex interactive experiments is made in real time and in situ/in operando conditions can be designed as an integral part of the beam line from the beginning of operation.

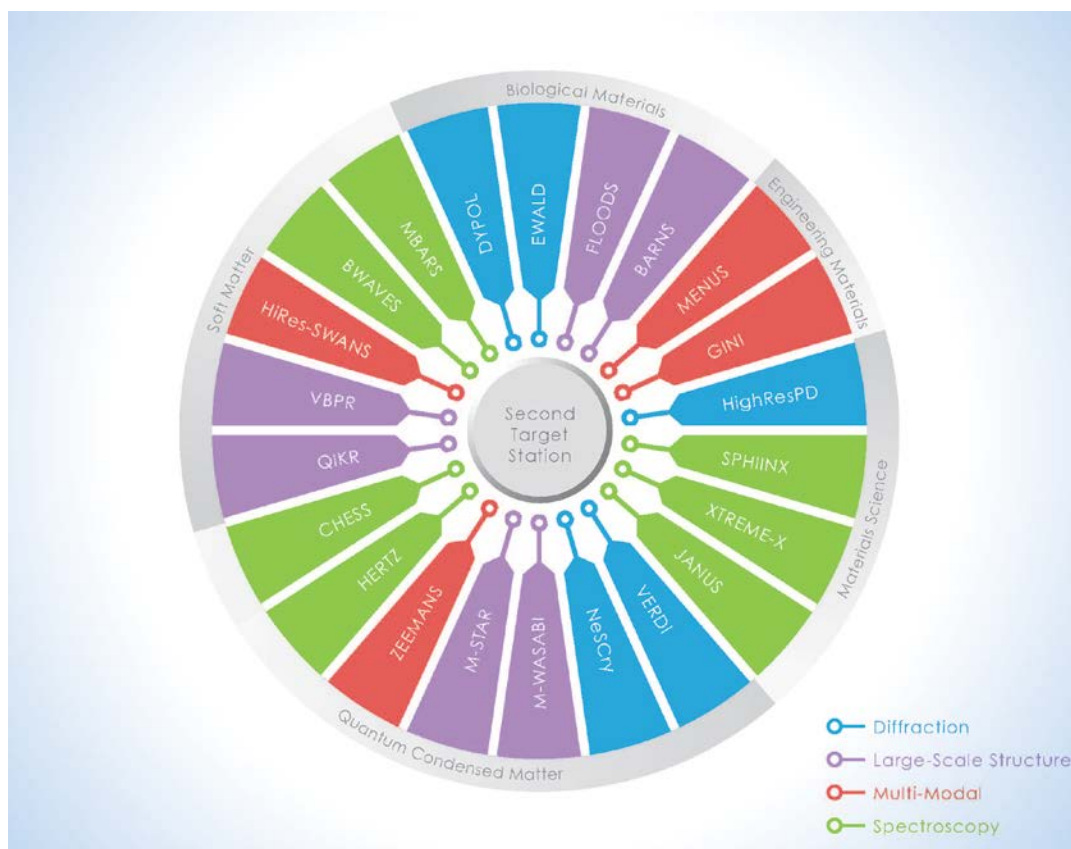


Fig. 1.5. The 22 neutron scattering instrument concepts explored for the Second Target Station span a range of science capabilities and science areas.

Overall, the development of the Second Target Station will ensure the US lead in neutron sciences for the foreseeable future. It will impact our understanding of materials by giving an integrated understanding from the atomic to real world scales. It will provide unprecedented access to mesoscale quantum and complex matter and ensure that the unique contributions of neutrons to discovery and understanding in these fields continue for decades ahead. The advent of 3D mapping and micro-spot technologies as well as the source intensity and novel instrumentation allow in situ and in operando studies, not just of exemplary materials but also of real operating systems, in the most challenging problems in technology and engineering. Automation and high throughput instrumentation, coupled with advanced modeling, databases and libraries, will put STS center stage coupling big data with computational resources to enable predictive control and design of materials. Already, the close relation between theory and experiment is putting neutrons at the forefront of the revolution in combining simulation and data. The high intensity beams and advanced handling capabilities will bring new insights into kinetics, out of equilibrium, and chemical reactions. They will facilitate not just the understanding of materials but also their synthesis and impact of processing conditions. Such capabilities, we predict, will become all the more important as the prediction of compelling material compositions makes advances in their synthesis all the more pressing. Finally, the major step forward in capabilities possible with STS will reach out into new science areas and bring whole areas of science, like biology and materials chemistry, into reach where the unique properties of neutrons can then play as important a role as they do today for quantum condensed matter and soft materials (Fig. 1.6).



Fig. 1.6. The second target station and instrumentation in this report provide transformative science capabilities impacting materials challenges and the new ways in which research is undertaken.

1.5 THREE SOURCE STRATEGY

STS will provide the means to address many of the outstanding challenges identified in the workshops, but neutron scattering techniques that are best optimized to different source characteristics are also a key requirement. The cold neutron beams and long repetition rate of STS perfectly complement the SNS First Target Station and HFIR. Together these facilities form an unbeatable combination that will give the United States clear leadership in neutron science capabilities for the next 20 years and beyond, allowing it to match or go beyond the capabilities of all existing or planned facilities worldwide. As part of our optimization strategy, we have explored instrument concepts at HFIR and FTS that can also take advantage of the advances detailed above to address the challenges identified in the science workshops. These new instrument concepts are also described in this document as part of a coherent approach to delivering an unparalleled and integrated set of neutron science capabilities. Figure 1.7 below summarizes the role of each facility and its strengths and the instrumentation types.

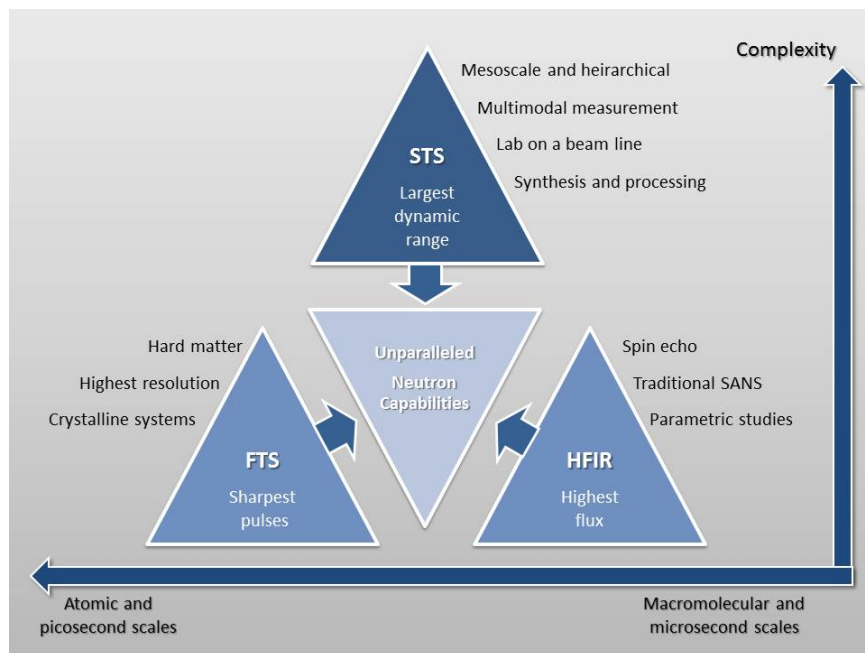


Fig. 1.7. The ORNL three source strategy.

1.6 FUTURE STEPS

The instrument concepts presented in this report are just a start. There are new instrument ideas and compelling science questions in the community that have not yet been explored. To access the creativity and collective wisdom of the whole US science community, we will hold a series of workshops to build on and add to the ideas presented in this document and continue the dialog about the role that neutrons will take in addressing the science challenges of today and the next decades. In addition, ORNL is investing directly in challenge experiments designed to demonstrate the capabilities that will be routinely available at STS for addressing the science of tomorrow. These experiments will use nuclear spin manipulation to transform the measurement of biosystems, establish infrastructure leading to inelastic measurements at extreme pressures of 40 GPa and above, and develop our strategy for simultaneous structural characterization of hierarchical materials over the broadest range of length scales. This is an exciting time for neutrons, and we hope you enjoy reading the report and encourage you to get involved in defining the future of neutron scattering in the United States.

1.7 CURRENT AND PROPOSED NEUTRON SOURCES AT ORNL

K. W. Herwig (ISD)

1.7.1 Introduction

ORNL is home to two powerful neutron sources: the High Flux Isotope Reactor (HFIR), an intense steady-state source, and the Spallation Neutron Source (SNS), the world's most powerful accelerator-based pulsed neutron source. During the past several years, these facilities have dramatically expanded both their science capabilities and capacity to support a diverse user community. These facilities currently represent about half of the US capacity to perform neutron scattering experiments. Continuing investments in new and upgraded instruments at these two facilities, along with on-going improvements

in technologies and techniques, will add science capabilities and increase capacity over the next five years.

The 1998 report of the Russell Subpanel [1] defining the technical specifications for SNS included recommendations to design the facility “such that it can be operated at a significantly higher power in a later stage” and to include the “capability of additional targets.” Both of these recommendations were incorporated into the original SNS design. The mission need for a SNS Second Target Station (STS) has been recognized by the Department of Energy with approval of CD-0 in January 2009 to “provide an additional target station at ORNL optimized for cold neutron beams.” Appendix A provides an abbreviated discussion on relative merits of the technical design requirements of STS. The current STS concept is a short-proton pulse, 10 Hz facility optimized for high peak-brightness, long-wavelength neutron pulses produced by coupled moderators. However, a number of the instrument concepts in the following sections propose taking full advantage of the 10 Hz STS operating frequency but require the sharper neutron pulses provided by a de-coupled, poisoned moderator. Current neutronics calculations indicate that such a moderator can be supported with minimal impact on the coupled moderators.

1.7.2 Source Characteristics and Strengths

HFIR

The HFIR cold-source is comparable to the world’s best reactor sources and provides the highest time averaged cold neutron flux of the ORNL sources, approximately 10× that of the proposed SNS STS as shown in Fig. 1.8 (a). In addition, HFIR produces approximately 40× the time-averaged thermal neutron flux of the SNS First Target Station (FTS).

The guide system delivering neutron beams to the cold instruments in the HFIR guide hall was designed in 1999 and started neutron beam operations in 2006. There have been major advances in neutron guide technology and neutron optics design in the past 15 years which have prompted an assessment of the HFIR neutron guide system. Section 6.3 provides a short description of a new guide concept for the HFIR cold source that would provide additional instrument end stations and improve neutron beam delivery for current instruments. Several of the proposed instrument concepts in the following sections would be supported by this new guide system.

SNS First Target Station

The SNS FTS is optimized for producing the highest wavelength resolution across a wide neutron spectrum. The two de-coupled, poisoned moderators that produce the shortest time neutron pulses and illuminate two-thirds of the SNS FTS neutron scattering instruments are placed in the most favorable positions relative to the Hg target. The two coupled H₂ moderators provide high fluxes of cold neutrons but have much broader time pulses than the de-coupled moderators and are placed in less optimum positions relative to the target, which limits their performance relative to the total number of neutrons they produce. Figure 1.8 (b) compares the pulse widths for the SNS moderators. FTS produces neutron

pulses at 60 Hz. The current STS project includes a doubling of the accelerator proton power from 1.4 MW to 2.8 MW with 2 MW available to FTS. The neutron scattering instruments and target shielding have all been designed for 2 MW operation, although some target modifications are likely needed because of the increased heat load. The current STS plan calls for operating the two sources in “pulse stealing” mode with five out of six pulses directed to FTS, and the remaining pulse directed to STS. One out of five of the FTS pulses will provide a longer counting time (broader wavelength band as discussed below) because of the missing pulse, but this will be of limited use because the choppers that define this band width cannot be re-set rapidly enough. The chopper systems on FTS will continue to operate as it currently operates, but with one pulse missing out of every 6.

SNS Second Target Station

STS is optimized for the highest cold neutron peak brightness, as shown in Fig. 1.8 (c). (Peak brightness is essentially the amplitude at the peak of the neutron time pulse emitted by the moderator as shown in Fig. 1.9.) In complementary fashion to FTS, coupled moderators will be placed in the most favorable positions relative to the target, maximizing their neutron production. Nonetheless, a number of the proposed instrument concepts require a much lower operating frequency than FTS but also require the sharp pulses of the decoupled moderators and would be well-served by the 10 Hz STS. The current STS concept includes three moderators: two coupled moderators of different geometry that are placed in the most favorable locations and a de-coupled moderator illuminating the remaining beam lines. Figure 1.9 shows pulse shapes at select wavelengths for the coupled moderators on both FTS and STS. Reducing the STS moderator dimensions to $3 \times 3 \text{ cm}^2$ will

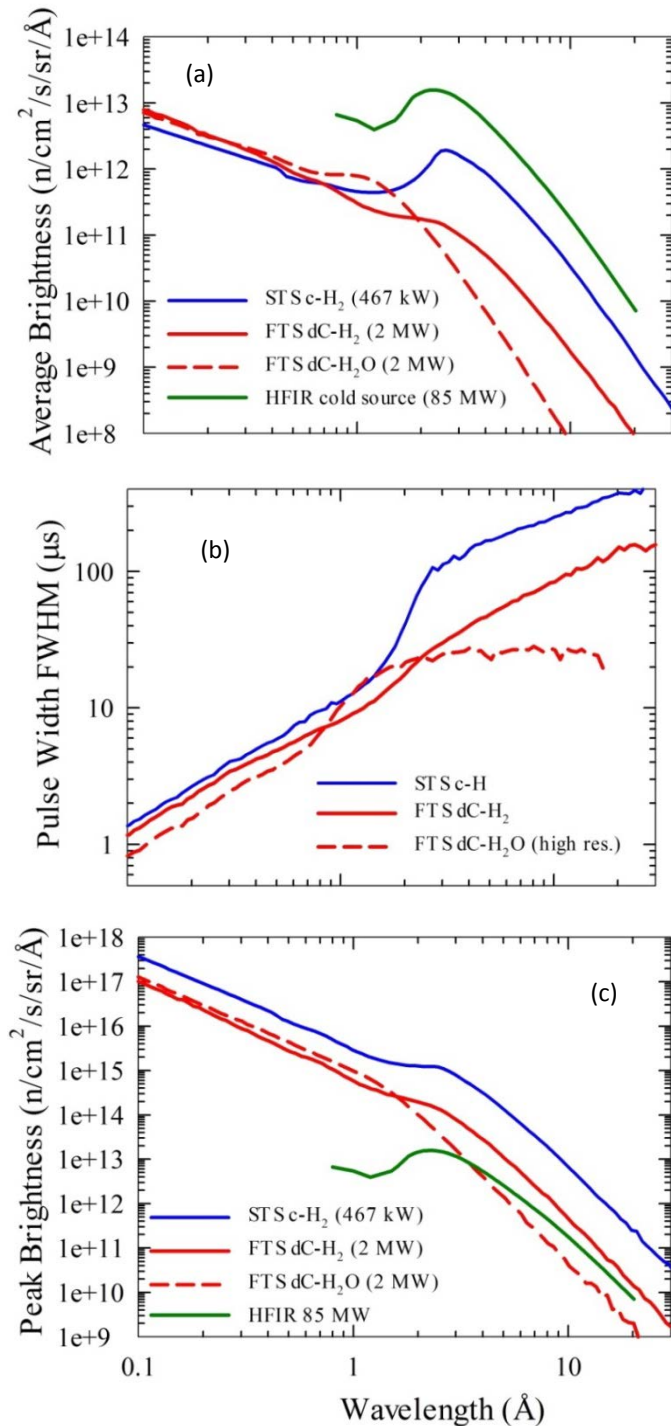


Fig. 1.8. Comparison of ORNL neutron source characteristics. (a) Time-averaged brightness of ORNL neutron sources. The SNS de-coupled and coupled moderators are shown for FTS and STS, respectively. These are the moderators for which the source was optimized. (b) Moderator pulse widths for the FTS de-coupled moderators and the STS coupled moderator. (c) Peak neutron brightness.

improve the peak brightness by an additional factor of ~ 2 relative to the $10 \times 10 \text{ cm}^2$ moderator.

Each of the three current and future ORNL neutron sources has characteristics that are highly desirable for different classes of neutron scattering instruments. The three ORNL facilities will provide a unique opportunity to match neutron scattering techniques and instrument design to the source that delivers the best performance. ORNL will be the only laboratory in the world to provide neutron scattering capabilities optimized across such a diverse set of sources.

1.7.3 Optimizing Instruments at Three ORNL Neutron Sources

The operating frequency, f , of a pulsed spallation source is a key parameter in optimizing its neutron scattering instruments. The neutron wavelength bandwidth, $\Delta\lambda(\text{\AA})$, available to the instrument is inversely proportional to f and the length, d (m), of the instrument, $\Delta\lambda = 3956/(d \cdot f)$. Higher source operating frequencies favor shorter instruments or instruments that use a small $\Delta\lambda$. For elastic techniques, the gains in employing time-of-flight (TOF) techniques are proportional to the number of useful instrument resolution elements available within this wavelength band. Consider the case of a high resolution powder diffractometer with a wavelength resolution $\delta\lambda/\lambda = 0.0005$ and a desire to use wavelengths from 0.5 to 6.0 \AA to obtain a complete data set. Such an instrument uses $\sim 5,000$ resolution elements and has the possibility for a TOF gain of 5,000 if all these elements can be obtained within a single pulse of the neutron source. If multiple pulses are required, the TOF gain is diminished accordingly. For inelastic instruments, gains are proportional to the peak neutron intensity at the desired λ and the ratio of the source frequency to the optimum instrument operating frequency. Repetition rate multiplication schemes can address the latter.

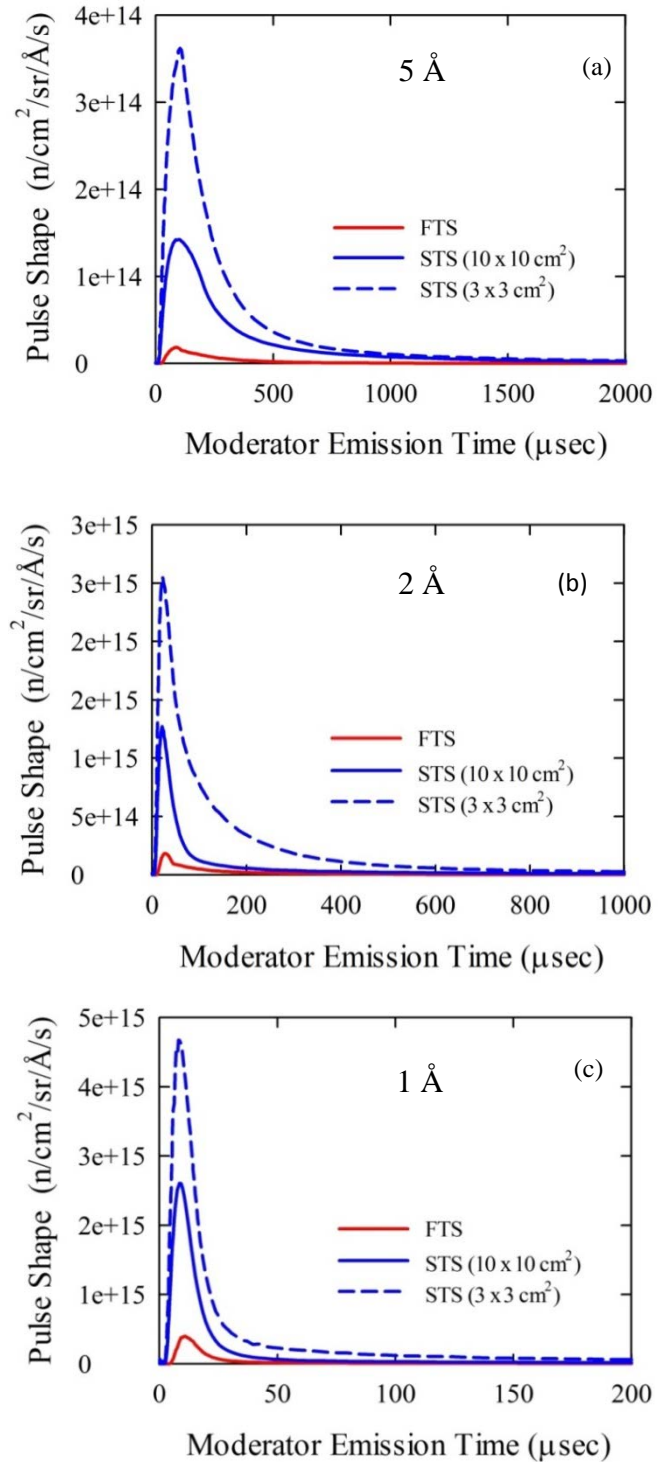


Fig. 1.9. Moderator pulse shapes for coupled moderators at FTS and STS at $\lambda = 5 \text{ \AA}$, 2 \AA , and 1 \AA in (a), (b), and (c) respectively.

Note that the time scale is changing in each plot.

Neutron scattering techniques and instruments that are optimized to use a small number of resolution elements have little opportunity to gain from TOF techniques and are best optimized to a reactor, continuous source that produces the greatest neutron time-averaged flux at the desired λ .

Figure 1.10 is an optimal performance map of elastic scattering techniques across ORNL neutron sources showing nominal ranges for many neutron scattering instrument types. The performance of most elastic scattering instruments depends on its range of accessible momentum transfers, Q , its Q -resolution, and its effective count rate. On most elastic instruments the Q -resolution is proportional to the wavelength resolution because the instrument geometry is designed to match geometrical contributions to the wavelength term. The x-axis in Fig. 1.10 is the desired wavelength resolution

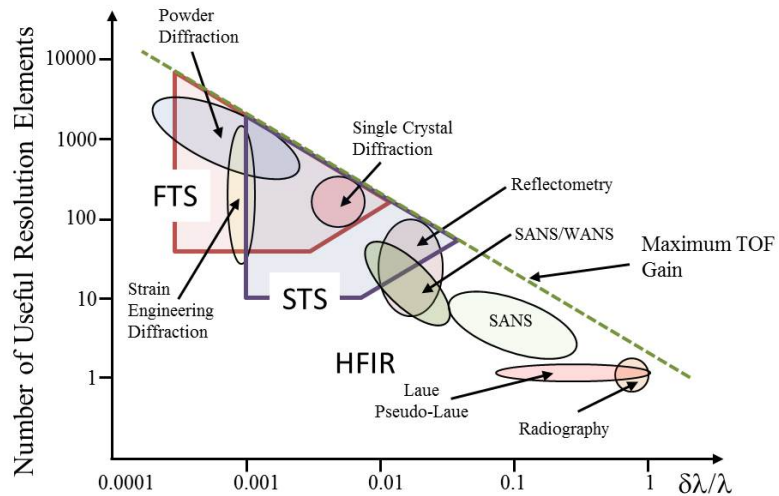


Fig. 1.10. Optimal performance map of elastic scattering instruments across the ORNL neutron sources.

Within the labeled boxes, the performance of the ORNL pulsed sources is expected to exceed that of HFIR. Outside the boxes, HFIR will obtain a desired data set more quickly.

expressed as $\delta\lambda/\lambda$. The y-axis is the number of these wavelength resolution elements required for any given measurement as discussed above and also represents the gain that an instrument can achieve from using TOF techniques. The approximate regimes of various elastic scattering techniques are indicated by the ovals. The maximum possible gain due to time-of-flight techniques is proportional to $(\delta\lambda/\lambda)^{-1}$ and is indicated by the dashed line. Within the labeled boxes, we expect the performance of the indicated pulsed source to exceed that of HFIR; outside the boxes, HFIR will obtain a desired set of data more quickly. That is, the gains from using TOF exceed the difference in time-averaged flux between the pulsed sources and HFIR. Notice that this simplified graph ignores features such as background, which can determine outcomes in some cases. The lower boundaries between HFIR and the pulsed sources are determined by the ratio of the time-averaged neutron flux of the SNS moderators and HFIR. The potential gain provided by the pulsed sources relative to HFIR increases as one moves upward in the chart. For example, at a $\delta\lambda/\lambda$ of 1%, STS can potentially measure a given sample as quickly as HFIR, provided more than 10 resolution elements are required to complete a data set. If 100 resolution elements are required, STS could potentially make a measurement 10 times faster than HFIR. Whereas there is a region in which FTS and STS overlap, there are also regions where each excels. The same conclusion applies to a comparison of HFIR with either pulsed source. The boxes for the pulsed sources are constructed for the moderator types they were optimized for—FTS: de-coupled, poisoned; and STS: coupled. The vertical and diagonal boundaries of the boxes are set by the maximum and minimum possible instrument lengths, 100 m and 15 m, respectively. (Although one or two instruments could be placed as far as 120 m from the moderator at STS, the majority must be located within ~90 m given restrictions on the site geometry.)

Figure 1.11 maps the performance of inelastic neutron scattering instruments. With the exception of backscattering and neutron spin echo, most inelastic studies use an energy resolution of a few percent and differ mainly in the magnitude of the incident energy. To separate the instruments, we choose the x-axis as the energy resolution (δE) in meV and the y-axis as the number of energy resolution elements required for the experiment.

Instruments to the right of this chart tend to use thermal to epi-thermal neutron energies, while those to the left tend toward use of cold neutrons, as indicated by the red and blue shading. The relative performance of the sources depends on the ratio of the time-averaged neutron flux modified by the number of resolution elements required.

FTS produces 40× fewer thermal neutrons than HFIR, so only in cases where more than 40 resolution elements are

required could FTS obtain data of a given quality more quickly than HFIR. As the plot indicates, Fermi chopper instruments fall into this category, but they are not competitive with triple-axis spectrometers (TAS) at HFIR when only a few resolution elements are required. Thus TAS will always perform best at HFIR. The performance of TOF chopper spectrometers scales with the peak neutron flux at the desired wavelength, provided the source is operated at a frequency that gives the desired number of resolution elements. The Fermi chopper spectrometers are best matched to the performance of the FTS water moderator. For cold neutron chopper spectrometers, the STS coupled H₂ moderator has about 5 to 7 times the peak brightness of the FTS moderator (see Figs. 1.8 [c] and 1.9). Assuming repetition rate multiplication is equally effective at both sources, these instruments will be best sited at STS. TOF backscattering spectrometers excel in their ability to sample a large dynamic range of energy transfers. The highest energy resolution requires the use of long wavelength neutrons ($\approx 20 \text{ \AA}$) and long beam lines, favoring STS. At shorter wavelengths, reasonable dynamic ranges can be obtained at the higher operating frequency of FTS and its poisoned, decoupled moderators provide ideal pulse widths. As was the case for the elastic scattering instruments, HFIR tends to be best matched to techniques that employ the smallest number of resolution elements. There is a significant overlap in capabilities between FTS and STS to support cold neutron TOF spectroscopy, and highly effective cold neutron chopper and backscattering spectrometers can be built at each source.

1.7.4 STS Instrument Strategies

Meeting the emerging science challenges of the next decade and beyond requires new paradigms in neutron scattering instrument design and optimization. Performance gains (flux on sample, sample size, resolution, extreme environments in pressure and magnetic field) on the order of 100 or greater are required (see some of the science case discussions in the instrument concept sections). As discussed above, the current maximum projected source gains of STS relative to FTS are $\sim 10\times$ in peak brightness (Fig. 1.9). The remaining order of magnitude must be achieved in the instrument design or development of associated sample environments. Some of this gain can be realized by use of the newest technologies,

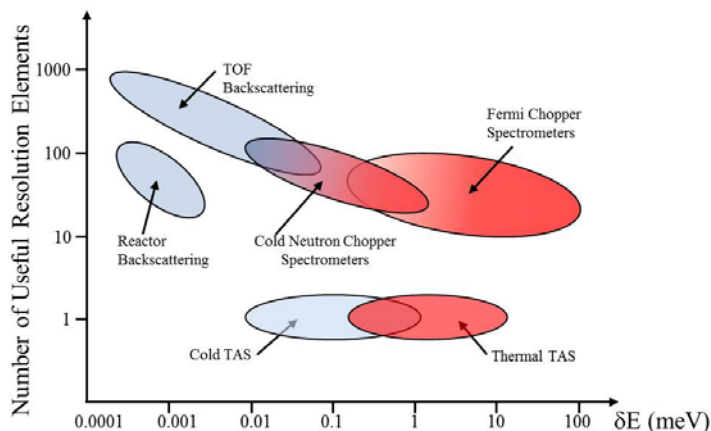


Fig. 1.11. Performance map of the inelastic spectrometers.

The colors indicate the incident neutron energy with red signifying thermal to epi-thermal neutrons and blue, cold neutrons.

particularly in the area of neutron optics (which is discussed in Section 6). In general, though, STS neutron scattering instruments will inevitably tend to more specialization and less flexibility. For example, measuring smaller samples may require not only better neutron optics and beam focusing but also an increase in acceptable beam angular divergence (see Section 2.2, the CHESSE concept) or development of background reduction technologies (see Section 3.3, the DyPol concept). Following are a few observations about STS instruments and their design:

- The science focus of each instrument must be well-defined because the desired performance gains are likely to push in the direction of less flexible, more specialized, and highly optimized instrument designs.
- Advances in neutron optics must be leveraged. This includes not only advanced guide technology but also development of more sophisticated optics systems such as illustrated by the HFIR IMAGINE instrument and the use of Wolter optics (Fig. 1.12).
- The smaller, high brightness moderators discussed above will enable better optimization of neutron optics systems but likely at the cost of increased mechanical complexity and possible active alignment systems. Particularly in the near moderator regions, care must be taken in the mechanical design of the target monolith to support the higher precision required. It will be important to support a close approach to the moderator of neutron optical systems, 60 cm or less.

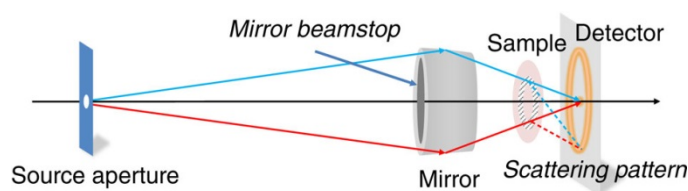


Fig. 1.12. Compact small angle neutron scattering instrument developed at MIT and tested at HFIR. [2]

- The low, 10 Hz repetition rate of STS will enable the use of much larger bandwidths per pulse, translating to the ability to simultaneously sample much larger length and/or time scales.
- Instrument concepts must mature on a time scale such that they can influence the final choices in moderator and source geometry and neutron spectral characteristics (pulse widths, brightness, and size).
- Development of neutron polarization techniques for use on TOF instruments is crucial because many of the methods commonly used on instruments at continuous sources are not directly applicable. Wide-angle polarization analyzers are particularly important because of the large solid angle detectors' coverage on most TOF spectrometers (see the science cases for CHESSE and HERTZ, Sections 2.2 and 2.3, respectively).

1.7.5 References

- [1] Report of the Basic Energy Sciences Advisory Committee on Neutron Source Facility Upgrades and the Technical Specifications for the Spallation Neutron Source, http://science.energy.gov/~media/bes/besac/pdf/neutron_source_rpt.pdf (1998).
- [2] D. Liu, et al, Nature Commun. 4, 2555 (2013).

2. CHALLENGES IN QUANTUM CONDENSED MATTER

Steve Nagler and Mark Lumsden (Quantum Condensed Matter Division [QCMD])

Although normally associated with physics at the atomic scale, quantum coherence can give rise to spectacular properties when it transcends the atomic scale through collective behavior in so-called quantum materials. Neutrons provide access to spatial and temporal electronic correlations in the relevant regimes and have played a pivotal role in our rapidly developing understanding of these materials.

A workshop on Quantum Condensed Matter at Lawrence Berkeley Laboratory on December 9 and 10, 2013, examined the current state of research on quantum materials, how the field might evolve over the next decade, and the role of neutron scattering in these developments. The workshop included sessions offering viewpoints on the current state and 10 year outlook for quantum materials, the synthesis of new materials, the complementary use of neutrons and x-rays, and muons and high magnetic fields. Participants in breakout sessions debated and reported their views on these topics to the full group.

The central messages of the workshop are: (1) the scientific field of quantum condensed matter is uncovering a rich variety of collective phenomena, some of which presents exciting opportunities for technological impacts; and (2) neutron scattering is an absolutely central technique for progress in the field. A list of problems in quantum materials research that will be important in the near future was generated and is summarized below. Guided by these science problems, a specific set of recommendations for neutron scattering development emerged. These recommendations, summarized below, have implications for source, instrumentation, and sample environment development as well as ideas to enable better coupling with the broader quantum materials community to maximize scientific impact.

Important Problems in Quantum Materials Research

Exotic ground states in quantum magnets

- Understanding the exotic ground states that emerge in quantum spin systems such as the quantum spin liquid state involves coordinated efforts in materials synthesis, theory, and scattering, coupled with thermodynamic measurements.

Unconventional superconductors

- The ultimate goal is to establish the mechanism for exotic superconductivity as well as the role of itinerant or local magnetism in these materials, including cuprates, Fe-based superconductors, heavy fermion superconductors, organic superconductors, etc.

Quantum critical phenomena

- Achieve a fundamental understanding of quantum critical points (QCPs) in both magnetic insulators and metals such as heavy fermion systems and understand their relevance to other phenomena observed in correlated electron systems.

Itinerant magnets

- Quantitative understanding of the influence of the electronic band structure on the magnetic properties of itinerant magnets requires coupling between experiment and theory/simulation and has implications for many other problems of interest, including unconventional superconductors.

Quantum materials out of equilibrium

- Currently, most experiments and theory focus on thermal equilibrium, but applications that use quantum materials often operate in or are influenced by non-equilibrium phenomena. It remains a significant challenge to measure and understand structure and dynamics in non-equilibrium conditions and involves developments both experimentally and theoretically.

Structure and dynamics in thin films/heterostructures/nanomaterials

- Understand static magnetism, epitaxial strain control, and magnetic and lattice dynamics in thin films, nanoparticles, and quantum dots.

Spatially resolved probes of (especially magnetic) structure of materials on the mesoscale

- Identify intrinsic and extrinsic inhomogeneities, the former from competing interactions and competing orders in strongly correlated systems and the latter because of the complex nature of the materials. Such inhomogeneities significantly influence function of materials in real devices.

Topological states of matter

- Determination of structure, kinematics, and dynamics of exotic mesoscale structures such as skyrmions.

Hydrogen in materials

- Study the properties of nanoconfined hydrogen containing matter such as water and understand why they differ from the bulk to shed light on the role that quantum mechanics has played in the origins of life.

Energy materials and industrial applications

- Strongly correlated materials are of increasing importance in a number of energy related technologies. Practical applications of such materials require understanding the science of interfaces as well as the mesoscale complexity of the materials' bulk form.

Determination of the structure of partially ordered materials including defect structures

- Synergistic efforts in neutron diffuse scattering measurements are coupled with theory and modeling to study the structure of inhomogeneous patterns in oxides.

Recommendations

To make progress in the challenging problems identified above, the following specific recommendations emerge for quantum materials research using neutron scattering:

1. **Cold neutrons**. Increasingly, forefront problems in quantum materials research involve complex materials consisting of large structures characterized by low energy fluctuations. Expanded capacity and capabilities for cold neutron elastic and inelastic neutron scattering will be essential to understand the structure and dynamics of such materials. Furthermore, emphasis on cold neutrons enhances complementarity with other experimental techniques such as inelastic x-ray scattering.
2. **Enable measurements with smaller samples**. Often, interesting materials are discovered where single crystals can be synthesized only by techniques such as high pressure synthesis, hydrothermal synthesis, and electrocrystallization resulting in small single crystal samples. Such sample sizes are challenging for neutron scattering. Optimized instruments at high flux neutron sources using advancements in neutron optics could enable both elastic and inelastic neutron scattering measurements on smaller crystals than had previously been possible, greatly expanding the impact of neutron scattering. This argument also extends to materials such as heterostructures and nanomaterials.
3. **Polarization analysis**. Implementation of polarization analysis, particularly when combined with time-of-flight instrumentation, can provide critical information to understand the nature of exotic ground states, including those with strong coupling between magnetic and lattice degrees of freedom. Polarized neutrons are also necessary to enable certain advanced techniques such as ultra-high resolution spectroscopy and diffraction using Larmor labeling.
4. **Coupling neutrons with materials exploration**. The discovery and subsequent investigation of new materials drives many of the scientific advancements in quantum materials research. High efficiency diffraction, both powder and single crystal, as well as in situ measurements during growth, is important to rapidly characterize both the crystal and magnetic structure of newly discovered materials. Better coupling of neutron diffraction with materials synthesis efforts calls for modified beam time access models that allow for more rapid access.
5. **Enhanced sample environments**. Many problems of interest can benefit from coupling of neutron scattering to extremes of pressure, temperature, and magnetic field. Significant development efforts are required to extend the limits, particularly for magnetic fields and pressure. Such developments will also benefit from and must be integrated with instrument development efforts (e.g., optimized instruments for measuring smaller samples). Developments in techniques such as pump probe approaches are also required to measure non-equilibrium phenomena.
6. **Better coupling of neutron scattering with theory and simulation**. The weak scattering nature of neutron scattering results in a cross-section for both elastic and inelastic scattering, which is well understood and can be calculated exactly by many theory and simulation techniques. Close coupling between theoretical efforts and neutron scattering is necessary to make progress in forefront problems. For neutron scattering, this requires detailed understanding of the instrumental resolution function, measurements in absolute units, and development of tools to enable quantitative comparison of theory and experiment.

7. **Facilitate measurements with multiple characterization techniques.** Increasingly, progress on many problems requires not a single technique but rather multiple complementary tools. The impact of neutron scattering can be enhanced by facilitating such measurements. This could have implications for methods of beam time access, such as joint beam time proposals at both neutron and x-ray sources. In addition, in situ techniques that combine neutrons and other techniques should be pursued. An example is TISANE (time dependent SANS experiments), which combines ac susceptibility and SANS to allow study of mesoscale systems such as skyrmions and vortex lattices.

2.1 COLD SPECTROSCOPY

Mark Lumsden and Jaime Fernandez-Baca (QCMD)

In response to community needs and scientific trends as discussed above, we propose the following instruments for cold neutron spectroscopy:

1. **CHESS**—Chopper spectrometer for small samples (SNS Second Target Station)
2. **HERTZ**—High energy resolution terahertz spectrometer (SNS Second Target Station)
3. **MANTA**—Multiple analyzer triple-axis spectrometer (HFIR)
4. Ultra-high resolution spectroscopy with neutron spin echo option for TAS (HFIR)

These instruments will:

1. Expand capabilities in high resolution spectroscopy. The proposed instruments will more than double the US availability of high resolution spectroscopy instruments optimized for the study of quantum materials. The first three instruments listed above are cold neutron spectrometers providing access to energy transfers from μeV to tens of meV , while the fourth is designed to provide μeV resolution at meV energy transfers. The cold neutron energy scale is well suited to many of the critical problems of both experimental and theoretical interest, such as quantum magnets, frustrated magnets, and heavy fermion superconductors. Furthermore, the cold neutron energy scale is well matched to the intrinsic energy scale associated with extreme sample environments including temperature, pressure, and magnetic field; studies in the presence of such parameters can yield critical information in the study of an array of topical scientific problems.
2. Offer close coupling between experiment and theory. One of the strengths of inelastic neutron scattering is that the measured cross-section is directly related to the dynamic spin correlation function $S(Q, \omega)$, which is accessible through theory and modeling. Therefore, inelastic neutron scattering allows for close connection with theory and computation, and neutron data can often provide definitive tests of theoretical models. Many problems at the forefront of condensed matter research involve competing interactions and ground states, and true comprehension requires high precision measurements that can be compared carefully to theory.
3. Enable inelastic scattering measurements on small samples. Inelastic neutron scattering remains an intensity-limited technique, which at the moment excludes many important materials that cannot be synthesized in large single crystal form. Advanced neutron optics combined with an

instrument specifically designed for small samples would enable inelastic neutron scattering on samples of dimensions as small as ~ 1 mm. Such an instrument would significantly expand the range of materials that could be explored with inelastic neutron scattering and dramatically broaden the impact of the technique. In addition, some complex sample environment equipment, such as high pressure, significantly restricts the sample volume. Instruments optimized for small samples are required to enable inelastic neutron scattering in the presence of such equipment.

4. Expand the use of polarization analysis with inelastic instrumentation. The first three instruments listed above will be designed to allow for three-dimensional polarization analysis enabling measurements of multiple components of the $S_{\alpha\beta}(Q, \omega)$ tensor. This combined with the broad angular and energy coverage of these instruments provides a wealth of information and more specific links to theory and simulation. Furthermore, there is growing interest in more complex materials with strong coupling between magnetism and orbital or lattice degrees of freedom. The ability to perform broad Q, ω coverage measurements with polarized neutrons allows for clean separation of lattice and spin dynamics, independent measurements of transverse and longitudinal spin fluctuations, and separation of coherent and incoherent scattering, of particular relevance in hydrogen containing materials such as soft matter.
5. Enable high efficiency mapping of excitations over a wide dynamic range. While modern chopper spectrometers such as those at SNS have greatly increased the ability to explore excitations over a wide range of Q, ω space, further progress is now possible at both SNS and HFIR because of new instrumentation concepts and the unique capabilities of STS. For SNS instruments at the lower repetition rate, the length of the time frame enables multiple incident energies to be measured simultaneously (so-called “rep rate multiplication”). Both the CHES and HERTZ instruments will be designed to enable on the order of 10 incident energies simultaneously. For HFIR instruments, there have been advancements in multi-analyzer configurations that enable simultaneous measurements over a broad range of scattering angles and final energies.
6. Enable high resolution measurements (μeV resolution) of dispersive excitations. As described in Section 5, Larmor labeling can break the conventional link between resolution and intensity and enable micro-electron volt resolution at meV energy transfer. This technique can be an option on a modernized thermal triple axis spectrometer to allow measurements of dispersive phonon or magnon lifetimes. The resonant spin echo methods can also be used to measure thermal expansion with 10^{-6} resolution that far exceeds the highest resolution of synchrotron instrumentation.

The following sections provide further information about the proposed instrumentation and the high impact science that would be enabled.

2.2 CHESS—CHOPPER SPECTROMETER FOR SMALL SAMPLES

G. Ehlers and M. D. Lumsden (QCMD)

Abstract

The planned STS at SNS will provide excellent opportunities for cold neutron spectroscopy. There are programmatic and capacity needs for two direct geometry inelastic spectrometers with different optimizations. CHESS is the first of these instruments and is a spectrometer optimized for very small samples ($\sim 1 \text{ mm} - 1 \text{ cm}$) and medium energy resolution. CHESS will take full advantage of the increased peak brilliance of the high brightness STS coupled moderators and of recent advances in instrument design and technology to achieve unprecedented performance in the cold energy range. For small samples, the performance will exceed that of CNCS by a factor of ~ 200 .

Science case

Traditionally, intensity limitations have meant that inelastic neutron scattering measurements could be performed only on large single crystal samples. However both source and neutron optics advancements now make it possible to break that paradigm so inelastic neutron scattering can be conducted on the most interesting high quality materials that typically are not available as large (cm sized) single crystals. CHESS will take advantage of the high brightness of the coupled hydrogen moderators at STS together with focusing neutron optics to optimize the flux of cold neutrons delivered to a small sample. Scientifically, CHESS offers the following capabilities:

1. A direct geometry time-of-flight spectrometer optimized for small samples ($\sim 1 \text{ mm} - 1 \text{ cm}$) and medium energy resolution. This will enable mapping excitations over a broad wave vector and energy range for samples with a cross-sectional area as small as 1 mm^2 .
2. The instrument will include full three-dimensional polarization analysis to enable separate measurements of multiple components of the $S_{\alpha\beta}(\mathbf{Q},\omega)$ tensor
3. The low repetition rate of STS will enable simultaneous measurements with multiple incident energies, greatly increasing measurement efficiency particularly in materials with excitations covering a broad range of energies

Extending the feasibility range for real experiments with respect to the minimally required sample size is one of the most promising areas for future growth. The last decade has seen the successful development and scientific deployment of several instruments specifically dedicated to small samples, including SNAP, MaNDI and TOPAZ at SNS. These are, however, diffraction instruments, and there is no inelastic spectrometer in operation that addresses this need.

The dynamic structure factor, $S(\mathbf{Q},\omega)$, as measured in an inelastic neutron scattering experiment contains information necessary to understand the microscopic interactions in a wide range of quantum materials. However, the traditional large sample size requirement has limited the applicability of this technique and prevented exploration of a great number of materials. The optimization described below and the expected gain factors for CHESS will enable inelastic neutron scattering on smaller samples than had previously been possible, opening the technique to a broader range of materials. One example is materials that can be grown only with high pressure synthesis.

This technique yields small single crystals as, for example, the $S = 1/2$ kagome staircase material β - $\text{Cu}_3\text{V}_2\text{O}_8$ [1]. Another interesting class of materials where inelastic neutron scattering has not been possible is organic superconductors. There are now several families of unconventional superconductors including the cuprates, Fe-based superconductors, and heavy fermion superconductors, all of which exhibit magnetism in close proximity to the superconducting state. Organic superconductors, composed of charge transfer salts [2], have phase diagrams with strong similarities to other unconventional superconductors as shown in Fig. 2.1 and have a superconducting state near an antiferromagnetic insulating state. These materials are thought to be unconventional superconductors, and magnetism is thought to play a role in the superconducting pairing mechanism [2,4]. While the magnetism in all other families of unconventional superconductors has been extensively studied with inelastic neutron scattering, to date no inelastic neutron scattering measurements have been performed on organic superconductors. Although organic superconductors can be deuterated to suppress the incoherent background, synthesis is based on electrocrystallization [5] from which only small single crystals can be obtained (see Fig. 2.2). The CHES instrument will allow for successful inelastic neutron scattering experiments on these materials (including studies in the presence of kbar applied pressure) allowing for detailed understanding of magnetism in these compounds and shedding light on the coupling between magnetism and superconductivity.

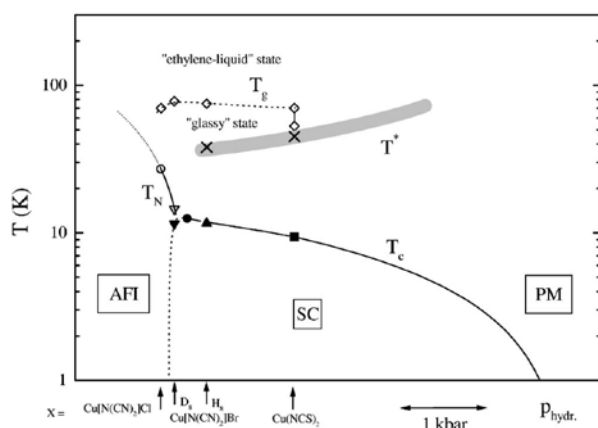


Fig. 2.1. Phase diagram of κ -(BEDT-TTF) $_2$ X as a function of pressure with arrows indicating the location of different compounds at ambient pressure [Müller].

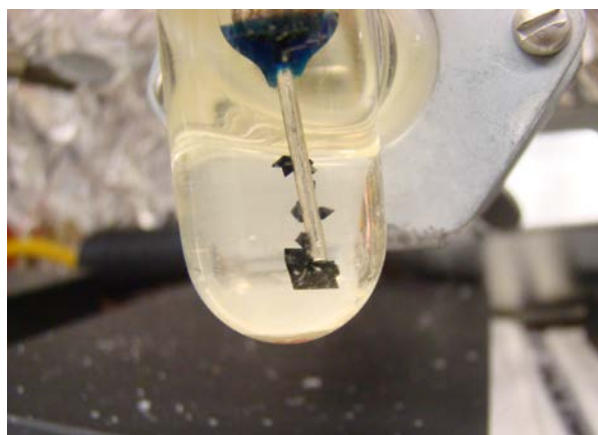


Fig. 2.2. Photos of single crystal samples of κ -(ET) $_2$ Cu[N(CN) $_2$]Br (Photo: J. A. Schlueter).

With measurements on small samples possible, one can consider inelastic neutron scattering measurements on epitaxially grown single crystals that are often used to develop new materials with tailored electronic, optical, or magnetic properties. If such crystals can be grown to micrometer thickness, studies of their excitations using CHES are feasible. Also possible are inelastic measurements of heterostructures where interface effects dominate. Exploration of spin and lattice dynamics in such systems could help to understand their unique magnetic properties and how they differ from the bulk.

The small sample optimization of CHES will also allow for expanded measurement capabilities in the presence of complex sample environments, such as high pressure cells, where the sample volume is limited. Pressure is, in principle, an ideal tuning parameter for unconventional superconductors including heavy fermion and Fe-based superconductors, but neutron scattering experiments are challenging on current instrumentation. While excitations have been studied across the phase diagram as a function of concentration, chemical doping introduces the unwelcome complexity of disorder and inhomogeneity on the observed properties. Pressure is a cleaner tuning parameter, but such studies will require expansion of the available pressure to ~ 15 GPa, which significantly restricts the sample volume. For heavy fermion superconductors, pressures of 3–10 GPa can tune the system from the magnetically ordered state to the superconducting state and eventually into the Fermi liquid state (for example, CePd_2Si_2 , in Fig. 2.3). For Fe-based superconductors, the pressures involved are typically higher. For instance, pure BaFe_2As_2 superconducts above ~ 7.5 GPa and transitions back into a Fermi liquid above ~ 16 GPa [7]. Exploring the evolution of the magnetic excitations in these materials versus pressure, and therefore without the disorder inherent to chemical doping, would allow stronger coupling to theory and thereby help to understand and exploit unconventional superconductors.

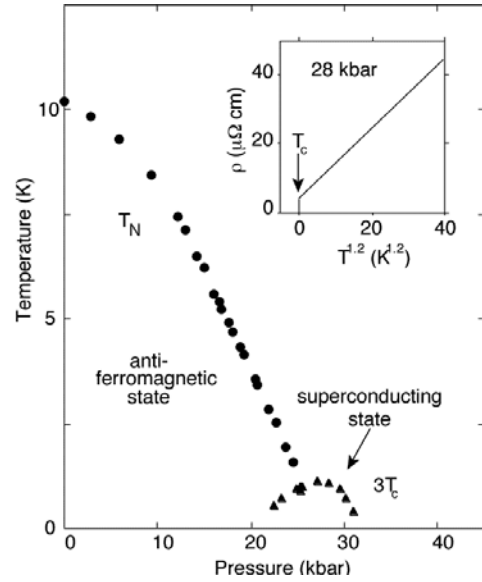


Fig. 2.3. Suppression of antiferromagnetic order and appearance of superconductivity in the heavy fermion compound CePd_2Si_2 [6].

CHES is also ideal for samples that absorb neutrons because of the presence of certain elements and where isotopic substitution is not an option. An example of such a case is iridium containing compounds where both stable isotopes absorb neutrons. The 5d electron transition metal oxides have received considerable attention in recent years because of the relative strength of spin-orbit coupling and the potential for realizing novel ground states [8]. Specifically, oxides based on Ir^{4+} are of interest because of the effective quantum spin-1/2 state resulting from octahedral oxygen coordination [9]. The compounds A_2IrO_3 ($\text{A} = \text{Li}, \text{Na}$) form a honeycomb lattice of Ir^{4+} ions and the proposed Hamiltonian (Kitaev-Heisenberg) has a rich phase diagram depending on the interaction strengths [10]. Inelastic neutron scattering is the ultimate tool to determine the low energy spin-Hamiltonian of these materials, but the neutron absorption of iridium poses a significant problem that has so far precluded successful single crystal inelastic measurements. To date, the only successful measurements have been on polycrystalline samples (Fig. 2.4) [Choi], and these data do not allow for unambiguous determination of the Hamiltonian. The absorption length defines a maximum sample dimension on the order of ~ 1 mm, meaning that an instrument like CHES,

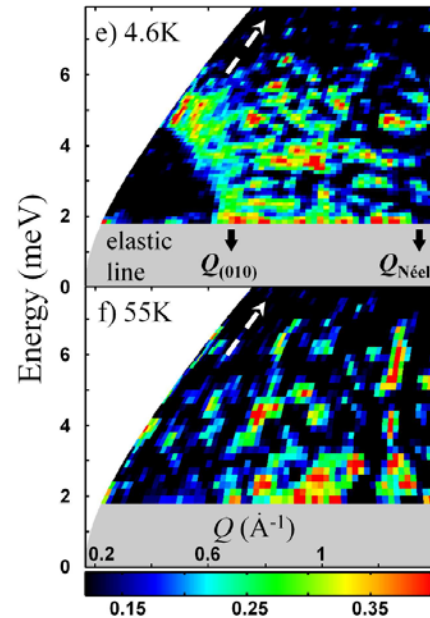


Fig. 2.4. Powder inelastic scattering from Na_2IrO_3 [11].

optimized for small single crystals, is required and could have an enormous impact on our understanding of this new class of materials.

Almost ubiquitous in the phase diagrams of strongly correlated electron systems, quantum criticality [12] is another scientific area the CHES spectrometer would impact. To date, there are very few comprehensive studies of quantum criticality in metals using inelastic neutron scattering [13], but neutron scattering can, in principle, provide information that is not available from other experimental techniques. The energy scales are too small for RIXS, and optical techniques do not provide access to finite wave vector transfer. The experimental difficulties are numerous, however: weak signals necessitate large samples where inhomogeneities and thermal gradients conspire to obscure the true nature of quantum fluctuations. Ideally, quantum critical fluctuations lack a characteristic energy scale, so measurements covering a wide dynamic range are required. To make progress, the ability to measure with small samples is critical to minimize the effects of disorder and thermal gradients. This scientific work also requires access to extremely low temperatures (20 mK), high magnetic fields (15 T), and pressure (0.5–10 GPa). It is also essential to cover several orders of magnitude of energy and wave vector transfer with high efficiency to explore the full extent of the quantum fluctuations and to document and find the limits of scaling relations. Both proposed time-of-flight spectrometers—CHES and the HERTZ instruments described in Section 2.2 and 2.3—are optimized for repetition rate multiplication, allowing such measurements to be performed efficiently.

Technical details common to both CHES and HERTZ

Relatively short overall length

It will be best to keep both instruments short (the overall length may not even exceed ~30 m); only at this shorter distance can one match the resolution contributions from the source pulse and the sample chopper pulse to give the best intensity for resolution performance because the incident source pulse width will not exceed ~200–400 μ s, depending on energy. The low frequency of the STS source (10 Hz) means that the bandwidth of the instrument will be very wide, and all incident energies down to below 1 meV will be accessed in the first frame.

Short wide-bandwidth instruments will benefit tremendously from recent innovations in chopper and guide technology.

Because neutron pulses at long wavelengths need much more time at the detector than short wavelength pulses—but will get to the detector in the same instrument setting—a pulse suppression device for the long wavelength pulses will be needed. Such a device has been invented and prototyped for the T-REX project at the European Spallation Source (ESS) [15]. It is commonly referred to as a “fan” chopper. Simply put, it is a combination of many frame overlap disks, rotating at base frequency (10 Hz)

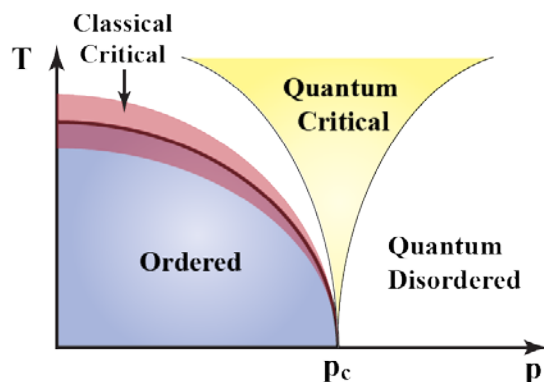


Fig. 2.5. Schematic phase diagram as a function of a tuning parameter, p . The quantum critical point is indicated as p_c , while the quantum critical region is shown in yellow (after [14]).

that are all shrunk to about 10° sectors. A large number (~ 5 – 10) of them are mounted in close vicinity to each other, rotating on different shafts. Such a device allows one to “fan out” the frame overlap chopper disk and to be flexible with suppressing individual pulses in one frame.

When putting ~ 10 – 20 pulses spanning a large wavelength range on the sample in one frame, a conventional instrument design will not work well because the sample chopper puts a constant pulse width (in time) Δt on the sample. Rather, for most applications it will be much better to aim for constant $\Delta E/E_i$ for all pulses, which implies $\Delta t \propto \lambda_i$. This can be done, as was shown for the VOR project at ESS [16], by allowing for a variable distance between the two disks of a double disk sample chopper. The required variation is on the order of only a few centimeters.

Fully integrated sample environment

It is essential to fully integrate dedicated sample environment equipment into the design of the secondary spectrometer. Both are required for scientific output, and enormous gains in quality and performance are possible by a holistic approach. Extreme conditions in temperature, magnetic field, pressure, strain, and any combination thereof drive the science and must be developed and accommodated within the initial project. Automated sample loading systems for low T measurements will also be required on this new generation of high count rate inelastic machines. Also, polarization analysis will be essential for many magnetic experiments because the general direction is toward systems with smaller moments (spin-1/2 half) with magneto-elastic effects or excitation continua, whereas traditional methods of isolating magnetic scattering (through temperature variation) are inadequate.

These requirements have the following implications:

- All ferromagnetic materials must be avoided within a radius of at least 2 m from the sample position.
- Strict limits must be imposed on the magnetic permeability of the steel of the tank and such components.
- Large coils for magnetic guide fields (several meters in diameter) must be incorporated in the design of the secondary spectrometer.
- There must be at least 50 cm of room between the guide exit and the sample position, and the beam must be shaped such that no diaphragm is needed between the guide exit and sample.
- An oscillating collimator between the sample and detector will be required.
- A maximum of flexibility must be kept around the sample such that unexpected environment or new conditions can be accommodated.

Technical details specific to CHES

The instrument will be optimized for a sample size between 1 mm and 1 cm. Therefore, the viewed moderator surface needs to be only a few centimeters horizontally and vertically with a guide-to-moderator distance chosen to illuminate the guide entrance with approximately ± 3 – 4 degrees of neutron beam angular divergence in both the horizontal and vertical directions.

The detector array will consist of ^3He tubes with a smaller diameter— ~ 1.5 cm—than at comparable FTS instruments. The solid angle covered by detectors will approach $\sim 2\pi$ ster. The neutron optics system will be designed to provide individual tuning of neutron beam size as well as vertical and horizontal beam divergences at the sample position. It will be essential to be able to increase beam divergence on sample to approximately ± 4 degrees (either horizontally or vertically), especially for small samples. The energy resolution will be tunable in the 2.5–4.5% range, which is typical for direct geometry inelastic instruments. Relaxing the resolution beyond $\sim 5\%$ rarely brings much useful information. The secondary spectrometer will be designed with polarization analysis in mind. This capability will be available from the first day of instrument operations.

The secondary flight path between sample and detector can be made rather short because high resolution will not be needed, and the small sample size minimizes its influence on the resolution. Thus the length of the secondary flight path will be driven by the need to maximize the solid angle covered by the detector array and the design requirements implied.

Table 2.1. Key instrument parameters for CHES

Source	STS
Wavelength/energy range	100 meV–0.5 meV
Resolution Q, E	2.5–4.5% variable $\Delta E/E$; $0.05 > \Delta Q$
Sample size range (beam size)	$1 \times 1 \text{ mm}^2$ to $1 \times 1 \text{ cm}^2$
Moderator—sample distance	25–30 m (TBD)
Sample—detector distance	2.5–3.5 m (TBD)
Detector type	^3He linear position sensitive
Moderator type	Cold, coupled H_2

References

- [1] N. Rogado, et al., *J. Phys: Condens. Matter* **15**, 907 (2003).
- [2] T. Ishiguro, K. Yamaji, and G. Saito, *Organic Superconductors*, 2nd ed. (Springer, Berlin, Heidelberg, New York, 1998).
- [3] J. Müller, et al., *PRB* **65**, 144521 (2002).
- [4] N. Toyota, et al., *Low-Dimensional Molecular Metals* (Springer, Berlin, Heidelberg, New York, 2007).
- [5] H. H. Wang, et al., *Chem. Mater.* **2**, 482 (1990).
- [6] N. D. Mathur, et al., *Nature* **394**, 39 (1998).
- [7] J. J. Wu, et al., *PNAS* **110**, 17263 (2013).
- [8] W. Witczak-Krempa, G. Chen, Y. B. Kim, and L. Balents, *Annual Review of Condensed Matter Physics* **5**, 57 (2014).
- [9] B. J. Kim, et al., *Science* **323**, 1329 (2009)

- [10]J. Chaloupka, G. Jackeli and G. Khaliullin, *Phys. Rev. Lett.* **105**, 027204 (2010).
- [11]S. K. Choi, et al., *Phys. Rev. Lett.* **108**, 127204 (2012).
- [12]S. Sachdev, “Quantum Phase Transitions,” Cambridge University Press, Cambridge, 2011.
- [13]H. V. Lohneysen, et al., *Rev. Mod. Phys.* **79**, 1015 (2007)
- [14]Matthias Vojta, Ying Zhang, and Subir Sachdev, *Phys. Rev. Lett.* **85**, 4940 (2000).
- [15]J. Voigt, et al., *Nuclear Instruments and Methods in Physics Research A* **741**, 26 (2014).
- [16]P. P. Deen, et al., arXiv:1407.0473 [physics.ins-det] (2014).

2.3 HERTZ—HIGH ENERGY RESOLUTION TERAHERTZ SPECTROMETER

G. Ehlers and M. D. Lumsden (QCMD)

Abstract

There are programmatic and capacity needs for two direct geometry inelastic spectrometers with different optimizations. Described in the previous section, CHES (chopper spectrometer for small samples) is optimized for small samples. However, there is a significant need for a second instrument, called HERTZ (high energy resolution terahertz spectrometer), that is optimized for larger samples and higher resolution. This instrument will enable measurements on samples as large as $5 \times 5 \text{ cm}^2$, a standard size on many thermal chopper and reactor based instruments, with a homogeneous and tunable intensity and divergence profile. The high brightness of the STS coupled moderators combined with advancements in instrument design will enable at least an order of magnitude gain in performance when compared with current, state-of-the-art instruments internationally.

Science case

Although CHES is optimized to enable inelastic neutron scattering on small samples, there are a large number of problems where one would like to study larger samples with finer energy and wave vector resolution. Such measurements can yield high statistics data providing critical tests for theory and can allow experimental separation of collective modes in complex materials. Ideally, one would like to cover the full range of sample sizes and resolution conditions in a single instrument, but it is difficult (if not impossible) to design a chopper spectrometer where the beam size at sample can be varied between 1 mm and 5 cm. Consequently, HERTZ is designed to enable the following:

1. A cold neutron direct geometry time-of-flight spectrometer optimized to provide a homogeneous beam as large as $5 \times 5 \text{ cm}^2$, a size that has become a standard for thermal chopper spectrometers and triple-axis instruments. Crystals grown with techniques such as floating zone often reach this size along the growth direction. This instrument will also allow for higher energy ($\sim 1\%$ of E_i or better) and wave vector resolution than the CHES spectrometer.
2. The instrument will be designed to allow full three-dimensional polarization analysis to enable measurements of multiple components of the $S_{\alpha\beta}(\mathbf{Q},\omega)$ tensor.

3. The low repetition rate of STS will enable simultaneous measurements with multiple incident energies, greatly increasing measurement efficiency particularly in materials with excitations covering a broad range of energies.

The last two points are important instrument design concepts for future direct geometry spectrometers at STS and are common to both HERTZ and CHES; the differentiation between the two instruments is primarily point 1 above.

One of the strengths of inelastic neutron scattering is that the measured cross-section is simply related to the quantity $S(Q, \omega)$, which is amenable to multiple theory or modeling approaches. As such, inelastic neutron scattering allows for close connections with theory and computation, and neutron data can often provide definitive tests of theoretical models. However, many problems at the forefront of condensed matter research involve competing interactions and ground states, and true comprehension requires high precision measurements that can be carefully compared to theory. To obtain inelastic neutron scattering data of sufficient statistical quality, an instrument with a large, homogeneous beam profile is required to facilitate measurements on large volume samples. HERTZ is optimized to provide such a large uniform beam with a high flux of cold neutrons. The cold neutron energy scale is well suited to many of the critical problems of both experimental and theoretical interest such as quantum magnets, frustrated magnets, and heavy fermion superconductors, and exploration of excitation spectra in such materials in the presence of extreme conditions of temperature, magnetic field, or pressure can provide additional, critical information. Furthermore, HERTZ will be designed to allow full polarization analysis providing measurements of multiple components of the $S_{\alpha\beta}(Q, \omega)$ tensor that can be further compared to theory and simulation. Consequently, HERTZ will provide a critical link between experiment and theory that is critical to enable progress in a number of forefront problems in quantum materials.

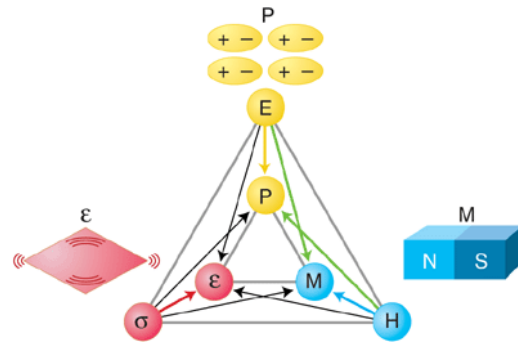


Fig. 2.6. Multiferroic materials exhibit at least two coexisting orders.

The figure represents ferromagnetic, ferroelectric, and ferroelastic order. The arrows indicate that different applied fields can control various states. For example, a magnetic field may control the electric or elastic properties of the material. [5]

One of the core capabilities provided by the proposed chopper spectrometers is a significant expansion of inelastic 3D polarization analysis and enabling such measurements over the full, broad Q, ω coverage of these instruments. By far the greatest need for polarized neutrons is in magnetism, which will be relevant for a significant part of the research at these instruments. The direction in which research is currently developing emphasizes increasingly complex materials in which magnetic scattering features are often weak (due to $S = 1/2$ entities) or diffuse (because magnetic correlations are short-ranged) [1–4]. The widely adopted strategy to separate magnetic scattering (using unpolarized neutrons) with temperature variation (to measure above and below a phase transition) cannot be applied with success if the magnitude of the magnetic scattering intensity is comparable—or weaker—than the variation with temperature of the nuclear scattering. Thus, in the future, polarized neutrons will be increasingly indispensable for the separation of lattice and spin dynamics in magnetic systems and also for independent measurements of transverse and longitudinal spin fluctuations.

When compared with CHES, which is optimized for small samples, HERTZ allows for higher resolution measurements in both energy and wave vector. Problems involving energy related materials such as thermoelectrics benefit from detailed microscopic understanding of heat transport, which is possible with measurements of phonon or magnon dispersions and line widths. As broadening of these excitations is often small, excellent resolution in both wave vector and energy transfer are required for such measurements. Furthermore, forefront problems in quantum materials are increasingly complex, often involving large molecular components resulting in crystalline materials with large unit cell parameters and small energy scales. The high flux of cold neutrons available on HERTZ is well suited to such materials, and good wave vector resolution is critical to measure coherent excitations from such large unit cell materials. The tunable resolution of HERTZ will enable the measurement of dispersive excitations in complex materials such as organic magnets.

One example well suited to HERTZ—which requires the use of polarized neutrons, good wave vector and energy resolution, and significant coupling between experiment and theory—is exploration of competing and coupled orders in multiferroic materials. Multiferroics are materials that exhibit multiple ferroic orders simultaneously, often ferromagnetic and ferroelectric order, and yield the potential for next generation device applications [5,6]. Note that coexistence of antiferromagnetism and ferroelectricity is typically also classified as multiferroicity. The coupled nature of the magnetic and electric properties of these materials naturally leads to strong interplay between various degrees of freedom, most notably magnetic and lattice. One manifestation of this is the observation of an “electromagnon,” a hybridized magnon–phonon excitation [7–9]. Full understanding of the interplay between magnons and phonons requires detailed measurements of both excitation spectra across the full Brillouin zone with good energy resolution. Furthermore, separation of the spin and lattice contributions and a wave vector dependent study of the extent of interaction between these modes require the use of polarized neutrons. Advancements in theory are also required to fully understand the coupled magnetic-lattice system. The broad Q, ω coverage and good wave vector and energy resolution of HERTZ and the ability to extend such measurements to enable a fully polarized determination of the relevant components of $S_{\alpha\beta}(Q, \omega)$ will allow for a much more comprehensive understanding of the coupling between spin and lattice degrees of freedom and can provide comprehensive “reference” data sets used to guide theoretical efforts.

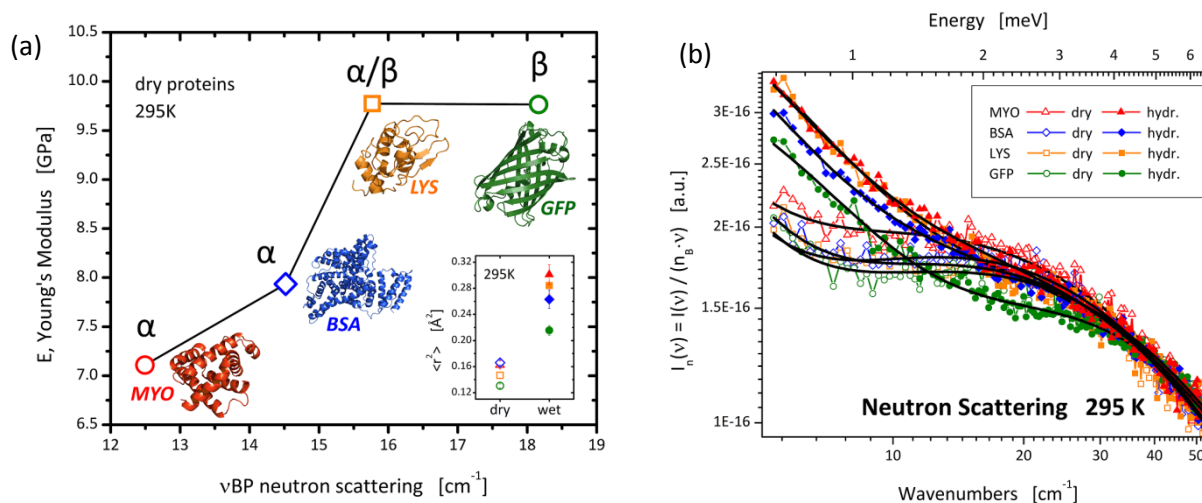


Fig. 2.7. (a) Elastic modulus for four dry proteins, myoglobin (MYO), bovine serum albumin (BSA), lysozyme (LYS), and green fluorescent protein (GFP), as a function of the boson peak frequency ν_{BP} . (b) CNCS measurements of the boson peak region for the four proteins at $T = 295$ K. [14]

It is important to note that cold neutron chopper spectrometers, such as CNCS, have significant interest from the soft matter and biophysics community, and currently, such studies make up about 15% of the experiments performed on CNCS. The instrument features common to both CHES and HERTZ of polarization analysis and repetition rate multiplication will allow for significant gains for such experiments. For soft materials (such as liquids, polymers, colloids, gels, or biological materials), static and dynamic correlations exist over large ranges (many orders of magnitude) of space and time, much of which is accessible by neutron scattering techniques (see, for example [15–19]). For a complete understanding of such materials, one needs to disentangle the contributions of self- and pair-correlations to the scattering. Self-correlations manifest themselves in incoherent scattering (which originates from the disorder of the individual scattering lengths of the atoms in a material), whereas pair-correlations are associated with coherent scattering (which is due to the average scattering lengths of the atoms). Polarized neutron techniques provide a model independent method of separating coherent and incoherent scattering experimentally [20]. The proposed HERTZ and CHES instruments will expand polarized neutron capabilities to time-of-flight instrumentation. These capabilities combined with repetition rate multiplication, enabling efficient measurements over a broad dynamic range, will enable routine separation of coherent and incoherent scattering across the relevant time and space parameters. Routine use of such capabilities can vastly increase the scientific content, which can be extracted from quasielastic neutron scattering measurements on such soft materials.

One final example that could be relevant to either CHES or HERTZ is the possibility of studying pump-probe, non-equilibrium phenomena. Elegant experimental and theoretical work on ultra cold atomic gasses shows the time evolution of an interacting quantum system beyond thermal equilibrium is unique, interesting, and important. While experiments and theory focus on thermal equilibrium, most of nature and many interesting phenomena in nature are associated with being out of equilibrium. One of the BESAC 10 Grand Challenges [10] reads, “How do we characterize and control matter away—especially very far away—from equilibrium?”

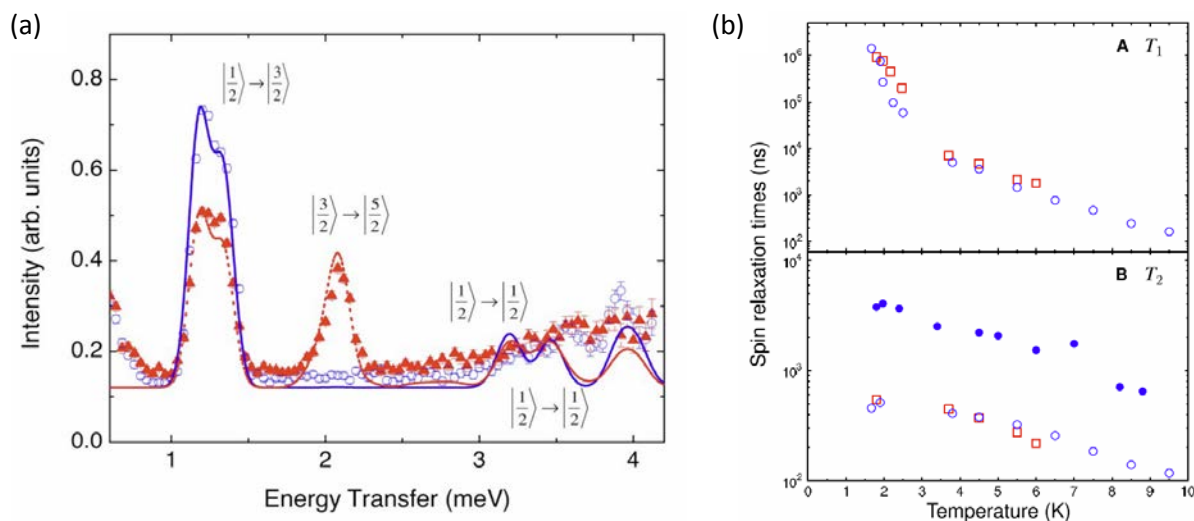


Fig. 2.8. (a) Inelastic neutron scattering spectra of Cr_7Ni molecular magnet at $T = 2\text{ K}$ (circles) and $T = 12\text{ K}$ (triangles) [11]. (b) T_1 (spin lattice relaxation times) and T_2 (phase-coherence relaxation times) as a function of temperature for Cr_7Ni (blue open circles), Cr_7Mn (red open squares), and perdeuterated Cr_7Ni (blue filled squares). At low temperatures, T_2 for perdeuterated Cr_7Ni approaches $4\ \mu\text{s}$ [12].

Apart from the obvious practical relevance of probing and understanding systems beyond thermodynamic equilibrium, the thermalization process can help to characterize the many body system. Workshops, conferences, and top theorists are focusing on this area. The intense pulsed neutron beams at SNS, particularly at STS, coupled with event mode data acquisition now offer the possibility of probing correlations in materials beyond thermal equilibrium. Because of the pulse width, the realistic time scale that can be addressed is microseconds. This implies we must focus on materials with relatively long relaxation times and, thus, slow dynamics. HERTZ will be ideal to probe the dynamic properties of systems out of equilibrium through pump-probe experiments. Examples include molecular magnets under pulsed microwave radiation or pulsed magnetic fields. These molecular magnet systems have received attention because of their potential in quantum computing applications [13]. Such applications require long relaxation times (for the Cr₇Ni system shown in Fig. 2.8, the relaxation time is on the order of microseconds) to enable fast coherent spin manipulation [12]. More interesting and challenging to researchers are experiments that probe time dependence in extended interacting systems. Spin singlet magnets under pulsed microwaves would be relevant for such experiments on HERTZ.

Technical details common to both CHES and HERTZ

This information is presented in the section “Technical details common to both CHES and HERTZ” in the CHES instrument description, Section 2.2.

Technical details specific to HERTZ

To achieve good energy resolution, the secondary flight path needs to be long, likely ~5 m. The solid angle covered by the detector array will thus be smaller than at CHES, perhaps ~ π ster. The sample chopper pulse will have to be short, ~10 μ s or less, and therefore a beam splitter design in the final part of the guide will be considered as prototyped at the Let instrument at ISIS [21]. The neutron optics system will be designed to provide individual tuning of neutron beam size and vertical beam divergence at the sample position.

Table 2.2. Key instrument parameters for HERTZ

Source	STS
Wavelength/energy range	100 meV–0.5 meV
Resolution Q, E	0.5–3.0% variable $\Delta E/E$; $0.02 > \Delta Q$
Sample size range (beam size)	$1 \times 1 \text{ cm}^2$ to $5 \times 5 \text{ cm}^2$
Moderator—sample distance	25–30 m (TBD)
Sample—detector distance	4–6 m (TBD)
Detector type	³ He linear position sensitive
Moderator type	Cold, coupled H ₂

References

- [1] M. A. de Vries, et al., *PRL* **103**, 237201 (2009).
- [2] G. J. Nilsen, et al., *PRB* **84**, 172401 (2011).
- [3] H. J. Silverstein, et al., *PRB* **89**, 054433 (2014).

- [4] K. Matan, et al., *PRB* **89**, 024414 (2014).
- [5] Nicola A. Spaldin and Manfred Fiebig, *Science* **309**, 391 (2005)
- [6] Sang-Wook Cheong and Maxim Mostovoy, *Nature Materials* **6**, 13 (2007).
- [7] A. Pimenov, et al., *Nat. Phys.* **2**, 97–100 (2006).
- [8] A. Pimenov, et al., *Phys. Rev. B* **74**, 100403 (2006).
- [9] A. B. Sushkov, R. Valdés Aguilar, S. W. Cheong, and H. D. Drew, *Phys. Rev. Lett.* **98**, 027202 (2007).
- [10] “Directing Matter and Energy: Five Challenges for Science and the Imagination.” A Report from the Basic Energy Sciences Advisory Committee, Chair: John Hemminger (2007).
- [11] R. Caciuffo, et al., *Phys. Rev. B* **71**, 174407 (2005).
- [12] Arzhang Ardavan, et al., *Phys. Rev. Lett.* **98**, 057201 (2007).
- [13] Michael N. Leuenberger and Daniel Loss, *Nature* **410**, 789 (2001).
- [14] Stefania Perticaroli, et al., *Soft Matter* **9**, 9548 (2013).
- [15] B. Farago, et al., *PRE* **65**, 051803 (2002).
- [16] A.-C. Genix, et al., *J. Chem. Phys.* **128**, 184901 (2008)
- [17] *J. Vac. Sci. Technol. A* **24**, 1191 (2006) and references therein, and *PRL* **103** 128104 (2009).
- [18] H. Morhenn, et al., *PRL* **111**, 173003 (2013).
- [19] Jonathan D. Nickels, et al., *Biophysical Journal* **105**, 2182 (2013).
- [20] B. J. Gabrys, *Physica B* **267-268** 122 (1999).
- [21] R. I. Bewley et al., *Nuclear Instruments and Methods in Physics Research A*, **637** 128 (2011).

2.4 MANTA (MULTIPLE ANALYZER TRIPLE-AXIS) FOR HFIR

Mark Lumsden, J. Fernandez-Baca, and Collin Broholm (QCMD)

Abstract

Recent experience has shown the combined strengths of time-of-flight and triple-axis spectroscopy can yield tremendous insight into a diverse set of problems in materials research associated with magnetism, superconductivity, and ferroelectricity. The MANTA instrument will expand this powerful

combination into the essential sub-thermal energy regime while increasing overall counting efficiency by three orders of magnitude relative to traditional cold TAS instrumentation.

Combined with the high incident neutron flux, an innovative wide-angle energy-dispersing detection system on MANTA will allow high efficiency measurements with a “foot print” in Q - ω space that is complementary to SNS-based time-of-flight spectrometers. MANTA will exploit and extend the most recent advances in focusing optics, multiplexing crystal spectrometers, and neutron polarization methods for a unique new capability to map excitations within a scattering plane over a selectable range of energy transfers.

Because of the planar nature of its detector systems, MANTA will be an ideal instrument for parametric studies with a range of complex sample environments. Development of the proposed detection system may also impact instrumentation for SNS where similar methods could be employed for a high efficiency spectrometer with a polychromatic beam before *and* after the sample.

Science Case

The MANTA cold neutron spectrometer at HFIR will use the latest advances in neutron optics and multi-analyzer configurations for high efficiency measurements over a distinct volume of Q - ω space that provides an important complement to SNS instrumentation. Specifically, MANTA will enable:

1. Very high efficiency mapping of Q -dependent scattering within a plane for a select range of energy transfer from 0.2 meV to 15 meV. When the energy range of interest matches the spectral range of the energy dispersive detector, MANTA may provide the highest efficiency of any ORNL instrument.
2. Fully polarized capability to separate magnetic and nuclear scattering and detect specific spin components of the magnetic scattering.
3. Through variable Bragg- and guide-based focusing, the instrument can accommodate a range of sample sizes and complement both the HERTZ and CHESS instruments proposed for STS.
4. The planar geometry makes MANTA an ideal instrument for high intensity parametric studies as a function of pressure, magnetic field, and ultra-low temperature.
5. A reconfigurable spectrometer allows for an ultra-high resolution option optimized for measuring lifetimes of magnetic and lattice excitations with μeV resolution. The scientific motivation for this will be described in the next instrument section on ultra-high resolution spectroscopy.

The colocation of SNS and HFIR at ORNL has proven to be powerful scientifically and, for the case of thermal neutrons, there are multiple examples where research groups have combined data from the two sources to enable high profile science. In general, the broad mapping capabilities of SNS instruments, such as ARCS and SEQUOIA, provide an overview of the scattering from a specific material that identifies features of interest, while the high monochromatic flux of thermal triple-axis instruments allows for parametric studies of these features. The combination of the proposed new STS direct geometry instruments and MANTA will expand such complementarity to the cold neutron regime.

Just as new instrumentation concepts are allowing orders of magnitude gains for pulsed source instrumentation, this is also the case for reactor-based instrumentation. The combination of Bragg- and guide-based focusing methods and the multi-analyzer configuration described below allows ultra-high efficiency mapping of inelastic scattering over a range of scattering angles and energy transfers based on the high time average cold neutron flux at HFIR. Because of its distinct native coverage of momentum-energy space, MANTA provides an important complement to the CHSS and HERTZ instruments described above.

One area where MANTA would have transformative impact is in the study of quantum spin liquids. Spawned in the quest to understand superconductivity in transition metal oxides, this area has turned out to be extraordinarily rich and holds promise for applications in quantum computing. Theoretical progress and progress in new materials synthesis indicate the time is ripe for a breakthrough in this area and inelastic neutron scattering will surely play a critical role. However, the bulk scattering cross section can be difficult to interpret because neutrons typically cannot create or annihilate the underlying quasi-particles individually. Theoretical work shows that studying the configuration of spin singlets that form in the vicinity of defects or at the edges of quantum spin liquids can help to determine the nature of the bulk spin liquid state [1]. Neutron scattering can access this pattern by mapping the Q dependence of the inelastic scattering associated with defects in the spin liquid. For localized excitations associated with defects, the influence on scattering exists over a restricted range of energy transfers (Fig. 2.9). The angular coverage of MANTA combined with simultaneous mapping of a range of final energies makes this an ideal instrument to probe the momentum space wave function of bound states in quantum spin liquids.

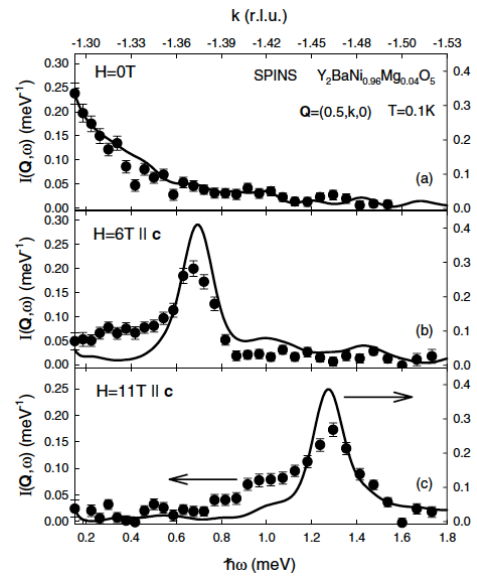


Fig. 2.9. Inelastic scattering from finite length spin-1 chains within $Y_2Ba(Ni_{0.96}Mg_{0.04})O_5$ in zero and applied field reveals the presence of topologically protected edge states [2]. MANTA would enable such work at lower defect density in 2D and 3D spin systems.

Many scientific problems can benefit from high efficiency measurements over a restricted range of Q, ω space. One problem of current scientific interest is the study of topological states in quantum spin ice. This type of materials is predicted to exhibit power-law “dipolar” correlations that are anisotropic in spin space and decay as r^{-3} in real space [3]. Power-law correlations without a broken symmetry and away from a critical point are remarkable signals of underlying gauge symmetry. After Fourier transformation of these correlations on the lattice, a static spin structure factor with “pinch points” at reciprocal lattice vectors in momentum space is obtained. These “pinch points” in spin ice materials are localized at specific regions of Q space where their signature in neutron scattering is that $S(Q)$ is singular in one direction and diffuse in all others. Extended in momentum space, yet with important sharp features, the elucidation of such scattering requires broad high-resolution coverage of momentum space. Figure 2.10 shows an example of elastic scattering from a classical spin ice material. The focus is now shifting towards quantum spin ice materials where energy resolution is also required [4]. MANTA could lead the way in this active field of research to probe quantum spin ice and other quantum spin liquids with emergent fractionalized quasi-particles versus field and ultra low temperatures (Fig. 2.10).

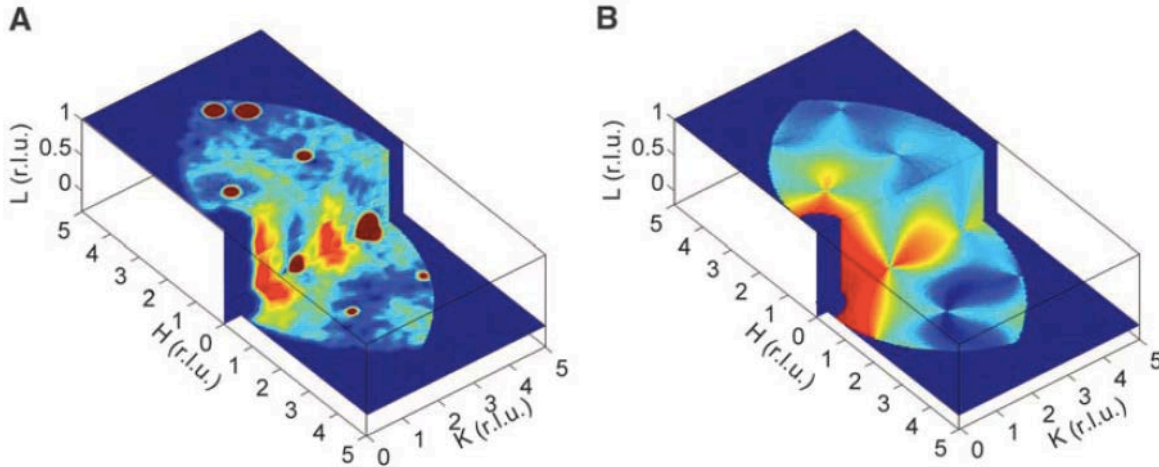


Fig. 2.10. (A) Measured and (B) calculated elastic neutron diffraction from classical spin ice in $\text{Dy}_2\text{Ti}_2\text{O}_7$. Measurements were carried out with a wide-angle thermal spectrometer at Helmholtz-Zentrum Berlin [5]. MANTA would extend such capabilities with the energy dimension as essential to understanding quantum spin ice and other quantum spin liquids.

Understanding the role of itineracy in heavy fermion materials is another area where the MANTA spectrometer would have strong impact. Heavy fermion compounds are strongly-correlated materials where interactions between f-electrons and itinerant electrons lead to a Fermi liquid-like state with effective electron masses that are two to three orders of magnitude larger than the bare electron mass [6]. Heavy fermion systems are naturally described in terms of a renormalized band structure with intricate features within meV of the Fermi level [7,8]. Cold neutron inelastic scattering is a critical tool to elucidate such band structure and the associated spin correlations. The relevant energy range is <10 meV, and wide angle coverage is essential to be able to reconstruct the underlying band structure (Fig. 2.11). Particularly in the fully polarized mode where broad magnetic scattering can be unambiguously separated from nuclear backgrounds, MANTA will open a new window on this fundamentally important class of materials that represent the vanguard in our understanding of strongly correlated electrons.

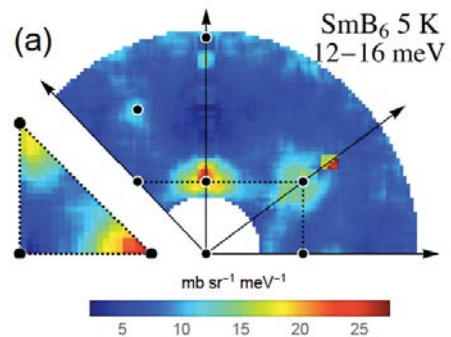


Fig. 2.11. Inelastic neutron scattering from the topological Kondo insulator SmB_6 measured on SEQUOIA.

The data illustrate the power of neutron scattering to probe correlated electron systems [9]. MANTA would extend such capabilities to low energies temperatures and high fields as particularly relevant to heavy fermion systems.

Another area where wide angle fully polarized capabilities will be essential is in the study of multiferroics, also discussed in the HERTZ section. While HERTZ will be ideal for a full mapping of interactions between magnons and phonons, MANTA will be the optimal instrument when there is a need to explore specific modes or branches that occupy a limited range of energy transfer as a function of external parameters such as electric or magnetic fields. As competition and interactions between multiple degrees of freedom are of growing importance at the forefront of quantum materials research, expansion of polarization analysis will be essential to separate the distinct components of composite

quasi-particles and provides a stronger link to theory. The combination of polarization analysis on MANTA and the proposed time-of-flight spectrometers would transform polarized neutron scattering from a highly specialized technique to a powerful tool in quantum condensed matter physics.

Finally, this instrument preserves the flexibility of triple-axis instruments and will include a specialized spectrometer option for ultra-high resolution measurements. The instrument will be reconfigured to perform such measurements as required. The scientific impact of these techniques will be described in Section 2.5, but enabling these ultra-high resolution measurements with both thermal and cold neutrons will broaden the scientific impact of this technique and allow for studies on a broader range of materials.

Technical Description

The incident beam optics of CG-1 were designed a number of years ago to allow for a vertically focused beam on a triple-axis instrument with minimal horizontal beam divergence, enabling measurements with high Q resolution. The calculated peak flux on sample for the existing optics configuration was 1.9×10^8 n/cm²/s (for $E_i = 9$ meV) [10]. The community's need to enable inelastic neutron scattering on smaller samples necessitates a redesign of these optics to provide the highest possible flux on the sample. Fortunately, developments in neutron guides now allow for higher m coatings and elliptically focused optics, which can greatly increase flux on the sample. This requires modification of the near source beam extraction to provide higher beam divergence to the downstream optics, together with an optimized guide design to properly transmit this divergence to the monochromator. As with many modern cold triple-axis instruments, the optics design will include a virtual source upstream of the monochromator and a double focusing PG 002 monochromator. In addition, a velocity selector will be included in the incident beam to eliminate higher order contamination and, thus, reduce background. Comparisons to other instrument upgrade projects internationally [11] indicate that gain factors of five to 10 are possible with such an upgrade and should result in a peak flux in excess of 1×10^9 n/cm²/s, making the CG-1 inelastic instrument the most intense monochromatic beam of cold neutrons in the world. This should allow for inelastic measurements on milligram samples, making it the ideal complement to the CHSS instrument proposed for STS with the flexibility to also use larger samples when available.

In recent years, significant progress has been made in multiplexing continuous source spectrometers to allow more efficient mapping of Q, ω space. At ORNL, it is important to take into consideration complementarity of such an instrument with SNS instruments now and in the future. As such, parametric measurement over a restricted range of Q, E space is a critical strength of inelastic instruments at HFIR that must be preserved. Fortunately, a recent multiplexed design allows for high efficiency mapping while maintaining the ability to measure with high time-integrated flux over a selectable range of Q, E space. This involves using analyzer crystals that scatter vertically, allowing for a nearly continuous coverage of scattering angles (the anticipated range of 2θ coverage would be greater than 160 degrees). The vertical scattering geometry allows multiple final energies to be measured simultaneously by stacking subsequent analyzers behind one another. It is anticipated that at least 10 final energies could be measured simultaneously over this full 2θ range for quasi-continuous angular and energy coverage. The fixed analyzer positions of such a spectrometer simplify motion control so that only the sample and the post sample spectrometer move during measurements. The broad, nearly continuous angular and final energy coverage vastly expands the number of simultaneous Q, E points that can contribute to a parametric study, is perfectly matched with the planar access of extreme

sample environments, and makes this instrument extremely efficient for mapping planes of inelastic scattering.

The above configuration also will allow for polarized neutron inelastic measurements with sample guide fields along any chosen direction. The incident beam polarization would be accomplished with either a supermirror polarizer or a ^3He cell. Post sample polarization analysis could be accomplished with a ^3He cell in a PASTIS-type configuration or possibly with a broad supermirror analyzer like the one fabricated for use on HYSPEC. With three orders of magnitude gain in overall counting efficiency, the polarized neutron scattering technique introduced by Moon et al. almost half a century ago [12] would come to full fruition and eliminate the need for the ambiguous methods now used to separate nuclear and magnetic scattering.

Finally, MANTA will preserve the strength of versatility of the triple-axis spectrometer and will allow for the possibility of ultra-high resolution measurements using Larmor techniques. Such an option could be combined with the current CTAX post sample analyzer, allowing such capability with a modest additional investment. The specific details of such a configuration together with the science case are described in Section 2.5.

Table 2.3. Key instrument parameters for MANTA

Source	HFIR CG-1
Moderator type	HFIR Cold Source
Energy range	E_i from 2.5 to 25 meV
Energy transfer resolution	0.07–1 meV at $\Delta E = 0$
Sample size range (beam size)	Variable. Samples as small as 10 mg possible
2 \square range	>160 degrees
Number of final energies	>10
Detector type (number)	^3He single tube (~1,000)—option of PSDs will be considered in instrument optimization

References

- [1] Y. Wan and O. Tchernyshyov, arXiv:1301.5008, *Phys. Rev. B* 87, 104408 (2013).
- [2] M. Kenzelmann, et al., *Phys. Rev. Lett.* 90, 087202 (2003).
- [3] Leon Balents, *Nature* 464, 199 (2010).
- [4] K. Kimura, et al., *Nature Communications* 4, 1934 (2013).
- [5] D. J. P. Morris, et al., *Science* 326 (5951), 411-414 (2009).
- [6] Z. Fisk, et al., *Science* 239, 33 (1988).
- [7] C. Pfleiderer. *Rev. Mod. Phys.* 81, 1551 (2009).
- [8] P. Schlottmann. *Phys. Rev. B* 36, 5117 (1987).

[9] W. T. Fuhrman, et al., arXiv:1407.2647 (2014).

[10] R. M. Moon, private communication.

[11] M. D. Le, et al., *Nuclear Instruments and Methods in Physics Research A* 729, 220 (2013).

[12] R. M. Moon, T. Riste, and W. C. Koehler, *Phys. Rev.* 181, 920 (1969).

2.5 ULTRA-HIGH RESOLUTION SPECTROSCOPY WITH NEUTRON SPIN ECHO OPTION FOR TAS AT HFIR

Jaime Fernandez-Baca (QCMD)

Abstract

Neutron spin echo techniques, in combination with triple axis spectroscopy at a high-flux reactor, can be used to determine lifetimes of dispersive excitations over the entire Brillouin zone with μeV resolution. Such measurements are the most direct way to unlock the relationship between the fundamental interactions and couplings in complex materials. Currently this ultra-high resolution spectroscopy can be achieved only by a technique called neutron resonance spin echo (NRSE). The recent development of superconducting magnetic Wollaston prisms provides the opportunity to implement an ultra-high resolution spectroscopic capabilities similar to the NRSE technique with some practical advantages. In this concept, the magnetic Wollaston prisms are used to encode the neutron spins instead of the radio frequency (RF) coils used in the NRSE technique. The implementation of this neutron-spin echo device on a polarized triple axis spectrometer (TAS) at HFIR will enable the measurement of lifetimes of lattice and magnetic excitations with μeV resolution. This is a capability that currently does not exist in North America.

Science Case

The combination of neutron spin echo and triple axis spectroscopy provides unique μeV resolution at a wide range of energy transfers, which are otherwise inaccessible to neutron or x-ray spectroscopies or any other method. The implementation of this technique will enable ultra-high resolution neutron spectroscopy to determine lifetimes of dispersive excitations over the entire Brillouin zone with μeV resolution [1–3]; this is the most direct way to unlock the relationship between the fundamental interactions and couplings in complex materials. This type of measurement will enable the understanding of the interplay of various subsystems in strongly correlated systems in the years to come. Three examples of high-impact science that will be enabled by the implementation of ultra-high resolution spectroscopy are listed below. These examples are consistent with the BESAC grand challenges report [6] and with the recommendations of the recent Berkeley workshop report.

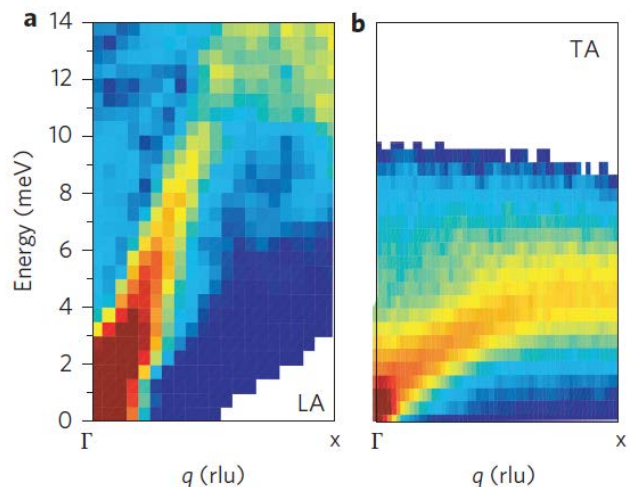


Fig. 2.12. Precise measurements of phonon dispersions and lifetimes will provide new insights on the thermal conductivity in thermoelectric materials (After [7]).

1. Phonon lifetimes in thermoelectric materials

Improving our current microscopic understanding of thermal conductivity is needed to design more efficient thermoelectric materials. Establishing a complete picture of phonon dispersions and mean-free-paths is crucial to providing a realistic microscopic characterization of phonon transport, against which atomistic models of thermal conductivity can be tested. Ultra-high-resolution inelastic scattering measurements on single crystals will provide quantitative information of phonon lifetimes resulting from scattering from nano- and mesoscale defects and will open the way to new processing routes that could improve key figures of merit for thermoelectrics.

2. Quantum effects in the spin dynamics of magnets

Ultra-high-resolution measurements in prototypical magnets will allow the determination of the various contributions of the different mechanisms of magnon broadening and their impact in the decay of thermal transport currents in these materials. The magnon broadening is indicative of the finite phonon lifetimes due to collisions with other magnons and domain boundaries, as well as different sources of disorder. The determination of these broadening mechanisms in complex magnets will contribute to the design of magnets with improved thermal properties

3. Electron–phonon interactions in strongly correlated electron systems

Early work on the possibility of electron–phonon coupling in Fe-based superconductors appears to rule out a conventional electron–phonon pairing mechanism but does not rule out an unconventional electron–phonon pairing mechanism that could primarily occur through a single or very few phonon modes, with the potential involvement of orbital order or fluctuations. Ultra-high-resolution inelastic neutron scattering will allow a close examination of the phonon widths in Fe-based superconductors and the extraction of precise electron–phonon coupling constants that will lead us to a better understanding of the potential role of this type of mechanism in Fe-based superconductors.

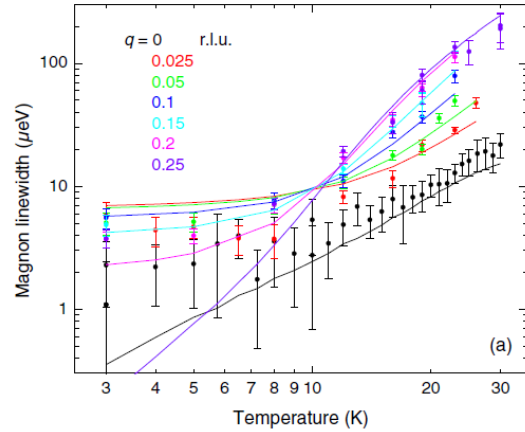


Fig. 2.13. Ultra-high-resolution spectroscopy enables the measurements of the phonon line widths with micro electron volt resolution (After [8]).

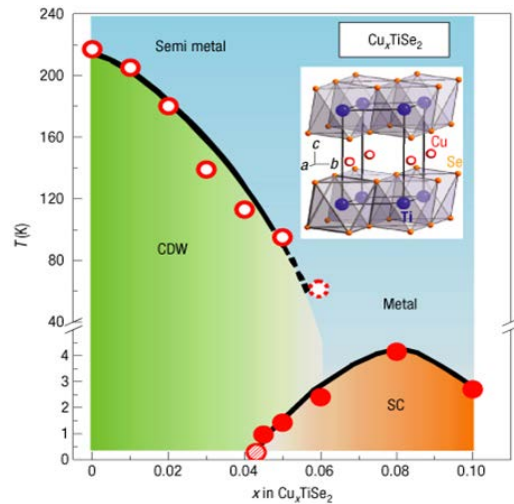


Fig. 2.14. The intercalation of Cu in TiSe₂ leads to the suppression of the CDW state and the appearance of superconductivity Cu_xTiSe₂ (After [10]).

The interplay of charge density wave physics and superconductivity is another important issue where the magnetic Wollaston prisms-based neutron spin echo technique can make an important contribution. For example, consider Cu_xTiSe_2 . TiSe_2 is a prototype charge density wave (CDW) system with a transition around 200 K. When Cu is intercalated between the TiSe_2 layers, the charge density wave is suppressed, and superconductivity appears. It has been suggested that electron–phonon coupling is responsible for the charge density wave order. This naturally leads to questions concerning the origin of superconductivity and a more complete understanding of the electron–phonon coupling via ultra-high-resolution measurements.

Technical Description

While conventional neutron spin echo techniques are known to provide ultra-high resolution at $E = 0$ meV [9], μeV resolution in measurement of dispersive excitations is possible because of a special technique developed by Gahler [1]. In this technique, the spin echo resolution is tuned to the slope of the energy-dispersion curve by tilting the boundaries of the precession fields relative to the neutron beam. The NRSE technique utilizes small RF spin flippers with precise flat surfaces to define the effective precession regions. Tilting of the field boundaries is achieved by rotating the RF coils to an alignment dependent upon the gradient of the phonon dispersion surface at the scattering vector Q ($Q = k_1 - k_2$, where k_1 and k_2 are the neutron wave vectors of the incident and scattered beams) (see Fig. 2.15).

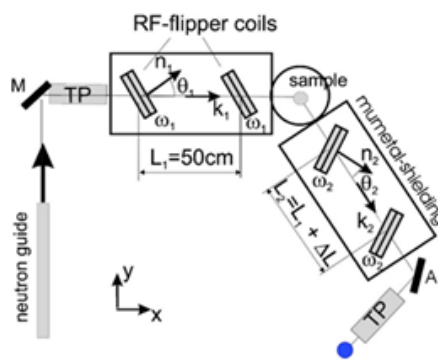


Fig. 2.15. Schematics of the Neutron Resonance Spin Echo instrument.

In this technique, the spin echo resolution is tuned to the slope of the energy-dispersion curve by rotating the RF coils (After [2]).

The instrument that we propose utilizes the recently developed superconducting magnetic Wollaston prism coils [4–5], which allow the tuning to the dispersion surface by changing of direct currents rather than by physical movement of coils. A magnetic Wollaston prism can spatially split a polarized neutron beam into two beams with different neutron spin states, in a manner analogous to an optical Wollaston prism [5]. Such a device can be used to encode the trajectory of neutrons into the Larmor phase associated with their spin degree of freedom. Magnetic Wollaston prisms with highly uniform magnetic fields and low Larmor phase aberration recently have been demonstrated and constructed using high temperature superconducting (HTS) materials [4–5]. The Meissner effect of HTS films is used to confine magnetic fields produced electromagnetically by current-carrying HTS tape wound on suitably shaped soft iron pole pieces. The device is cooled to ~ 30 K by a closed cycle refrigerator (CCR), eliminating the need to replenish liquid cryogenics and greatly simplifying operation and maintenance. An HTS film ensures that the magnetic field transition within the prism is sharp, well-defined, and planar because of the Meissner effect. The spin transport efficiency across the device was reported to be $\sim 98.5\%$ independent of neutron wavelength and energizing current. The reason for choosing this technology is that it has already been shown to have high neutron transmission and low parasitic scattering; it also can accept larger beams, unlike the RF coils, where the maximum beam size depends upon the tilt angle.

The basic unit for the ultra-high resolution option for a TAS that we propose consists of two Wollaston prisms in a single vacuum vessel (cooled by a CCR), with a rectangular magnetic field region between them. This would replace the two tilted RF coils in the NRSE method. This unit will be placed in a polarized neutron beam before the sample to be studied. A second, similar unit will be placed after the sample and before a polarizing analyzer. A schematic view of this system is shown in Fig. 2.16, where the neutrons come from the left, and the magnetic fields are perpendicular to the paper. By changing the fields in each of the regions in a way that is easy to calculate, the surfaces of constant spin echo phase can be aligned with the dispersion surface of the excitation to be studied. The observed depolarization of the spin echo is related directly to the spectral form of the scattering via a Fourier transform, just as it is for traditional NSE close the zero energy transfer. Generally, because no standard scatterer is available to calibrate the instrument, one measures variations of the spectral shape as a function of an external parameter, such as temperature.

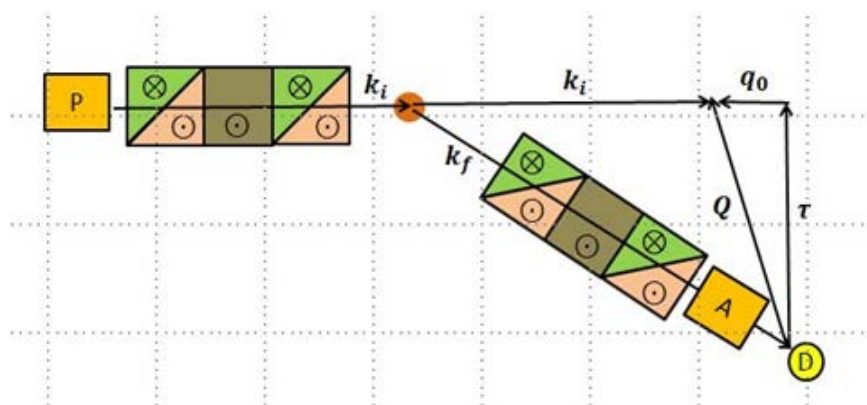


Fig. 2.16. Schematics of a neutron spin echo instrument based on the newly developed superconducting magnetic Wollaston prisms (4,5) instead of the RF coils of the NRSE instrument.

References

- [1] R. Gähler, R. Golub, and T. Keller, "Neutron resonance spin echo—a new tool for high resolution spectroscopy." *Physica B* **180 & 181**, 899–902 (1992).
- [2] T. Keller, K. Habicht, H. Klann, M. OH, H. Schneider and B. Keizer, "The NRSE-TAS spectrometer at the FRM-2," *Apple Phys A* **74**, S332 (2002.)
- [3] K. Habicht, R. Golub, F. Mezei, B. Keimer and T. Keller, "Temperature-dependent phonon lifetimes in lead investigated with neutron-resonance spin-echo spectroscopy." *Phys. Rev. B* **60**, 104301 (2004).
- [4] The superconducting magnetic Wollaston prism was recently developed at Indiana University by a DOE funded STTR project.
- [5] F. Li, et al., "Superconducting magnetic Wollaston prism for neutron spin encoding," accepted for publication in *Rev. Sci. Instrum.*

- [6] See for example “Directing Matter and Energy: Five Challenges for Science and the Imagination,” A Report from the Basic Energy Sciences Advisory Committee. US Department of Energy, December 2007.
- [7] J. Ma, et al., “Glass-like phonon scattering from spontaneous nanostructure in crystalline AgSbTe₂,” *Nature Nanotechnology* **8**, 445 (2013).
- [8] S. P. Bayrakci, et al., “Lifetimes of Antiferromagnetic Magnons in Two and Three Dimensions: Experiment, Theory, and Numerics,” *Phys. Rev. Lett.* **111**, 017204 (2013).
- [9] F. Mezei, in *Neutron Inelastic Scattering* (IAEA, Vienna), p. 125 (1978).
- [10] E. Morosan, et al., *Nature Physics* **2**, 544 (2006).

2.6 MAGNETIC STRUCTURE

Bryan Chakoumakos (QCMD)

Neutron diffraction is the most powerful probe to determine magnetic crystal structures, and the continued development of user-friendly software tools to apply representational analysis has greatly expanded the number and complexity of magnetic crystal structures reported annually. Magnetic structural studies are needed for diverse sample forms, which include powder, single-crystal, thin film, and nanoparticle. A major research interest is the effects of reduced dimensionality, not only of the physical dimensions of the crystallite size, but also of the dimensionality of the magnetic exchange on the magnetic lattice. In addition, frustrated spin systems (spin ices, spin glasses, etc.) are a hot topic. Polarization of the neutron beam and polarization analysis of the scattered beams provide enhanced fidelity to separate magnetic scattering from nuclear scattering. In conjunction with ultra-low temperature sample environments, these are essential capabilities for world-class neutron scattering facilities. Magnetic ordering constitutes a phase transition, and neutron studies often track order parameters for these, as well as fully characterizing the magnetic structure (propagation vectors of the magnetic lattice, magnetic moments, moment orientation, magnetization densities, etc.). Determining increasingly complex magnetic structures (e.g., multi-k, modulated [commensurate and incommensurate], helices, cycloids, cones, etc.) often requires multiple data sets and increasingly necessitates the use of single-crystal diffraction data. The uniqueness of solutions is worsened in the case of powder diffraction, because different Bragg reflections contribute to a particular observed peak, so that the magnetic structure of compounds with symmetry higher than orthorhombic cannot be unambiguously determined [1]. For collinear magnetic structures in cubic crystals, the direction of the magnetic moments cannot be determined by powder diffraction [2]; for tetragonal, rhombohedral, and hexagonal systems, only the assumed common angle of the magnetic moments with the c-axis can be determined, and there is no sensitivity to the in-plane orientation angle [1]. Fully polarized single-crystal neutron diffraction offers the best opportunity to determine and constrain the correct magnetic structural model. STS instruments offer major advantages to this approach because the small, higher flux beams from the proposed compact moderators will enable the use of smaller sized crystals, reduce background scattering, provide greater ease of neutron polarization, and allow for more extreme sample environments. Powder and single-crystal diffractometers that have greater ΔQ resolution at low Q and high intensity are most suitable, given the magnetic form factor fall-off and the need to detect small magnetic moments.

References

- [1] J. Rodríguez-Carvajal and F. Bourée, "Symmetry and magnetic structures." *EPJ Web of Conferences* **22**, 00010 (2012).
- [2] G. Shirane, "A note on the magnetic intensities of powder neutron diffraction." *Acta Crystallographica* **12**, 282-285 (1959).

2.7 M-STAR (MAGNETISM–SECOND TARGET ADVANCED REFLECTOMETER)

Valeria Lauter (QCMD)

Abstract

M-STAR is the new concept advanced polarized neutron reflectometer optimized for studies of magnetism and structure in small nanosystem samples. It will define new limits in nanoscience and spintronics investigations with versatile experimental conditions of magnetic and/or electric fields, light and temperature applied in situ. It will explore a range of science from new nanosystems a few atomic monolayers thick to complicated prototype device-like systems with multiple buried interfaces having small lateral dimensions of only several millimeters. This will be possible because of the unique combination of high brightness of the source at STS and the new concept of optimized advanced optics, which will provide a gain factor of more than 200 over the magnetism reflectometer on FTS. With its low repetition rate, STS is the prerequisite to build this world-leading polarized neutron reflectometer. M-STAR is optimized for a fully integrated complex sample environment with an extended temperature range of $3\text{ K} < T < 750\text{ K}$, magnetic field of $-1.5\text{ T} < H < 1.5\text{ T}$, electric field E , and pumped light optics L (THEL).

Science Case

Spintronics is an emerging technology that exploits the intrinsic spin and its resulting magnetic moment in addition to the fundamental electric charge of the electron in novel solid-state devices. M-STAR can address an extended range of science topics, including topological heterostructures, multifunctional oxide heterostructures, domain dynamics (switching and relaxation), multiferroics, self-assembled magnetic heterostructures, and others. Many of these nanostructures exhibit unusual physical properties that are important for science and technology and that represent key innovations in the field over recent years. The availability of high performance polarized neutron reflectometry (PNR) is vital for the understanding of magnetism in these systems.

A revolutionary new generation of heterostructures has emerged based on integrating topological insulators (TIs) with conventional materials. Proximity coupling with a ferromagnetic insulator (FI) allows the TI surface states to experience ferromagnetic interactions, where symmetry breaking occurs right at the interface. Examining dual-proximity effects by introducing ferromagnetic order onto the surface of TI thin films is being realized by using ultra-thin FI and small heterostructures.

A high intensity and broad wavelength band of the polarized neutron beam with polarization analysis (I, Q, P, A) is required to perform experiments on complicated multilayers with small lateral spot sizes of a few square millimeters in diameter. M-STAR is optimized to provide the world's best combination of (I, Q, P, A) parameters.

Multifunctional Oxide Heterostructures is the rapidly developing field of thin film systems that exhibit unusual physical properties important from the fundamental point of view and for device application. The field of ferroelectric and ferromagnetic oxides as epitaxial thin films poses challenges and directions toward the advancement of these materials systems in applications of low-energy consumption devices, with a particular focus on the room temperature magnetoelectric multiferroic, BiFeO_3 , exchange coupled to a ferromagnet. The nature of exchange coupling and mechanisms of the voltage control of ferromagnetism observed in these heterostructures are particularly interesting problems.

In situ studies of kinetics and relaxation processes (domains and re-magnetization process in nanostructures and multilayers) require a broad spectral range and a higher flux combined with complex sample environment (THEL). Emergent interface magnetization has been claimed for several novel interface states but is expected to be weak, so these experiments require large statistics up to large Q on limited sample sizes (I,Q,P,A).

Highlight Science Enabled by M-STAR

1. **In situ studies of kinetics and relaxation processes (domains and re-magnetization process in nanostructures and multilayers)** require a broad spectral range and a higher flux combined with a complex sample environment.

The reorientation transition of the magnetization at surfaces and interfaces is important for applications and understanding magnetic anisotropy. Such a transition may be driven by temperature, film thickness, and film topology. The domains and their relaxation depend on atomic structure of the film, anisotropy, and temperature. The reversal of a domain magnetization may be relatively slow and can be studied by time-of-flight polarized neutron reflectometry with off-specular scattering in the following systems:

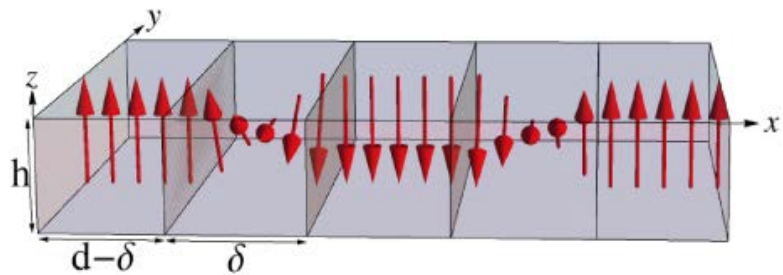


Fig. 2.17. Domain in uniaxial thin films [1].

- Kinetics and relaxation processes (domains and re-magnetization process in nanostructures and multilayers)
- High frequency in spintronics (periodically alternating magnetic fields at the sample)
- Application of electric field for spintronics devices (small samples)

Hybrid multilayers, which consist of ultra-thin ferromagnetic layers alternating with either antiferromagnetic or superconducting ones, are considered to be promising structures for spintronics. Of great importance is the investigation of the magnetization reversal process of magnetic hybrid structures with adjacent ultrathin soft/hard ferromagnetic layers or ferromagnetic/antiferromagnetic layers. The spin-valve, resistive switching and giant magnetoresistance effects are found in such structures, and some of them have been used as write-reading elements. Significant attention currently is focused on the study of ferromagnetic/superconductor heterostructures (FM/SC), in which the magnetic layer is supposed to be used to control the superconductor properties. Therefore, the

knowledge of static and dynamic properties of the ferromagnetic film, which is the key element of FM/SC heterostructures, is important.

An example heterostructure for the experimental study of magnetization reversal kinetics is an ultra-thin manganite layer $\text{La}_{0.7}\text{Sr}_{0.3}\text{MnO}_3$ (LSMO) grown on a LaAlO_3 substrate (LAO) and covered by a high temperature superconductor layer ($\text{YBa}_2\text{Cu}_3\text{O}_{7-d}$). The main attention will be paid here to the magnetization kinetics for the in-plane magnetic field aligned with the easy axis because such a field saturates the film more easily than the out-of-plane field, and that geometry is more important for applications.

2. Magnetic tunnel junction devices with a small lateral size

Long-ranged magnetic proximity effects take place in magnetic tunnel junction devices with a small lateral size of 1–2 mm in diameter.

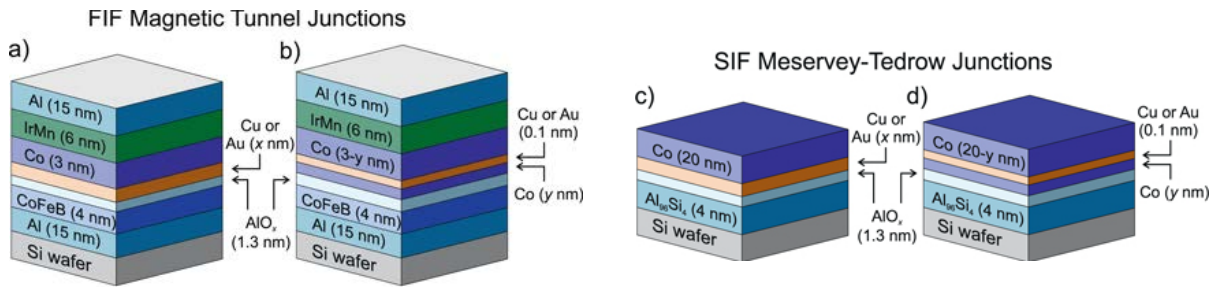


Fig. 2.18. Schematic structure showing the layer stacking sequence deposited on a silicon substrate. FIF (ferromagnet-insulator-ferromagnet) magnetic tunnel junctions with (a) interface doping layers and (b) δ -doping layers of copper and gold.

SIF (superconductor-insulator-ferromagnet) Meservey–Tedrow junctions with (c) interface doping layers and (d) δ -doping layers of copper and gold. The layer thicknesses are not drawn to scale [2].

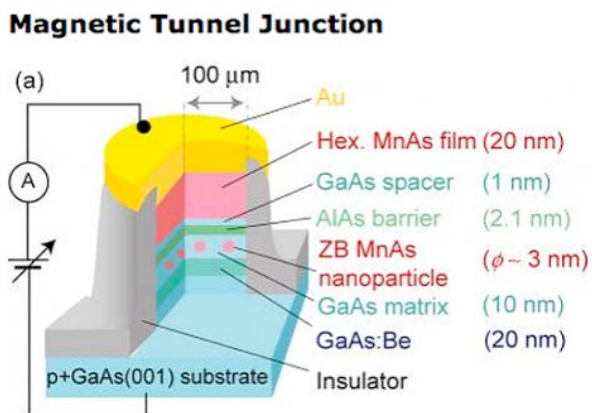


Fig. 2.19. Example of a magnetic tunnel junction (MTJ) device, which can be studied with polarized neutron reflectometry. The lateral size of the sample can be 1–2 mm in diameter.

3. Fractional topological insulators

A fractional topological insulator (TI) ground state can be obtained only by a combination of strong interactions between electrons and a strong spin-orbit coupling. This can be realized through fabrication of a heterostructure device with a TI quantum well in contact with a superconducting material (Fig. 2.20). The superconductor will induce Cooper pairing in the TI quantum well via the “proximity effect.” By applying a gate voltage, it is possible to drive a quantum phase transition in the quantum well between an insulating and a superconducting state. The TI’s spin-orbit coupling significantly modifies the character of this transition and gives rise to stable incompressible quantum liquids in the phase diagram.

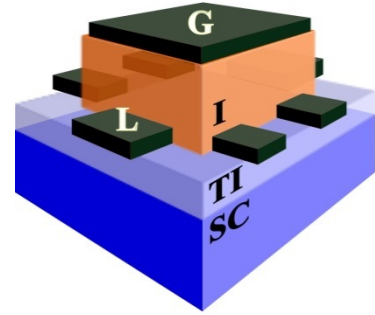


Fig. 2.20. A heterostructure device with a TI quantum well [3].

The TI quantum well can host electrons in two states of spin projection and two orbital states. Inter-orbital Cooper pairs can carry spin and feel the spin-orbit coupling. This produces two helical modes, one of which has energy that decreases with momentum. That helical mode can condense at large momenta and produce a superconducting state with a TR-invariant vortex lattice of spin supercurrents. The quantum phase transition out of this vortex state, tuned by the gate voltage, is generally the first-order vortex lattice melting. The resulting vortex liquid phase is an incompressible quantum liquid, a candidate for a fractional TI.

4. **Multifunctional Oxide Heterostructures** are a rapidly developing field in thin film systems. They exhibit unusual physical properties **that** are important from the fundamental point of view and for device applications that have represented the key innovations in the field in recent years. The field of ferroelectric and ferromagnetic oxides as epitaxial thin films poses challenges and directions toward the advancement of these materials systems in applications of low-energy consumption devices, with a particular focus on the room temperature magnetoelectric multiferroic, BiFeO_3 , exchange coupled to a ferromagnet. The nature of exchange coupling and the mechanisms of the voltage control of ferromagnetism observed in these heterostructures is a particularly interesting problem.

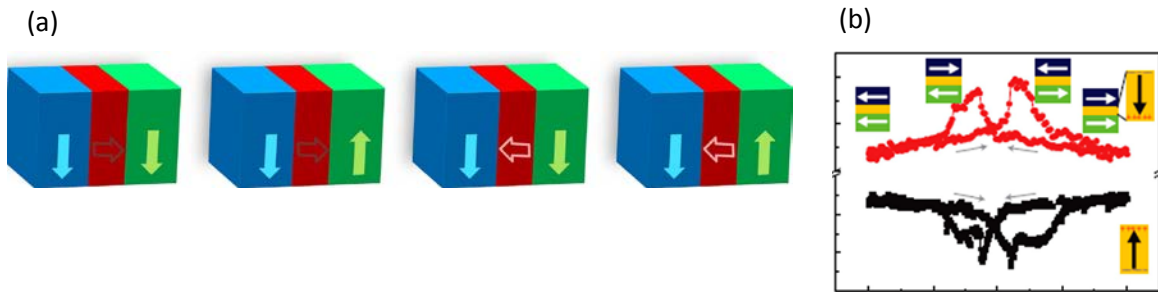


Fig. 2.21. Ferroelectric (FE) tunnel junctions for information storage and processing.

(a) sketch of artificial multiferroic tunnel junctions consisting of two ferromagnetic (FM) electrodes separated by a FE tunnel barrier. The FE polarization (open arrow) is controlled by an electric field, whereas the configurations of the electrodes' magnetizations (solid arrows) are controlled by a magnetic field, giving rise to four non-equivalent resistance states. (b) Resistance versus magnetic field curves measured at $V_{dc} = 10$ mV and 50 K in the as-grown state of a Co/PZT (3.2 nm)/LSMO junction (black squares) and after polarization with a +3-V applied electrical bias (red circles). The polarization states of the barrier and magnetization directions in each magnetic layer are schematically shown for each non-volatile state [4].

Technical Description

Source

The low repetition rate and high brightness of the peak of STS is ideally designed for the new generation polarized neutron reflectometer. The low repetition rate allows for a broad wavelength band necessary to obtain the large Q range with only one incident angle and therefore, to perform experiments at constant geometry. Another advantage is the bigger incident angle for the increased separation of reflected and direct beams, which provides a low background and high angular resolution for the Q region of small momentum transfer.

Key elements of the instrument:

- Source size 50 mm × 50 mm
- Distance moderator—sample 32 m
- Distance sample—detector 2–2.5 m
- Detector type: size 500 mm × 500 mm, resolution 1.5 mm horizontal × 2–2.5 mm vertical
- No direct view to the source from the sample/detector position for polarized and unpolarized beams, which provides low background
- Sample geometry is vertical; scattering geometry is horizontal

A constant sample position for polarized and unpolarized beams is provided with a polarized–unpolarized optical assembly. Each optical system (for polarized and unpolarized beams) consists of two SM 1,200 mm long beams with identical optical properties $m = 6$. Polarizer is optimized for the wavelength band 0.5 Å – 15 Å with polarization 99%.

Novel optics will image the moderator directly on the sample, which will allow for measuring unprecedented small samples of $2 \times 2 \text{ mm}^2$ and single dots as parts of larger samples. The focusing optics are shown in the side view in Fig. 2.22. The focusing optics represent an assembly of two (top and bottom) 10 cm wide optical mirror bands starting at a distance of 3 m from the moderator right after the choppers up to a distance of 29 m from the moderator. The assembly is installed in a vacuum and consists of several sections with different m values (Fig. 2.22). The total length of the focusing system is $2 \times [26 \text{ m long and } 10 \text{ cm wide}]$. The focusing system will give a gain factor of 20 at the sample position. The resolution is flexible at 2–10 %.

The sample environment (magnetic field, closed cycle refrigerator) is optimized for M-STAR, so that a change of the experimental conditions is performed with minimum loss of beam time.

Table 2.4. Key instrument parameters for M-STAR

Source	STS
Moderator type	Cold, coupled H ₂
Wavelength range	0.5–15 Å
Resolution Q	Variable: 2–10 %
Sample size range (beam size)	50 mm max
Moderator—sample distance	32 m
Sample—detector distance	2–2.5 m
Detector type	2D PSD Resolution 1.5 mm horizontal, 2–2.5 mm vertical

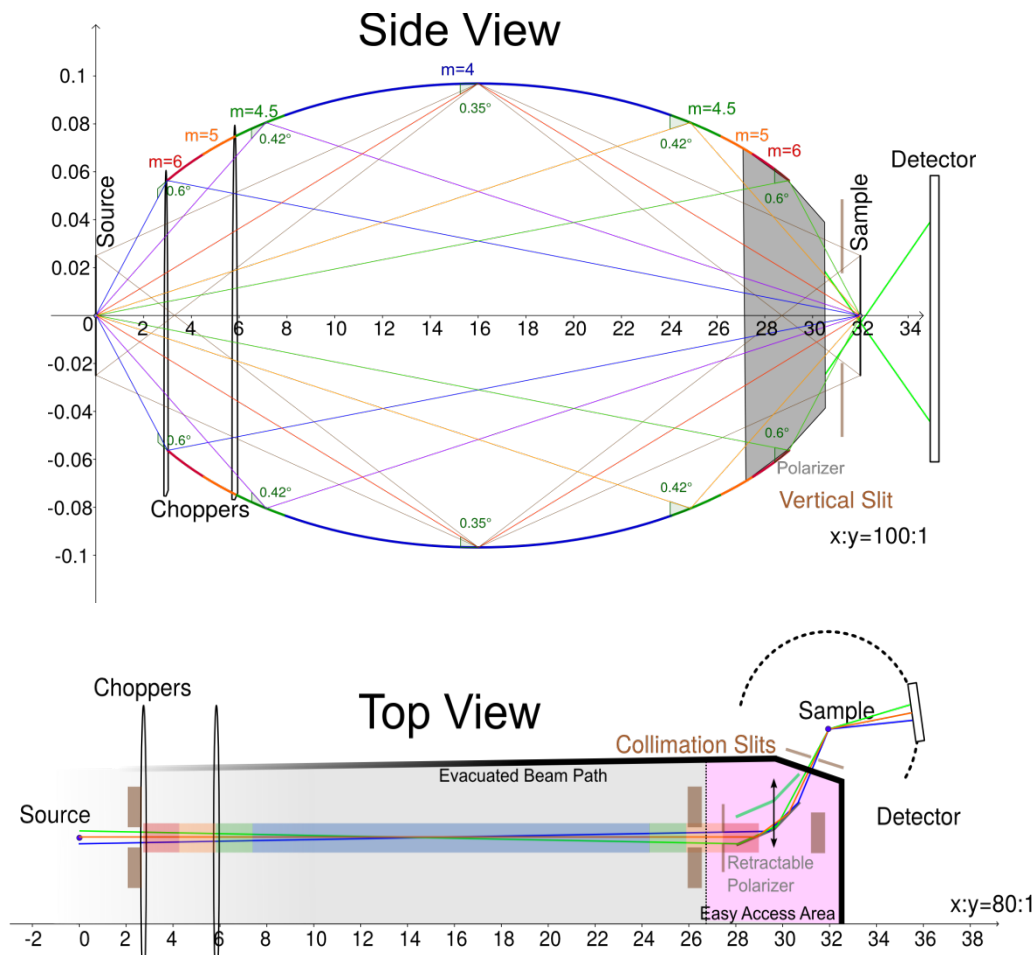


Fig. 2.22. Schematic view of the focusing optics scheme proposed for M-STAR.

References

- [1] F. Viot, et al. *J. Phys. D: Appl. Phys.* **45**, 405003 (2012).
- [2] M. S. Gabureac, et al., *New J. Phys.* **16**, 043008 (2014).
- [3] <http://physics.gmu.edu/~pnikolic/topological-insulators.html#tihet>
- [4] Vincent Garcia and Manuel Bibes. *Nature Communications* **5** (2014). doi:10.1038/ncomms5289.

2.8 M-WASABI (MAGNETISM—WIDE AND SMALL ANGLES WITH BIG INTENSITY)

Valeria Lauter (QCMD)

Abstract

M-WASABI is the new concept instrument for complete reflectometry, comprising specular reflection, off-specular scattering, and GI-SANS; it is optimized for studies of magnetism and structure in nanosystems with multiple lateral length scales. With high intensity and resolution, it will open new

doors for studies of laterally patterned samples of magnetic and non-magnetic systems using GI-SANS with a polarized neutron beam and polarization analysis. Laterally patterned nanosystems characterization will be performed in 3D. This will be possible because of the unique combination of the high brightness of the source at STS and the new advanced design with optimized optics, which will provide a gain factor of more than 30. M-WASABI is optimized for fully integrated complex sample environments with an extended temperature range of $3\text{ K} < T < 750\text{ K}$, magnetic field $-1.5\text{ T} < H < 1.5\text{ T}$, electric field E , and pumped light optics L (THEL).

Science Case

Recent meetings and conferences on different aspects of the investigation of magnetism, magnetic materials, and spintronics display the main contemporary trends in the field of magnetoelectronics and materials and devices in spintronics. Lateral structures obtained with different planar patterning techniques represent the key innovations in the field of nanoscience applications in recent years. This benefits many of the science areas that require high performance polarized and neutron GI-SANS.

A high intensity and broad wavelength band of a polarized neutron beam with polarization analysis (I, Q, P, A) is required to perform experiments on complicated patterned multilayers. M-WASABI is optimized to provide the world's best combination of (I, Q, P, A) parameters and advanced optics for GI-SANS.

Highlight Science Enabled by M-WASABI

- 1. Power of Oxide Interfaces: Directing and Accelerating Ions in Vertically Aligned Nanoscale Architectures,** investigating functional oxide materials with exceptionally high ionic transport based on vertically aligned interfacial (VAI) architectures by designing and tailoring such interfaces in self-assembled complex oxides. Neutron scattering (NS) establishes a *direct* and *precise* correlation between the local interfacial characteristics and the global physical properties. Grazing incidence polarized NS (GI-SANS) and off-specular scattering can map both lateral and depth information of oxygen distribution, expediting our understanding of the mechanism of oxygen generation and migration in VAI structures. This 3D insight into buried structures over the whole sample is unique to grazing incidence neutron scattering.

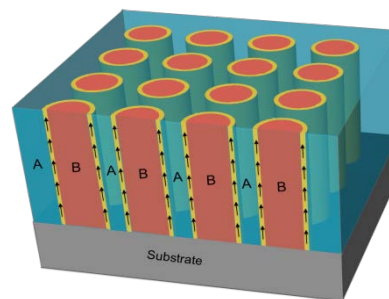


Fig. 2.23. Schematic drawing of VAI nanocomposite architecture.

Potential materials to be studied include perovskites (e.g., $[\text{La},\text{Sr}]\text{MnO}_3$, CaCoO_3 , and SrTiO_3) paired with binary oxides (e.g., CeO_2 and Sm_2O_3) or spinel oxides (CoFe_2O_4). For an initial proof of concept and validation, we will begin with the benchmark systems of $\text{La}_x\text{Sr}_{1-x}\text{MnO}_3$ (LSMO): CeO_2 and LSMO: CaFe_2O_4 , owing to the controllable lattice mismatch and phase insolubilities within these two material pairs.

Because the lattice of CeO_2 sits between the two end members of LSMO, a systematic study of the effect of lattice mismatch on interfacial strain and resultant ionic conductivity can be studied by varying phase composition and/or dopant concentration (Fig. 2.24). The comparison of the two starting systems will provide us with information regarding how the interfacial ionic conductivities can be tuned through selection of different crystal structures and morphologies (matrix vs. column components).

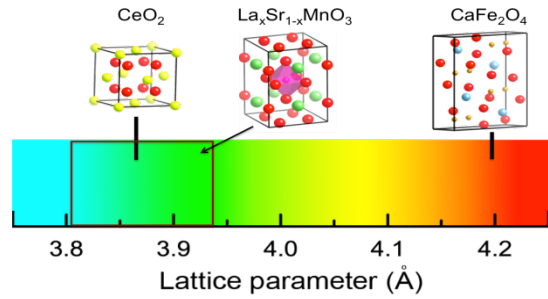


Fig. 2.24. Lattice parameters of the proposed starting model materials.

2. **Exchange-coupled composite elements comprising soft and hard layers** represent a rapidly developing field in thin film systems, which exhibit magnetization reversal in bit patterned media with vertical and lateral exchange. Magnetic recording on continuous granular media has reached areal densities on the level of 500 Gb/in^2 . The areal density limit for conventional perpendicular recording is around 1 Tb/in^2 . Reducing the grain size beyond this mark, to achieve yet higher storage capacity, may compromise the thermal stability because of the superparamagnetic effect. In response, much research has focused on alternative media architectures and recording schemes. Foremost among these is bit-patterned media (BPM) magnetic recording. BPM consists of an arranged array of magnetic islands, fabricated using lithography techniques and/or self-assembly methods. Separation between the islands ensures a large signal to noise ratio, while increased magnetic volume of bits in BPM increases thermal stability of the stored data. Dipolar interactions may also significantly reduce the thermal stability. Dipolar interactions are most significant between neighboring elements. Capped BPM (CBPM), which is composed of magnetically hard patterned islands coupled to a continuous low anisotropy film, was recently introduced to address the magnetostatically induced switching field distribution (SFD) problem. In this design, the continuous capping layer enables compensation of dipolar interactions through lateral exchange between the bits, which is tuned to counterbalance the effects of the magnetostatic fields and reduce SFD. These media can reduce the switching fields, as well. However, because of optimization toward minimum SFDs, the potential of the capping layer in explicitly reducing switching fields may not be fully exploited. Moreover, the domain walls in the capping layer can reduce media stability for certain parameter ranges. These questions can be addressed with polarized GI-SANS with polarization analysis, accessing the magnetic correlations between the covert cells while switching.

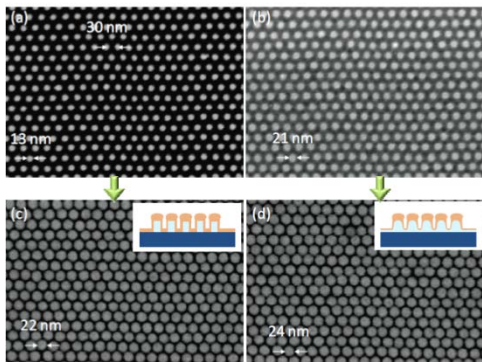


Fig. 2.25. SEM images of 30 nm pitch dots before (a,b) and after (c,d) cobalt or palladium multilayer deposition.
<http://nextbigfuture.com/2011/10/singapore-develops-nanopatterning-for-6.html>

3. **Magnetic tunnel junctions (MTJs)** are components consisting of two ferromagnets separated by a thin insulator. If the insulating layer is thin enough (typically a few nanometers), electrons can tunnel from one ferromagnet into the other. Because this process is forbidden in classical physics, tunnel magnetoresistance is a strictly quantum mechanical phenomenon. Magnetic tunnel junctions are manufactured in thin film technology. On an industrial scale, the film deposition is done by magnetron sputter deposition; on a laboratory scale, molecular beam epitaxy, pulsed laser deposition, and electron beam physical vapor deposition are also used. The junctions are prepared by photolithography. Investigations of domains and domain correlations on different lengths scales can give additional insight into the physics of these devices when reducing the magnetic layer thicknesses.
4. **Nanoring Magnets and Nanoring-MTJs.** Nanorings offer a new geometry for exploring nanomagnets and devices. The two main configurations of a nanomagnet are the vortex state and the onion state. Previously we have studied the switching characteristics of nanorings. There are several schemes for exploring nanoring MTJs (Fig. 2.26 [a]). The reference and the storage layers are in the onion state (Fig. 2.26 [b]), similar to the dipole configuration in traditional MTJs, except that the switching current is significantly less. The reference and the storage layers are in the vortex state, and the two different chiralities in the storage layer provide the memory states (Fig. 2.26 [c]) but require a higher switching current.

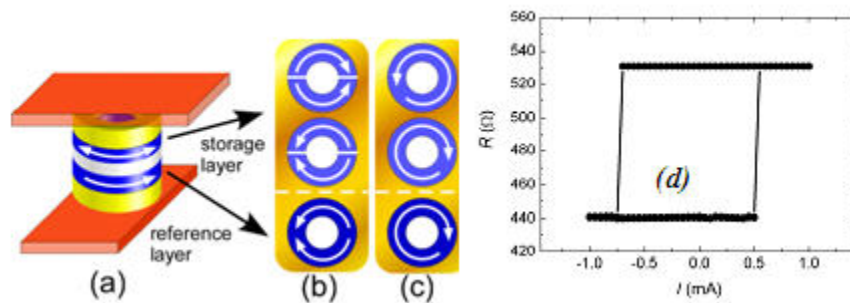


Fig. 2.26. Nanorings. (a) A nanoring MTJ with (b) onion/onion and (c) vortex/vortex states.
 (d) Spin torque switching of a 100 nm nanoring MTJ. Investigation of nanorings/MTJs with a variety of ring diameters all with the same narrow ring width of 25 nm was completed to determine the switching current dependence on ring geometry. (<http://mrsec.jhu.edu/research-highlights/Nanoring%20Magnets/Nanoring%20Magnets%20and%20Nanoring%20MTJs>)

Technical Description

Source

The low repetition rate and high brightness of the peak of STS is ideally designed for the new generation GI-SANS with polarized neutrons. The low repetition rate allows for a broad wavelength band necessary to obtain the broad Q range at one incident angle and to perform experiments at constant geometry. Another advantage is larger angular separation of reflected and direct beams, which provides a low background and high angular resolution for low Q range momentum transfers.

Key elements of the instrument:

- Source size 50 mm × 100 mm
- Distance moderator—sample 40 m
- Distance sample—detector 2–2.5 m
- Detector type—size 500 mm × 500 mm, resolution 1.5 mm horizontal × 2–2.5 mm vertical
- No direct view of the source from the sample position, low background
- Sample geometry is vertical, scattering geometry is horizontal

Constant sample position for polarized and unpolarized beam is provided with a polarized–unpolarized optical assembly with identical optical properties, $m = 6$. The polarizer is optimized for the wavelength band 0.5 Å–15 Å with polarization of 99%.

Focusing optics at the detector position is based on a new concept, which will allow for measuring large samples with GI-SANS by using an advanced optical focusing system with focus at the detector position. This way the vertical resolution of the instrument is given by the focus spot and not the beam divergence and size as for a pinhole instrument. This allows construction of a much shorter instrument with the same angular resolution, avoiding an unnecessary good wavelength resolution with its associated loss in bandwidth. The focusing optics are shown in Fig. 2.27 (side view). It represents an assembly of two (top and bottom) optical mirror bands 10 cm wide, starting at a distance of 3 m from the moderator right after the choppers, up to the distance of 20 m from the moderator. Assembly is installed in a vacuum and consists of several sections with different m values (Fig. 2.27). The total length of the focusing system is $2 \times [17 \text{ m long and } 10 \text{ cm wide}]$. The focusing system will give a gain factor of 20 at the sample position. Resolution is adjustable from 2 to 10 %. The sample environment (magnetic field, closed cycle refrigerator) is optimized for M-WASABI, so that a change of the experimental conditions is performed with minimum loss of neutron beam time.

Table 2.5. Key instrument parameters for M-WASABI

Source	STS
Moderator type	Cold, coupled H ₂
Wavelength/energy range	2–15 Å
Resolution Q	Variable: 2–10 %
Sample size range (beam size)	50 mm max
Moderator—sample distance	38–40 m
Sample—detector distance	2–2.5 m
Detector type	2D PSD Resolution 1.5 mm horizontal, 2–2.5 mm vertical

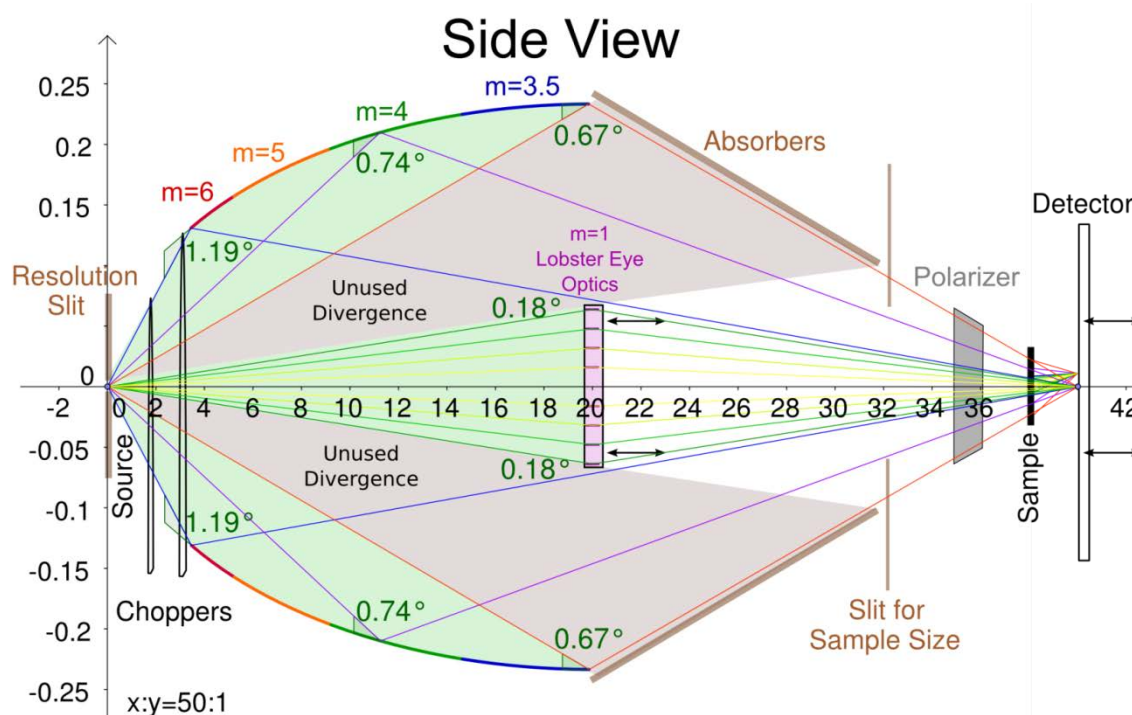


Fig. 2.27. Schematic view of the focusing optics for M-WASABI.

2.9 NESCRY (NEUTRON SINGLE CRYSTAL DIFFRACTOMETER) FOR STS

Huibo Cao, Ovi Garlea, and Bryan Chakoumakos (QCMD)

Abstract

The cold-neutron single-crystal diffractometer, NeSCry, optimized for studies of small crystal size (0.01–8 mm³) will accommodate a diverse range of sample environments to enable ultralow temperatures with and without pulsed magnetic fields, high pressure combined with low temperature, and applied electric fields. The main distinction of NeSCry is the ability to study small single-crystals, $\geq 0.2 \times 0.2 \times 0.2$ mm³, with high-resolution at low-Q and superior flux owing to high brightness, compact, moderator designs for STS. This instrument will have large 2D, highly pixelated detectors close to the sample

position and low background to enable high throughput and large reciprocal space coverage. Considering the ratio in neutron flux provided by STS with respect to FTS, the optimized optical guide, and significantly improved background, the NeSCry is estimated to gain a factor of over 50 in efficiency compared with the existing single crystal instrument TOPAZ.

Science Case

Ever expanding synthesis efforts to realize materials that couple spin, orbital, and lattice degrees of freedom are an essential step in developing next-generation technologies. Many synthesis methods (e.g., flux growth, solvothermal, high pressure, etc.) typically yield small crystal sizes most amenable to x-ray study, but many of these materials would directly benefit from study by neutron diffraction as well. Neutron diffraction is still the method of choice for elucidating the microscopic magnetic structure of materials and detecting the light atoms in battery or fuel cell materials. Given the increasing complexity of materials (e.g., more elements, low dimensional structures, larger unit cell size, etc.), there is a critical need for diffractometers that have sufficient signal to study much smaller crystals than presently possible. Moreover, at present in the United States, controlled environmental conditions are lacking for single crystal neutron diffraction, which is crucial to detecting emergent phenomena in many areas. In particular, in situ studies of crystal growth and ion exchange will be possible, and this will provide new opportunities to study transition and metastable states of a great variety of materials.

Exotic structure and emergent phenomena because of coupling spin, orbital, electron, and lattice degrees of freedom generally occur with small structural distortion, spin canting, or long period modulation of the nuclear and spin structures simultaneously, which requires high Q-resolution and large Q-range, which both can be provided directly by a cold neutron source. Good examples are skyrmion and soliton spin structures, which could be developed as futuristic quantum information storage media. For the slight lattice distortion caused by forming spin density waves in the superconductors, cold neutron diffraction provides the unique capability to distinguish how the lattice distortions and spin density waves are coupled during in situ thermal processing. Equipped with combined extreme sample conditions, NeSCry will serve as an explorer into emergent physics (quantum fluctuation and frustrated magnetism) and functional materials (high T_c superconducting, multiferroic, thermoelectric, piezoelectric, magnetocaloric materials, and so on).

Composite materials that have small lattice misfits are industrially attractive, and in many of these cases, neighboring atoms in the periodic table are also present, necessitating high-Q resolution and neutrons (as opposed to x-rays) (e.g., the phase and microstructure determination of nickel-based superalloys, which are employed in jet engines).

Measuring spin density maps also is a powerful tool to explore emergent physics and functional materials. The high flux and high Q-resolution provide a great opportunity to see nuclear and magnetization densities unambiguously.

The molecular magnetism is another natural research area for NeSCry. The potential applications reside in the areas of spintronics, quantum computing, information storage, and nanomedicine.

The energy conversion and energy storage materials are another fruitful area to pursue. The large wavelength band provides a great opportunity to study those materials and, more importantly, the multiple extreme condition environments are of great importance for in situ studies. Single-crystal diffraction can often reveal the true intrinsic physical behavior of materials, which then can be further optimized using nanostructural engineering.

Three Highlight Experiments

1. Skyrmion lattices

A skyrmion lattice is a topological spin state driven by thermal fluctuations. It has attracted a lot of attention because of the nontrivial physical phenomena such as the topological Hall effect, but it is not easily studied by many experimental methods. The observation and manipulation of this spin configuration becomes of great interest because the expectation is that understanding and controlling such states could lead to new physical phenomena and technological innovation. However, the long periodicities of skyrmion lattices exceed the resolution of the conventional single-crystal neutron diffraction for the magnetic structure determination. So far, only diffraction on small angle neutron scattering instruments has been used to determine the propagation vector. The MnSi crystal represents a large class of these materials that can be studied much more effectively using NeSCry.

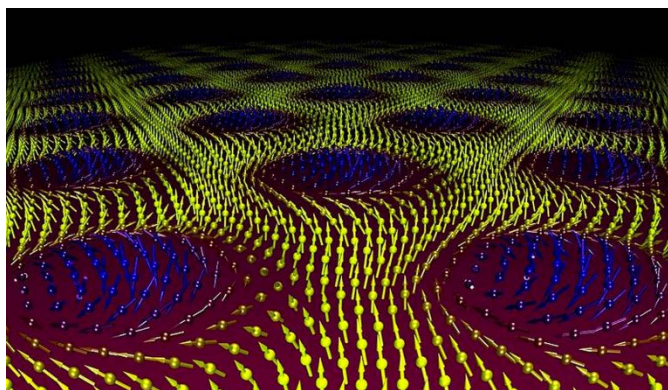


Fig. 2.28. Skyrmion lattice in the MnSi chiral magnet [1].

Reference

[1] S. Mühlbauer, et al., “Skyrmion Lattice in a Chiral Magnet.” *Science* **323**, 915–919 (2009).

2. Photo-induced magnetism

Various classes of transition metal compounds are known to exhibit light sensitive electronic structural changes accompanied by dramatic changes in their magnetic and/or optical properties. These roughly fall into several possibilities: (1) spin crossover complexes, (2) metal-to-ligand charge transfer complexes, (3) metal-to-metal charge transfer compounds, (4) ligand isomerization with change of spin state, (5) valence tautomerism, and (6) open/close switching of ligands with change of spin state [1]. These classes of switchable molecular systems are actively studied with the goal to develop technological applications, such as displays, information and energy storage, and sensors. For instance, in a magnetic hetero-junction, photocarrier injection through the interface can change its magnetic properties. In general, magnetization and demagnetization occur through intermediate states in photomagnets, where electromagnetic energy enables the system to reach the intermediate states.

Photo-induced magnetism has attracted overwhelming attention since photo-induced magnetization was reported in a Prussian Blue analog by Sato et al. [2]. Photo-irradiation can trigger electronic excitation, which can further rearrange the lattice and affect other related physical properties, such as the magnetism. Manipulation of the magnetism by photons opens a door to new technologies.

However, the large unit cell volumes and large number of atoms for many of these interesting materials has effectively blocked experimental studies using neutrons. Thanks to the high flux, high-resolution polarized cold-neutrons and accommodating sample environment conditions, NeSCry will provide a key to in situ measurements of the lattice distortions, the spin disorder–order transition, magnetization densities, and their relationships. From the experiment, we expect to elucidate the mechanisms of the photo-induced magnetism and help to design useful materials.

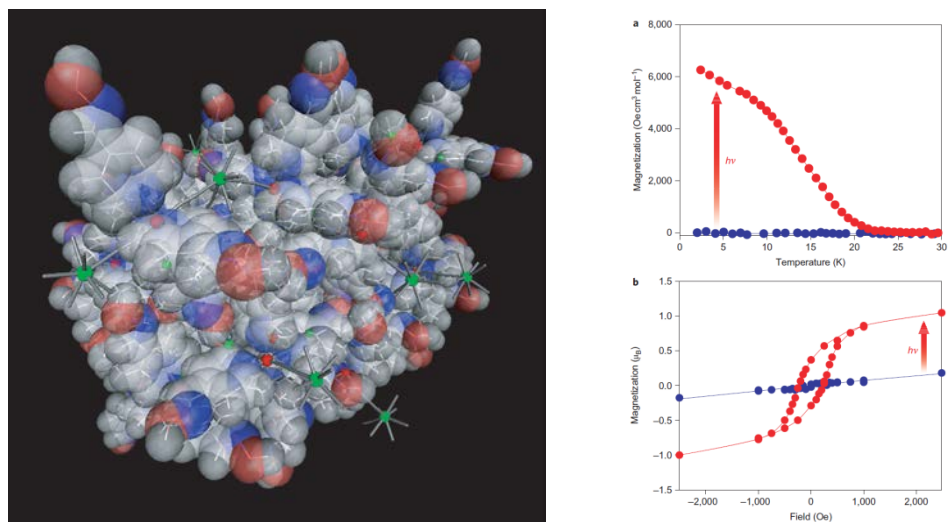


Fig. 2.29. Crystal structure of $\text{Fe}_2[\text{Nb}(\text{CN})_8]\text{-(4-pyridinealdoxime)}_8\text{-2H}_2\text{O}$ (left). Magnetization change caused by photo-induced spin-crossover (right). [3]

Recently reported 3D Fe–Nb mixed-metal compounds— $\text{Fe}_2[\text{Nb}(\text{CN})_8]\text{-(4-pyridinealdoxime)}_8\text{-2H}_2\text{O}$ and $\text{Fe}_2[\text{Nb}(\text{CN})_8]\text{-(4-bromopyridine)}_8\text{-2H}_2\text{O}$ —are proposed as first experiments for this class of materials [3, 4]. NeSCry offers a new capability to study photomagnetism with neutron diffraction because it allows for measurements using crystals of a small enough size to enable light stimulation.. Many of these crystals cannot be grown in large sizes (> 1 mm) anyway, but studies by neutron diffraction complement x-ray studies by having ideal sensitivity to the spin states and magnetization density.

References

- [1] Jun Tao, H. Maruyama, and O. Sato, “Valence tautomeric transitions with thermal hysteresis around room temperature and photo-induced effects observed in a cobalt-tetraoxolene complex.” *Journal of the American Chemical Society* **128**, 1790–1791 (2006).
- [2] O. Sato, T. Iyoda, A. Fujishima, and K. Hashimoto, “Photo-induced magnetization of a cobalt-iron cyanide.” *Science* **272**, 704 (1996).
- [3] Shin-ichi Ohkoshi, et al., “Light-induced spin-crossover magnet.” *Nature Chemistry* **3**, 564–569 (2011).
- [4] Shin-ichi Ohkoshi, et al., “90-degree optical switching of output second-harmonic light in chiral photomagnet.” *Nature Photonics* **8**, 65–71 (2013).

3. Boracite-type multiferroic crystals

The general formula for boracite is $M_2B_7O_{13}X$, where M is a divalent metal (Mg, Cr, Mn, Fe, Co, Ni, Cu, Zn, Cd), and X is a halogen atom (Cl, Br, I). Even though boracites were the first multiferroic materials discovered nearly 50 years ago (long before the term multiferroic was coined), their relatively complicated crystal structures (unit cell volumes 925–1,800 Å³ and ≥ 24 unique atoms) have retarded unraveling the coupling between their magnetism and electric polarization. Neutron single-crystal diffraction offers great fidelity to determine the long-range ordered magnetic states, transition temperatures, and primary atomic displacements.

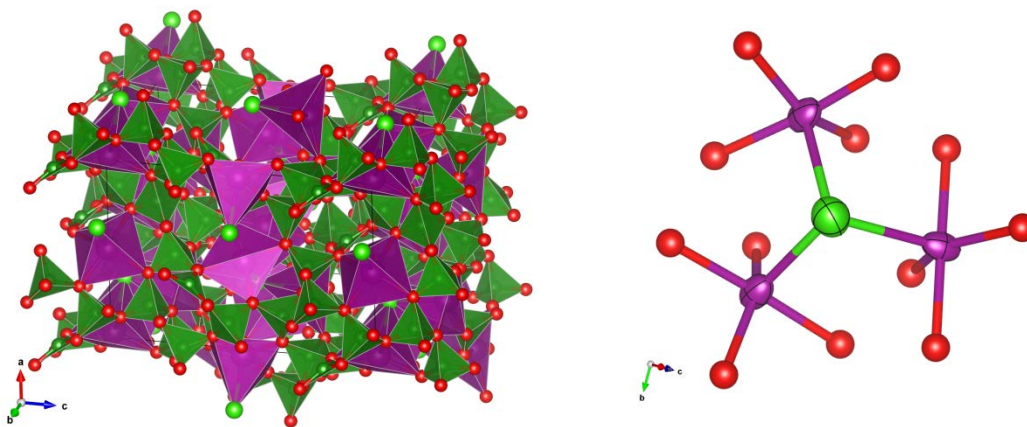


Fig. 2.30. Polyhedral view of an example acentric polar crystal structure of boracite, $Mn_3B_7O_{13}Cl$ (left) and its Mn cluster (right).

Boracites are generally grown by hydrothermal methods, by flux-growth, or by vapor transport, and the crystal size can be several cubic millimeters, but typically, crystal size is ≤ 1 mm. The high temperature forms are cubic (tetrahedral) and undergo phase transitions to lower symmetry, polar acentric, structures below about 400 K to 550 K. This necessarily introduces twin domains in the crystals. At lower temperature some of these compounds become simultaneously ferroelectric and ferromagnetic or antiferromagnetic, and all of these non-centrosymmetric phases allow the piezoelectric effect. For the halogen boracites, the transition temperatures to the ferroelectric phase vary widely (hundreds of degrees) depending on composition but follow the order $Cl > Br > I$. For neutron diffraction, the large amounts of boron in boracites require isotopic enrichment with ¹¹B to make neutron experiments feasible. These challenges are fully addressed by NeSCry, given its projected high flux and polarizability. The rich science topic of multiferroic properties of boracites directly benefits from neutron diffraction and the capabilities offered by STS instrumentation.

Technical Details

NeSCry will be optimized for measurements of very small single crystal samples, such as 0.01 mm³, and consequently the moderator surface only needs to be 2–3 cm horizontally and vertically, allowing for a very intense cold neutron beam on the sample.

The moderator to sample distance will be chosen between 30 and 50 m, and a broad wavelength range ($\sim 8 \text{ \AA}$) will be enabled. The neutron optics system will be designed to have interchangeable guide sections to allow for the tuning of the vertical and horizontal beam divergences in the range of $\pm 0.5\text{--}2^\circ$. A relaxed beam divergence on sample of $\sim \pm 2$ degrees could be especially beneficial for measuring very small samples. A separate section of the guide could be assigned to a neutron polarizer (supermirror). The polarization will be manipulated by using an RF neutron spin flipper.

The secondary flight path between sample and detector will be short, ranging from 0.25 m to 1 m, determined by the need to minimize the background signal and to maximize the solid angle covered by the detector array.

The detector will consist of an array of multiple banks to cover a large Q-range and will have sufficient pixelation to resolve Bragg peaks from unit cell volumes up to $120,000 \text{ \AA}^3$.

A full range of sample environment equipment (cryostats with mK inserts, closed cycle refrigerator with automatic sample changer, pressure cells, pulsed magnetic fields) will be available for this instrument.

Table 2.6. Key instrument parameters for NeSCry

Source	STS
Moderator type	Cold, coupled H ₂
Wavelength/energy range	1.2–14 Å
Resolution Q/E	$\Delta Q/Q$: 0.2–0.4%
Sample size range (beam size)	$0.2 \times 0.2 \text{ mm}^2$ to $2 \times 2 \text{ mm}^2$
Moderator—sample distance	30–50 m
Sample—detector distance	0.25–1 m
Detector type	Highly pixelated detector/angular detector

2.10 VERDI (VERSATILE DIFFRACTOMETER FOR COMPLEX MAGNETIC STRUCTURES) FOR STS

O. Garlea (QCMD)

Abstract

The cold-neutron diffractometer, VERDI, optimized for studies of magnetism and large unit cell structures, will excel by its high-resolution at low-Q and a much-increased flux owing to the high brightness of the source at STS. Designed to deliver efficiency and versatility, this instrument will serve for both powder and single crystal studies under extreme conditions of temperature, pressure, or magnetic field. This instrument will be equipped with polarization capability and will combine and extend the strengths of two of the currently most reputable magnetism diffractometers, WISH at ISIS and D7 at ILL, providing the US user community with the platform for new scientific breakthroughs. Even assuming a minimal level of optimization with respect to the WISH instrument at ISIS, the VERDI instrument can be expected to be at least five times faster. At the same time, its versatility will make it a one-of-a-kind instrument.

Science Case

The ever increasing complexity of magnetic systems, which often involve coupled spin, orbital, and lattice degrees of freedom, calls for much improved instrumentation that provides high resolution at low-Q, high intensity, and reduced extrinsic background. The proposed cold-neutron diffractometer VERDI proposed here will meet all these criteria and will be well adapted for in-depth magnetic structure studies as specified below:

- **Complex incommensurate structures.** VERDI will be optimally suited for studying complex incommensurate structures that arise in multiferroic compounds, which are recognized as one of the new emerging technologies for information processing. The high-resolution and the wide-Q coverage obtained by using a single-frame bandwidth will enable simultaneous characterization of crystal structure as well as local ferroelectric and magnetic properties in these materials.
- **Reduced ordered magnetic moments and itinerant magnets.** The 4d, 5d, and possibly 6d transition metal oxides have recently become a fertile ground for studies of new magnetic phenomena driven by spin-orbit interaction. The extended nature of the magnetic electrons in such systems requires measurements at small wave-vectors to avoid form-factor suppression of the already weak magnetic signal. This problem is well addressed by the VERDI instrument, which will be able to access a very low-Q regime, down to 0.1 \AA^{-1} , with extremely low background. For specific cases, a significant improvement in the signal-to-noise ratio will be achieved by using a monochromatic incident beam produced by a Fermi chopper.
- **Magnetization density studies and short-range magnetic correlations.** VERDI will be equipped with polarization capability; applications will include studies of the magnetization distribution across magnetic organic molecules as well as studies of the redistribution of electrons accompanying the combined magnetic–crystallographic transitions in martensitic materials. Compounds where covalence effects result in the sharing or transfer of magnetization density between transition metals and anions also represent excellent candidates for study. In addition, the ability to perform neutron polarization analysis over a wide angle will allow the separation of nuclear, magnetic and nuclear spin-incoherent scattering for unambiguous magnetic diffuse scattering studies.
- **Neutron diffraction under extreme conditions.** Intriguing new phenomena in quantum materials can be exposed by combining the cold-neutron source related advantages with new sample environments such as extreme low temperatures, high pressures, and high magnetic fields. A variety of materials—of which one can name the multiferroics, magnetocaloric materials, frustrated magnetic systems, and magnetic molecular materials—are known to exhibit dramatic changes in their magnetic behavior under high pressures and/or applied magnetic fields.

Highlight Science Enabled by VERDI

1. Expanding the magnetic phase diagram of solid oxygen to higher pressures and lower temperatures

Oxygen is the only elemental molecule that carries a magnetic moment. When it is cooled to below 24 K, long-range magnetic order is observed, giving rise to the simplest antiferromagnetic solid in nature: α -O₂ [1]. This phase transforms under pressure of 6–7 GPa to δ -O₂ [1], which is also long-range ordered [2] and contains three distinct magnetic phases [4,5]. The unexpected

richness of oxygen's phase diagram is a consequence of the weak interplane exchange interaction, which depends strongly on the mutual orientation of the molecules [3].

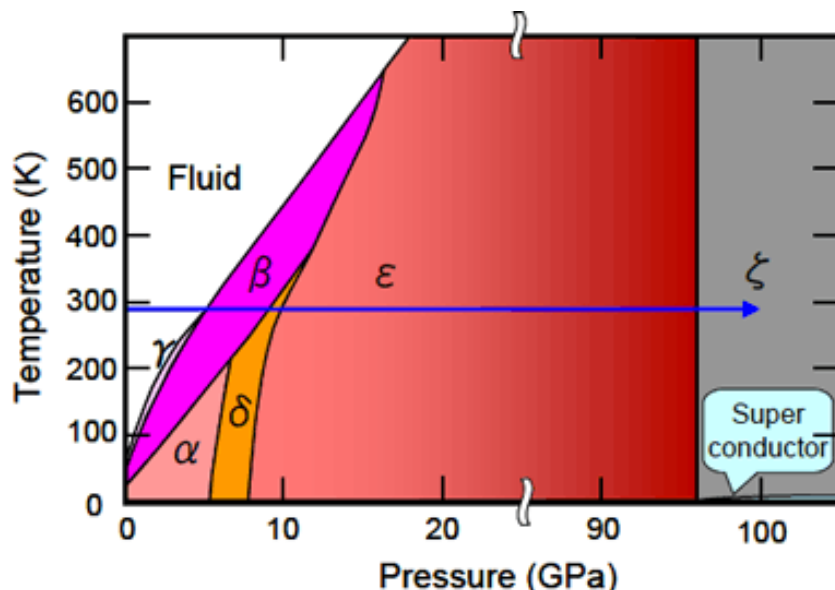


Fig. 2.31. Pressure–temperature phase diagram of oxygen.
[<http://www.azonano.com/article.aspx?ArticleID=1797>]

References

- [1] Y. Freiman and H-J. Jodl, "Solid Oxygen," *Physics Report* **401**, 1-228 (2004)
- [2] N. Goncharenko, O. Makarova, and L. Ulivi, "Direct determination of the magnetic structure of the delta phase of oxygen," *Phys. Rev. Lett.* **93**, 055502-1-4 (2004).
- [3] S. Klotz, et al., "Magnetic ordering in solid oxygen up to room temperature," *Phys. Rev. Lett.* **104**, 115501-4 (2010).
- [4] S. Klotz, Th. Strässle, and Th. Hansen, "Magnetism of solid oxygen under pressure by neutron scattering," *Notic. Neutr. Luce Sinc.* **17**, 1004, 10–15 (2012).
- [5] S. Klotz, Th. Strässle, and Th. Hansen, in preparation.

2. Determination of complex field-induced incommensurate long-range magnetic order in quantum magnets

The quantum magnets are natural realizations of gases of interacting bosons whose relevant parameters such as dimensionality, lattice geometry, amount of disorder, nature of the interactions, and particle concentration can vary widely [1]. The particle concentration can be tuned easily by applying an external magnetic field that plays the role of a chemical potential, and the system can be driven from a state with no bosons to a state with a finite number of bosons, thereby creating a quantum phase transition [2]. Elastic neutron scattering can directly probe the ordered magnetic moment in the field-induced ordered state to understand the nature of the ordered phase, the direction of the easy axes, and the size of the ordered

moments. In some cases, the spin ordering becomes extremely complex, characterized by one or more incommensurate wave-vectors [3]. For instance, there are rather unusual broken symmetry states that could be stabilized in frustrated quantum magnets. $\text{Ba}_3\text{Mn}_2\text{O}_8$, $\text{Sul-Cu}_2\text{Cl}_4$, and Cs_2CuCl_4 are three examples where frustration leads to spiral structures with incommensurate wave vectors.

The high-resolution, the wide-Q coverage, and the enhanced signal to background ratio of the VERDI instrument will enable for studying complex incommensurate structures induced by applying high magnetic fields.

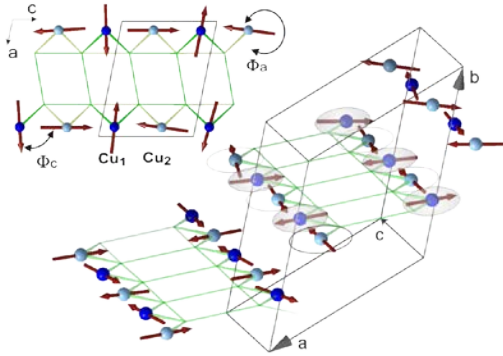


Fig. 2.32. Proposed model of the incommensurate helical structure induced by magnetic fields in $\text{Sul-Cu}_2\text{Cl}_4$ [3].

References

- [1] Vivien Zapf, Marcelo Jaime, and C. D. Batista. “Bose-Einstein condensation in quantum magnets,” *Rev. Mod. Phys.* **86**, 563 (2014).
- [2] Thierry Giamarchi, Christian Rüegg, and Oleg Tchernyshyov, “Bose–Einstein condensation in magnetic insulators,” *Nature Physics* **4**, 198–204 (2008).
- [3] V. O. Garlea, et al., *Phys. Rev. B* **79**, 060404 (2009).

3. Measurements of pinch-points, like diffuse features in highly frustrated magnets with a local ice-rule type constraint, using polarized neutrons

The two-in/two-out spin configuration observed on certain pyrochlore lattices arises from the magnetic dipole–dipole interaction between the spins with local exchange interactions being of secondary importance. The “ice-rule” is not purely a local effect but is stabilized by both the near-neighbor and long-range part of the dipolar interaction [1, 2]. It can therefore be seen as an emergent, many-body property. The key experimental signatures of either the “real” or “effective” dipolar correlations are expected to be pinch-point singularities, bow-tie like diffuse features centered on nuclear Bragg positions. Polarized neutron experiments can be designed at VERDI to measure two independent components of the tensor $S^{\alpha\beta}(\mathbf{Q})$ that are typically labeled as spin flip (SF) and non-spin flip, making it possible to separate the contributions of the components of spin correlations in and out of the scattering plane. Experimentally probed pinch-points features could be the signature of any type of topological constraint in a frustrated system that can be mapped to the ice rules.

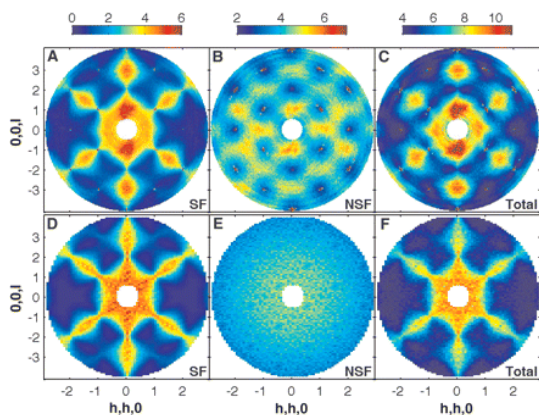


Fig. 2.33. Diffuse scattering maps from spin ice, Ho₂Ti₂O₇. Experimental SF, non-spin flip scattering at T = 1.7 K with pinch points at (0, 0, 2), (1, 1, 1), (2, 2, 2) [(A) to (C)] versus theory [(D) to (F)] (see Ref [1]).

References

- [1] T. Fennell, et al., "Magnetic Coulomb Phase in the Spin Ice Ho₂Ti₂O₇," *Science* **326**, 415 (2009).
- [2] T. Fennell, et al., "Pinch points and Kasteleyn transitions in kagome ice," *Nature Physics* **3**, 566–572 (2007).

Technical Details

VERDI will be designed to provide maximum versatility based on operational needs, as a powder or single crystal diffractometer, with or without polarization capability. The instrument will benefit from the use of a broad wavelength range ($\sim 8\text{--}9 \text{ \AA}$) so that most of the Q-range of interest can be covered by a single frame. The choice of the moderator will be made to take full advantage of the STS high brilliance. The moderator to sample distance will be optimized between 40 and 60 m, and the secondary flight path between sample and detector will be in the range of 2–3.5 m.

The chopper system will consist of a T_0 chopper and the required bandwidth defining disk choppers. A Fermi chopper will also be available on a translation table for providing monochromatic beam for use in studies of magnetic diffuse scattering using polarized neutrons. To ensure versatility, the instrument will have a series of interchangeable guide sections that will allow adjustment of the geometrical resolution. The instrument will be optimized for a sample size between $2 \times 2 \text{ mm}$ and $10 \times 20 \text{ mm}$. Separate types of elliptical guides could potentially be used for the powder and single crystal measurements considering the difference in sample size and the required divergences. For instance, in the case of powder measurements, the incident divergence of the beam could range from 0.2 to 1° in the horizontal direction and from 2 to 3° in the vertical; for the single crystal, a more symmetric geometry of maximum $1 \times 1^\circ$ is needed. A set of slits and a Soller collimator positioned in the last section of the guide could offer additional flexibility in trading the incident neutron flux for instrument resolution. The Q resolution will be tunable in the 0.2–0.4% range.

A separate section of the guide will be assigned to a neutron polarizer (supermirror of ^3He). The polarization will be manipulated by using a Mezei-type neutron spin flipper or Cryoflipper (when using high magnetic fields). A set of orthogonal xyz field coils situated around the sample position will be used to sequentially rotate the polarization of the incident beam in each direction. The instrument will also be

equipped with a supermirror analyzer array that will cover the horizontal scattering plane over the $\sim 120^\circ$ angular range for xyz-polarization analysis.

The detector will consist of an array of 8 mm diameter ^3He tubes (with no gaps between them) arranged in a cylindrical shape covering an angular range of 175° in the horizontal plane and $\pm 20^\circ$ in the vertical plane. The use of scintillator detectors may be considered as alternative if a continuous coverage needed for the single crystal experiments can be accomplished. An oscillating, fine, radial collimator made of blades of Mylar coated with Gd_2O_3 paint will ensure a low background and high signal-to-noise-ratio.

A full range of sample environment equipment (12 T cryomagnet, cryostats with mK inserts, closed cycle refrigerator with automatic sample changer, pressure cells) will be available for this instrument.

Table 2.7. Key instrument parameters for VERDI

Source	STS
Moderator type	Cold, coupled H_2
Wavelength/energy range	1.2–14 Å
Resolution Q/E	$\Delta Q/Q$: 0.2–0.4%; $\Delta E/E$: > 3%
Sample size range (beam size)	$2 \times 2 \text{ mm}^2$ to $10 \times 20 \text{ mm}^2$
Moderator—sample distance	40–60 m
Sample—detector distance	2–3.5 m
Detector type	(8mm ^3He PSD)

2.11 ZEEMANS: A HIGH MAGNETIC FIELD BEAM LINE

Garrett Granroth (NDAV) and Collin Broholm (QCMD)

Abstract

Scientific impact, user demand, and two recent National Academy of Science reports[1,2] identify neutron scattering in high magnetic fields as a priority area. The enhanced brightness of the proposed second target station and progress in high field technology now offer the opportunity for a quantum leap. With continuous fields in excess of 35 T and versatile neutron instrumentation capable of all forms of scattering, the ZEEMANS facility would define the frontier in high field neutron scattering and offer unprecedented new scientific opportunities. As summarized below, the groundbreaking experiments enabled would:

1. expose the structure and dynamics of previously inaccessible quantum matter in correlated metals and insulators;
2. characterize vortex matter in new regimes of high temperature superconducting materials;
3. determine the multiplicity of collective electronic resonances in technologically relevant materials;

4. locate hydrogen in materials relevant to medicine, biology, physical chemistry, and materials science through nuclear spin labeling; and
5. elucidate of the texture and structure of materials during high field processing.

Science Case

The wide-ranging scientific program of the National High Magnetic Field Laboratory (NHMFL) indicates the scientific value of controlling the electronic and nuclear state of materials with magnetic fields in the range from 1 to 100 T. Adding through neutron scattering, the capability of probing electronic and nuclear structure and dynamics at the atomic scale opens an exciting array of scientific opportunities.

At the present, fields up to 12 T are generally available and in high demand at neutron scattering facilities worldwide. The limits are 17 T (at the Helmholtz-Zentrum Berlin) for steady fields and 30 T for limited pulsed field diffraction (at the Spallation Neutron Source). A keyword search using the Web of Science indicates these capabilities generate approximately 90 publications and 3,000 citations per year. Pushing to higher fields dramatically expands the range of materials and phenomena that can be subject to the powerful combination of high fields and neutron scattering. In recognition of this, the Helmholtz-Zentrum Berlin is about to launch a ~19 million euro (about \$24.2 million US) facility for neutron scattering in steady fields up to 25 T. The importance of this area for the materials based sciences was also recognized in two recent reports from the National Research Council (NRC), the latest of which offers the following conclusion and recommendation [2]:

Conclusion: *Neutron and x-ray scattering measurements have played a central role in explicating the behaviors of virtually every class of strongly interacting matter. However, there continues to be almost no progress in the United States on bringing higher fields to neutron and x-ray scattering user facilities. It is clear that difficulties in establishing and maintaining an effective steward-partner relationship between scattering facilities and the NHMFL, as well as their respective sponsors, have been a contributing factor to this lack of progress. This is rapidly becoming a lost opportunity for US science, and bold action is needed now to take the lead in this important area.*

Recommendation: *New types of magnets should be developed and implemented that will enable the broadest possible range of x-ray and neutron scattering measurements in fields in excess of 30 T. This requires as a first step the expeditious procurement of modern 10–16 T magnet/cryostat systems for US facilities, together with the recruitment of low-temperature/high-field specialists. Second, a 40 T pulsed-field magnet should be developed with a repetition rate of 30 s or less. Third, building on the development of a high-temperature all-superconducting magnet, which was recommended earlier, a wider-bore 40 T superconducting dc magnet should be developed specifically for use in conjunction with neutron scattering facilities. New partnerships among federal agencies, including the Department of Energy, the National Institute of Standards and Technology, and the National Science Foundation, will likely be required to fund and build these magnets, as well as to provide the funds and expertise that will be needed to operate these facilities for users once they are built.*

The ZEEMANS project would pursue the opportunities for new materials based science with neutrons indicated by the strength of the existing research programs at fields up to 17 T and so clearly identified and enunciated by the NRC studies.

The goal is to create nothing less than the *world center for high magnetic field neutron scattering at Oak Ridge National Laboratory* in conjunction with the construction of STS. A facility reaching fields beyond

35 T and offering the full range of neutron spectroscopy, diffraction, reflectometry, and SANS with the intensity, resolution, and coverage offered by STS, would have major impact across the whole range of materials based sciences.

While the most exciting results will undoubtedly come from areas we cannot predict, we shall highlight several scientific areas where the ZEEMANS facility would surely have a major impact: There is strong interest in quantum materials where the non-intuitive world of quantum mechanics—usually associated with the atomic scale—finds expression in anomalous “quantum coherent” properties at the macroscopic scale. The superconducting state is an excellent example, but the rich and varied properties of so-called “quantum spin liquids” are only now beginning to be appreciated and explored. Potential applications lie in the areas of energy and information, though the initial excitement is simply associated with exploring and controlling the fundamental properties of quantum correlated systems. High magnetic fields open an exciting new dimension along which to create, manipulate, and explore quantum matter. Already apparent in the active research programs that surround the current suite of magnetic fields, it is safe to predict a very active scientific program that closely connects with new materials synthesis and the theoretical frontier of quantum field theories in condensed matter.

Rekindled by the discovery of iron superconductivity in 2008, the possibility of superconductivity beyond room temperature continues to motivate a worldwide multidisciplinary research effort. To support high current densities needed for high power applications, the dissipative motion of flux lines must be kept at bay. SANS in high magnetic fields provides essential information about the modulated internal fields of type II superconductors. A ZEEMANS facility would enable such experiments in a new field regime where the spacing between flux lines approaches the superconducting coherence length. New knowledge about the interplay between magnetism and superconductivity that may help to develop even stronger superconductivity can be anticipated there. The experiments will also be able to probe flux line order and motion in a regime of fields that is appropriate for high current applications ranging from MRI magnets to electrical energy transport.

The Zeeman effect is associated with the ability of magnetic fields to split atomic transitions. Such experiments were crucial in the development of the quantum theory of atoms because they reveal the degeneracy of atomic levels. The analogous solid state experiments are now essential to understand the collective modes of quantum materials. A prominent example is the so-called “spin resonance,” a defining feature of high temperature superconductors near magnetic quantum criticality. High field experiments to explore the nature of collective resonances in high temperature superconductors and correlated topological insulators with technologically relevant energy scales would become possible with the proposed ZEEMANS facility.

Sufficiently high magnetic fields applied at low temperatures can also be used to manipulate nuclear spins. This is of great interest when combined with neutron scattering, which is sensitive to nuclear spins through the strong nuclear force. For H^+ the scattering length actually changes sign with the relative spin state, which yields the notoriously large nuclear incoherent cross section of hydrogen. The effects of manipulating the nuclear spin state of hydrogen in materials are dramatic. The ZEEMANS high field facility makes possible the combination of high-resolution NMR methods for nuclear spin manipulation and neutron diffraction for unprecedented structural information about hydrogen in solids. It is difficult to predict where the impact will be greatest, but there are many opportunities because accurate information about hydrogen locations is critical in fields of science ranging from medicine, biology, and geology to metallurgy.

High fields have interesting and useful effects on materials processing in materials ranging from polymers to metals. A better understanding of the mechanisms underlying high field processing of materials could lead to new anisotropic functional materials and structural alloys based on field-induced microstructures. In metallurgy, for example, there is an active program of research into the use of magnetic fields to stabilize significantly stronger forms of steel. The basic effect of the field is to shift the free energy of magnetic versus non-magnetic phases of iron. Neutron diffraction and SANS at the proposed ZEEMANS facility could dramatically advance this area by enabling the mapping metallurgical phase diagrams and the development of texture during field processing in the highest accessible dc fields.

The proposed ZEEMANS facility would enable a broad research program and open new directions of inquiry that make use of neutrons' unique magnetic and nuclear interactions with materials. The technology and the science would form a strong link between the programs at NHMFL and ORNL's Neutron Sciences Directorate so that a partnership between these organizations in making ZEEMANS a reality will be natural.

Technical Description

A previous study [3-5] shows that a beam line that is competitive to non-dedicated beam lines could be built on FTS. The following description is based on those calculations, scaled up for the increases to STS. Without taking into account anything but source flux, the instrument would be roughly 2 × HYSPEC and 3 × TOPAZ. Details of such comparisons are shown in Figs. 2.34 and 2.35.

The time between pulses for STS is six times longer; that means rather than using a sub frame repetition of at least three for RRM operation, a sub frame operation of at least 18 can be used. Similarly, the bandwidth for diffraction type experiments would expand six times by moving from 0.88 Å to 5.3 Å. This bandwidth expansion means reflectometry could be done in two steps, and most diffraction experiments could be done in a single step rather than multiple steps, thus cutting the measurement time at least in half. Multiplying bandwidth and RRM gains means that on STS, the measurement time would be ~20 × TOPAZ and 40 × HYSPEC. This already assumed a factor of 10 gain from improved focusing optics, so further gains could be had with newer advanced focusing optics.

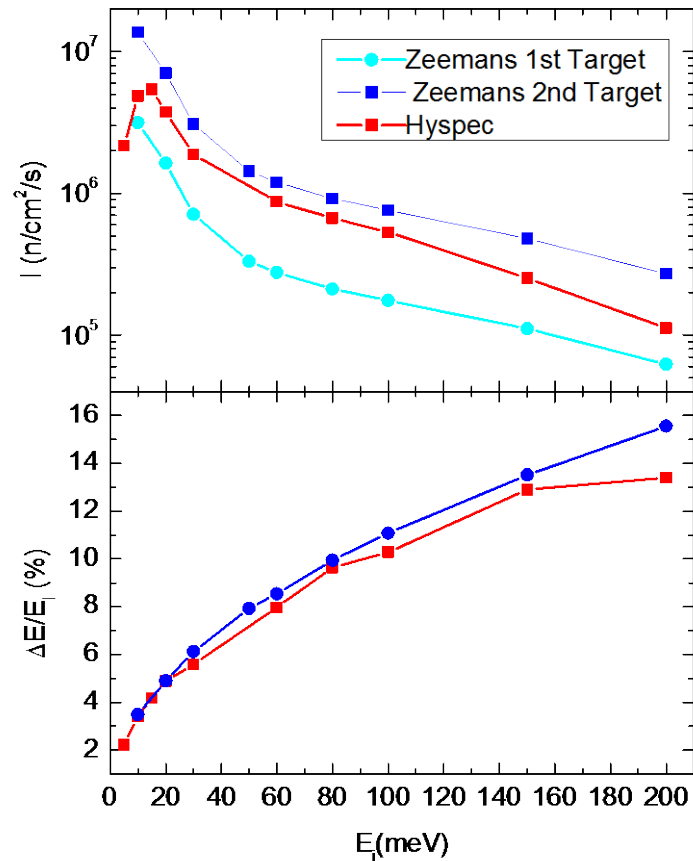


Fig. 2.34. Comparison of flux on a sample between ZEEMANS in the spectrometry configuration and HYSPEC.

The instrument would be on the coupled hydrogen moderator. The sample position is located 70 m away from the target to minimize magnetic interference with neighboring beam lines. The detectors are located 5 m away from the sample position. The detectors are envisioned to be 7 mm diameter He³ tubes and should be effective to a wavelength as short as 0.5 Å.

The beam line as envisioned uses an elliptical guide with the capability of changing the last 5 m of optics to focus to smaller samples. The largest sample envisioned is a 4 cm on a side cube. Along the guide, there will be four bandwidth choppers to define the beam for white beam use. A high speed double disc chopper will be needed to allow for direct geometry spectroscopy. An additional chopper that controls the number of subframes for RRM mode of operation will be needed. This chopper may need to spin faster than a bandwidth chopper.

To interface to the magnet, provide vacuum for the detectors, and provide a feed-through for sample environment, a detector vessel with a rotation flange is envisioned for the beam line. This includes a 2 m diameter differentially pumped seal. Though this seal is big, it is not beyond the scalability of the technology. A view of the magnet, vessel, and seal is shown in Fig. 2.36.

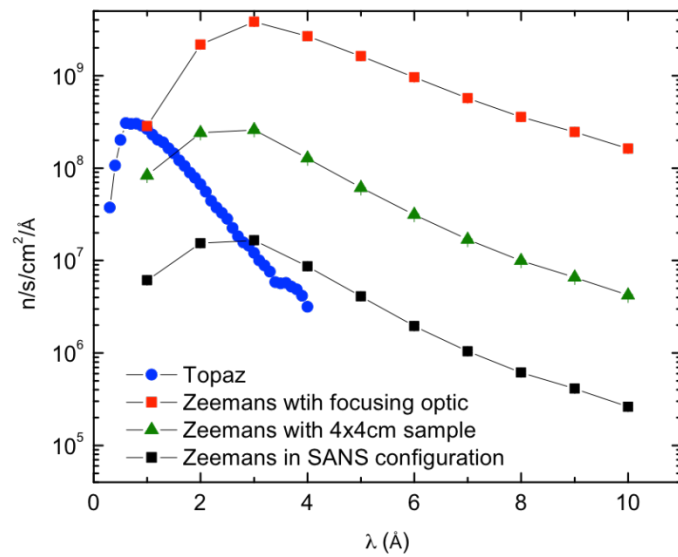


Fig. 2.35. The flux on sample per pulse for white beam ZEEMANS configurations with TOPAZ for comparison.

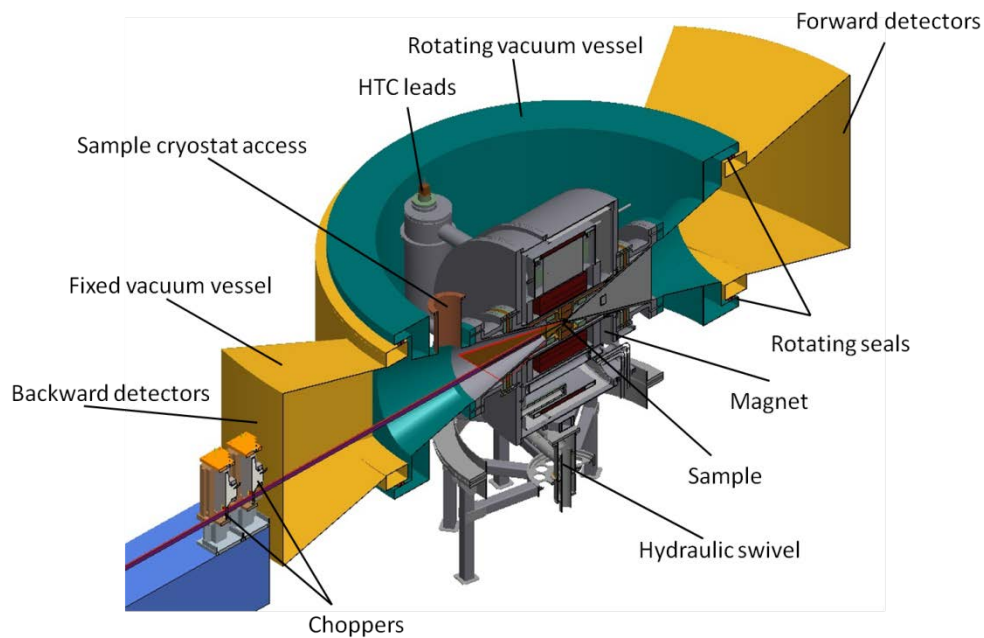


Fig. 2.36. Detector vessel, magnet, and differentially pumped rotation seal.

The central piece of this beam line would be a high field facility scale magnet. Recent estimates from NHMFL are that a 35 T magnet could be built with all superconducting technology. If one includes Bitter magnet technology in a series connected hybrid form, at least 40 T is achievable, and everything is in place for additional high field upgrades. However, this requires more infrastructure.

For the all superconducting case, a significant helium liquification plant, a modest dc power, and water cooling utilities are required. For the hybrid form, 12 MW of dc electrical power are needed, and a cooling water system sized to take those 12 MW of heat away along with an additional 1 MW of cooling overhead for the dc power supply makes the utilities a significant an effort. The hybrid method is preferable, because it allows an upgrade path to 60 T when the technology becomes available.

To realize the full scientific impact of a high field neutron scattering facility, thermal control of the sample from the extreme cryogenic limit of 50 mK to high temperatures 1,000°C will be necessary. This is feasible but must be planned for and built into the system from the start.

Table 2.8. Key instrument parameters for ZEEMANS

Source	STS
Moderator type	Cold, coupled H ₂
Wavelength range (diffraction and SANS)	1 Å ≤ λ ≤ 10 Å
Inelastic energy range	10 meV ≤ E _i ≤ 200 meV
Resolution	1% ≤ ΔE/E _i ≤ 15%
Sample size range (beam size)	maximum: 2 × 2 cm ²
Moderator—sample distance	60 m
Sample—detector distance	5 m
Detector type	³ He LPSD

References

- [1] National Research Council (US). Committee on Opportunities in High Magnetic Field Science., National Academy of Sciences (US) and National Science Foundation (US), Opportunities in high magnetic field science. 2005, Washington, D.C.: National Academies Press.
- [2] National Research Council (US). Committee to Assess the Current Status and Future Direction of High Magnetic Field Science in the United States., National Academy of Sciences (US), High Magnetic Field Science and its Application in the United States. 2013, Washington, D.C.: National Academies Press.
- [3] A. T. Savici and G. E. Granroth, in SNS Technical Report, SNS-NSSD-TOF-TR-0002-R00 (2009).
- [4] G. E. Granroth, et al., in ICANS XIX, 19th meeting on Collaboration of Advanced Neutron Sources.
- [5] A. T. Savici, et al. J. Phys.: Conf. Ser. 251 0120573 (2010).

3. GRAND CHALLENGES IN BIOLOGY

P. Langan (Biology and Soft Matter Division)

Gaining a predictive understanding of the behavior of complex biological systems is one of the greatest scientific challenges that we will face over the next decade. This understanding will guide us in protecting and repairing physiological systems, allow us to mimic the architectures and processes of living systems to create new biomaterials and bio-inspired technologies, and provide the information necessary to manipulate microorganisms and their ecosystems to create new biotechnology and biorefinery solutions to emerging energy and environmental challenges. A workshop at the University of California, San Diego (UCSD) engaged the scientific research community in further identifying grand challenges in biological sciences that ORNL's neutron user facilities can help to address. The major workshop outcome was that neutrons can provide several types of unique information that will be important in addressing the identified challenges. Areas where neutron scattering is poised to have a major potential impact include membrane associated biological processes and the dynamic assembly and regulation of large biological complexes.

Neutron scattering will be applied most powerfully if combined with advanced deuterium labeling techniques and high performance computing. Neutrons are highly sensitive to hydrogen (H), the most abundant element in biological systems, and are sensitive in a different way to its isotope deuterium (D). This sensitivity to H and D allows for enhancing the visibility of specific parts of complex biological systems through isotopic substitution. Computer simulations using high performance computing allow for prediction and interpretation of neutron scattering data from systems that are too complex for analytical theory. Neutrons will also be applied most powerfully when combined with complementary experimental techniques that use photons and electrons. Photons and electrons interact with the atomic electric field and are most sensitive to heavy atoms; with just one electron, H is all but invisible. Neutrons interact with nuclei; light atoms such as H are highly visible. Neutrons are also complementary to photons and electrons because they cause little radiation damage and are highly penetrating, enabling use of complex sample environments. These properties allow neutron scattering to be used to obtain precise information on the location and dynamics of H at the atomic level, as well as truly unique information on large, dynamic, multidomain complexes at longer length and time scales using contrast variation.

Despite the advantages in using neutron scattering, significant technical gaps must be bridged not only in neutron scattering instrumentation but also in molecular biology, deuterium labeling, and computational technologies. These gaps, which are discussed in this report, include

- the need for more advanced deuterium labeling techniques,
- better access to neutron beam lines,
- increased neutron flux on available beam lines,
- neutron beam lines optimized for membrane diffraction,
- the development of innovative techniques for polarizing neutron beams and H atoms in samples to enhance scattering power and to dynamically control scattering contrast,

- the development of new instrumentation that allows simultaneous access to broad regions of time and space,
- better integration of high performance computing techniques with neutron scattering experiments, and
- the development of computational tools that allow the combination of experimental data from multiple complementary techniques to generate more complete models of complex biological systems.

Furthermore, a major effort must be made to recruit a larger segment of the biology community to the new neutron resources that are becoming available at ORNL. Bridging those gaps will allow neutrons to be used in a transformative way to unify the structural and dynamical description of biological systems across length and time scales. This will transition the concept of a predictive understanding of biological systems to a reality. Emerging grand challenges at the interface of biology and neutron science over the next 10 years, and our recommendations to ORNL to help address them, are given below.

3.1 10 GRAND CHALLENGES

1. **Bioengineering:** Understand and redesign plants, organisms, and enzymes with new or improved properties and function.
2. **Drugs:** Design multibillion dollar drugs for human disease targets that have better target specificity, improved binding, and no susceptibility to drug resistance.
3. **Integration of structure and dynamics:** Unify the structural and dynamical description of biological systems.
4. **Living cells and microorganisms:** Understand how multidomain and multicomponent molecular complexes are assembled and regulated during life processes, by dynamically visualizing and (computer) simulating complete living cells and microorganisms.
5. **Complex biological systems:** Seamlessly integrate information from different experimental techniques across length and time scales and across different information types, using computational methods to obtain a predictive understanding of complex biological systems such as plant cell walls, complete living microorganisms, and multicellular systems such as microbial communities and the brain, from DNA sequences to systems biology.
6. **Biomaterials:** Understand the basic scientific principles that underpin photosynthesis, and other biological processes, as a basis for new manmade systems.
7. **Biotechnology:** Transition from a biorefinery concept to its realization.
8. **Membranes:** Understand natural bilayer membrane structure and dynamics; fusion; and vesicle, pore, and domain formation. Understand the structural and functional interplay between membranes and other molecules; membrane protein folding, structure, and function; and perturbation of membranes in disease.

9. **Disorder and Flexibility:** Understand the roles of disorder and flexibility in biological systems; molecular communication mediating signaling and regulatory functions.
10. **Kinetic Processes:** Determine the kinetics of signaling events within multiprotein assemblies.

These grand challenges are a summary of several discussed in this report. Also discussed is how the advanced neutron user facilities at ORNL can provide unique information to address these grand challenges. The new knowledge afforded will complement and extend information obtained from other user facilities utilizing techniques employing, for example, photons or electrons. Neutrons can probe large ranges of length and time scales, from Å to microns and picoseconds to microseconds; furthermore, neutrons are ideal for studying multiscale phenomena intrinsic to biological processes.

3.2 RECOMMENDATIONS

1. **Cold neutron flux:** Radically increase the flux of neutron beam lines at long wavelengths, in particular for small-angle scattering, crystallography, and spin echo.
2. **Deuteration:** Establish advanced deuteration and sample preparation expertise and facilities.
3. **Access to facilities:** Improve access to neutron beam lines and high performance computing.
4. **New beam lines:** Build an improved spin echo beam line and a second beam line for studying aligned samples of membranes and biological fibers.
5. **Computational tools:** Develop improved computational methods and tools that exploit high performance computing and that can integrate diverse experimental techniques with models and calculations.
6. **Living cells:** Develop new cell and molecular biology techniques that will allow biological processes to be followed within living cells, model protocell platforms, and microorganisms using neutron scattering in combination with deuterium labeling.
7. **Time-resolved studies:** Develop technologies that allow more rapid data collection for time-resolved studies of kinetic processes.
8. **Experiment and theory:** Develop a rigorous link from the theory of atomic systems to experimentally observable quantities.
9. **Data sharing:** Develop integrated repositories for sharing data and computational tools for seamless access to complementary data for model building and systems analysis.
10. **Community outreach:** Expand community awareness of the advantages of neutron scattering and recruit the biology community to the neutron sources that are available. At present the number of experiments that can be accommodated on available neutron beam lines is limited by the relatively weak flux of neutron beam lines. Accommodating more investigators will therefore require enhancing the efficiency of neutron beam lines to increase access.
11. **Flagship experiments:** A small number of systems should be targeted for programs that can drive the technological developments, as discussed in the body of the report.

12. Improve integration of neutron and x-ray scattering

On the following pages, we present examples of studies that may be performed on instruments at the Second Target Station (STS) at ORNL's Spallation Neutron Source (SNS) or on new instruments installed at an upgraded HFIR cold guide hall.

3.3 DYNAMICALLY POLARIZED CRYSTALLOGRAPHY (DYPOL) FOR STS

JK Zhao, ISD, and D. Myles, BSMD

Abstract

The Dynamically Polarized Crystallography (DyPol) instrument at the STS will deliver a > thousandfold gain in performance for diffraction analysis of hydrogenous materials and enable breakthroughs in our understanding and control of complex biological systems. Polarizing the neutron beam and aligning the proton spins in a polarized sample drastically change the coherent and incoherent neutron scattering cross-sections of hydrogen, amplifying the coherent scattering by almost an order of magnitude and suppressing the incoherent background to zero. Harnessing this revolutionary technology at STS will drive advances in bioenergy materials and biofuel production, synthetic biology, new diagnostics, and therapeutics of disease.

Science Case

Visualizing H atoms in biological materials is one of the biggest remaining challenges in biophysical analysis. While NMR and x-ray techniques have unrivaled capacity for high-throughput structure determination, neutron diffraction is uniquely sensitive to H atom positions in crystals of biological materials and can provide a more complete picture of the atomic and electronic structures of bio-macromolecules. This information can be essential in providing predictive understanding and engineering control of key biological processes—for example, in catalysis, ligand binding, and light harvesting—and to guide bioengineering of enzymes and drug design. Realizing this potential using neutrons requires breakthrough advances that will produce 100–1,000 gains in performance and has been identified by the structural biology community as a key scientific driver and technological challenge.

DyPol will meet this challenge at STS and deliver > thousandfold gains for diffraction analysis of hydrogenous materials by combining (1) a high intensity STS polarized neutron beam line (> twenty-fivefold gain over MaNDi at FTS) with (2) a revolutionary dynamic polarization sample environment that will align the spin of hydrogen nuclei in the sample, which amplifies the coherent scattering term by a near-order of magnitude and simultaneously suppresses the incoherent background to zero (> hundredfold gains in signal to noise ratio of the diffraction data) (Fig. 3.1). Harnessing this disruptive new technology will deliver breakthrough capabilities at STS, removing the intrinsic limitations of sample background limited diffraction and tuning and maximizing the scattering from—and visibility of—hydrogen atoms in biological materials. This will break through a critical threshold in application of neutrons in biology by enabling analysis of radically smaller samples than has been possible to date and will open the way to fundamentally new science by permitting the following:

1. Analysis of novel macromolecular structures and rapid structure-activity analysis for the development of inhibitors to human disease targets, engineering enzyme active sites for novel

chemistry, and re-engineering enzymes for design properties such as thermal and acid stability for industrial uses.

2. Analysis of photochemistry in biology: understanding how hydrogen atoms modulate the site energies and spectral properties of pigment-protein complexes in photosynthetic complexes and the light harvesting machinery that converts light to chemical energy.
3. Analysis and refinement of complex active-site electronic structures in metallo-proteins, which are key throughout biology and are used in catalysis, energy capture and conversion, transport and storage, signal-transduction, and genome replication and repair.

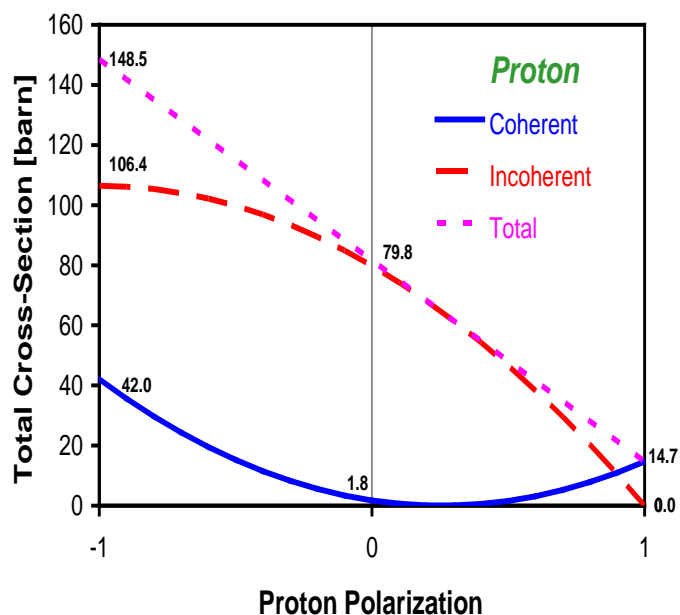


Fig. 3.1. Proton scattering cross-section from polarized neutrons as a function of proton polarization. When protons are fully polarized parallel to the polarization of neutrons, the incoherent cross-section reduces from 79.8 to 0 barns, while the coherent cross-section increases from 1.8 to 14.7 barns.

Initial Science Objectives

1. Photosynthetic machinery

Research Theme's Associated Workshop: Biology

Potential Partners (*Attendees of Associated Workshop):

Robert Blankenship* (Washington University in St. Louis)

Richard Cogdell (University of Glasgow)

An understanding of the molecular details that underlie solar energy capture in photosynthetic organisms will lead to a better understanding of energy transfer in natural photosynthetic systems, and, in addition, will aid in the development of biohybrid photosynthetic systems. Current x-ray crystal structures of photosynthetic machinery reveal details of the pigment-protein architecture and interactions that regulate and control energy transfer but do not resolve hydrogen atoms (Fig. 3.2). This is significant because, in many cases, hydrogen bonding interactions are critically important in the stabilization of antenna pigments and in fine-tuning and control of their site-energies. One of the most

contentious and debated questions concerns how the individual site energies of protein bound chlorophyll molecules are modulated and tuned by local hydrogen bonding and electrostatic interactions with the protein scaffold. The extra level of detail provided by neutron diffraction experiments can contribute to better understanding of the spatio-energetic landscape and exquisitely tuned properties of the photosynthetic apparatus.

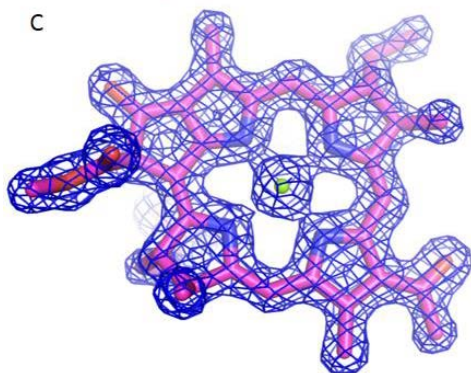


Fig. 3.2. Structure of a bacteriochlorophyll (BCL) pigment from the *P. aestuarii* FMO. While the x-ray structure (blue mesh) shows that the BCL (magenta) is encapsulated entirely within a protein scaffold, DyPol will enable the hydrogen bonding interactions that fine-tune and modulate the energy excitation and transfer energies to be determined precisely.

2. G protein-coupled receptors

Research Theme's Associated Workshop:

Biology

Potential Partners (*Attendees of Associated Workshop):

Geoffrey Chang* (University of California, San Diego [UCSD])
 Robert Lefkowitz (Duke University)
 Brian Kobilka (Stanford University)

G protein-coupled receptors (GPCRs) are involved in a wide variety of physiological processes in humans, where they function in regulating cellular responses to numerous types of external signals. Properly functioning GPCRs are required for human health, and mutations in GPCRs can lead to many different types of acquired and inherited human diseases such as retinitis pigmentosa, cancers, thyroid disorders, and many other endocrine-related disorders. Indeed, 40–60% of all modern drugs target GPCRs.

Fundamental to the drug discovery process is an understanding of the potential molecular interactions drugs can form with GPCRs, in addition to improvement of drugs through subsequent structure function studies of drug-bound GPCRs, and a more complete understanding of GPCR allosteric activation. However, lacking from the x-ray crystal structures of these molecular interactions are the hydrogen atoms, which form the majority of the contacts between GPCRs and drug targets (Fig. 3.3). Knowledge of

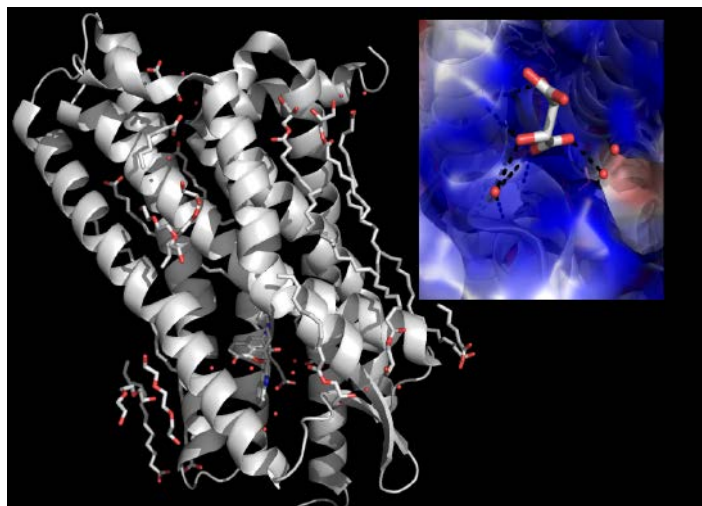


Fig. 3.3. Overall structure of a G-protein coupled receptor (gray).

Inset: hydrogen bonding interactions between the GPCR (surface representations) and a modulator (grey stick representation). Elucidation of the molecular interactions between GPCR and non-covalent modulators is required to ensure the next generation of drugs.

the localization of hydrogen atoms in apo GPCRs, and in their drug bound states, will provide a profound level of information that can ultimately have a major impact on human health.

3. Ribozymes

Research Theme's Associated Workshop: Biology

Potential Partners (*Attendees of Associated

Workshop):

Marin Egli* (Vanderbilt University)

Barry Stoddard (Fred Hutchinson Cancer Research Center)

Jennifer Doudna (University of California, Berkeley)

The central dogma of molecular biology was ultimately altered in 1982 with the discovery of ribozymes. No longer was RNA strictly a transient state of genetic material in the pipeline to produce "true enzymes," the proteins. The discovery of ribozymes demonstrated that RNA can act not only as a genetic template but also as an enzyme, thereby supporting the idea of the RNA origin of life. One of the most studied ribozymes, the hammerhead ribozyme (Fig. 3.4), carries out a self-cleaving phosphodiester isomerization reaction that is accelerated 10,000 times relative to the un-catalyzed reaction. The underlying mechanism of this rate acceleration has been extensively studied, and potentially important nucleotides involved in catalysis are hypothesized, yet there has been no direct observation of the atoms involved in the catalysis because it involves hydrogen atoms. Although some ribozymes are being pursued as potential therapeutic targets, understanding ribozyme mechanism would shed insights into a chemical reaction that was potentially found at the beginning of the biological universe.

Technical Description

DyPol has two key components: (1) A high intensity polarized neutron beam line on STS that will view a coupled moderator and deliver to the sample; and (2) the DNP sample environment, which will be developed, implemented, and optimized at ORNL (once developed, the DNP can be deployed on other neutron beam lines).

Instrument: DyPol will be a 90 m long instrument on a coupled moderator, optimized for a bandwidth of 3 Å, and will deliver broad bandpass ($\delta\lambda/\lambda \sim 25\%$) polarized neutrons produced by a ^3He spin-filter to the sample with as close to 4π detector coverage as achievable. The instrument gain-factor is >25 relative to the FTS MaNDi diffractometer (see the technical discussion on EWALD below).

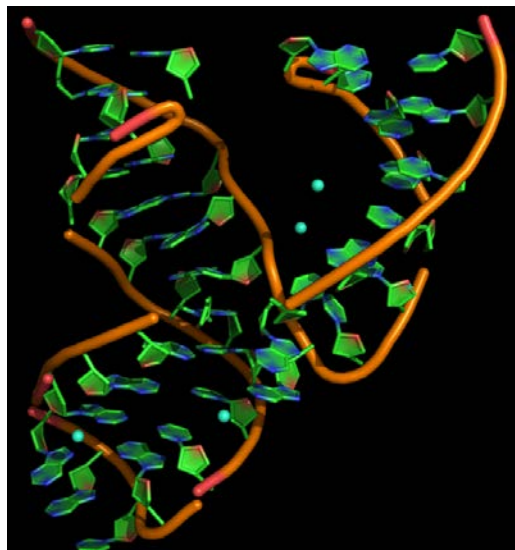


Fig. 3.4. Overall structure of the hammerhead ribozyme.

Although the structure of a ribozyme has been known for over 20 years, no direct observation of the atoms involved in catalysis are known. Metal ions (cyan spheres) and the interactions with the RNA, are known to play a role in the mechanism of this primordial enzyme.

DNP sample environment: The key components of DNP are (1) magnetic fields of $\sim 2.5\text{--}5\text{T}$; (2) 2–4 mm microwaves; and (3) low temperature cryostat with high cooling power (Fig. 3.5). In addition, an NMR system is needed to measure and manipulate the nuclear polarization. Free electron spins are introduced into the sample either by mixing paramagnetic centers into the sample or by radiating the sample with electrons of other ionizing beams. The required 2.5 to 5T magnet field can be supplied by a compact superconducting magnet with field homogeneity of $10^{-4}\text{T}\cdot\text{cm}^{-1}$. Higher magnetic fields will enable higher nuclear polarization and allow a sample to stay polarized longer. The required frequency of the microwave is a function of the magnetic field. For 5T, 2 mm microwave is needed. The required low temperature is supplied by a dilution refrigerator, which needs to be able to remove the heat from the microwave while the sample is being polarized and to maintain the sample at $<100\text{ mK}$ after the polarization process is finished. At temperatures of $<100\text{ mK}$, nuclear spins will be “frozen” in place for an extended period of time, allowing the nuclear polarization to be manipulated by NMR, which will in turn enable advanced scattering techniques.

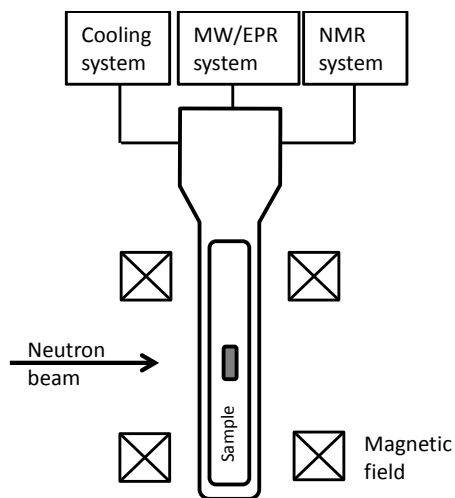


Fig. 3.5. Schematic of the DNP sample environment.

The required 2.5 to 5T magnet field can be supplied by a compact superconducting magnet with field homogeneity of $10^{-4}\text{T}\cdot\text{cm}^{-1}$. Higher magnetic fields will enable higher nuclear polarization and allow a sample to stay polarized longer. The required frequency of the microwave is a function of the magnetic field. For 5T, 2 mm microwave is needed. The required low temperature is supplied by a dilution refrigerator, which needs to be able to remove the heat from the microwave while the sample is being polarized and to maintain the sample at $<100\text{ mK}$ after the polarization process is finished. At temperatures of $<100\text{ mK}$, nuclear spins will be “frozen” in place for an extended period of time, allowing the nuclear polarization to be manipulated by NMR, which will in turn enable advanced scattering techniques.

Additional R&D: Possible modification/development of detector types to compensate for the stray magnetic field produced by the 2 T holding field.

3.4 EWALD: ENHANCED WIDE ANGLE LAUE DIFFRACTOMETER FOR STS

Leighton Coates, Biology and Soft Matter Division

Abstract

EWALD is designed to study small single crystal protein samples typically 0.001 mm in volume with unit cell edges greater than 100 \AA on edge. This will open new frontiers in neutron structural biology by enabling x-ray sized crystals to be used for neutron experiments. Protein crystals are typically weakly scattering and can only be grown to small volumes, thus EWALD will benefit significantly from the $\times 10$ high brightness of the STS coupled moderator. Advances in neutron detector technology and instrument design will result in a gain factor of around $40\times$ in performance compared to MaNDi at the Spallation Neutron Source’s first target station.

Science Case

One common and large capability gap for all atomic resolution single crystal neutron diffractometers is the weak flux of available neutron beams, which results in limited signal-to-noise ratios, giving a requirement for samples volumes of at least 0.1 mm^3 . A community driven workshop in January 2014 at the University of California, San Diego, identified as the number one priority the ability to collect data from protein crystals an order of magnitude smaller than can currently be collected on MaNDi. The ability to operate on crystals an order of magnitude smaller, $\sim 0.01\text{ mm}^3$, will open up the new and more complex systems to studies with neutrons including the development of improved drugs against

multiresistant viruses and bacteria, understanding enzyme mechanisms, and the regulation of metabolic pathways for synthetic biology.

Resistance to antibiotics poses a major global threat to public health [1]; the World Health Organization (WHO) analyzed data from 114 countries and concluded resistance was happening in every area in the world [2]. Unfortunately, we are moving toward a post-antibiotic era, in which people die from simple infections that have been treatable for decades. Two key antibiotics no longer work in more than half of people being treated in some countries. One of them—the β -lactam antibiotic carbapenem—is the so-called “last-resort” drug used to treat people with the most serious life-threatening infections such as pneumonia and bloodstream infections caused by the bacteria *K. pneumoniae*. Neutron diffraction studies on the New Delhi metallo- β -lactamase enzyme, NDM-1, will reveal how it interacts with carbapenems and will help explain how this particular β -lactamase is able to break down last choice antibiotics.

Initial Science Objectives

1. Protein nucleic acid complexes

Research Theme’s Associated Workshop: Biology

Potential Partners (*Attendees of Associated Workshop):

Martin Egli* (Vanderbilt University)

Walter Chazin* (Vanderbilt University)

John Tainer* (Scripps Institute)

DNA polymerases play fundamental roles in maintaining the integrity of the genome from one generation to the next. Ever since their discovery in 1956, DNA polymerases have been extensively studied to reveal how these enzymes replicate genomic information with remarkable accuracy. Many high-resolution x-ray structures of DNA polymerases have been solved (Fig 3.6.). With the snapshots provided by x-ray crystallography, mechanisms of how DNA polymerases incorporate nucleotides and discriminate the correct nucleotide from the incorrect ones have been proposed. However, there is no direct evidence because hydrogen atoms are missing in those snapshots. Determination of hydrogen atom positions will allow for elucidation of how DNA polymerases discriminate and incorporate nucleotides and how spontaneous mutations may arise during this process. This information will fill fundamental gaps in enzymes that are linked to numerous cancers and are potential therapeutic targets.

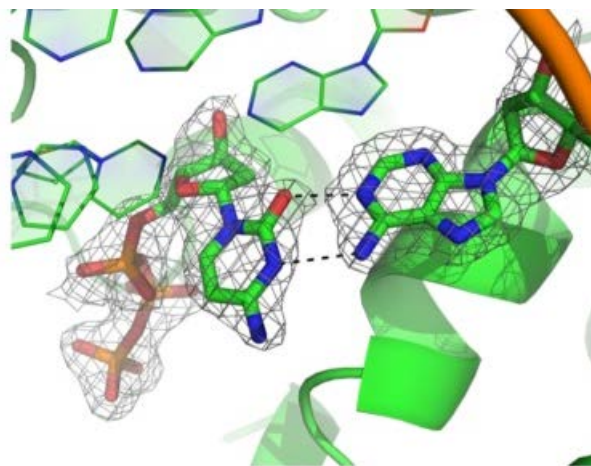


Fig. 3.6. The DNA polymerase active site.

Inter-base hydrogen bonding interactions (dashed lines) are important for polymerase mechanism and fidelity, yet are not visible in electron density maps (gray mesh) from X-ray crystallographic experiments.

2. HIV Reverse Transcriptase

Research Theme's Associated Workshop: Biology

Potential Partners (*Attendees of Associated Workshop):

Irene Weber* (Georgia State University)
Robert London (National Institutes of Health [NIH])
Wei Yang (NIH)
Eddy Arnold (Rutgers University)

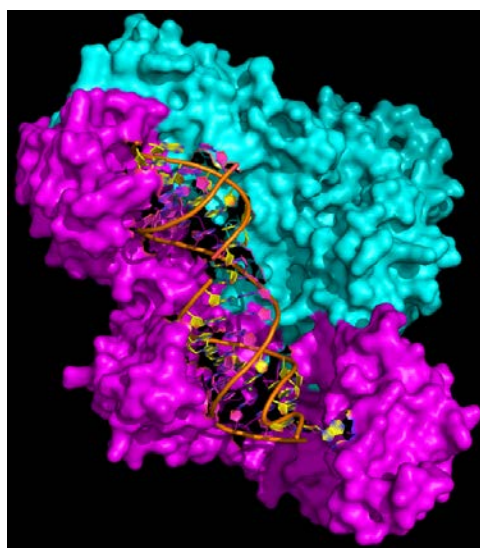
Replication of retrovirus, such as HIV, requires the activity of a reverse transcriptase (RT) to generate a complementary DNA strand from the viral RNA genome. This process requires three separate enzymatic activities to be encoded in a single protein:

1. RNA dependent DNA polymerase activity to synthesize the complementary viral DNA genome and a DNA/RNA heteroduplex.
2. RNaseH activity to degrade the RNA strand of the DNA/RNA heteroduplex.
3. DNA dependent DNA polymerase activity to synthesize the duplex DNA strand from the single stranded complementary DNA strand.

The HIV RT is a metamorphic enzyme with two polypeptides that dimerize, known as P51 and P66, with identical amino acid sequences folding into two different tertiary structures, each with distinct enzymatic activities (Fig. 3.7). Over 60% of all HIV drugs target the HIV RT and specifically bind to the active site, dimerization interface, or allosterically inhibit the enzyme. Although many effective HIV RT drugs exist, the incorporation of spontaneous drug resistance mutations can reduce drug efficacy. There is a need to fully understand and identify all of the potential drugable sites in the HIV RT and how to potentially expand the current drugs to be effective against resistance mutations. Neutron crystal structures of the HIV RT bound to duplex DNA and heteroduplex DNA/RNA and bound to the different classes of HIV RT drugs will aid in supplying new drug leads to the pipeline required to constantly address HIV drug resistance mutations.

Fig. 3.7. Overall structure of the HIV-1 RT.

The HIV RT is composed of two conformationally distinct subunits, P66 (magenta) and P51 (cyan), that fold from an identical polypeptide. Mutations arising in both subunits are a major cause of drug resistant HIV cases. The molecular interactions between the RT and drugs, which largely mediated by hydrogen atoms, need to be studied at a level of detail that can only be provided by neutron diffraction experiments.



3. Protein Kinases

Research Theme's Associated Workshop: Biology

Potential Partner (*Attendees of Associated Workshop):

Susan Taylor* (University of California, San Diego)

Protein kinases are involved in the regulation of a number of signaling pathways in human cells through the phosphorylation of proteins involved in signal transduction pathways. Estimates suggest as much as 30% of the proteins encoded by the human genome are targets of protein kinases and hyper/hypo-malfunctioning kinases have a significant impact on human health. Protein kinases are the second most prevalent drug target, after G protein coupled receptors, in human pharmacotherapy. The protein kinase family is diverse, yet the most studied and viewed as a model for all kinase enzymes is protein kinase A (PKA) (Fig 3.8). Numerous kinetic, structural, and theoretical methods have studied the PKA mechanism, which has been hypothesized to be an S_N2 nucleophilic substitution reaction involving an active site proton transfer. However, without knowing the position of the hydrogen atoms in PKA, it is not known whether the proton transfer from the nucleophile happens before the phosphoryl transfer or after the reaction has gone through the transition state. Neutron crystallography is the only technique that will allow for visualization of the active site hydrogen atoms of PKA, allowing for detailed insights into this important class of regulatory proteins.

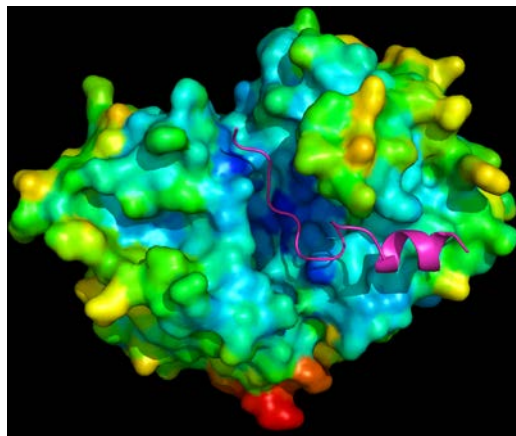


Fig. 3.8. Overall structure of protein kinase A (surface representation) bound to a substrate analog peptide (magenta).

Peptide substrate phosphorylation by protein kinase is an important regulatory response in many signaling pathways relevant to human pathology, yet a detailed understanding of mechanism has not been presented through X-ray crystallographic experiments.

Technical Description

Smaller beam sizes and high-brilliance cold neutron fluxes will allow for much smaller samples of more complex systems to be studied, thus allowing high-resolution neutron crystallography to be applied to characterize membrane proteins and their function for the first time. Spanning this sample-size capability gap would provide new opportunities for using neutron crystallography in the development of improved drugs against multiresistant viruses and bacteria, understanding enzyme mechanisms, and the regulation of metabolic pathways for synthetic biology.

This gap will be closed by increasing neutron flux, increasing detector coverage by adding more detectors to maximize data collection efficiency, using longer wavelength neutrons to maximize reflectivity, or preparing deuterated samples to increase the scattering power of samples.

Moderator comparison for protein crystallography

The coupled para-hydrogen moderators proposed for STS will have a bit larger FWHM (full width at half maximum; 49 and 172 μsec at 2 and 5 \AA respectively) and are expected to have $10 \times$ the brightness ($3 \times 3 \text{ cm}^2$) relative to the first target station coupled $10 \times 12 \text{ cm}^2$ moderators that MaNDi currently views now (Table 3.1).

Table 3.1. First target station source parameters

λ (Å)	Decoupled, poisoned para-hydrogen		Coupled para-hydrogen	
	FWHM (μsec)	Integrated intensity (n/ster/pulse/eV)	FWHM (μsec)	Integrated intensity (n/ster/pulse/eV)
2.02	17.4	2.35×10^{13}	43.1	1.20×10^{14}
5.09	45.1	5.07×10^{13}	156	4.65×10^{14}

MaNDi currently has a total flight path length (moderator-sample-detector) of 30.45 m. To get approximately the same timing resolution, one needs an instrument at STS that is 2.5 to 3.5 times longer to account for the moderator pulse width difference at 2 or 5 Å, respectively. Taking a factor of 3 as a reasonable compromise, one gets a total instrument length of around 91.35 m including the detector distance from sample. At this length and a 10 Hz repetition rate, the instrument will have a bandwidth of 4.33 Å, perfect for neutron protein crystallography. At 60 Hz, MaNDi has a bandwidth of 2.17 Å, but MaNDi often operates at 30 Hz, which doubles that to 4.33 Å, which is perfectly matched by the proposed STS instrument. The penalty in repetition rate is then 10 Hz/30 Hz = 0.333. The gains are 10 (brighter moderator) × (ratio of FTS coupled/decoupled moderator intensity) × 1.5 for detectors. Therefore, expect a count rate gain of 25 and 45 at 2 and 5 Å, respectively.

Table 3.2. Key instrument parameters for EWALD

Source	STS
Moderator type	Cold, coupled H ₂
Wavelength/energy range	2–8 Å
Resolution $\Delta d/d$	0.0015
Sample size range (beam size)	1 mm ²
Moderator—sample distance	90 m
Sample—detector distance	0.35 m
Detector type	Anger camera detectors

References

- [1] S. Drawz and R. Bonomo, “Three Decades of β -Lactamase Inhibitors.” *Clinical Microbiology Reviews* **23** (1): 160–201 (2010).
- [2] “Antimicrobial resistance global report on surveillance: 2014 summary.” World Health Organization. WHO/HSE/PED/AIP/2014.2.

3.5 COLD NEUTRON DIFFRACTOMETER WITH POLARIZATION FOR QUASI-CRYSTALLINE MATERIALS (ALIGN)

J. Katsaras and P. Langan, BSMD

Abstract

A proposed high-resolution, low-background horizontal scattering diffractometer, ALIGN, will enable studies of aligned membranes (stacks of multibilayers) and fibrous materials (e.g., biomass, biological polymers, muscle, etc.). The realization of such an instrument will bridge a capability gap, enable new science and engage a new community of researchers.

Science Case

For bilayers, ALIGN with its suite of one- (1D) and two-dimensional (2D) detectors will have the ability, for example, to simultaneously collect both 1D specular data associated with structure perpendicular to the bilayer normal and 2D non-specular data arising from in-plane structure. For fibrous biological tissues and polymers, the large 2D detector of ALIGN, with high spatial resolution, will allow fiber diffraction patterns to be collected. The instrument will allow flexible selection of incidence wavelength ($3 \text{ \AA} < \lambda < 5 \text{ \AA}$) and sample to detector distance, making it suitable for characterizing structure both in the nanometer and \AA range.

1. **Instrument optimized for aligned stacks of membranes and fibers.** Neutron beams, for the most part, lack considerable beam intensity. This, in conjunction with the sample background arising from the incoherent scattering from hydrogen (biological and soft materials are inherently hydrogen rich), ultimately determine the limit for structural resolution. The primary goal of the ALIGN diffractometer is to maximize the signal-to-noise ratio, but not at the expense of spatial resolution. This will be achieved using highly aligned samples, a focusing monochromator, low background sample environments, judicious shielding of materials, and neutron polarization techniques.
2. **Aligned and fiber samples.** Compared to isotropic samples (i.e., powders), aligned systems generally offer a better signal-to-noise ratio, resulting in better resolved structural information and the potential to clearly differentiate between signals arising from in-plane and out-of-plane structure.
3. **Dedicated sample environments.** The instrument's horizontal scattering geometry requires that samples adsorbed to solid supports (e.g., Si) are hydrated either from liquid water or at some percent relative humidity. For high-resolution 1D measurements, flat supports will be used, but in the case of lower resolution 2D measurements, membranes can be coated onto cylindrical supports, giving rise to in-plane and out-of-plane structure data simultaneously. Fiber or tissue samples will be mounted on a goniometer, which will allow coordinated movement of the sample and, in conjunction with the 2D detector, will be able to map out complete regions of cylindrical reciprocal space.
4. **High-resolution structural data resulting in better biological models.** The higher resolution structural data that can be obtained from ALIGN will restrict the number of models that can fit the experimental data, giving rise to a more accurate description of the real system.

5. **AND/R instrument at NIST.** The proposed instrument will make use of developments implemented over the past decade at the advanced neutron diffractometer/reflectometer (AND/R) at NIST.

Initial Science Objectives

1. Lipid Rafts

Research Theme's Associated Workshop: Soft Matter

Potential Partners (*Attendees of Associated Workshop):

G. W. Feigenson (Cornell University)

G. Pabst (University of Graz)

E. London (Stony Brook University)

Cell membranes, once thought to be homogeneous assemblies of lipids and proteins, are now believed to contain nanoscopic domains ("lipid rafts") (Fig 3.9). It is widely accepted that rafts play a central role in cellular processes, notably signal transduction. Recently, we have used small-angle neutron scattering (SANS) to determine the size of nanoscopic membrane domains in unilamellar vesicles using a four-component model system—SANS data were fit using Monte Carlo analysis. Employing the proposed ALIGN instrument and selective deuteration, the size and lateral ordering, if any, of nanoscopic domains can be obtained directly (in-plane scattering), including the thickness of the liquid-ordered and liquid-disordered phases (out-of-plane scattering), something we are unable to determine by SANS when both phases are present. From these and complementary SANS experiments, we will be able to determine, for the first time, the role of line tension in controlling domain size in model membranes, and possibly even in real membranes.

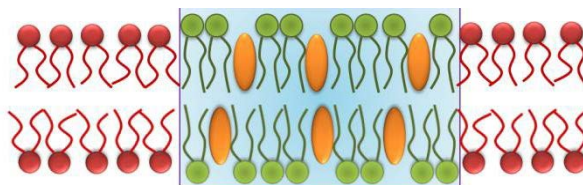


Fig. 3.9. Schematic diagram of a raft-containing lipid bilayer.

The raft and its surrounding lipid bilayer can have different thicknesses, depending on the size of the raft.

2. Biomass to bioethanol conversion cycle optimum utilization: Lignin Fiber structure

Research Theme's Associated Workshop: Soft Matter

Potential Partners (*Attendees of Associated Workshop):

Brian Davison (ORNL Biosciences Division)

Richard Dixon (University of North Texas)

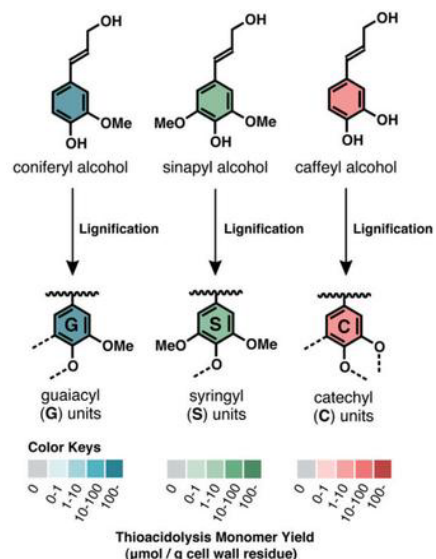
C-Lignin comprising only catechyl alcohol units that are completely non-methylated and form a linear homopolymer can be derived from the seed coats of a larger number of unrelated and relatively exotic plant species, both monocots and dicots, and is a very interesting polymer (Fig 3.10.). In the species so far examined in which this C-lignin co-exists with mixtures of guaiacyl (G) and syringyl (S) G/S lignin (G/S), it is not attached to the classical lignin polymer. We propose the C-lignin represents an ideal system for relating the physical properties of lignin to computational simulations in a quantitative way.

The importance of quantified verification is that it allows the extension of molecular dynamics approaches to more complex lignin molecules with a high degree of confidence. Further, the presence of naturally high levels of C-lignin in *Jatropha curcas* seed coats, a high volume by-product of biodiesel production from the seed oil of this species, suggests a near term resource for exploitation of this polymer.

The linear form of this homopolymer could exhibit reasonable crystalline nature in one direction such as fibers, and understanding the interactions that promote such forms would enable critical values to the novel form of lignin material.

Fig. 3.10. Seed Coat Lignin Compositions of Euphorbiaceae and Cleomaceae Plants.

Yields of monomeric guaiacyl (G), syringyl (S), and catechyl (C) type trithioethylpropylphenols ($\mu\text{mol/g}$ cell wall residues) released by analytical thioacidolysis (taken from Tobimatsu et al., *The Plant Cell*, 25, 2587 [2013]).



3. Protein misfolding

Research Theme's Associated Workshop: Biology and Soft Matter

Potential Partners (*Attendees of Associated Workshop):

Richard Kriwacki (St Jude Children's Research Hospital)

Zimei Bu (City College of New York)

Amyloid plaques comprising misfolded proteins are the hallmark of several presently incurable diseases, including Alzheimer's, Parkinson's, Huntington's, type-II diabetes, Creutzfeldt-Jakob, and others. The interaction of these proteins with the surface of lipid bilayers is of fundamental importance as it relates to the above-mentioned protein-misfolding diseases. Although the aggregation of amyloid-forming proteins has been extensively studied in bulk solution, very little is known about protein aggregation associated with membrane surfaces (Fig. 3.11). A detailed understanding of how these proteins aggregate and are stabilized could provide new insights into the toxic effects associated with these diseases. The ALIGN instrument will be used to study membrane-induced cross-fibrillation of amyloidogenic peptides using oriented membranes to better understand how lipid membrane surfaces mediate and influence protein aggregation as well as how they may be targeted by toxic protein aggregates.

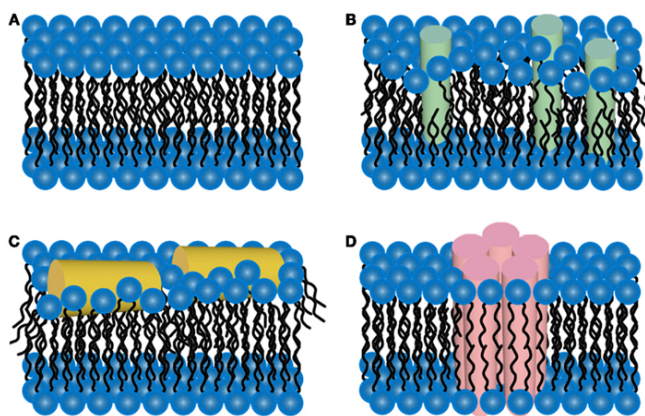


Fig. 3.11. Schematic representations of different amyloid/lipid association scenarios.

(A) Unperturbed lipid bilayer. (B) Amyloid-protein insertion or (C) surface association. (D) Aggregation of amyloid-forming proteins [1].

4. Fiber Diffraction of Cellulose

Research Theme's Associated Workshop: Biology

Potential Partners (*Attendees of Associated Workshop):

Daniel Cosgrove (Pennsylvania State University)

Brian Davison (ORNL Biosciences Division)

Blake Simmons (Sandia National Laboratory)

Cellulose, the most abundant renewable material on earth, is biosynthesized by polymerization of glucosyl residues at the cell membrane by an ordered synthase complex, followed by assembly of the extended parallel chains into nanometer thick crystalline microfibrils. In effect, the synthase complex acts as a biological spinneret producing high tensile strength microfibrils as the fundamental structural unit in the cell walls of plants and certain algae, bacteria, fungi, sea animals and amoebae. A number of industrial applications involve biological or chemical conversion of cellulose into bioproducts, such as biofuels or plastics. Further, cellulose fibers can be isolated and then used in new composite materials, such as films and gels. Neutron fiber diffraction studies based in Europe have played a leading role in revealing the fundamental structure and properties of cellulose. Fibers are characterized as consisting of structural aggregates that are preferentially aligned along a particular direction, called the fiber axis, but that have random orientation about this direction. No existing neutron beam line at ORNL is capable of collecting diffraction data to atomic resolution from biological fibrous tissues. The proposed ALIGN beam will bridge a capability gap in the US for neutron fiber diffraction and will provide transformative opportunities for developing and characterizing new cellulosic materials. ALIGN also will create a new community of researchers who study other fibrous systems ranging from muscle to synthetic polymers and polymeric assemblies such as DNA and filamentous viruses.

Technical Details

The instrument will be located at HFIR on a cold neutron guide, outfitted with polarization capabilities (both incident and diffracted sides). A suite of 1D (pencil) and 2D (area) detectors will be used for high- and lower-resolution studies, respectively. The diffractometer will have adjustable incident and diffract side collimation and an adjustable sample-to-detector distance (SDD). A pyrolytic graphite focusing monochromator will be used to take full advantage of a tall incident beam of neutrons (i.e., ~ 15 cm tall) with a $\Delta\lambda/\lambda \sim$ of a few %, thus allowing optimization of neutron flux on the sample (or detector) at the expense of an acceptable increase in beam divergence and energy resolution. The instrument will be capable of measuring both specular and non-specular diffraction from aligned membrane (multibilayers) and complete diffraction patterns from fibrous materials.

Incoherent scattering is formidable for hydrogen-rich materials because of hydrogen's (^1H) intrinsically large incoherent scattering cross section. Incoherent scattering, which contributes to the background noise signal, determines the limit of maximum momentum transfer ($Q = 4\pi \sin(\theta) / \lambda$, where λ is the neutron wavelength and 2θ is the scattering angle) that can be realistically analyzed from a neutron scattering experiment. Because of this high background signal, a great deal of the system's structural information is irretrievably lost (i.e., the signal is buried in the noise). By either reducing or eliminating the background noise, the usable Q-range can be extended, resulting in higher fidelity data and, ultimately, better resolved and robust structural features. Maximum momentum-transfer can be extended through various means, including the suppression or elimination of the incoherent background signal. Spin-polarized neutrons, which are produced using spin-filters such as Heusler crystals, polarizing supermirrors, and polarized ^3He , are one way to address the incoherent background problem (substituting deuterium for hydrogen is another) in the case where multiple scattering from the sample

is minimal, and the 1/3–2/3 rule of incoherent scattering applies. Importantly, however, the polarization capability will allow for the use of magnetic reference layers for the direct inversion of diffraction data. The optional polarized-beam setup will include two sets of polarizers and neutron spin-flippers. In the high-resolution mode (1D pencil detector), the incident neutron beam polarizing assembly (i.e., before the sample) will be a high reflectivity Fe/Si supermirror, and the same setup will be repeated at the analyzer position (after the sample). In the case of lower resolution data (2D detector), the Fe/Si supermirror analyzer can be replaced with a ^3He analyzer.

The pyrolytic graphite focusing monochromator increases the neutron flux on the sample. It will consist of a series of 002 ($d = 3.335 \text{ \AA}$) oriented pyrolytic graphite plates (containing nearly perfect crystallites) mounted on a focusing assembly, which will accept the full height (15 cm) of the incident neutron beam. Immediately after the monochromator, a liquid nitrogen-cooled beryllium filter will be placed to remove neutrons with wavelengths $< 3.97 \text{ \AA}$, which can potentially increase background and contribute to higher order Bragg scattering.

Table 3.3. Key instrument parameters for ALIGN

Source	HFIR
Moderator type	HFIR Cold Source
Wavelength range	$3 \text{ \AA} < \lambda < 5 \text{ \AA}$
Resolution	$Q \sim 20 \text{ \AA}^{-1}$ $\Delta\lambda/\lambda \sim 1\text{--}4\%$
Sample size range (beam size)	2.5–10 cm diameter Si wafers
Sample-detector distance	1–2.5 m
Detector type	1D ^3He pencil and 2D detector with 2 mm resolution

Reference

[1] Burke, et al., *Frontiers in Neurology* **4**, 1 (2013).

3.6 NEUTRON RADIOGRAPHY AND TOMOGRAPHY STATION (NEURATOM)

Hassina Bilheux, CEMD

Abstract

Imaging with cold neutrons is an important part of ongoing science in engineering materials and geosciences and is an increasingly key component in plans for imaging of biological systems. We propose to build a novel grating-based cold neutron imaging beam line, Neutron Radiography and Tomography Station (NEURATOM), which will utilize cold neutrons to detect small changes in samples such as small amounts of hydrogen atoms in geological, biological, and engineering samples.

A unique complementary set of data including attenuation, differential phase, and ultra small-angle scattering will provide micrometer and sub-micrometer structural information that cannot be achieved using current conventional imaging capabilities.

Science Case

Low space resolution (~ 50 microns) will enable measurements of processes with fast dynamics (millisecond events) in areas of research such as functioning complex engineering parts, fracking studies, and fluid flow in geosciences. It will also allow the images of large biological tissues such as tumors. A grating system that can be translated in and out of the beam line provides the advantage to tune the resolution to the science application.

Compared to the existing neutron imaging capability at HFIR, this new concept offers high spatially resolved imaging capability that will open unique new science opportunities for samples that (1) are significantly thinner (a few microns) than what is currently achievable on thick (a few mm) samples, and (2) have low contrast such as in mesoporous carbon electrodes.

- 1–5 microns capability
 - Energy materials: Understanding energy storage device performance is limited by the inability to accurately model lithium (batteries) or hydrogen (fuel cells) distribution around the boundaries of the electrodes and membranes, respectively. Currently, a large portion of the industrial battery/fuel cell research is dedicated to modeling ion transport. High spatial resolution (i.e., 1 micron) neutron computed resolution is the only tool capable of visualizing lithium mass transport in 3D in battery electrodes. The lithium concentration changes in both cathodes and anodes as a function of charge/discharge are essential to validate 3D modeling transport tools. Real time mapping at different C-rates will help understand the rate limitation and the origin of various polarization factors that limit the capacity utilization. The tomography analysis provides the local lithium concentration at a given spatio-temporal location. This information can be utilized to feed a multi-physics based transport model that ultimately forms the basis for a predictive capability for determining the cycle life and safety of Li-ion batteries both at the cell and at system level. Moreover, the edge enhancement provided by neutron phase contrast is key to determining the location of aggregates of atoms in these interface regions (fuel cell membranes).
 - In situ cavitation effects in transportation research injectors
 - Porous quantification in additive manufacturing and geological materials
 - Cellular imaging of biomass and biological tissues
- Sub-micron microscopy (will require longer wavelengths)
 - Energy materials: Reaching high spatial resolution will address important materials properties such as changes in morphology and changes caused by red-ox reactions (dissolution, reduction, nucleation), and elemental 3D mapping of aggregates of atoms under both ex situ and in situ conditions.
 - Subcellular imaging of biomass and biological tissues

H₂O/D₂O contrast variation and selective D-labeling will reveal unique information about the dynamic assembly of functioning biological membranes in living systems.

Technical Description

Compared with thermal and epithermal neutrons, cold neutrons are more sensitive to small changes in a sample and can detect, for example, small amounts of hydrogen atoms in a sample. This makes cold-neutron imaging well suited for engineering samples that have very low hydrocarbon content, such as diesel particulate filters, injectors, or heat exchangers. For large, complex engineering structures, the facility will need to accommodate large samples; a grating set-up that can be translated will be needed when increased contrast and/or high spatial resolution is required (i.e. for energy materials and biological samples).

Preferably, the instrument should not have a guide system. If guides are necessary, the use of a nanoparticle diffuser is required. A variable aperture system with L/D's from 400 to 1,000 is acceptable.

Table 3.4. Key instrument parameters for NEURATOM

Mode	Field of View	Spatial resolution	Time to acquire a radiograph	Detector/capability
Low-resolution (sCMOS)	5 cm × 5 cm	~ 50–100 microns	ms	sCMOS or large-coverage MCP
Medium-resolution	10 cm × 10 cm	50 microns	s	CCD
High-resolution	1 cm × 1 cm	< 100 nm	< 30 min	Gratings

3.7 BARNs (BROAD ANGULAR RANGE NEUTRON SCATTERING)

Sai Venkatesh Pingali and Lili He, BSMD
Kenneth Littrell, CEMD

Abstract

A broad angular range neutron instrument will enable us to acquire structure features that cover a variety of sizes in a single exposure of supramolecular samples, such as cell-substructures, tissues, biomass, fibrils, self-assembly of soft matter, structure of complex fluids, magnetic nanocomposites, structure of porous media, and phase behaviors of metallic materials. Major instrument design improvements such as a better guide system, closer proximity of guides to the cold source, and insertion of beam condensing optics would allow optimal utilization of the HFIR cold source's high brilliance, achieving ~10 times higher overall flux compared to the current flux on Bio-SANS samples.

Science Case

An area of interest related to hierarchically structured systems spanning a large range of length scales requires a significant improvement in the neutron flux and single-exposure accessible Q-range available to the small-angle neutron scattering (SANS) instrument. Recent community workshops (February and March 2014) identified complex biomacromolecules, hierarchical structures, and self-assembled advanced materials advancements as current and emerging fields of significant interest. Broad Angular Range Neutron Scattering (BARNs) will address hierarchical or supramolecular structured systems such as biomass in the biofuel and bioenergy industry, substructures in cells and tissues for medical applications, and fibrils in the medical and advanced materials industries. Capabilities include the following:

1. **Wide Q-range accessible in a single exposure for supramolecular structures.** The study of supramolecular structures will involve variations in neutron signals over multiple orders of magnitude, and the structures will exhibit intrinsically weak to strong scattering characteristics over a wide range of length scales. The ability to examine these systems in a single exposure will enable critical studies that are currently not possible, such as the correlation between structural changes at different length scales of the hierarchical system. These studies will be especially useful for cell function, biomass structural change during chemical and enzymatic breakdown processes, and a reaction process that promotes self-assembly of supramolecular structures. Instruments where a broad Q-space is surveyed and where flux is increased are ideal.
2. **Better time resolution for in situ studies.** Time resolved studies on supramolecular self-assembly or deconstruction processes currently are limited because the same reaction has to be repeated two to three times to access the entire accessible Q-range. Fibril growth from single peptide strands, the breakdown of biomass structures, and the self-assembling process of soft matter are some examples of studies that would benefit from the development of this instrument, which is unlike anything currently available. Using this new instrument, time-resolved, multiple-order length scales studies would unravel a deep understanding of complex processes providing valuable guidance for optimization.
3. **Enhanced neutron flux.** A key requirement for the success of BARNS is improved neutron flux that will benefit the two capabilities suggested above. Increased flux will provide better neutron signal-to-noise ratios over the span of the accessible Q-range, which would consist of several structural features of the hierarchical system.
4. **Polarization analysis enables distinguishing coherent and incoherent scattering and measuring magnetic materials.** The use of the polarized neutron technique on SANS instruments will provide significant results in the field of nano-magnetic structure analysis. Differences between spin-up and spin-down neutron scattering cross sections of magnetic precipitates can be combined with chemical contrast variation to allow analysis of the interference term of nuclear and magnetic scattering, respectively, resulting in extraction of the composition and magnetization profiles of the samples.

Initial Science Objectives

1. Unraveling plant photosynthesis process

Research Theme's Associated Workshop: Biology

Potential Partners (*Attendees of Associated Workshop):

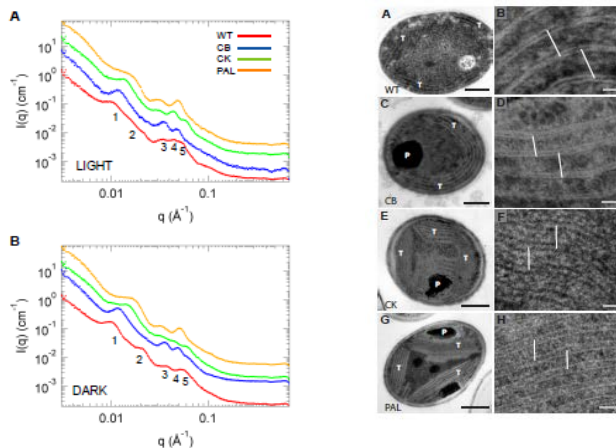
Robert Blankenship* (WUSTL)

Himadri Prakasi (WUSTL)

The thylakoid membrane undergoes significant structural changes between its functionally active (light) and inactive (dark) states. The leaflet spacing within the membrane is responsible for the different peaks, referenced to as 1 to 5 (Fig. 3.12). However, the larger structural features of the cyanobacteria cell are not fully accessible with the current design of this instrument. Furthermore, to obtain these light and dark profiles, the data was acquired over three different configuration settings in a sequential manner. This implies that the ensemble of structures observed in the different configurations could potentially be different because the membrane arrangement is highly sensitive to various environmental

settings. For these reasons, an instrument that provides the capability to obtain structural features over the entire expanded Q-range is highly desirable.

Fig. 3.12. Thylakoid membranes in cyanobacteria mutants and their response to light.
Right panel: Transmission electron micrographs of wild type (WT) and phycobilisome antenna mutants. Whole cell images and enlargements illustrating thylakoid membrane spacing are shown (top to bottom) for WT, and mutants CB, CK, and PAL. *White bars* depict the center-to-center thylakoid membrane spacing. *T*, thylakoid membranes; *P*, polyphosphate bodies. *Scales bars* = 500 nm (*A, C, E, and G*) and 50 nm (*B, D, F, and H*). *Left panel:* SANS data from cyanobacterial cells under light and dark conditions. Scattering intensities from WT (*red*), CB (*blue*), CK (*green*), and PAL (*gold*) in the light (*A*) and dark (*B*) over the entire experimental Q-range are shown. Peaks are labeled 1–5. Intensities of curves were shifted for better readability (taken from Liberton et al., *Journal of Biological Chemistry* 288, 3632 [2013]).



2. Optimization of biomass to bioethanol conversion

Research Theme's Associated Workshop: Biology
Potential Partner (*Attendees of Associated Workshop):

Brian Davison (ORNL Biosciences Division)

Efficient conversion of biomass (Fig. 3.13) to bioethanol is a two-step process: (1) thermochemical pretreatment to break open the complex, composite nature of the biomaterial; and (2) enzyme breakdown of cellulose chains to glucose that is further fermented to ethanol. The purpose of the first step is to improve the efficiency of the second step by increasing enzymatic access to the cellulose chains. However, the recalcitrant behavior of lignin biopolymer renders this process inefficient. The hierarchical nature of this system calls for a technique that examines a wide range of length scales, and the ability to access this range simultaneously especially will assist in observing the effect of the breakdown process over a wide range of sizes of features in this complex system.

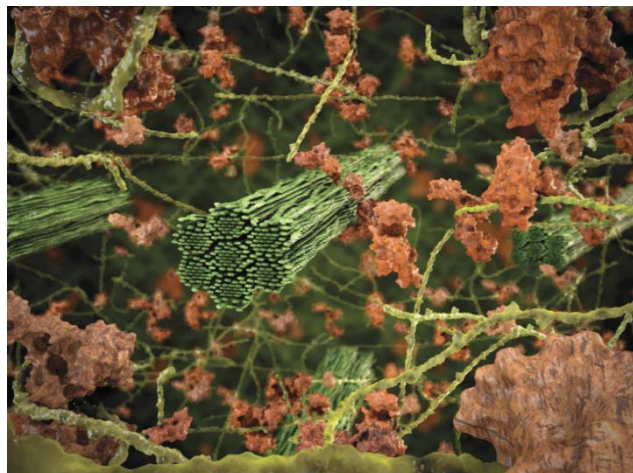


Fig. 3.13. Complex structure of cell-wall biomass during the pretreatment process in a computational model. Fibrous bundle of cellulose molecules (green, center) surrounded by other lignin (brown) and hemicellulose (light green) components.

3. Protein/peptide misfolding pathways

Research Theme's Associated Workshop: Biology
Potential Partner (*Attendees of Associated Workshop):

Valerie Berthelie (University of Tennessee–Knoxville)

Protein misfolding is responsible for many fatal diseases, and understanding the folding mechanism often provides valuable clues critical in arresting the progress of these folding/unfolding pathways. The onset of neurodegenerative diseases such as Huntington's and Alzheimer's, to name a few, have a signature observation—the formation of fibrillar structures. However, the lower degree oligomers of these peptides that exhibit a high propensity to associate are considered highly toxic. The study of the association mechanism of these peptides result in studying structures that exhibit large structural features that form during the process while still the small features exists. Understanding this mechanism requires the ability to observe structural features over a broad length scale range (or Q-range). Furthermore, the ability to observe the entire range in one experimental setting in conjunction with enhanced flux will permit observing the time-resolved progress of the folding/unfolding mechanisms (Fig. 3.14).

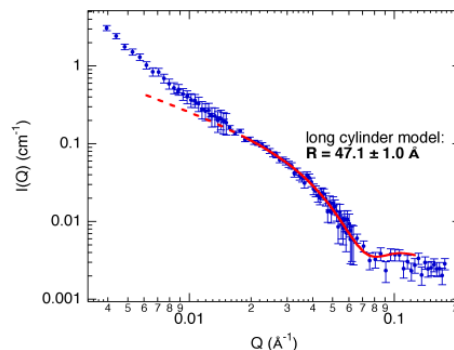


Fig. 3.14. SANS data obtained over a larger Q-range allow the NtQ₄₂P₁₀ fibril structure to be carefully probed.

A long-cylinder form factor fit (red solid line) accounts for the SANS profile at high and intermediate Q values. Deviations observed between the experimental scattering data and the extrapolated fit (dashed line) at $Q < 0.02 \text{ \AA}^{-1}$ are due to favorable fibril-fibril interactions (taken from Stanley et al., Biophysical Journal 100, 2504 [2011]).

4. Morphologies and Defects of Nanostructured Organic–Inorganic Hybrid Thin Films using in situ SANS

Research Theme’s Associated Workshop: Soft Matter

Potential Partner (*Attendees of Associated Workshop):

Yu Lei (University of Alabama in Huntsville)

Atomic layer deposition (ALD) is a thin film growth technique (Fig. 3.15) that relies on self-limiting binary reactions between gaseous precursor molecules and a substrate to deposit uniform films in a layer-by-layer fashion. Its impressive feature has expanded its application in the synthesis of both metal and metal oxide nanomaterials for applications in energy conversion and storage. ALD could also be applied to grow organic-inorganic hybrid films that contain ordered organic components within an inorganic matrix. In this case, sequential exposures of ALD precursors and organic coreactants will be used to react with a substrate’s surface. The resulting heterobifunctional thin films can possess tunable optical, electronic, and chemical properties with proper choices of ALD cycles and sequences. The post treatment of these thin films, under different conditions, also will bring different physical and chemical properties to the thin films. However, the morphologies and growth mechanisms of the organic-inorganic thin films using ALD, as well as the effects of the post-treatment, are still not well-understood. The understanding of the hybrid thin film growth mechanisms and effects of post-treatment will be a significant step toward atomic-precision synthesis of bifunctional ultra-thin films for important applications in energy conversion and storage, artificial organs, water purification, etc. SANS is critical to provide information on growth mechanisms of the hybrid thin film, including film thickness, growth rate, domain size, shape, density, and arrangement of organic-inorganic components. SANS is also an ideal tool to resolve the mechanisms of the porous structure formed during post-treatment, revealing pore formation and collapse with respect to increasing temperature and different gas environments. The success of this experiment will open a new window for rational design of hybrid organic-inorganic thin films.

Our ex situ experiment recently performed unsuccessfully at GP-SANS was attributed to neutron flux that was too low to detect the film growth. We need to stack more than 300 ultra-thin films to get reasonable statistics, which is nearly impossible. This experiment should be achievable with a tenfold increase in neutron flux at the sample position while optimizing usage of the current cold source flux from the reactor at HFIR and replacing current guides with newer, improved guides with an overhaul of the collimator box design.

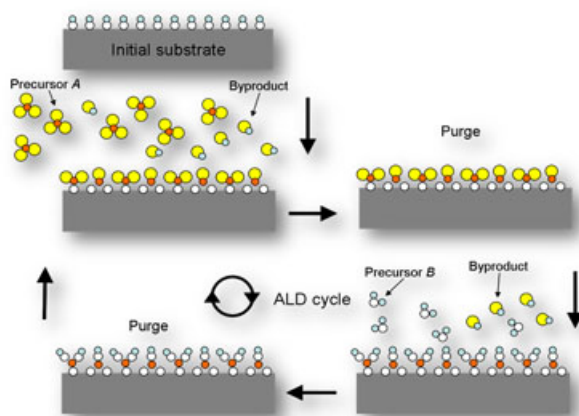


Fig. 3.15. Atomic layer deposition (ALD).

(Source: <http://www.merc.zju.edu.cn/htw/research.htm>)

Technical Details

The performance of BARNs hinges on optimizing usage of the current cold source flux from the reactor at HFIR. The following design upgrades to the Bio-SANS/GP-SANS at HFIR could potentially produce a tenfold increase in neutron flux at the sample position in the following manner. The distance from the cold source to the start of the guide system distance can be reduced/optimized to provide a view of the entire cold source. The neutron flux could potentially increase fivefold by this modification. In addition, replacing current guides with newer, improved guides with an overhaul of the collimator box design that encloses these guides would substantially minimize loss of neutron flux, reduce backgrounds at the detector, and extend the useful wavelength range to shorter neutron wavelengths. Finally, using beam condensing optics could potentially produce another twofold increase in neutron flux at the sample.

The instrument will be optimized for sample apertures measuring 1 mm and 2 cm in diameter.

Using the reactor based instrument, the detector array will consist of ^3He tubes arranged in multiple banks at different distances. The enhanced solid angle covered by detectors will allow a broader range of length scales to be measured simultaneously. In this design, detector banks will aim at a $Q_{\text{max}}/Q_{\text{min}}$ ratio of ~ 300 by placing the detector banks at a closest distance of $\sim 0.5\text{--}1$ m to the sample, an intermediate distance of $6\text{--}8$ m, and a long distance of $15\text{--}20$ m to sample. The detector banks at closest and intermediate distances will be offset transversely, and all the detector banks will be placed in a manner to allow for a sufficient overlap region for stitching of the data. Furthermore, a tenfold increase in neutron flux will enable the use of smaller sample apertures for high scattering samples to further improve the achievability of Q_{min} . Additionally, neutron focus lens and/or multiple circular converging collimators can potentially improve Q_{min} by 10 times without significantly compromising the neutron flux at the sample position. Another characteristic that could improve our ability to achieve lower Q_{min} values is reducing the detector pixel size from 8 mm to below $3\text{--}4$ mm. If the instrument were placed at the SNS second target station, the total flight path should be minimized while retaining the secondary flight path to be as long as possible. A long secondary flight path permits access to lower Q and thus longer length scales. A shorter overall length allows a broader range of wavelengths to be used without frame overlap from the 10 Hz source frequency and reduces the size and cost of the detector array. These lengths are constrained by the required Q resolution.

A major aspect of an instrument catering to the study of time-resolved processes is a robust sample environment suite of equipment. This instrument will be designed to allow incident beam polarization control and will have a flexible, accessible sample area for a wide variety of sample environments. The suite of sample environments will include a conventional changer, temperature control in controlled atmosphere or vacuum between 300 and 1,200 K, pressure cells capable of pressures in excess of 1 kbar at temperatures between 300 and 500 K, flow-through cells, electromagnets and a rheometer; all of these features should be available from the day the instrument becomes operational.

Table 3.5. Key instrument parameters for BARNs

Source	HFIR Cold Source/STS
Moderator type	Cold Source or Coupled H ₂
Wavelength/Q range	6 Å ≤ λ ≤ 18 Å 0.01 Å ⁻¹ ≤ Q ≤ 6 Å ⁻¹
Resolution Q	Δλ/λ ≤ 10% to 15% (variable)
Sample size range (beam size)	1 mm to 1.6 cm (diameter)
Moderator—sample distance	To be determined if instrument is at STS
Sample—detector distance	1–15 m
Detector type	³ He linear position sensitive

3.8 FLUX-OPTIMIZED ORDER/DISORDER SANS (FLOODS) FOR STS

Chris Stanley and Volker Urban, BSMD

Abstract

A neutron flux-optimized SANS instrument with a reduced focal spot on the sample affords many new scientific opportunities. In particular, high impact biological and soft matter experiments will become achievable with this instrument, where neutron flux and sample quantity requirements previously have been critical barriers. Flux-Optimized Order/Disorder SANS (FLOODS) requires the highest available flux density, but with a focus on relatively small length scales (for SANS) and disordered structures, divergence can be relaxed, and instrument length can be moderate (for a SANS). The instrument should perform well on a high flux cold source provided by STS or at a re-optimized guide hall at HFIR. FLOODS could provide a total integrated flux of $1.2 \cdot 10^9$ neutrons per second on a sample area of 0.1 cm². This is 100 times more neutrons/s and 1,000 times more flux than currently available at CG-3 Bio-SANS, for example.

Science Case

The structure-function paradigm in biology is shifting as it becomes clear that so-called “intrinsically disordered” proteins, or protein regions, are highly prevalent in the human proteome (50% of all human proteins are either wholly disordered or contain disordered regions) and essential for function in many biological processes. This emerging trend was identified as one of the key new drivers in biological research at the Biology Grand Challenges Workshop at the University of California, San Diego, in January 2014. In addition to folded domains, many proteins possess intrinsically disordered regions (IDRs) that exhibit heterogeneous, dynamic conformations that are influenced by their environment (e.g., pH, ionic strength, extent of molecular crowding, cellular localization, etc.) and interactions with multiple cofactors, substrates, and regulatory partners. For example, many IDRs within proteins fold into discrete conformations upon binding to their functional partners. Many others, however, function in their disordered state—establishing relationships between disorder and function is a major challenge in this research area. Several techniques may be employed for studying the dynamic shape of these macromolecules, NMR spectroscopy (through uniform isotope labeling of individual subunits within multi-protein assemblies or of individual domains or regions within multi-domain proteins) and fluorescence spectroscopy (through specific labeling of individual, or pairs of, amino acids within individual proteins or individual subunit within multi-protein assemblies). Neutrons can greatly contribute to advancing this challenging area of research because of their unique ability in probing the

heterogeneous conformations of disordered systems, in particular disordered regions of proteins. This capability is analogous to the groundbreaking contributions that SANS has made to our understanding of synthetic polymers; for example, the fundamental insight of the random coil nature of polymers in the melt state has been proven by SANS and is not otherwise directly observable experimentally. SANS has the potential to make similar groundbreaking and unique contributions to biology by exploring the conformations of flexible protein regions in multi-subunit functional complexes. To fully exploit this potential, three ingredients are required:

1. Segmental deuterium labeling to enable study of specific disordered protein regions with complex, multi-component systems
2. Molecular simulations of flexible disordered regions (within complex assemblies) that can be compared to structural data
3. A SANS instrument that has sufficient beam power and flux density to extract a very low intensity signal from small volume biological samples, with high signal-to-noise ratios, and in reasonable amounts of time

New scientific opportunities are possible with a flux-optimized SANS instrument capable of measuring smaller samples and providing increased time resolution.

The need for working with smaller sample quantities/volumes:

Many critical-functioning and disease-relevant proteins are difficult to prepare in sufficient quantities for a conventional SANS measurement. For example, numerous drug targets are membrane-associated proteins that typically have low expression yields and are inherently difficult to crystallize for high-resolution structure determination. Obtaining structural details by SANS would assist in rational drug design and would lead to significant biomedical breakthroughs. SANS is uniquely suited for this research because of its natural contrast between protein and lipid. A particular challenge with intrinsically disordered proteins (IDPs) is that many become unstable with increasing concentration, leading to undesired precipitation. Amyloid proteins responsible for a number of neurological diseases, such as Alzheimer's and Huntington's, also have upper concentration limitations. Furthermore, amyloids are typically found at nanomolar levels in vivo, while current SANS requires micromolar concentrations. Performing SANS at significantly lower amyloid concentrations reduces the gap between in vitro and in vivo conditions.

The need for enhanced time resolution:

Time-resolved SANS has been increasingly utilized in recent years, and current neutron flux affords time resolution on the order of minutes. In comparison, synchrotron small-angle x-ray scattering (SAXS) experiments are following protein-folding events on the milliseconds time-scale and can probe even shorter times. Empowering SANS to resolve millisecond time changes, coupled with the contrast advantages of neutrons over x-rays, will undoubtedly lead to new scientific discoveries. An unanswered question concerns the coupled folding–binding interaction mechanism of an IDP. With bio-deuteration and SANS contrast matching, the IDP folding component of the interaction could be monitored specifically. Improved time resolution also is imperative for following amyloid protein aggregation kinetics because the earliest structures formed are believed to be the most toxic. Obtaining a more detailed picture on the early structural evolution of the aggregation process will aid in identifying and characterizing these transient species. SANS with enhanced time-resolution capabilities will benefit

many other areas. In polymer and materials science, phase transition kinetics drive phase separation, gelation, and self-assembly phenomena. For example, obtaining long-range order in self-assembling polymer systems is a key to many materials applications. However, a better grasp of the kinetics is essential to effectively control and tune properties. FLOODS will be equipped with sample environments optimized for time-resolved experiments. Stopped-flow and continuous-flow devices will support controlled mixing in-beam. Mounting microfluidic devices will be possible to probe solutions within these channels, taking advantage of the small-focus beam.

Initial Science Objectives

1. Proteins with Intrinsically Disordered Regions

Research Theme's Associated Workshop: Biology

Potential Partner (*Attendees of Associated Workshop):

Richard Kriwacki* (St. Jude Children's Research Hospital)

Intrinsically disordered proteins or protein regions are essential for function in many biological processes, and they present a key new driver in biological research [1]. In addition to folded domains, many proteins possess intrinsically disordered regions (IDRs) that exhibit heterogeneous, dynamic conformations that are influenced by their environment (e.g., pH, ionic strength, extent of molecular crowding, cellular localization, etc.) and interactions with multiple cofactors, substrates, and regulatory partners. For example, many IDRs within proteins fold into discrete conformations upon binding to their functional partners. Many others, however, function in their disordered state—establishing relationships between disorder and function is a major challenge in this research area.

FLOODS will enable studies of the conformations of intrinsically disordered regions within larger multidomain proteins through combination with segmental deuterium labeling. We will open up this new field of structural biology research by demonstrating this new capability with the example of p27^{Kip1} (p27), as a prototype disordered protein (Fig. 3.16). It is thought that the intrinsic flexibility of p27 provides a molecular basis for the sequential signal transduction conduit that regulates p27 degradation and cell division [2].

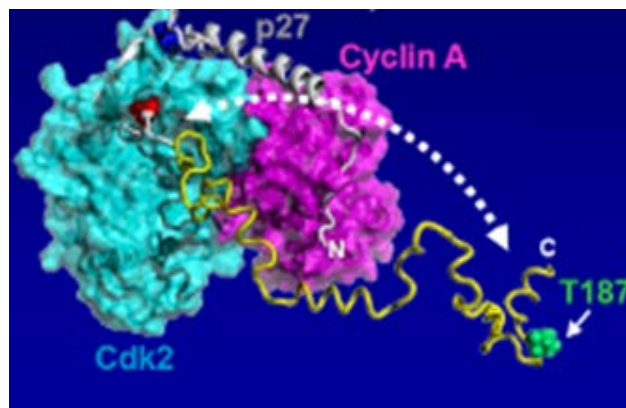


Fig. 3.16 Structure of the p27/Cdk2/cyclin A complex.

Schematic view prepared with the program PyMOL [<http://pymol.sourceforge.net>] of full-length p27 bound to Cdk2/cyclin A showing the solvent-accessible surface for Cdk2 (cyan) and cyclin A (magenta). The kinase inhibitory domain (KID) (grey) and C-terminal domain (yellow) of p27 are illustrated as ribbons (taken from [2]).

2. Time-resolved study of early stages of protein aggregation in neuro-degenerative disorders

Research Theme's Associated Workshop: Biology

Potential Partner:

Valerie Berthelie (Graduate School of Medicine, University of Tennessee Health Science Center)

FLOODS will dramatically improve time resolution for the studies of amyloid protein aggregation (Fig. 3.17) kinetics. This is of high impact because the earliest structures formed are believed to be the most toxic. Obtaining a more detailed picture on the early structural evolution of the aggregation process will aid in identifying and characterizing these transient species. We will demonstrate this new capability with a hundredfold improved time resolution over previous studies for the case of Structural Formation of Huntingtin Exon 1 Aggregates [3].

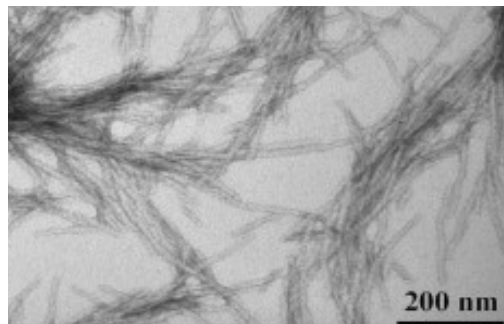


Fig. 3.17. TEM image of the fibrils formed by NtQ42P10 with a calculated fibril radius, $R = 40 \pm 8 \text{ \AA}$.

3. Dynamic changes in membrane protein structure

Research Theme's Associated Workshops: Biology, Soft Matter

Potential Partners (*Attendees of Associated Workshop):

Heidi Hamm* (Vanderbilt University)
Robert Blankenship* (Washington University in St. Louis)
Michael Brown (University of Arizona)
Linda Columbus (University of Virginia)

Membrane proteins, which are encoded by ~30% of all known genes and are the target of over 50% of drugs, engage in myriad activities including signaling, transportation, apoptosis, defense, and others. While recent progress has been made in crystallization of membrane protein and solving atomic structures in the crystalline form, there is still a significant gap in studying the membrane protein structure in a more native membrane-like environment. The structure of membrane proteins in the crystal could be significantly different from the structure in a functional state constrained by the structure and chemistry of the lipid membrane. In addition, many membrane proteins currently cannot be crystallized, presenting a great challenge for researchers to understand their functions with little or no structural information. Recently, small-angle scattering (SAS), which provides low-resolution envelope structure, has become an indispensable tool for not only validating atomic protein structure but also providing valuable structural insight to many proteins regarding the function–structure relationship. Small angle neutron scattering (SANS) is advantageously positioned to develop into such a tool for membrane protein studies because the contrast match technique enables researchers to eliminate lipid scattering present in the protein-lipid

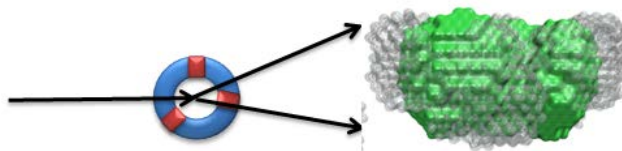


Fig. 3.18. SANS resolves shapes of membrane protein reconstituted in liposome. Red rectangles represent membrane protein in liposome (Blue). On the right side, a reconstruction of protein structure (green) was surrounded by lipids (gray).

complex. Another major advantage is that the energy of cold neutrons used in biological studies is in the range of meV, which poses no radiation damage to bioactive samples.

Currently, membrane protein solution structure can be studied by solubilizing with detergent micelles, liposomes (Fig. 3.18), or amphiphilic polymers in solution. The natural neutron scattering contrast between protein and those materials is small, although it is significantly better than electron density contrast, which is detectable by x-rays. The flux enhancement provided by FLOODS will improve the signal-to-noise ratio greatly. In addition, membrane proteins are usually difficult to express and purify, and the small sample amount requirement of FLOODS could enable many such experiments that otherwise would be impractical. Moreover, the higher flux at FLOODS allows time-lapse experiments that could help us understand ligand binding protein structure changes such as in GPCR proteins.

4. Optimization of biomass to bioethanol conversion

Research Theme's Associated Workshops: Biology, Soft Matter

Potential Partners (*Attendees of Associated Workshop):

Brian Davison (ORNL Biosciences Division)

Yannick Bomble (National Renewable Energy Laboratory)

Michael Himmel (National Renewable Energy Laboratory)

Tracy Nixon (Penn State University)

Efficient conversion of biomass to bioethanol is a two-step process:

1. Thermochemical pretreatment to break open the complex, composite nature of the biomaterial
2. Enzyme breakdown of cellulose chains to glucose that is further fermented to ethanol

Understanding enzyme interaction to substrate (Fig. 3.19) will facilitate innovative approaches in optimizing the enzymatic breakdown process. A major roadblock currently is the lack of knowledge on interactions that promote as well as destabilize the digestion process. These enzymes have a cellulose binding module (CBM) connected to the catalytic domain by a linker. Two major aspects of this system—the highly mobile nature of the linker-CBM and the low contrast between the enzyme and the substrate due to the contrast matching condition—clearly indicate the need for the FLOODS instrument.

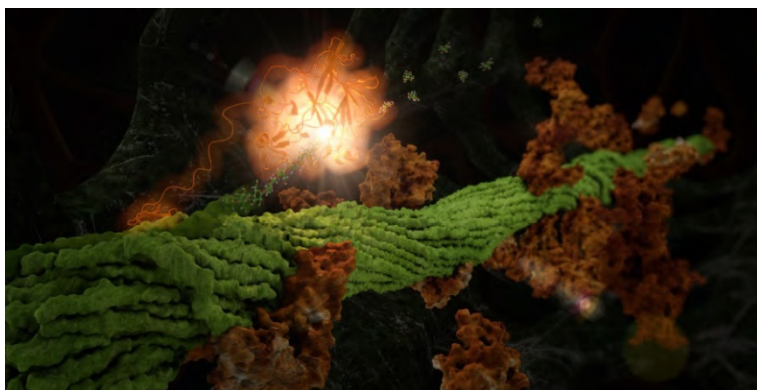


Fig. 3.19. A cellulase enzyme (orange) hydrolyzing a cellulose (green) strand despite the presence of lignin aggregates (brown) on the cellulose surface.

(Taken from Davison, et al., renewal proposal of Scientific Focus Area ERKP752 Dynamic Visualization of Lignocellulose Degradation by Integration of Neutron Scattering Imaging and Computer Simulation).

Technical Description

FLOODS is a SANS instrument that increases flux on the sample by convergent optics, placing the sample at the focal length and the detector at the imaging length (Fig. 3.20). In comparison with standard SANS instruments, FLOODS will have relaxed constraints for minimal Q and divergence and will optimally use the resulting gain factors for a high incident neutron rate ($1.2 \cdot 10^9$ n/s) and high flux ($1.2 \cdot 10^{10}$ n/s/cm²) on the sample. These numbers were based on the calculated performance of the high-brightness coupled, cold STS moderator assuming an ideal neutron optics system, a 0.1 cm² sample area, and a 2° beam divergence (FWHM). These performance increases will represent gain factors over current world-class SANS instruments by a factor of 100 in integrated flux and 1,000 or more in flux on the sample. Optimizing a SANS instrument in this parameter space will be possible because other instruments across the 3-source SANS suite will cover complementary spaces, in particular to much smaller Q (BARNs), and to high $\delta Q/Q$ resolution Small/Wide Angle Neutron Scattering (SWANS). As a result, the approach for this instrument will likely violate commonly held beliefs about the “optimum compromise” for a SANS instrument. In particular, if placed at the STS, the instrument will use the high wavelength resolution afforded by time-of-flight to further relax divergence in favor of a higher flux on the sample. Moreover, the scientific focus is on isotropically scattering samples, and consequently, the option of increased flux by using slit collimation or slit focusing will be considered. This instrument should be relatively short from source to detector (in particular for a SANS instrument).

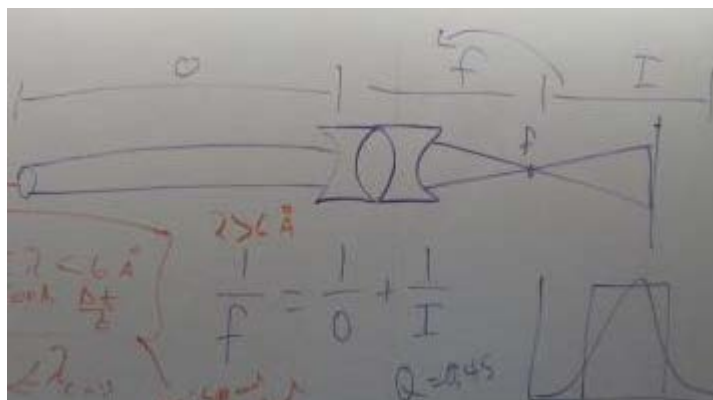


Fig. 3.20. Concept of a SANS instrument with the sample at the focal length and the detector at the imaging length.

White board discussion at the SANS brainstorming meeting in February of 2014 at the SNS.

As a design guideline, the equivalent of CG-3 Bio-SANS configured with an approximately 2 m sample to detector distance can be considered. However, taking that situation as a reference,

FLOODS should have additional detectors at higher angles to provide both higher dynamic Q -range and better solid angle coverage. Existing detector technology (³He tube arrays) would be sufficient; on the other hand, if detectors with higher pixel resolution are available, the source could be imaged with demagnification on the detector, allowing for a further reduction of instrument length. The shortness of the instrument will be advantageous for utilizing a maximum wavelength bandwidth, again for the highest integral neutron flux. FLOODS will be a cold neutron instrument that should capitalize on the simultaneous use of a broad neutron bandwidth; e.g., below 1 Å to greater than 10 Å. The scattering signatures that are targeted by this instrument typically will be broad curves as exhibited by random coils and by the low- Q region of form factors such as ellipsoids. Therefore, FLOODS should typically operate in a relaxed Q -resolution of $\Delta Q/Q \sim 20\text{--}50\%$ and fully utilize this broad resolution for increased divergence that allows focusing the beam on the sample. With a focus on small coherent scattering cross sections in samples that typically have high incoherent background from hydrogen (an even deuterium), methods for suppression of incoherent scattering will be extremely valuable. Methods that should further be investigated for potential suitability include: (a) choppers that remove in background from inelastic scattering (i.e., thermalization of cold neutrons in hydrogen-rich samples), (b) dynamically

polarized neutrons, and (c) spin-polarization/analysis. All of these methods have specific limitations and drawbacks, and their suitability for FLOODS needs further R&D.

The FLOODS instrument will have optics that focus on the sample position and image the virtual neutron source on the detector with minimum neutron loss; mirror focusing may be best suited for this purpose. The optimal sample size used in FLOODS will be 1 mm² to 10 mm². This presents an improvement over current liquid sample volumes by a factor 10 to 100 and will enable biological experiments that are to date not feasible because of limited availability of selectively deuterium-labeled enzymes. Beam divergence of this instrument will be defined by the minimum Q that needs to be measured. It needs to be adjustable; for the new scientific focus area of flexible linker regions in enzymes, Q_{min} could be made as large as 0.1 to 0.2 Å⁻¹. However, to include a broader range of studies with time resolution, FLOODS should be built to be capable of allowing experiments with a more conventional dynamic Q-range of 0.01 to 0.5 Å⁻¹. The expectation for this instrument is to outperform the current CG-3 Bio-SANS by approximately a factor of 100 in counting rate and simultaneously by a factor of 1,000 in flux on sample, allowing samples that are 10 times smaller than what currently can be used. The gain factors are based on improvements to the source/neutron delivery system and focusing optics. The latter will significantly limit the accessible minimum Q (as compared to CG-3 Bio-SANS). However, this is not a problem because experiments requiring smaller Q will be run on other complementary instruments across the FTS/STS/HFIR suite of SANS beam lines. FLOODS will utilize new SANS sample environments, in particular with smaller volumes (~10 to 30 microliter) and flow cell systems, including stopped flow for kinetic experiments.

Table 3.6. Key instrument parameters for FLOODS

Source	STS
Moderator type	Cold source or coupled H ₂
Wavelength/Q-range	1 Å ≤ λ ≤ 15 Å 0.01 Å ⁻¹ < Q < 2 Å ⁻¹
Resolution Q	ΔQ/Q ~20–50%
Sample size range (beam size)	1 mm ² to 1 cm ²
Moderator—sample distance	To be determined
Sample—detector distance	~2 m
Detector type	Area detector—large solid angle

References

- [1] Grand Challenges in Biological Neutron Scattering, Workshop Report, University of California, San Diego, January 17–18, 2014.
- [2] Galea, et al., *Journal of Molecular Biology* **376** (3), 827–838 (2008).
- [3] Stanley C. B., et al., *Biophysical Journal* **100**, 2504-2512 (2011).

4. GRAND CHALLENGES IN SOFT MATTER

G. S. Smith (Biology and Soft Matter Division)

One of the goals of modern science is to create materials by design with specific functionalities. Soft matter composed of covalently bound molecular building blocks (including polymers, surfactants, nanoparticles, gels, etc.) provides almost endless complexity and tunability for making new materials to achieve this goal. As the complexity of these systems grows, so do the challenges for developing our fundamental understanding of the materials properties with the ultimate goal of controlling static and dynamic function. To identify these challenges for the next decade, a workshop was organized to examine how neutrons can play a role in solving these problems.

Neutron scattering has played and continues to play a major role in magnetism (spin dependent interactions associated with the spin of the neutron) and in soft matter (isotopic labeling). Thus it is not accidental that three of the neutron oriented workshops are intimately related to these areas of condensed matter. At the Soft Matter Workshop, 39 invited leading researchers (including 4 NAE members and 1 NAS member) from 14 universities, 5 other national laboratories, and 3 industrial research centers, joined 5 participants from ORNL on the University of California, Santa Barbara, campus on May 17–18, 2014. The workshop—organized by Matt Tirrell of the University of Chicago and Fyl Pincus of UC Santa Barbara—included presentations and discussions on experiments, synthesis, theory, and modeling/simulation.

While neutrons are an essential tool for studying soft matter today, new techniques and new sources in the future will provide even more information on these complex systems. For example, the proposed Second Target Station (STS) at the Spallation Neutron Source (SNS) at Oak Ridge National Laboratory (ORNL) will be optimized to provide a high flux of long wavelength neutrons over a wide bandwidth. Such a source will be ideally suited to simultaneously studying multiple temporal and spatial scales, which is crucial to understanding complexity in soft systems. To exploit and fully interpret the data, a closer coupling between modeling and experiment will be essential. Significantly increased facilities for selective isotopic labeling (primarily deuteration) will be needed. Soft matter has a growing synergistic relationship with molecular and cellular biology in the area of synthetically reproducing and enhancing the functionality found in living systems. Achieving these goals may involve the marriage of synthetic and biological moieties.

The outcome of the workshop was to produce a report on these challenges and to anticipate how to address the challenges with new techniques. While the focus was on the future, the recommendations and discussions represent a graded set of actions from the near term to the end of the decade. Below is a summary of the challenges and the recommendations for ways to confront the challenges using neutrons.

4.1 AREAS OF SOFT MATTER WHERE MORE RESEARCH IS REQUIRED TO DEVELOP FUNDAMENTAL UNDERSTANDING

Response of mechanical deformation—jamming, glassy materials, gels, and non-equilibrium phenomena in soft matter

Soft/hard composite materials

How to manipulate particles/dispersions in composites and understand properties to improve functionality

Understand anisotropic (particle shapes or interactions) systems

Behavior of organic shells (application to soft matter hierarchical systems)

Weakly ordered systems

Tissue structure and scaffolds

Transport in soft matter—Electron/ion/water/phonon transport across large length scales in a multicomponent system; e.g., bicontinuous structures, composites, etc.

- a. From segmental motion through the glass transition (small length scale) relevant to larger scale transport (macro performance)
- b. Ionic movement in gels, flows, brushes
- c. Interplay of convection and charge transport
- d. Interplay of charge transport and humidity

Polyelectrolytes

- a. Multiple charge states, amphiphilic architectures
- b. Surface structures
- c. Multipolar and polarizability effects

Complex structures in solution—hierarchical assemblies

Soft matter under industrial processing conditions—including the effects of flow, shear, high temperature, high pressure, etc.

Active soft materials

- a. Steady state morphologies of active systems
- b. Structure and functionality of decorated membranes
- c. Enzyme dynamics
- d. Scattering from whole cells; imagine deuterating only microtubules or only membranes in a living cell

Expand our ability to make quantitative measurements such as

- a. Membrane curvature and fluctuations and equilibrium dynamics
- b. Methods to probe non-equilibrium behavior and dynamics
- c. Providing in situ, short range local information in soft materials

How to define interfaces and set boundary conditions in soft matter/hybrid systems to understand their properties (structure, dynamics, chemistry); how to design interfaces with defined structures and functions

Polar solvents other than water

Identify the effects of polydispersity on properties (physics)

4.2 RECOMMENDATIONS TO HELP ADDRESS THESE AREAS OF NEED

Pursue a reflectometer (including Grazing Incidence Diffraction capabilities) on a brighter Second Target Station. This could increase the Q-range, provide for single shot kinetics measurements, and improve spatial resolution to define interfaces and interface structure.

Advance time-dependent kinetics techniques and experiments for SANS, USANS, and GI-SANS. These are currently limited to minutes, but a Second Target Station could achieve a hundredfold increase in flux to achieve 1 s to enable a new realm for single-shot kinetics measurements.

Advances in neutron lens and mirror technology are needed. Use to achieve spatial profiling at the micron-scale for neutron imaging, phase contrast imaging neutron tomography, SANS, and reflectometry to obtain fine local structure. Also, use for very-high resolution SANS (VSANS).

Develop “conventional” spin echo at HFIR to allow order of magnitude faster measurements with higher dynamic and Q-range. Currently, ILL in Grenoble, France can do 800–1000 ns.

Enhance backscattering instrumental resolution to cover a broader time range

Develop Larmor precession techniques such as SESANS to extend spatial resolution to very large length scales

Need wide variety of advanced experimental environments specific to soft matter research to achieve “lab at the instrument”

- a. For applying fields (e.g., electric, magnet, flow)
- b. Impose extreme conditions (e.g., flow, shear, evaporation, humidity, gas vapor pressure, confinement)
- c. Arbitrary duration, phasing, and spatial configuration for non-equilibrium structures
- d. Need better infrastructure at facilities for sample environment development by external researchers—Europe has this but the United States does not

Expand capabilities for computationally-involved data analysis

- a. Integrate with data simulation methods that can be constrained using data and supplementary information
- b. Develop tools for more detailed computation/simulation methods where complex data can be modeled in real time for data where “traditional” analysis fails
- c. Real time data visualization
- d. Dedicated high speed computers
- e. Theory combined with experiment—a key component to these challenges is harmonizing both approaches

Provide facilities for sample preparation and characterization on site and in close proximity to the instruments, particularly for biological or interfacial samples.

Design and build complementary and simultaneous in-beam characterization with positional sensitivity (e.g., fluorescence, x-ray reflectivity, Brewster angle, SEM/TEM, AFM, etc.)

New methods to measure local distributions of stress or anisotropy in soft materials such as homogeneously polarized spins in the sample (stress) combined with labeling materials with nuclear spin probes

Extend the times scales for dynamics measurements far beyond 1 μ s. High flux of very long wavelength neutrons coherent beams might be used (neutron speckle)

Provide abundant facilities for specific deuteration of materials. For example, deuteration of just one peptide sequence in a whole protein—such as just one alpha helix of a 7 alpha helix GPCR— or expanded capabilities for isotopic labeling of molecular components of polymers.

Need flexibility with beam time for an iterative experimental design process. This could also serve for training students in neutron scattering. Funding and new paradigms are needed to take full advantage of neutron facilities and to supply neutron scattering expertise in the future

Broadly advertise and highlight advantages of neutrons to the Soft Matter Community; make a greater effort to expand the neutron scattering community.

Following are descriptions of instrument concepts and initial science targets that address these recommendations.

4.3 HIRES-SWANS (HIGH RESOLUTION SMALL/WIDE ANGLE NEUTRON SCATTERING) FOR STS

Shuo Qian and William Heller (Biology and Soft Matter Division)

Abstract

A capability gap exists between traditional high-resolution diffractometers and small-angle neutron scattering instruments that lies between the ability to resolve nanoscale features in newly developed

complex, disordered materials in which local ordering is equally critical for material performance, as is commonplace in the soft matter sciences. Specifically, photovoltaic materials, polymer-nanomaterial composites, superhydrophobic materials, and biomaterials have properties that arise from interplay between nanoscale and molecular structures. To fill this capability gap and enable new science through the implementation of grazing-incidence scattering as part of its design to optimize it for studies of thin films, the HiRes-SWANS combines features of a high-resolution neutron diffractometer with the ability of a small-angle neutron scattering instrument to probe length scales spanning from the interatomic out to tens of nanometers simultaneously. The combination of broad dynamic range ($0.01 \text{ \AA}^{-1} < Q < 6 \text{ \AA}^{-1}$), high Q resolution ($\Delta Q/Q < 1\%$) and grazing-incidence scattering capabilities that could be achieved on a beam line at the high-flux, low repetition rate STS, a truly unique instrument optimized for studying many of the newly developed, novel materials with technological game-changing potential can be studied as has never been capable previously.

Science Case

Soft matter science encompasses a broad range of topics and materials, such as nanomaterials, polymer-nanoparticle composites, high-performance fibers, and biological materials ranging from biomembranes to biofilms. All of these are in the forefront of basic and applied research because they hold possible key answers to solve many problems in energy, biomedical, and bioengineering. The soft matter sciences have been identified as a growth field. DOE supports many programs in which the length scales that the HiRes-SWANS will address, such as batteries, photovoltaic materials, and functional nanomaterials. Other funding agencies also see great potential in soft materials. For instance, the National Science Foundation sponsored the “Workshop on Opportunities in Theoretical and Computational Polymeric Materials and Soft Matter” in 2013.

An important feature of soft matter is the range of length and energy scales that produce bulk material properties. Chemistry gives rise to both bonded and non-bonded interactions that produce local structure and function while simultaneously driving macromolecular behaviors such as self-assembly and long-range dynamics that ultimately give rise to bulk properties. These materials often lack highly ordered local structure but display varying degrees of long-range order. Further, the material’s structures and dynamics can respond dramatically over small temperature ranges commonly encountered in everyday life. The HiRes-SWANS instrument will be optimized to directly address these length scales simultaneously. Focusing optics that direct the beam and reduce the size of the beam at the sample will be integrated into the design to enable grazing-incidence scattering while simultaneously enabling studies of smaller samples (1 mm^2) more effectively than is presently possible. The focused beam will also enable more detailed time-resolved studies of materials. When combined with the unprecedented wide dynamic range of measurement, time-resolved in situ studies of materials can be performed to gain new insight into processes such as nanoparticle synthesis, self-assembly in soft materials, and device processing. Examples of new science that would be enabled by the HiRes-SWANS include the following:

- **Assembly Processes in Polymer-Nanoparticle Composites.** The unique properties of nanoparticles arise from their size, high surface-to-volume ratio, and geometry. However, making nanomaterials into devices often requires the growth of macroscopic materials either composed entirely of or containing nanoparticles. For example, polymer–nanoparticle composite organic photovoltaics have been extensively studied, yet the relationship between the starting solution state and the final bulk heterojunction that collects light, separates charge, and transports it is not well understood. Local

chain packing, crystallization, and nanoscale self-assembly affect the performance of the resulting bulk heterojunction.

- **Biomaterials and Bio-Inspired Materials.** Nature uses soft materials to create the functional nanoscale systems that make up the machinery of cells. Researchers have long looked to nature for both inspiration and ingredients when seeking to make materials with specific functionalities, such as capturing solar energy by mimicking photosynthesis. Similarly, the self-assembly behavior of lipids can be leveraged to optimally structure a nanomaterial such that its function is optimized. By understanding how the interplay of lipids and proteins gives rise to structure, the ability to guide creation of new materials will result.

Initial Science Objectives

1. Tuning Local Interactions to Direct Self-Assembly in Polymer-Nanocomposites

Research Theme's Associated Workshop: Soft Matter

Potential Partners (*Attendees of Associated Workshop):

Thomas P. Russell* (University of Massachusetts)

Sanat K. Kumar (Columbia University)

Igal Szleifer* (Northwestern University)

Dvora Perahia* (Clemson University)

Gary Grest* (Sandia National Laboratory)

Robert M. Briber (University of Maryland)

Pinar Akcora (Stevens Institute of Technology)

The unique properties of nanoparticles arise from their size, geometry, and high surface-to-volume ratio, as well as from the materials from which they are made. Their potential for creating revolutionary applications is well understood, but realization of real-world uses requires bridging from the nanoscale to the macroscale. One means of doing so is through the formation of polymer-nanoparticle composites. Such materials are more commonplace than many people realize, with automotive tires being one of the most prevalent examples where the additives to rubber create a plethora of performance characteristics. The formation of the structures that give rise to desirable performance in tires is the result of years of experience gained through extensive trial and error that has only very recently benefitted from the development of the nanosciences. In fact, the actual interactions that form across a wide range of functionally relevant length scales to make a high-performance racing tire instead of a daily-use one having excellent wear properties are only partially understood; a similar situation also exists for other polymer-nanoparticle composites encountered every day. Development of new functionalities and optimizing performance in polymer-nanoparticle composites must be approached from the ground up in which the structure and function of the nanoparticles and polymers are well-understood and can be leveraged to drive their self-assembly from their starting mixture into a final macroscopic material with the desired performance characteristics.

The development of polymer-grafted nanoparticles affords a truly unique opportunity to develop tunable polymer-nanoparticle composites. The specific physicochemical properties of the polymers attached to the surface of the nanoparticle give rise to a tunable interaction between the nanoparticles, as well as with the surrounding medium into which they are dissolved. These properties arise not only from chemistry but also from the polymer chain length, as can be seen in Fig. 4.1. Further, the polymers grafted to the surface of the nanoparticles may experience additional confinement effects that further modify their behavior relative to their bulk state. The result is a rich parameter space for driving material properties through the selection of nanoparticles, grafting polymers, and the matrix material. The relatively recent advent of anisotropic polymer grafting methods further enhances the potential for guiding self-assembly processes. However, understanding how these properties drive self-assembly into the bulk presents both a daunting challenge and an incredible opportunity. In particular, the study of the local

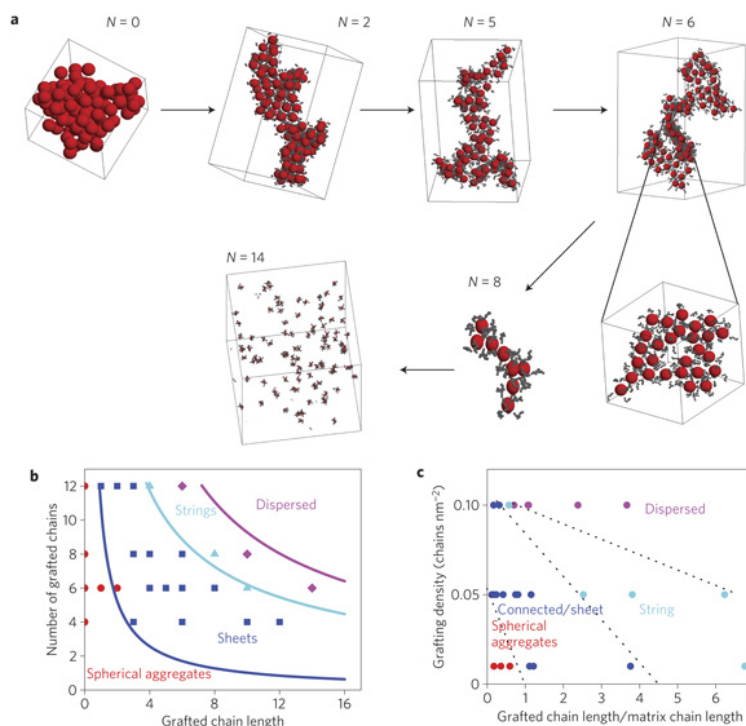


Fig. 4.1. Polymer-grafted nanoparticles in a polymer nanocomposite self-assemble in a polymer chain length- and grafting density-dependent manner [1].

interactions (0.1–10 nm) that give rise to assembly at the 10s of nanometers and beyond is experimentally difficult to realize. The HiRes-SWANS instrument is optimized to probe these length scales with sufficient resolution to elucidate detailed features in the scattering data arising from specific molecular-level interactions while simultaneously probing length scales that can show the nanoscale assembly in the material. Therefore, the instrument has the potential to provide previously inaccessible experimental insight into the interactions within polymer–nanoparticle composites when combined with the unique structural information afforded by deuterium labeling and neutron scattering techniques.

By studying the impact of nanoparticle chemistry, grafting polymer and matrix polymer chain chemistry, and chain length on the structure and local interactions between the components of the system with the HiRes-SWANS instrument and deuterium labeling of the polymers, a new understanding of the relationship between the physicochemical properties of the materials and the resulting polymer–nanocomposite will result. Novel insight into the nanoparticle-grafting polymer-matrix polymer interactions will be gained using high-performance atomistic and coarse-grained simulations of these materials to interpret the scattering data collected for the wide range of length scales uniquely probed by the HiRes-SWANS. SANS and USANS measurements will expand the range of length scales studied structurally out to those readily studied by complementary microscopy studies, thereby affording a holistic view of the structure. Further, detailed characterization of the performance of the resulting materials will be performed to complement these nanoscale characterizations to relate macroscopic

behavior to nanoscale structure. The resulting knowledge gained about the polymer-nanocomposite materials will truly enable the first integrated understanding of the ground-up relationship between the nanoscale and the macroscale in materials science.

2. Grazing-incidence Neutron Scattering on Protein-Membrane Assembly

Research Theme's Associated Workshops: Soft Matter (University of California, Santa Barbara) and Biology (University of California, San Diego)

Potential Partners (*Attendees of Associated Workshops):

Steve White* (University of California, Irving, Biology Workshop)
Huey Huang* (Rice University, Biology Workshop)
Gianluigi Veglia* (University of Minnesota, Biology Workshop)
Margie Longo* (University of California, Davis, Soft Matter Workshop)
Tonya Kuhl* (University of California, Davis, Soft Matter Workshop)
Donald Engelman (Yale University)
Mei Hong (Massachusetts Institute of Technology)

One of the grand challenges mentioned more than once at both the biology workshop at UCSD and the soft matter workshop at UCSB was to understanding membrane proteins in a membrane context and lipid-protein dynamics.

The cellular membrane, made of phospholipids, proteins, and other smaller molecules, is one of the most important structures in all living things. It serves as a barrier that separates the cytoplasm of cells from the surrounding environment, and it encloses organelles inside cells to segregate biological functions. Membrane proteins, which are encoded by ~30% of all known genes and are the target of over 50% of drugs, engage in myriad activities including signaling, transportation, apoptosis, and energy production. In addition, the membrane self-assembly and diffusion process is used to test curvature directed nanopatterning and sol-gel entrapped nanolipoprotein particles, etc. The structure and dynamics within this natural, nanostructured material are well served by the capabilities of the HiRes-SWANS instrument.

Grazing-incidence neutron scattering (and diffraction) (GINS) is an excellent technique for studying proteins in such native-like membrane environments because aligned planar membranes with their surface parallel to the substrate provide preferential orientation of any membrane-associated structure with respect to the incident beam. Developed for studying surfaces and buried interfaces in the materials sciences—such as the quantum dots on semiconductor surfaces and metal deposits on oxide surfaces—the grazing incident scattering techniques have also been adopted for studying soft matter systems such as polymer films, block copolymer films, self-organized nanostructured thin films, and lipid-protein interfaces. The GINS scattering data from a thin film on a 2D detector contains structural information in-plane and out-of-plane (Fig. 4.2) (i.e. structure perpendicular and parallel to the normal of the membrane), and provides additional information including lateral organization and correlations of components in layered samples. Neutron membrane diffraction, based on GINS geometry, which uses a highly ordered membrane assembly, makes it possible to solve high-resolution lipidic structures such as membrane fusion intermediates, membrane pores, etc., without artificial labeling.

Currently, there is a significant gap in the understanding of membrane proteins that arises from difficulties in obtaining high-resolution structural information. Additionally, the interplay between the lipids and membrane-integral proteins and the organization of various macromolecules in the membrane bilayer is not well understood. With the HiRes-SWANS and selective deuteration, the impact

of different lipid species on the self-assembly of membrane-integral proteins can be studied. These systems may adopt long-range order over 10s of nanometers while simultaneously giving rise to local ordering of the lipids around the protein. Such lateral organization of the cellular membrane in response to membrane proteins spans length scales uniquely probed by the HiRes-SWANS. The results will provide a truly unique view of the organization in the cellular membrane, the structure of membrane proteins, and the interfacial structure with unprecedented resolution that cannot be obtained by any existing instrument.

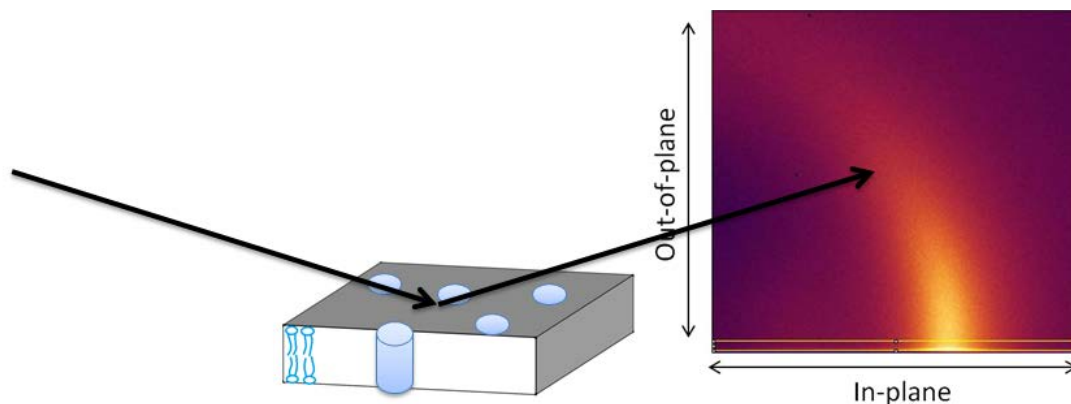


Fig. 4.2. The geometry of grazing-incidence scattering with a simulated 2D scattering pattern showing in-plane and off-plane structure of a protein-membrane assembly. The blue cylinders represent membrane proteins reconstituted in the planar lipid bilayer.

3. DNA Origami and Templating for Programmable Nanoparticle Superlattice Assembly

Research Theme's Associated Workshop: Soft Matter

Potential Partners (*Attendees of Associated Workshop):

- Oleg Gang* (Brookhaven National Laboratory)
- William Shih (Harvard University)
- Hao Yan (Arizona State University)
- Erik Winfree (California Institute of Technology)
- Chad Mirkin (Northwestern University)
- Sanat K. Kumar (Columbia University)
- Julie Kornfield* (California Institute of Technology)

Chemistry and materials science have made incredible advances in producing new materials that affect virtually all aspects of daily life. The advent of the nanosciences has expanded the range of possible materials by leveraging size effects that give rise to new functionalities for materials that cannot exist in the bulk state. Biology has long used exquisitely controlled nanoscale structure and chemistry to impart highly specific behaviors to the cellular machinery that makes life possible. The development of DNA-templating and DNA origami has enabled the nanosciences to leverage this specificity through the inherent chemical complementarity of double-stranded DNA (dsDNA) to create novel synthetic structures such as hollow boxes 10s of nanometers on a side having a hinged lid (Fig. 4.3) and even nanomaterials engineered for specific optical response (Fig. 4.4). These structures do not arise from simple self-assembly but instead are directly engineered through the use of specific complementary sequences of single-stranded DNA (ssDNA) that constrain how they can link to create dsDNA. The possibilities for engineering materials within such a framework are nearly limitless. In particular, the ability to use a DNA framework to drive specific assembly of nanoparticles into superlattices with

engineered properties has the potential to lead to novel materials for applications ranging from biomedicine to optical sensors.

While it is tempting to think that specifying and grafting the appropriate sequence of DNA is all that is required to construct the desired superlattice of material, the inherently flexible and disordered natures of ssDNA and dsDNA do not give rise to precise Lego™-like behavior.

Understanding the interaction of the DNA framework with an inorganic nanoparticle is the key to truly improving control in the assembled structures, which is particularly important if a transition is to be made from the laboratory to large-scale industrial production where the exquisite control possible on a small scale cannot be attained in bulk synthesis.

Neutron scattering, which is sensitive to hydrogen, provides an excellent way for studying DNA-functionalized inorganic nanoparticles. Understanding the interactions that take place at the 0.1 nm to 1 nm length scales, uniquely possible on the HiRes-SWANS with sufficiently high resolution for resolving fine features in the data, is the key to advancing control over these fine intermolecular interactions that give rise to the formation of the superlattice of nanometer scale particles as they grow into structures on the 10s of nm scale.

Understanding the interactions that take place at the 0.1 nm to 1 nm length scales, uniquely possible on the HiRes-SWANS with sufficiently high resolution for resolving fine features in the data, is the key to advancing control over these fine intermolecular interactions that give rise to the formation of the superlattice of nanometer scale particles as they grow into structures on the 10s of nm scale.

Understanding the interactions that take place at the 0.1 nm to 1 nm length scales, uniquely possible on the HiRes-SWANS with sufficiently high resolution for resolving fine features in the data, is the key to advancing control over these fine intermolecular interactions that give rise to the formation of the superlattice of nanometer scale particles as they grow into structures on the 10s of nm scale.

DNA origami templating methods have the potential to make it possible to grow colloidal crystals of mixtures of different species of nanoparticles in a manner akin to how sodium and chloride ions assemble into a crystal lattice. The nanoparticles effectively become “superatoms” within the superlattice. Once assembled via the DNA–DNA interactions from an initial solution state, such materials could be dried to remove the solvent and even subjected to high temperature processing that burns away the organic materials, leaving a heterogeneous superlattice of metallic domains within a truly robust macroscopic material that has the potential to retain features of the individual nanoparticles and may give rise to synergistic effects. The growth of such materials would be ideally studied by the HiRes-SWANS. Specific nanoparticle surface interactions that form during thermal processing could be resolved, and insight into creep of atomic species between different nanoparticles during the thermal processing could be observed. The neutron scattering experiments with the HiRes-SWANS will provide key critical information related to engineering and optimizing such materials for specific performance and will provide novel insight into the relationship between a wide range of length scales and functions.

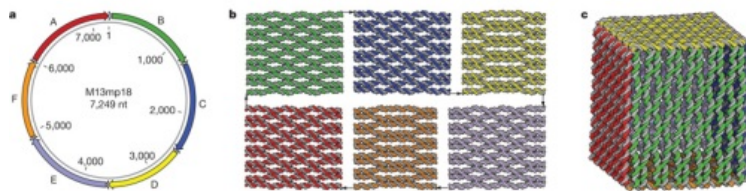


Fig. 4.3. Formation of a DNA Origami box from the DNA framework, to the assembled sides of the box, and ultimately to the final 3D structure. [2].

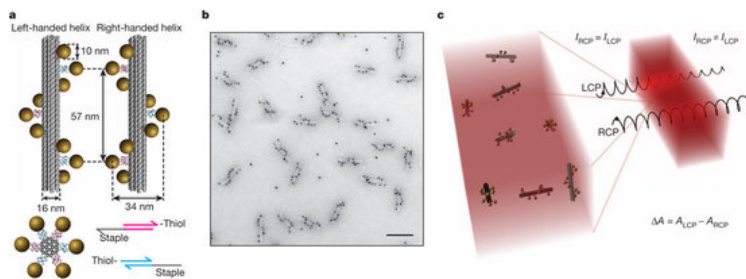


Fig. 4.4. Plasmonic nanostructures formed through DNA templating. Using DNA grafted to nanoparticles, it is possible to develop materials with an engineered optical response [3].

4. Investigating the Effect of Short-Range Interaction of Nanoparticles on the Formation of Nanocrystal Colloids

Research Theme's Associated Workshop: Soft Matter

Potential Partners (*Attendees of Associated Workshop):

Thomas P. Russell* (University of Massachusetts)

Bradley Olsen (Massachusetts Institute of Technology)

Oleg Gang* (Brookhaven National Laboratory)

Brett Helms* (Lawrence Berkeley Laboratory)

Colloidal nanocrystals (NCs) with at least one dimension in the range of 1–10 nm exhibit unique size- and shape-dependent physicochemical properties arising from low-dimensional quantum confinement effects, which makes them excellent building blocks for advanced materials in nanotechnology. Therefore, much interest and effort have been devoted to control NC size, shape, and organizational characteristics. For examples, monodispersed CdSe NCs, capped with hydrophobic ligands having long alkyl chains, can self-assemble into micron-sized colloidal crystals with highly ordered periodicity. Recent developments show that non-spherical NCs such as rods, wires, tubes, arrows, and tetrapods can also be fabricated by using tailored CdSe nanorods. These NCs not only exhibit various appealing physicochemical properties because of low dimensional quantum confinement effect but also provide new building blocks for anisotropic nanostructures. Because these physicochemical properties emerging from various NCs are directly related with the organization of nanoparticles and the overall shape of NCs, a characterization tool that can cover 0.1–100 nm length scale with high resolution becomes crucial. The HiRes-SWANS instrument is optimized to probe these length scales with sufficient resolution to elucidate detailed features in the scattering data arising from nanoparticle–nanoparticle interactions and arrangements as well as the overall shape of assembled NCs. Therefore, the instrument has the potential to provide previously inaccessible experimental insight into the NC formation process as well as the relationship between the organization structure of nanoparticles and the resulting properties of NCs (Fig. 4.5).

By utilizing the wide Q-ranges and resolutions expected from HiRes-SWANS, pair distribution function (PDF) type analysis is also possible and can provide direct pictures of a nanoparticle arrangement in the NCs via $g(r)$. At the same time, the low-Q ranges accessible by HiRes-SWANS can characterize the overall shape of NCs via conventional form-factor type analysis. The neutron scattering machine also provides a unique chance to study multi-component NCs by using different scattering lengths for constituting nanoparticles. The formation of NCs is largely governed by the surface chemistry or the interaction between nanoparticles, which can be modeled in various types of computer simulations, including both atomistic and coarse-grained simulations. Therefore, the combination of computer simulation and scattering experiments can facilitate complete understanding and interpretation of experimentally collected data from HiRes-SWANS. Further, in situ growth of NCs can be investigated to provide critical information for the formation mechanism of NCs.

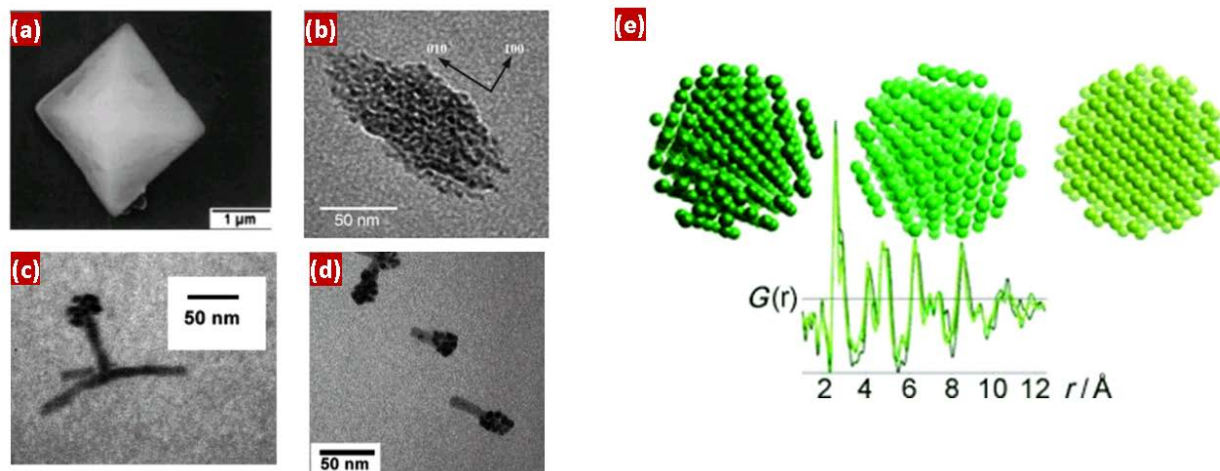


Fig. 4.5. (a) Colloidal crystal of CdSe NCs.[4] (b) Ellipsoidal NC of CuO [5]. (c) CdTe tetrapod. (d) Asymmetric CdTe rods [6]. (e) Pair distribution function analysis example showing insights into the electrochemical reaction of $\alpha\text{-Fe}_2\text{O}_3$ with lithium [7].

Technical Description

The HiRes-SWANS, with its broad dynamic range and higher Q-resolution than a traditional SANS instrument, is only enabled by being located on a high-resolution moderator at the short pulse, low-repetition rate STS at SNS. A key requirement of the instrument is that it be located relatively close to the moderator to afford the broadest wavelength band possible while minimally compromising the resolution of the instrument. Ideally, the Q-resolution of the instrument will be such that $\Delta Q/Q \leq 1\%$ through the entire Q-range, which will enable high-resolution studies of nanoscale materials while also enabling studies of local structure without compromising the data quality by losing features to the resolution of the instrument. Choppers will be employed to provide a tunable resolution and define the wavelength band while avoiding issues related to frame overlap.

The use of a bending and focusing guide will make possible a great reduction in the size of the beam at the sample while simultaneously deflecting the beam down from the horizontal to enable grazing-incidence scattering. We envisage a maximum beam size at the sample position of 1 cm by 1 cm. Collimating optics will be an integral part of the design to reduce the size of the beam at the sample position further to both reduce the sample size (a key requirement of grazing-incidence scattering geometries) and improve the angular resolution of the instrument. The sample area must be kept open and versatile, with the ability to mount a wide variety of sample environments suited to studies of soft materials. Sample environments such as vacuum ovens, humidity chambers, illumination systems, simultaneous in situ spectroscopy instruments, and the like are envisioned, although there is no limit to the range of possibilities that will ultimately be driven by the scientific program of the instrument as it develops.

The sample-to-detector distance can be relative short (≤ 3 m) because of the use of a focusing guide and small beam size. The detector system will have to address the needs of both SANS and diffraction, but large solid angle coverage is required to enable the broad simultaneous Q-range. A potential solution would be to use both ^3He tube detectors for the small-angle banks and a solid state design better suited for high spatial resolution measurements of the scattered neutrons. Sub-millimeter pixels would be ideal

for such detectors and should be feasible. Using the high-resolution detectors for the entire solid angle coverage would actually improve the resolution of the instrument at low-Q.

Table 4.1. Key instrument parameters for HiRes-SWANS

Source	STS
Moderator type	Cold, coupled H ₂
Wavelength/energy range	0.25 Å ≤ λ ≤ 10 Å with as broad of a bandwidth as possible for a single setting of the choppers
Resolution Q	0.01 Å ⁻¹ ≤ Q ≤ 6 Å ⁻¹ ΔQ/Q ≤ 1%
Sample size range (beam size)	1 mm ² up to 1 cm ²
Moderator—sample distance	≤ 15 m
Sample—detector distance	≤ 3 m with broad solid angle coverage
Detector type	Mixture of ³ He and high spatial resolution (< 1 mm ² pixel size) solid state detectors

References

- [1] Akcora, et al. *Nature Materials* **8**, 354–359 (2009).
- [2] Andersen, et al. *Nature* **459**, 73–77 (2009).
- [3] Kuzyk, et al. *Nature* **483**, 311–314 (2012).
- [4] *Science* **270**, 1335–1338 (1995).
- [5] *Adv. Mater.* **17**, 42–47 (2005).
- [6] *Nano Lett.* **4**, 2397–2401 (2004).
- [7] *Angew. Chem. Int. Ed.* **51**, 4852–4855 (2012).

4.4 KINETICS REFLECTOMETER

John Ankner, Biology and Soft Matter Division

Abstract

The Kinetics Reflectometer will be a versatile multipurpose instrument featuring horizontal sample geometry and a broad “single-shot” Q-range for structural and kinetic studies of solid, liquid/solid, and free liquid surfaces and interfaces. By placing the instrument on a short (15 m) flight path at the 10-Hz SNS Second Target Station (STS), one will be able to collect specular reflectivity data at a single (ϑ , $\Delta\lambda$) instrument setting over a full decade of Q (e.g. $0.02 \text{ \AA}^{-1} < Q < 0.20 \text{ \AA}^{-1}$). In addition to radically simplifying data collection and reduction, “one-shot” measurements eliminate the 60–90 s required to change chopper phases and move motors between Q bands on existing SNS reflectometers, enabling broad-Q

specular reflectivity to be measured in seconds or less. This purely kinematical advantage, coupled with improved STS cold flux, can yield $\times 100$ improvements in time resolution for the study of self-assembly of surfactants, polymers, and proteins at solid and liquid interfaces; diffusion, annealing, and exchange processes in thin films; encapsulation and release in drug delivery materials, sensors, and energy storage; switchable materials; and chemical and biochemical surface reactions.

Science Case

Neutron reflectometry covers a broad spectrum of science involving the growth, self-assembly, structure, and interactions of a wide variety of thin film materials ($1 \text{ nm} < d < 500 \text{ nm}$) and impacts many core areas of polymer, chemical, biological, and materials science. Because the advanced thin film materials of the future will be increasingly complex, there is an urgent and ongoing need to develop high performance neutron reflectometers to elucidate their structure.

The challenges to be met in soft condensed matter and the life sciences are as wide ranging as the topics investigated. While the sensitivity of neutrons to structural features offers a significant advantage in all types of multicomponent system, the recent literature shows a clear trend toward following time-dependent processes. These processes include, but are not limited to [1]:

- Self-assembly of surfactants, polymers, and proteins at solid and liquid interfaces
- Rearrangement processes in thin films: polymer interdiffusion, inter-layer movement, lipid flip-flop, and annealing/drying/exchange/wetting processes in composite films such as photovoltaic materials
- Encapsulation and release of components in plastics, polymer blends, drug delivery and implant materials, and chemical and biological sensors
- Switchable materials that undergo structural changes in response to external chemical, mechanical, electrical, or magnetic stimuli
- Surface reactions that involve change in film structure or chemical composition; e.g., enzyme catalysis, oxidation or other film degradation reactions, receptor-ligand binding, drug-target interactions, surface functionalization, etc.

The recent literature contains a number of interesting kinetic studies, capturing the early development of this nascent field. The performance of organic photovoltaic materials depends crucially on intimate contact between light-absorbing and electron-conducting polymers. In Fig. 4.6 below, researchers at Australian Nuclear Science and Technology Organisation (ANSTO) [2] tracked the diffusion of light-harvesting phenyl-C61-butyric acid methyl ester (PCBM) into conducting poly(3-hexylthiophene) (P3HT). Films annealed at 130°C exhibited dramatically improved transport properties. Time-resolved neutron reflectivity measurements (5 min shots during a temperature ramp) tracked the onset and rapid diffusion of PCBM into the P3HT matrix beginning at 120°C (right figure).

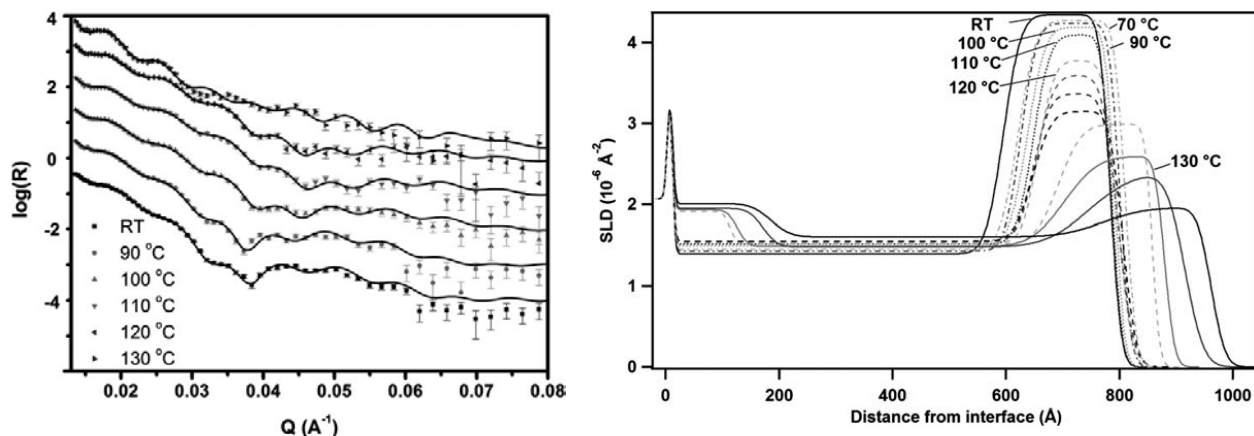


Fig. 4.6. Neutron reflectivity (left) and fitted scattering length density profiles (right) of PCBM/P3HT bilayer. Data were collected in 5-minute time intervals, from which can be seen the rapid redistribution of PCBM beginning at 120°C [2].

In another study, researchers working at ISIS at Rutherford Appleton Laboratory and ILL investigated the interaction of ozone with a lung surfactant monolayer deposited on the surface of water in a Langmuir trough [3]. Unsaturated lipids in lung surfactant are required for proper respiratory function. The prevalence of pollutants such as ozone in the environment is an ongoing human health concern. In Fig. 4.7, the lipid Pd_{17}OPC was exposed to ozone in a Langmuir trough within a sealed box. The destruction of the lipid layer is tracked by the reduction of reflectivity in 750 s time shots.

As a final example of research in this nascent field, our colleagues at ILL studied lipid rearrangement in model bilayers [4]. The relative proportion and arrangement of lipids in natural and model membranes is a subject of ongoing study. By tracking the time dependence of lipid bilayer structure, they were able to determine that lipids transfer from one leaflet to the other only when both leaflets are in the liquid phase. The $T = 53^\circ\text{C}$ curve in Fig. 4.8 depicts a time-weighted average because the data could not be collected rapidly enough to depict a single state.

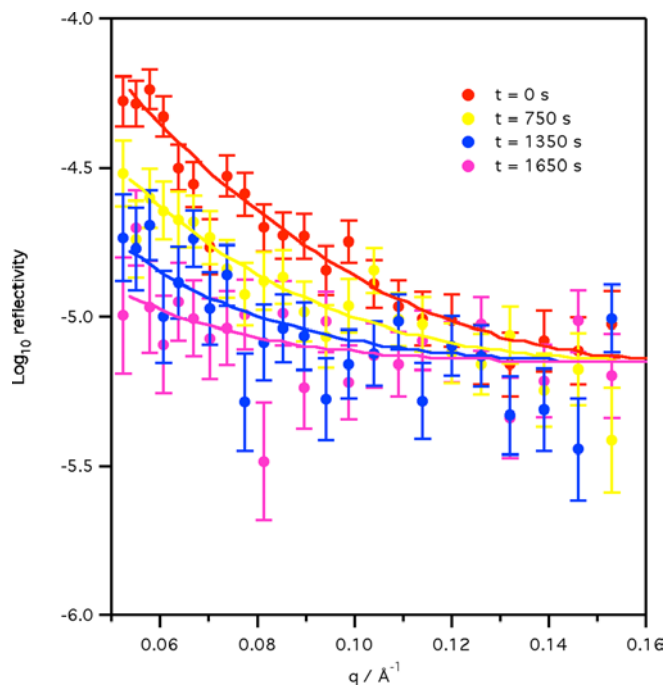


Fig. 4.7. Dissolution of lipid monolayer on water surface upon exposure to ozone tracked in 750 s time shots [3].

None of the above experiments could have been carried out at the current SNS FTS because of bandwidth restrictions. Using the Liquids Reflectometer, we can measure, for example, $0.02\text{--}0.05 \text{\AA}^{-1}$, $0.05\text{--}0.10 \text{\AA}^{-1}$, and $0.10\text{--}0.20 \text{\AA}^{-1}$, but not all at once in a single setting. To extract structure from specular

reflectivity data, the researcher needs to fit the whole curve, and in time-dependent measurements, the researcher cannot always anticipate where changes will occur. Measurements such as those described above require a reflectometer with a large Q bandwidth.

Initial Science Objectives

1. Understanding the nature of the glassy surface-solvent interaction

Research Theme's Associated Workshop:

Soft Matter

Potential Partners (*Attendees of

Associated Workshop):

Matt Tirrell* (University of Chicago)

Juan de Pablo* (University of Chicago)

Tom Russell* (University of Massachusetts)

Often in soft materials, the materials are prepared or used in a glassy state. This non-equilibrium, frozen, and disordered structure is typically induced by slowly supercooling the material below the glass transition temperature. More recently it has been shown that by direct vapor deposition of molecular materials at low temperatures, high density glasses may be created. Unlike thermally produced glasses, these high-density glasses show little aging with time reminiscent of thermally annealed samples that have aged for thousands of years [5]. Recent experiments on the spreading of liquids across polymer surfaces show that the way in which these glassy materials interact with solvents depends strongly on their state [6]. For example, measurements of the contact angle as a function of the spreading velocity of a polar solvent drop on a polymer thin film suggests the polymer is solvent melting and changes from a glassy to a liquid state at the solvent front. The behavior is also strongly dependent on the initial humidity. With the kinetics reflectometer, we will have the opportunity to study the surface interaction of solvents with polymer surfaces as we vary environmental conditions that determine the glassy state of the materials. We will perform time-dependent reflectometry experiments where we can hold the temperature of the film below or above the glass transition temperature and study the solvent density profile on a molecular level as a function of controlled solvent vapor pressure.

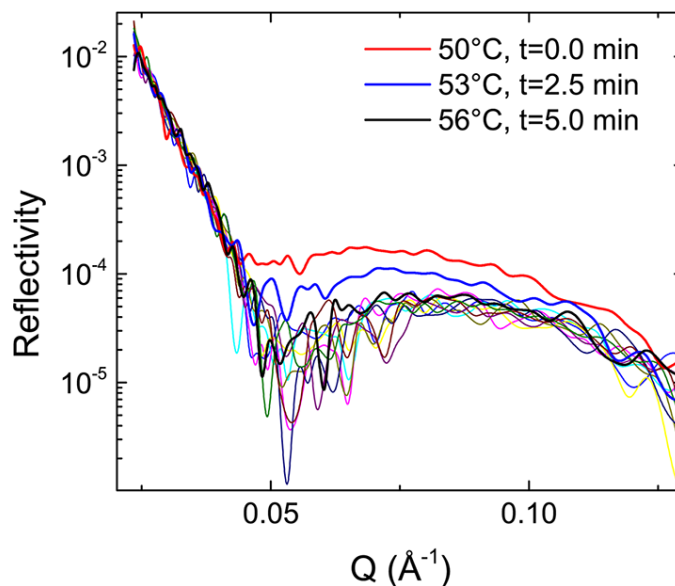


Fig. 4.8. Neutron reflectivity of DSPC/DMPC bilayer against D_2O collected in 2.5 min shots [4].

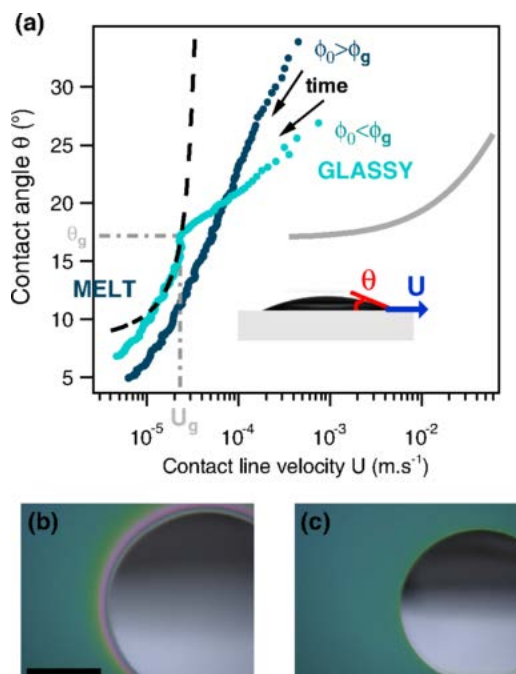


Fig. 4.9. (a) Contact angle as a function of the contact line velocity of a water droplet spontaneously spreading on a $2.7 \mu\text{m}$ thick layer of maltodextrin.

(b), (c) Color images from the top of a droplet of DMSO spreading onto a 550 nm thick layer of maltodextrin [6].

This will be done on a series of polymer films prepared by spin coating and then slowly brought below the glass transition temperature as well as glassy films vapor deposited. With these experiments, we expect to learn more about the fundamental interactions between polymer surfaces in the glassy state and polar solvents.

2. Kinetic pathways of multicomponent hierarchical assembly in soft materials

Research Theme's Associated Workshop: Soft Matter

Potential Partners (*Attendees of Associated Workshop):

Brett Helms* (Lawrence Berkeley National Lab)

Michael Chabiny* (University of California, Santa Barbara)

Tom Russell* (University of Massachusetts)

The surface and interfacial structure developed in composites of directed, self-assembled, nanocrystalline materials in a soft matrix are often a non-equilibrium result of highly path dependent processing conditions. For example, many soft films are deposited by spin coating or spray coating where the surface quality is highly dependent on solvent concentration, solvent vapor pressure, spinning speed and acceleration, and annealing treatment. In this study, design rules for the self-assembly of these hierarchical materials at arbitrary inorganic interfaces will be explored. Examples of rearrangement processes in thin films include polymer interdiffusion, inter-layer movement, annealing/drying/exchange/wetting, and layer flip-flop processes in composite films such as photovoltaic materials. In particular, the kinetics reflectometer will permit real-time exploration of the interfacial and surface structure developed during non-reversible thin film assembly in controlled environmental conditions and at a variety of surface types including solid-vapor and solid-solution interfaces and surface morphologies (flat polished versus patterned). By using selectively deuterated materials, we can determine the layered structure of the film as a function of processing conditions. Introduction of atmospheric jumps including temperature, pressure, or solvent chemical potential may be explored in situ and in real time for each excursion. Presently, any such changes in conditions must be quenched, or only the final conditions may be explored. In either case, these experiments presently are performed ex situ and do not permit the exploration of intermediate states.

Technical Description

The characteristics of the SNS FTS place limitations on the manner in which reflectivity data can be collected. In particular, operating at 60 Hz severely limits the available wavelength bandwidth, necessitating multiple instrument settings to collect data sets. Piecing these data sets together not only introduces complexity and sources of error into data reduction and analysis but also precludes studying kinetic processes on time scales less than 10 min (due to motor and chopper phasing delays). Operating the SNS Liquids Reflectometer at 10 Hz would add a world-beating capability that simply does not exist currently at SNS. Placing a very similar instrument at STS featuring enhanced cold flux will yield factors of 20–50 improvements in time resolution relative to the best existing instruments.

By making relatively modest changes to the design of the current SNS FTS Liquids Reflectometer, one can realize the “single-shot” paradigm on a 10 Hz STS.

- Source: SNS STS
- Instrument length: moderator to sample, 13.5 m; sample to detector, 1.5 m
- ^3He 2D PSD, $20 \times 20 \text{ cm}^2$, 1 mm pixel resolution, or equivalent
- $2.5 \text{ \AA} < \lambda < 30 \text{ \AA}$ (a shorter Maxwell distribution peak would greatly enhance Q range)
- Resolution: $\delta\lambda/\lambda < 0.01$
- Moderator type: coupled H_2
- Polarization option
- Sample size: flat surfaces $1\text{--}15 \text{ cm}^2$
- Optics system: curved multi-channel bender, possibly elliptical horizontal focusing
- Chopper system: a bandwidth chopper or two
- Beam divergence: Defined by guide system and slits
- Performance estimate and basis: 10–20 \times ISIS Inter; 20–30 \times ILL Figaro and ANSTO Platypus (flux and bandwidth scaling)
- Wet chemistry laboratory adjacent to instrument

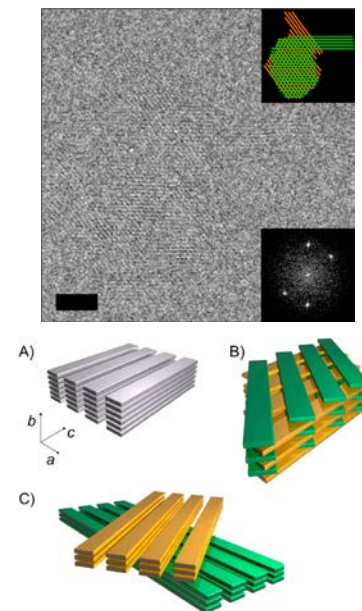


Fig. 4.10. Schematic representation of (A) a lamellar crystal, (B) a crystal with a nonparallel backbone structure, and (C) a quadrite, an epitaxial arrangement of two lamellae across the ac plane.

The film is made from many such crystallites. Neutron reflectometry can help elucidate the real time construction of the average surface properties [7].

- Langmuir trough, environment chamber, potentiostat, and other sample environments fully integrated as part of the construction project

Table 4.2. Key instrument parameters for Kinetics Reflectometer

Source	STS
Moderator type	Cold, coupled H ₂
Wavelength/energy range	2.5 Å < λ < 30 Å
Resolution	$\delta\lambda/\lambda < 0.01$
Sample size range (beam size)	1.5 × 3 cm ²
Moderator—sample distance	13.5 m
Sample—detector distance	1.5 m
Detector type	³ He 2D PSD

References

- [1] H. Wacklin and A. Vickery. “ESS Instrument Construction Proposal—FREIA” (2014).
- [2] K. H. Lee, et al., “Correlation of diffusion and performance in sequentially processed P3HT/PCBM heterojunctions films by time-resolved neutron reflectometry,” *J. Mater. Chem. C* **1**, 2593 (2013).
- [3] K. C. Thompson, et al., “Degradation and Rearrangement of a Lung Surfactant Lipid at the Air-Water Interface during Exposure to the Pollutant Gas Ozone,” *Langmuir* **29**, 4594 (2013).
- [4] Y. Gerelli, L. Porcar, and G. Fragneto, “Lipid Rearrangement in DSPC/DMPC Bilayers: A Neutron Reflectometry Study,” *Langmuir* **28**, 15922 (2012).
- [5] P.-H. Lin, et al, *J. Chem. Phys.* **140**, 204504 (2014).
- [6] J. Dupas, et al., *PRL* **112**, 188302 (2014).
- [7] C. J. Takacs, et al., *Nano Letters* **14**, 3096 (2014).

4.5 VBPR (VARIABLE BEAM PROFILE REFLECTOMETER)

*Jim Browning, Chemical and Engineering Materials Division
John Ankner, Biology and Soft Matter Division*

Abstract

A horizontal geometry neutron reflectometer capable of delivering a variable beam profile extending to millimeter size samples enables surface and interfacial studies to a broader class of materials and sample type than is currently accessible. The Variable Beam Profile Reflectometer (VBPR) will allow a user to accurately define the beam profile on a sample’s surface to as small as 1 mm² without the use of apertures in the immediate sample position, leaving room for large or extended sample environments. VBPR will take advantage of the pulse characteristic and brightness of STS to deliver a broad wavelength band at high fluence. This permits the acquisition of an extended Q-range from a single instrument

setting while greatly reducing measurement time and opening the possibility for kinetic studies on a sub-second time scale.

Science Case

Interest in surface and interfacial phenomena continue to increase across diverse scientific areas ranging from biology to geoscience. When coupled with isotopic substitution or complicated sample environments, neutron reflectometry (NR) remains a method of choice in the study of interfaces. However, current interest is beginning to shift to samples that do not meet the traditional NR sample criteria of a large, homogeneous surface area. Examples of such systems include patterned or graded surfaces used to understand layer conformation and its effect on surface properties, solid-state diffusion over short length scales, hybrid (organic/inorganic) materials of technological interest with limited lateral dimension or heterogeneous surface structure, or materials in extreme environments.

1. **Soft-Layer Conformation at Interfaces.** Nanopatterned surfaces formed by e-beam lithography have been proposed as platforms to investigate structure such as the conformation of suspended soft-surface coatings or protein conformation at the surface of a suspended lipid bilayer [1]. E-beam lithography is a time-consuming process that can take days to produce the large surface area patterns needed for conventional NR measurement. The ability to probe such systems on a millimeter length scale will eliminate the need to produce large patterned surfaces and open new areas of research.
2. **Interphase Formation.** In battery materials research, understanding the formation of the solid-electrolyte interphase (SEI) is critical to the performance and safety of energy storage materials, yet SEI formation is poorly understood. NR is ideally suited for the study of SEI formation in situ. However, it can be difficult to obtain a uniform electric field over large surface area electrodes, leading to lateral inhomogeneity in layer formation. The ability to define a small beam profile on the sample makes it possible to select specific areas or eliminate the need for large-area electrochemical cells altogether.
3. **Diffusion in Solids.** The study of diffusion processes over short length scales (\sim nm) is a developing area of research in energy storage, nanostructured, and semiconductor materials. In situ NR can play a major role in the study of such systems by using stable isotope substitution (e.g., $^6\text{Li}/^7\text{Li}$ in energy storage materials) and multilayered film configurations. However, this approach may be viewed as too expensive because of the high cost of many stable isotopes. The technique can be greatly enhanced with the use of smaller samples. VBPR will enable the use of much smaller samples, with surface areas as much as two orders of magnitude smaller than those currently used, therefore proportionally lowering the cost per sample. More significantly, the use of smaller samples will greatly improve time resolution by improving the response time of heating and cooling samples.

In general, large beam profiles that extend large sample areas result in an averaging of the scattering length density profile, perpendicular to the surface, over the entire surface of the sample. The result is that information regarding lateral inhomogeneity is lost. The ability to focus the beam to as small as 1 mm^2 will allow the user to “raster” a sample, effectively measuring variations in the scattering length density profile as a function of lateral position on the sample. This could allow NR measurements of nontraditional materials such as naturally occurring minerals or samples deposited onto irregular surfaces.

Initial Science Objectives

1. The neutron surface forces apparatus

Research Theme's Associated Workshop: Soft Matter

Potential Partners (*Attendees of Associated Workshop):

Matt Tirrell* (University of Chicago)

Tonya Kuhl* (University of California, Davis)

Jacob Israelachvili (University of California, Santa Barbara)

One of the most fundamental questions in the molecular structure of polymers is, "What is the nature of the interactions between molecules, and how do those interactions affect the molecular structure?" Among the most successful tools devised to measure the surface forces is the Surface Forces Apparatus (SFA) invented by Jacob Israelachvili [2]. This device measures the forces between two cylindrical mica surfaces, each coated with a layer of the materials to be measured. The forces between the surfaces can then be

measured as a function of surface separation. With the small footprint of the VBPR, we can begin to reduce the size of the contact area between surfaces in confined geometry. Although we cannot approach the SFA contact area, we can envision building a cell that can achieve confinement gaps of ~ 10 nm (currently with large area cells, we can obtain separations of several 10s of nm). With this cell, we can simultaneously measure the detailed structure and forces between two surfaces coated with soft thin films. In addition, the smaller size will permit us to incorporate sliding surfaces, which will allow us to reproduce the frictional forces measured using SFA and, therefore, the surface structure under shear. The ability of the neutron to penetrate through the substrate materials (single crystal quartz or silicon) will permit us to study the surface structure of confined polymers. By selective deuteration and by contrast matching with a solvent, we can highlight the effect of the forces on the surface structure.

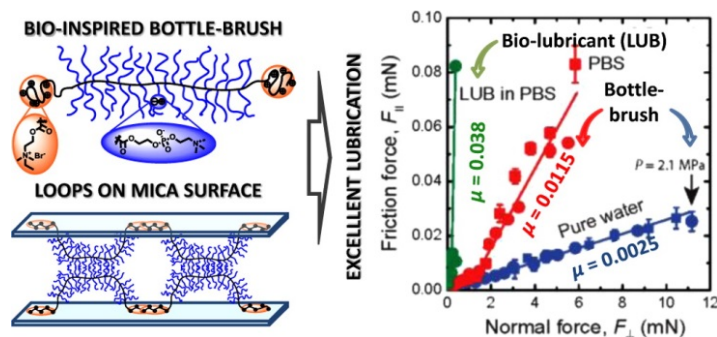


Fig. 4.11. Schematic representation of surface forces experiment on a biomimetic bottlebrush polymer. [3]

2. What is the molecular nature of contact adhesion?

Research Theme's Associated Workshop: Soft Matter

Potential Partners (*Attendees of Associated Workshop):

Matt Tirrell* (University of Chicago)

Oleg Gang* (Brookhaven National Laboratory)

Bret Helms* (Lawrence Berkeley National Laboratory)

Matt Helgeson* (University of California, Santa Barbara)

When soft surfaces are brought into contact in the melt or in a solvent, they may or may not form a bonded interface. These experiments are intended to explore the nature of thin films in confined geometry. Some of the questions to explore include the following:

- How does adhesion develop between confined films?
- How do charged, uncharged, or mixed polymers interpenetrate on approach, and how does their structure vary with applied force?
- How do hierarchical multicomponent film structures change in confined geometry?
- How does change in confinement or applied stress affect the kinetic restructuring of tethered molecules (e.g., DNA) at a surface, and what are the associated time scales?

These experiments will complement SANS studies of linkers and directed self-assembly between nanoparticles by a detailed understanding of the surface structure between surfaces at separations below 10 nm. The small surface areas probed by the mmLR will enable experiments using a confined surface cell to understand how soft materials respond to applied uniaxial surface stress at the nanoscale. At present, variable confinement experiments using neutron reflectometry require that the alignment of two opposing and parallel surfaces on the order of 10s of cm^2 in area be brought into contact to confine a thin film. With state-of-the-art polished surfaces (with a surface waviness of $\lambda/20$) and great experimental effort, two such surfaces can be used to define a gap size \sim several 10s of nm. However, with a surface area of only a few mm^2 , surface waviness and surface contamination can be reduced. In this case, surface approach and confinement may be improved to less than 10 nm permitting studies of polymers and DNA, surfactant and lipids, and even simple fluids as they approach each other. Combined with selective deuteration, new insight into the detailed molecular nature of these surface interactions may be gathered as they form and change with changing gap size.

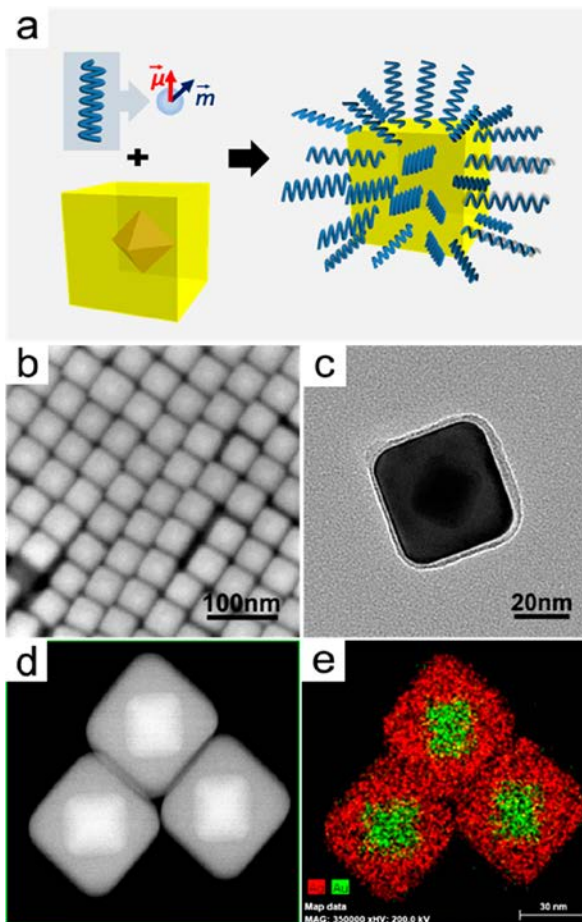


Fig. 4.12. Plasmonic nanoparticles built with hard core nanoparticles and soft linking materials at the interfaces. [4].

Technical Description

The VBPR comprises an elliptical guide system that will focus a divergent beam allowing its profile, or footprint on the sample, to be tuned and avoid over-illumination [5]. The length of the instrument from moderator to detector is approximately 15 m with a sample to detector distance of ~ 2 m. The VBPR would require a relatively large area position sensitive detector with a resolution ~ 1 mm. The beam profile on sample is expected to range from ~ 1 mm² to several hundred square millimeters.

Table 4.3. Key instrument parameters for VBPR

Source	STS
Moderator type	Cold, coupled H ₂
Wavelength/energy range	$2.5 \text{ \AA} < \lambda < 15.5 \text{ \AA}$
Resolution	$\delta\lambda/\lambda < 0.05$
Sample size range (beam size)	$1.0 \times 1.0 \text{ mm}^2$
Moderator—sample distance	30 m
Sample—detector distance	2 m
Detector type	³ He 2D PSD (1 mm resolution)

References

- [1] G. Smith, et al., “Bilayer self-assembly on a hydrophilic, deterministically nanopatterned surface,” *Nano Research* **6**, 784 (2013).
- [2] J. Israelachvili, et al., *Rep. Prog. Phys.* **73**, 36601 (2010).
- [3] X. Banquy, et al., *JACS* **136**, 6199 (2014).
- [4] F. Lu, et al., *Nano Letters* **13**, 3145 (2013).
- [5] J. Stahn, U. Filges, and T. Panzner, “Focusing specular neutron reflectometry for small samples,” *The European Physical Journal Applied Physics* **58**, 11001 (2012).

4.6 MBARS (MICA BACKSCATTERING SPECTROMETER) FOR STS

E. Mamontov (CEMD)

Abstract

A mica-based backscattering spectrometer, MBARS, optimized for small samples, will open new frontiers in biology and soft matter science. In combination with a companion broad-range inverted geometry spectrometer (BWAVES), MBARS will provide coverage over 7 orders of magnitude in relaxation time. In the quasielastic neutron scattering (QENS) regime, these two spectrometers will provide access to the same lower-Q range (particularly relevant to soft matter and biology systems), thanks to identical choice of the scattering angle coverage and the final wavelength of 20 Å. The latter requires a high flux of long-wavelength neutrons available at STS, where both spectrometers need to be placed.

Science Case

Inelastic neutron scattering—in particular, backscattering spectroscopy—is the only experimental technique that probes not only the time, but also the spatial characteristics of microscopic dynamics in various systems on the highly relevant nanometer length scale, through the Q-dependence of the inelastic and quasielastic spectra. As such, this technique is uniquely suited for comparison with and validation of molecular dynamics simulations. The success of the FTS backscattering spectrometer, BASIS, has demonstrated the preference by the scientific community for a combination of the high energy resolution and the broad accessible range of energy transfer (dynamic range) for studying microscopic relaxation dynamics. Access to lower Q values and longer relaxation times (to probe larger structural units involved in slower motions) is needed for studying more complex biological and soft matter systems. At the same time, many biological samples would be difficult or impossible to synthesize in quantities sufficient to use the traditional (about 10 cm²) neutron beam cross-section available at backscattering spectrometers. MBARS will be the answer to these challenges, featuring the highest energy resolution of any neutron backscattering spectrometer, the broad accessible dynamic range, the access to low Q values, and the neutron beam cross-section 10 times smaller compared with today's backscattering spectrometers.

1. **Optimization for measurements of small samples that are difficult to obtain in sufficient quantities or that require selective deuteration.** Because of the large incoherent neutron scattering cross-section of hydrogen (large when compared with all the other elements including deuterium), partial deuteration of biological molecules is a powerful tool for studies of the microscopic dynamics of, for example, protein residues and chains. For most samples, selective deuteration is challenging and time- and resource-consuming, and the quantity of the deuterated protein is usually the limiting factor. MBARS can measure samples that are 10 times smaller compared to those presently required by neutron backscattering spectrometers.
2. **Access to much longer relaxation times.** MBARS will offer an energy resolution 15 times better compared to BASIS while providing a comparable dynamic range. This will provide access to the relaxation processes 15 times slower than currently possible to probe, which is especially important for complex biological systems.
3. **Continuous overlap, at all Q values, with a companion spectrometer to achieve very wide dynamic range.** For the first time in the practice of neutron scattering facilities, a combination of the very high-resolution backscattering spectrometer and the very broad-range inverted geometry spectrometer will yield spectra comparable to those obtained by dielectric spectroscopy, but with the unique advantages offered by neutron scattering, such as hydrogen/deuterium selectivity and spatial resolution capabilities (through the Q-dependence of the scattering signal).

Specific Science Examples

1. Protein-solvent coupling (Biology and Biophysics)

The function of proteins is strongly affected by their interaction with the solvent molecules. Because of the complex character of solvent relaxations, researchers commonly strive to probe the temperature dependence of the protein-solvent dynamics. As the temperature is gradually increased from the very low baseline temperature, where only the vibrational degrees of freedom are present, the relaxational degrees of freedom become activated. The numerous

unresolved controversies in the field largely stem from the energy resolution limitations of present day neutron backscattering spectrometers; which dynamic effects in proteins-solvents are truly resolution-independent, and thus characterize the properties of the system, not the particular spectrometer? The STS very high-resolution backscattering spectrometer, MBARS, will answer these unresolved questions through achieving far better resolution, on the 200 nano-eV energy scale, than anything possible on backscattering spectrometers today (Fig. 4.13).

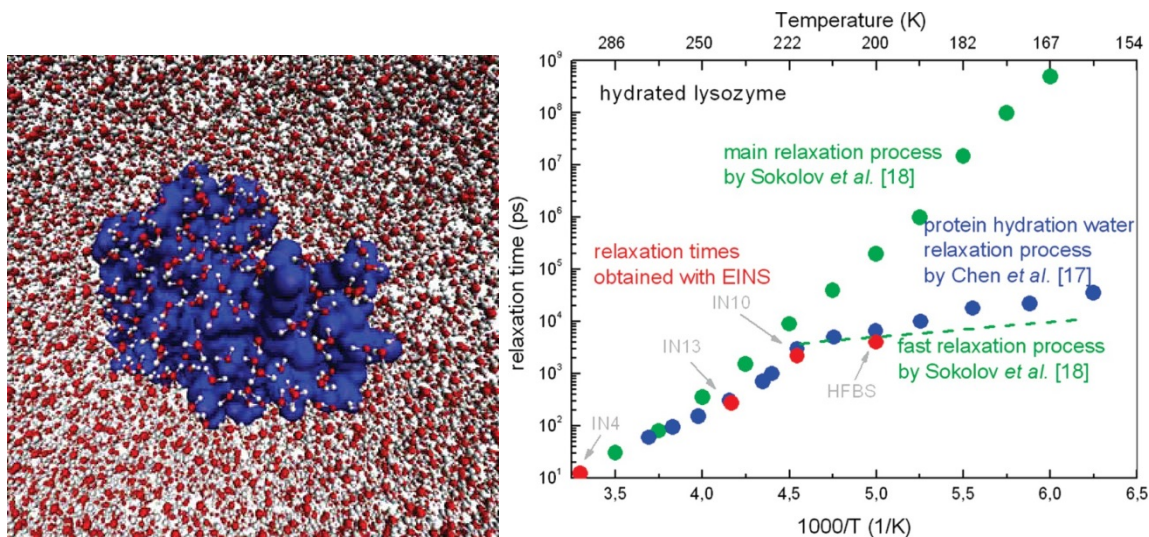


Fig. 4.13. The protein-solvent dynamic processes in hydrated/solvated proteins (left figure [1]) have been studied using neutron spectrometers of variable energy resolution (right figure [2]). However, even the best present day backscattering spectrometers lack sufficient resolution to resolve the multiple controversies remaining in the field that preclude our understanding of the protein-solvent coupling and function.

2. Lithium diffusion in solid state battery component materials under ambient conditions (Chemical Physics and Advanced Functional Materials)

Lithium batteries work by transport of lithium ions across multilayer porous electrodes with concurrent electron transport in the external circuit (Fig. 4.14). Most often, the rate limiting step in the transport process is due to the low mobility or diffusion of lithium ions in the solid electrode phase or due to mass transport issues arising from the movement of ions through the tortuous electrode bulk. The rate or power density is mostly dependent on the ionic transport coefficient of lithium in the host structures. QENS has a unique capability, as a characterization technique, of investigating the details of lithium ions diffusion in the host structures, yielding information such as the diffusion jump length and the residence time between the successive jumps. The current SNS backscattering spectrometer, BASIS, has already demonstrated a potential for QENS studies of lithium diffusion in battery component materials. This is no small feat, given that lithium, unlike hydrogen, does not have a large neutron scattering cross-section, and lithium-bearing compounds, unlike hydrogen-bearing compounds, are not routinely studied by QENS because of the very stringent requirements to the spectrometer's signal strength and signal-to-noise ratio. Unfortunately, we have found that the current energy resolution of neutron backscattering limits QENS experiments on lithium diffusion to the temperatures above *ca.* 350 K. Below this temperature, the QENS broadening from lithium diffusion cannot be resolved (e.g., ref. [3] and unpublished results by J. Nanda's group). QENS studies of lithium

diffusion under realistic conditions (ambient and slightly below ambient temperatures) thus require improved energy resolution, which will be achieved by MBARS.

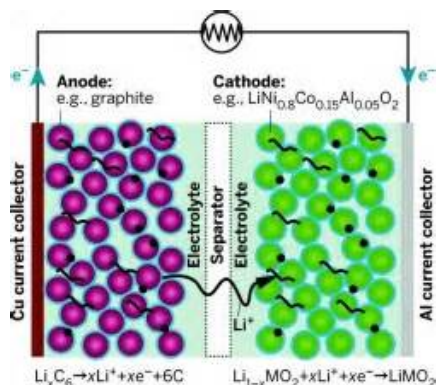


Fig. 4.14. Schematic of lithium transport in a solid state battery.

The microscopic parameters of lithium diffusion in the battery component materials (e.g., the jump length and the residence time between the successive jumps) can be directly probed by QENS, but the energy resolution of today's backscattering spectrometers needs improvement to probe these parameters at near ambient temperatures.

3. Data bank of protein dynamics (in tandem with BWAVES spectrometer) (Biology)

MBARS will be used in tandem with another STS instrument, a very broad-range high-resolution spectrometer BWAVES, to cover 7 orders of magnitude in the energy transfer (relaxation times). This will yield spectra comparable to broadband dielectric spectroscopy data, but with sensitivity to the scattering momentum transfer (that is, the microscopic length scale) and deuterium/hydrogen selectivity (Fig. 4.15). Such spectra will be particularly suitable for the neutron Dynamics Data Bank (DDB), recently initiated by the group of G. Zaccai [4]. Because of the limitations of today's neutron spectrometers, the present day data for the Dynamics Data Bank are collected in "piecemeal" fashion, with only a small energy range of excitations (that is, a small range of relaxation times) probed in a given neutron scattering experiment. Such approach is not adequate for biosystems (and, in general, soft matter systems), which exhibit broad, overlapping excitation, both quasielastic and inelastic in character. The present day attempts to merge the data from different spectrometers are hampered by the mismatch in their momentum transfer coverage. On the other hand, MBARS and BWAVES will feature an identical momentum transfer range, allowing for perfect data overlap resulting in spectra of unprecedented quality for the Dynamics Data Bank.

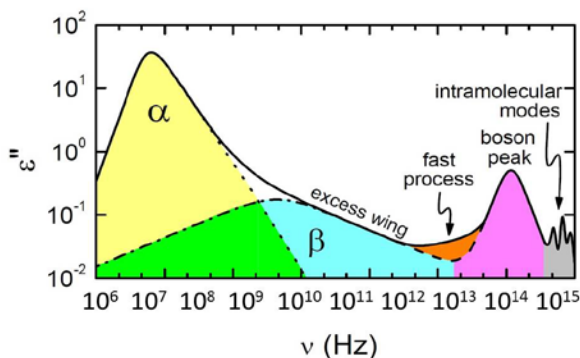


Fig. 4.15. Schematic presentation of the microscopic dynamic processes in complex glass-forming systems spanning many orders of magnitude in relaxation time.

This picture also represents some essential features of protein dynamics, albeit greatly simplified.

Technical Details

MBARS can be built only at a short-pulse, long-wavelength source with a low repetition rate, such as the 10 Hz STS. The very high energy resolution requires long neutron time-of-flight (that is, a long neutron wavelength and a long primary flight path). The long flight path, in turn, requires a low repetition rate to preserve a sufficiently wide dynamic range. The specified energy resolution of 200 neV (FWHM) calls for a cold decoupled moderator with a pulse width of 90 μs or narrower for the primary flight path of 63 m. To match the energy resolution of the primary flight path for a 0.25 cm^2 sample and a 2 m sample-to-analyzer flight path, we will employ fluorophlogopite mica analyzer crystals with 0.30° mosaic spread (FWHM) ($\delta d/d = 2.3 \times 10^{-4}$ for (002) reflection at $E = 0.2045 \mu\text{eV}$) at a Bragg angle of 88.5°. The specified dynamic range of $\pm 0.060 \text{ meV}$ will be free of potential contamination from the neutron up-scattering in the sample to the higher order mica reflections ([004], [006], [008], etc.) with the use of WAVES, the recently proposed wide-angle velocity selector for the scattered neutrons. Although the concept of WAVES has been developed, practical implementation requires research and development. The long neutron wavelength used by MBARS will result in the lower Q values (0.03 to 0.60 \AA^{-1}), providing additional benefits to biological and soft matter research. Because of the small sample size, the moderator needs to be only a few cm in size horizontally and vertically. The desired divergence of the neutrons incident on the sample is limited by WAVES in the vertical directions, and should not exceed $\pm 0.5^\circ$ in both directions. A curved guide will be used to eliminate the direct view of the moderator by the sample. Four low-speed (10 Hz) incident bandwidth selection choppers will be used. A relatively small detector array consisting of linear position-sensitive ^3He tubes will intercept the neutrons reflected by the analyzer mica crystals at scattering angles from 5° to 160° . Both the primary and secondary flight path will be evacuated. Given the long neutron wavelength, an effort will be made to use sapphire (as opposed to aluminum) windows along the secondary flight path to reduce neutron absorption. Likewise, the sample holders need to be manufactured using sapphire because traditional aluminum sample holders would produce undesirable background at the lowest Q values. The implementation of WAVES will allow the use of the higher-order mica reflections whenever the wider Q-range, at the expense of the energy resolution, is desired.

Table 4.4. Key instrument parameters for MBARS

Source	STS
Moderator type	Cold, de-coupled H_2 (<90 μs pulse at $\lambda = 20 \text{ \AA}$)
Energy transfer range	$\pm 0.060 \text{ meV}$
Resolution E	0.2 μeV
Sample size range (beam size)	$0.5 \times 0.5 \text{ cm}^2$
Moderator—sample distance	63 m
Sample—detector distance	3.75 m (2 m sample-analyzer)
Detector type	^3He linear position sensitive

References

- [1] Chu et al., *J. Phys. Chem. Lett.* **3**, 380–385 (2012).
- [2] S. Magazu et al., *J. Phys. Chem. B* **115**, 7736–7743 (2011).
- [3] H. Nozaki et al., *Solid State Ionic* **262**, 585–588 (2014).
- [4] L. Rusevich et al., *Eur. Phys. J. E* **36**, 80 (2013).

4.7 BWAVES (BROAD-RANGE WIDE ANGLE VELOCITY SELECTOR) FOR STS

E. Mamontov (CEMD)

Abstract

BWAVES, a high-resolution, broad energy transfer range, inverted geometry spectrometer optimized for small samples, will open new frontiers in biology and soft matter science. BWAVES alone will cover 5 orders of magnitude in energy transfer, from several μeV to several hundred meV, making it a one-stop instrument for vibrational spectroscopy of biomolecules. The combination of MBARS and BWAVES will cover more than 7 orders of magnitude in relaxation time. In the quasielastic regime, these two spectrometers will provide access to the same lower-Q range (particularly relevant to soft matter and biology systems) because of identical choice of the scattering angle coverage and the final wavelength of 20 Å. The latter requires a high flux of long-wavelength neutrons available at STS, where both spectrometers need to be placed.

Science Case

Inelastic neutron scattering (INS) is indispensable for studying microscopic dynamics of complex biological and soft matter systems because of a combination of the following characteristics.

1. High sensitivity to hydrogen and hydrogen/deuterium selectivity, unmatched by other probes except NMR.
2. High energy resolution, far exceeding the energy resolution attainable in synchrotron x-ray inelastic scattering experiments.
3. Information on the geometry of motions obtained through the signal sensitivity to the scattering momentum transfer, Q , which NMR and dielectric spectroscopy do not possess.

However, there are barriers limiting the use of INS for studying biomolecules, including the relatively large incident beam size, which requires large samples, and the limited dynamic range of neutron spectrometers. The challenge is exacerbated by the complex microscopic dynamics exhibited by soft matter systems, and even more so by proteins, which show more features than the dynamics in hard matter because of the simultaneous presence of the vibrational and relaxational processes. This calls for continuous, rather than piecemeal, coverage of the accessible energy transfer in a single experiment. Such a continuous coverage is provided by inverted geometry spectrometers of TOSCA/VISION type, which, however, lack the energy resolution to simultaneously study the quasielastic signal originating from relaxations in soft matter. To this end, we propose to build BWAVES, a small beam size, broadband

inverted geometry spectrometer optimized for biological and soft-matter samples that utilizes a novel wide-angle velocity selection device, WAVES, instead of traditional crystal analyzers, for the final energy selection of scattered neutrons. The case for small samples and complementarity with MBARS is stated in the MBARS description above.

Specific Science Examples

1. Biomolecules in real-life biological solvents (Biology and Biophysics)

Even though the function of proteins and other biomolecules critically depends on their interaction with the solvent, neutron scattering studies of microscopic dynamics of biomolecules to date are commonly performed on powder samples of biomolecules with a limited hydration level. Such model systems profoundly differ from the real-life biomolecules solvated in aqueous, biologically active media. The current SNS backscattering spectrometer, BASIS, has demonstrated some potential for studying proteins solvated in realistic aqueous environments. To date, spectrometers with the energy resolution similar to that of BASIS, needed to match the internal protein dynamics, invariably suffer from a limited accessible dynamic range. The BWAVES will have energy resolution similar to that of BASIS but also the extremely broad dynamic range to probe the faster dynamics of the solvent simultaneously with protein dynamics. The advent of BWAVES will change the existing research paradigm and open a new era of simultaneous measurements of the microscopic dynamics of biomolecules and their real-life solvents. Studies of the influence of co-solvents, solvent pH, etc., on the dynamics of the solvated biomolecules, which are not possible with hydrated powders, will become standard (Fig. 4.16).

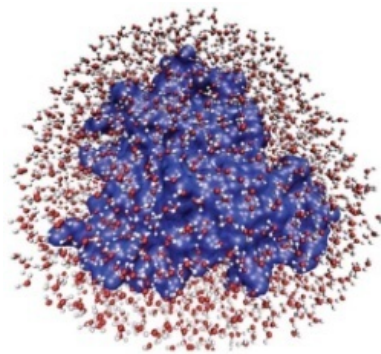


Fig. 4.16. Instead of commonly performed to date model system studies of proteins as hydrated powders (left figure, adapted from [1]), we aim at studies of proteins in real-life biological solvents (right figure), with simultaneous characterization of the microscopic dynamics of both the solute and solvent.

2. Microscopic dynamics in complex liquid electrolytes (Chemical Physics and Advanced Functional Materials)

The research focus for better liquid electrolytes has recently shifted to complex systems such as room-temperature ionic liquids (RTILs). The performance of RTILs in applications is tied to the microscopic dynamics of their cations and anions, which can be quite complex. The vibrational dynamics of ions in RTILs can be measured using traditional probes such as IR and Raman scattering but would be studied more effectively by vibrational neutron spectroscopy (e.g., employing selective deuteration). However, in the practically important liquid state, the low-energy modes overlap with the quasielastic signal because of both the center-of-mass and side group ion relaxation dynamics. BWAVES, which can measure both quasielastic and inelastic

scattering signals simultaneously, will provide an unprecedented, detailed picture of the microscopic dynamics of RTILs responsible for their application performance, which is impossible to obtain with present day spectrometers.

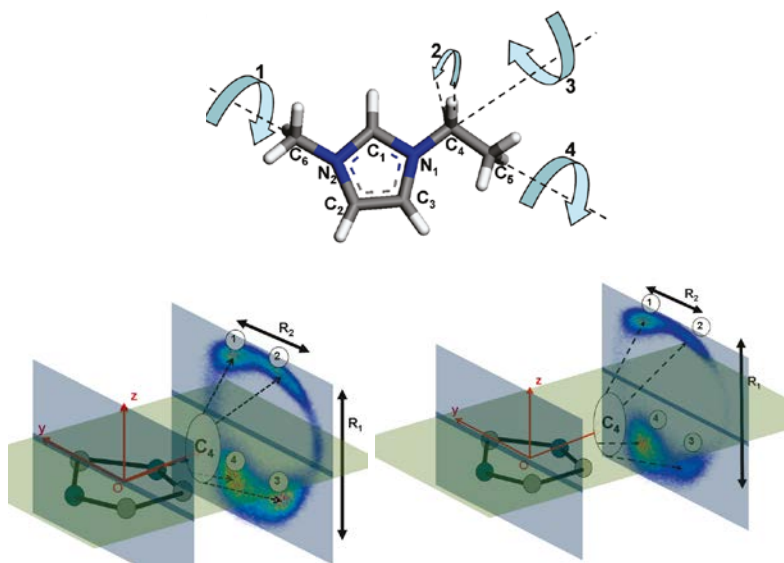


Fig. 4.17. Possible reorientational motions of the Emim cation (top) and contour plots (bottom) of the spatial distribution of the C₅ carbon atom relative to the N₁ carbon atom in the solid (right) and liquid (left) phases in a room temperature ionic liquid 1-ethyl-3-methyl-imidazolium bromide [2].

3. Data bank of protein dynamics (Biology) (in tandem with MBARS spectrometer)

As discussed above in the MBARS instrument description, the combination of these two spectrometers will provide an unprecedented 7 orders of magnitude dynamic range of energy transfers (relaxation times). This will yield spectra comparable to broadband dielectric spectroscopy data, but with sensitivity to the scattering momentum transfer (that is, the microscopic length scale of the dynamic processes) and deuterium/hydrogen selectivity.

Technical Details

BWAVES can be built only at a long-wavelength source with a low repetition rate, such as 10 Hz STS. The high energy resolution in the quasielastic regime is primarily determined by the WAVES device and is proportional to λ^{-3} . Thus, BWAVES relies on a high flux of long-wavelength neutrons at STS. The very broad dynamic range requires a short primary flight path (16 m) to avoid the frame overlap; thus, the low source frequency of 10 Hz is a must. The concept of WAVES has been worked out, whereas its practical implementation requires some research and development. BWAVES will have a T0 chopper (two counter-rotating T0 choppers if allowed by the space available) and two low-speed (10 Hz) incident bandwidth selection choppers. Because of the small sample size (0.5 cm by 0.5 cm), the moderator (coupled) only needs to be a few cm in size horizontally and vertically. The desired divergence of the neutrons incident on the sample is limited by WAVES in the vertical directions and should not exceed $\pm 0.5^\circ$ in that direction. The divergence in the horizontal direction could be much greater. A short secondary flight path of only 0.75 m will result in a relatively small detector array, consisting of linear position-sensitive ³He tubes at scattering angles from 5° to 160°. Similar to the sample holders for the companion backscattering spectrometer MBARS, the BWAVES sample holders need to be manufactured using sapphire because traditional aluminum sample holders would produce undesirable background at the lowest Q values in the quasielastic regime, where $0.03 \text{ \AA}^{-1} < Q < 0.60 \text{ \AA}^{-1}$. Despite its high resolution and the very broad dynamics range, which makes BWAVES a unique quasielastic and an outstanding

inelastic spectrometer at the same time, it will be a compact instrument, with a short primary flight path and small evacuated vessel.

Table 4.5. Key instrument parameters for BWAVES

Source	STS
Moderator type	Cold, coupled H ₂
Energy transfer range	-0.060 meV to +500 meV
Resolution E	$\Delta E/E=1.7\%$, 3 μeV at the elastic line, Q resolution varies
Sample size range (beam size)	0.5 × 0.5 cm ²
Moderator—sample distance	16 m
Sample—detector distance	0.75 m
Detector type	³ He linear position sensitive

References

- [1] H. Frauenfelder et al., *PNAS* **106**, 5129–5134 (2009).
- [2] B. Aoun et al., *J. Phys. Chem. Lett.* **1**, 2503–2507 (2010).
- [3] L Rusevich et al., *Eur. Phys. J. E* **36**, 80 (2013).

4.8 MICROSECOND NEUTRON SPIN ECHO (MICROSE) FOR HFIR

Changwoo Do, Wei-Ren Chen, and Gregory Smith, BSMD

Abstract

We propose to build a neutron spin echo (NSE) instrument on the HFIR cold source to complement the existing time-of-flight NSE instrument at FTS. The longer wavelength NSE instrument on the HFIR cold source will be optimized for the larger lengths scales and slower motions of mesoscopic objects such as cell membranes, polymer composites, and large colloids. The time scale of NSE instruments scales with the cube of the neutron wavelength. By taking full advantages of the 10 times higher flux at long wavelengths ($\lambda > 10 \text{ \AA}$), NSE at HFIR will reach up to true $\sim 1 \mu\text{s}$ dynamics time scale with much faster data collection time, achieving ~ 100 times better overall performance compared to NSE at FTS.

Science Case

As pointed out in the recent report on opportunities for mesoscale science by the BES Advisory Committee (BESAC) [1], meeting future energy challenges requires revolutionary new materials that operate at dramatically higher levels of functionality and performance than current systems. To reach the full potential of materials complexity and functionality, unraveling and controlling the complexity at the mesoscale have been recognized to provide the critical intellectual link between the top-down design of new material with macroscopic building blocks and the bottoms-up design with nanoscale functional units. Realizing mesoscale science opportunities requires advances not only in our knowledge but also in our ability to observe and characterize. Therefore, the availability of an NSE capable of studying length scales $\sim 100 \text{ nm}$ will enable the assessment of slow dynamics at meso-length scales. It is essential to facilitate breakthroughs in developing previously unrealized functionality of new materials by expanding our understanding at the mesoscale phenomena. The NSE at HFIR characterized by the

following two principles will aid research projects within the soft matter research, condensed matter physics, materials science, and biophysics communities.

1. **Optimize as a high throughput instrument.** A single NSE user experiment typically takes about 10–14 days for reasonable collection of data, including resolution and background measurements. Often the initial 10–14 days of experiment is not enough to produce scientific publications, and one or two additional measurements are planned or performed before resulting in publications. A major bottleneck of slow NSE performance is the low flux of neutrons at long wavelength. The flux of long wavelength neutrons at HFIR is surveyed to be at least 10 times higher. Therefore, the slow measuring time can be, at least, improved by a factor 10, achieving 5–7 days of beam time per user experiment with more (Q, t) space coverage and statistics.
2. **Enable unique and high-impact science via wide Q and t range.** While NSE has huge advantages as a non-destructive probe of slow-dynamics, time scales above 300 ns are still considered to be less than efficient time ranges for practical experiments. Full coverage of $0.01 \text{ \AA}^{-1} < Q < 1 \text{ \AA}^{-1}$ and $1 \text{ ps} < t < 1 \text{ \mu s}$ can enable dynamical PDF analysis via direct Fourier transformation of $S(Q, t)$. This opens up a unique opportunity to investigate localized motions of soft colloids or water in driving soft matter collective motions using dynamical PDF, which are expected to have a very high and immediate impact in soft matter research. Additional scientific problems of current interest to which NSE can provide critical information include the following:
 - Dynamics of Polymers
 - Dynamics of polymers in confinement
 - Dynamics of polymer–nanoparticle composites
 - Dynamics in mesoscale structures by block copolymers
 - Ion transportation and chain dynamics of polymer batteries
 - Dynamics of polyelectrolytes (energy related materials)
 - Dynamics of Colloids
 - Hydrodynamic interactions
 - Intra-colloidal collective dynamics
 - Dynamical PDF study of localized inter-colloidal collective motions
 - Dynamics of Membranes
 - Interaction with cholesterol and peptides
 - Transportation in biomembranes
 - Dynamics of polymer films and vesicles
 - Glass Phenomena
 - Dynamics of glass-forming liquids
 - Supercooled liquids
 - Critical phenomena at confinement

Initial Science Objectives

1. Localization Dynamics of Soft Matter

Research Theme's Associated Workshop: Soft Matter

Potential Partners (*Attendees of Associated Workshop):

Takeshi Egami (University of Tennessee)

Yang Zhang* (University of Illinois, Urbana-Champaign)

Understanding dynamics in disordered media is of great interest for the field of soft matter.

Various scattering techniques, including neutron,

x-ray, and light, have been commonly used to investigate the dynamical features manifested in different spatial and temporal regimes. In the theoretical framework, their dynamics is usually described in terms of the dynamic structure factor $S(Q,\omega)$ or intermediate scattering function $F(Q,\tau)$. However, these systems are strongly non-periodic and, therefore, their excitations are often localized in a mesoscopic scale. Within the experimentally accessible Q range, the information of this desired local collective dynamics not only is partially concealed in the measured dynamical correlation functions, such as $S(Q,\omega)$ and $F(Q,\tau)$, but also is masked by other dynamical processes such as the phonon-like longitudinal diffusion. In this regard, the localized dynamical processes, ubiquitously existing in liquids, colloids, polymers, and glasses, are hardest to identify based on the current experimental protocol operating in the reciprocal Q space. The proposed NSE at HFIR, with the accessibility of multiple orders of Q regimes not available from any currently available NSE spectrometer, presents an alternative approach to address these important problems. Via Fourier transforming the experimentally measured $F(Q,\tau)$ to obtain the statistically meaningful $g(r,\tau)$, the important problems of localized dynamics can be addressed for the first time through the analysis of mesoscale dynamics in real space.

2. Mechanism of Flow in Sheared Colloidal Solutions

Research Theme's Associated Workshop: Soft Matter

Potential Partners (*Attendees of Associated Workshop):

Takeshi Egami (University of Tennessee)

Matt Helgeson* (University of California, Santa Barbara)

Mike Weaver* (Procter and Gamble)

The flow of a liquid has been described theoretically by the hydrodynamic theories. Much less attention has been paid to the local level dynamics, because it has been believed that the particle motion in a liquid was so random that details of the particle motion were irrelevant to the physics of liquid flow. However, computational and theoretical evidences have shown that various dynamical processes taking place at different length scales of soft matter are indeed characterized by multiple temporally heterogeneous events. For example, the key event in determining the caging phenomenon is not the long-time cage breaking; instead, a short-time breaking/associating process between the neighboring particles has been identified as the elementary excitation in liquid and glass. The associated characteristic time has been shown to be highly heterogeneous.

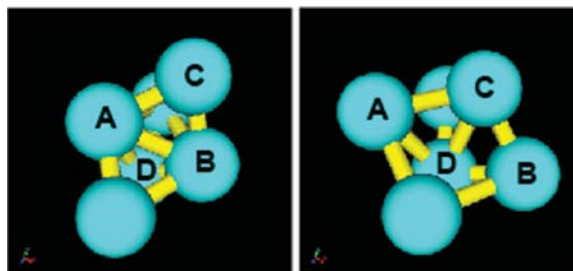


Fig. 4.18. A schematic representation of the topological change in the nearest neighbor configuration when one bond between colloid A and colloid B is broken and a new bond between colloid C and colloid D is formed in the immediate neighborhood.

Rheo-SANS measurements demonstrated that the correlation length of a strained field caused by applied external shear (a manifestation of the breaking/associating process) can be extracted unambiguously. Combined with the shear cell, the high flux of NSE at HFIR will allow separate determination of the longitudinal density relaxation process (which is a transverse mode) and the size fluctuation and lifetime of the strained field as a function of shear/flow rate a different values of Q . NSE at HFIR also will allow the test of the computationally predicted dynamical picture of heterogeneousness and will differentiate the dynamical collectivity for different processes. The aforementioned methodology can be generalized to a much broader field. Given the availability of a sample environment, NSE at HFIR will allow revolutionary studies of the general susceptibility $\chi(Q, \tau)$ for the condensed matter system perturbed by the presence of other external fields such as electrical or magnetic fields.

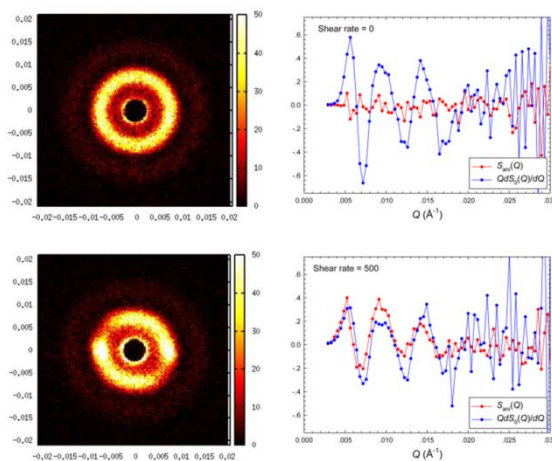


Fig. 4.19. Left panels: SANS absolute intensity of silica solutions projected in the velocity (v) – velocity gradient (∇v) plane at shear rate 0 and 500 1/s. The anisotropy qualitatively reflects the change in the suspension microstructure. Right panels: The isotropic (blue) and anisotropic part (red) of the inter-particle structure factor $S(Q)$.

3. Dynamics of Soft Materials at Very High Salt Environment

Research Theme’s Associated Workshop: Soft Matter
Potential Partners (*Attendees of Associated Workshop):

- Fyl Pincus* (University of California, Santa Barbara)
- Juan de Pablo* (University of Chicago)
- Gary Grest* (Sandia National Laboratories)

Ion transportation is a commonly observed process that is not only important in batteries in general but also has a critical role in understanding various cell mechanisms in the human body and in designing biocompatible electronics. Although more flux of Li^+ can provide high current and high capacity energy storage devices, in polymer lithium batteries, too many Li^+ ions reduce the performance of batteries because of the hindered ion mobility caused by a strong interaction between polymers and Li^+ ions. In living cell organisms, while the average ion concentration is not very high, a locally concentrated environment can occur around proteins and membranes and introduce changes in local hydration structure and dynamics. Understanding structure and dynamics of soft materials at high concentrations of ions or salts has a potential impact in both fundamental sciences and practical applications. However, because concentrated ion systems inevitably reduce scattering signals from the polymers under investigation and sometime absorb neutrons (Li^+), high flux neutrons are required for dynamic studies. In addition,

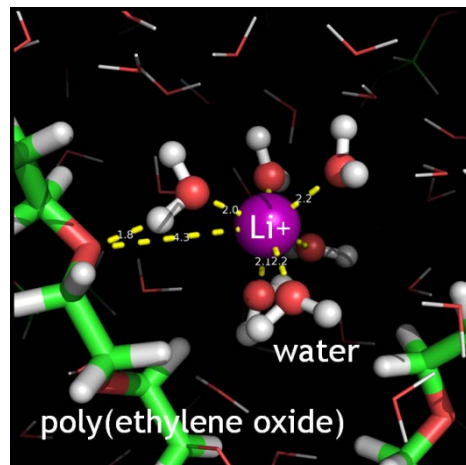


Fig. 4.20. Molecular model illustrating the associating and caging effect of a lithium ion by water at it moves through a hydrated poly(ethylene oxide) matrix.

multiple scales of dynamic processes by polymers, water, and ions can be studied only with wide ranges of time and Q space that are available from the proposed NSE at HFIR.

Technical Details

Taking full advantage of the recent progress in neutron optics, superconducting magnets, and spin polarization, the Jülich Center for Neutron Science (JCNS) has made viable the use of neutrons with a wide wavelength distribution for NSE at SNS at ORNL for the first time. Since it was commissioned in 2009, this instrument's general usefulness for dynamical investigation has been demonstrated. Nevertheless, the capability of the SNS NSE to explore the slow dynamics in the larger, mesoscopic length scale ($Q < 0.05 \text{ \AA}^{-1}$) is severely constrained by its intrinsic limitation posed by the short pulse neutron spectrum and front-end instrument optics. For example, exploration of larger length scales and longer correlation times requires long wavelength neutrons. Because the SNS cold source is not optimized for long wavelengths, the capability of the NSE at SNS to explore these spatial and temporal regions is severely limited by the lack of long wavelength neutrons (the wavelength λ is required to be around 20 \AA to reach the Fourier time of 400 ns or more). Thus there is a strong need for constructing the second NSE instrument, which will be optimized for long wavelengths.

An opportunity exists at HFIR at ORNL for the construction of such a spectrometer, because a planned CG-4 or CG-1 guide upgrade can increase the time-averaged brightness of long wavelength flux. NSE is an inherently low resolution measurement in Q, so the availability of long wavelength neutrons with sufficient flux (~ 10 times higher averaged flux at long wavelength $> 10 \text{ \AA}$), a relaxed wavelength resolution from HFIR, and a large space for high field-integrals of precession coils will certainly strengthen our capability to complete dynamical measurements of the mesoscale using neutron scattering by reaching higher Fourier time ($\sim 1 \text{ \mu s}$) and low-Q ($Q_{\text{min}} \sim 0.01 \text{ \AA}^{-1}$). By just using the high flux, at least an order of magnitude overall improvement is expected from the (Q, t) ranges and fast measuring time. The large space availability for the long precession coil opens the possibility of reaching very high-Q ($\sim 1 \text{ \AA}^{-1}$) and a homogenous magnetic field at the same time. Consequently, fewer data points compared to the existing NSE will be required to obtain echo amplitude, resulting in a data collection rate at least 5 times faster.

Combined with the intense brightness of neutrons at moderate wavelength ($4 \text{ \AA} < \lambda < 8 \text{ \AA}$) at HFIR (which is ~ 2 times brighter than ILL), the NSE at HFIR can be optimized for smaller sample volumes (as small as $1.5 \text{ cm} \times 1.5 \text{ cm} \times 0.1 \text{ cm}$) that are highly desired by biology communities for moderate time scale (< 50 ns) studies. The overall smaller sample size range compared to existing NSEs can guarantee a more homogeneous magnetic field within the sample area, even with existing correction coil technology. A 2D position sensitive detector will be used as a typical NSE instrument to provide multiple Q-ring analysis.

Combining all technical improvements, the expected improvement over any NSE in the United States is at least 100 times—10 (flux & [Q,t] range) \times 5 (optimized magnetic field stability with better algorithm) \times 2 (sample area).

Table 4.6. Key instrument parameters for MICROSE

Source	HFIR
Moderator type	Cold Source
Wavelength/energy range	$4\text{\AA} < \lambda < 25\text{\AA}$
Resolution	$\Delta\lambda/\lambda = 15\%$
Beam divergence	< 18 mrad
Sample size range (beam size)	$1.5 \times 1.5 \text{ cm}^2$ to $3 \times 3 \text{ cm}^2$
Precession coils	Max field: 5 kG Max field integral: 1 T·m
Polarizer/analyzer	FeCo-Si, FeCo supermirrors
Sample—detector distance	4–5 m, rotatable from 0° to $\sim 180^\circ$
Detector type	2D position sensitive Area $\sim 32 \times 32 \text{ cm}^2$ Pixel size $\sim 1 \text{ cm}^2$

Reference

- [1] “From Quanta to the Continuum: Opportunities for Mesoscale Science.” September 2012

5. CHEMISTRY AND ENGINEERING MATERIALS

5.1 CHALLENGES IN MATERIALS DISCOVERY, CHARACTERIZATION, AND APPLICATION

Materials are at the heart of technologies that will define the future economy and provide solutions to the compelling challenges facing society from energy security to future transport and infrastructure. Predictive modeling of materials holds the promise of accelerating the development of new solutions; however, as a prerequisite, this requires an understanding of materials' structure and dynamics from the atomic scale to real world components and systems. In addition, understanding and modeling, synthesis, and processing are vital to achieving transformative impact.

A workshop titled "Frontiers in Materials Discovery, Characterization, and Application" was held at Schaumburg Illinois, on August 2–3, 2014, to explore the needs of the materials science community, future directions, and the most significant problems that could be addressed in the next decade by neutron diffraction, imaging, and spectroscopy.

The workshop brought together leaders from academia, industry, and national laboratories covering chemistry, materials science, geoscience, and engineering materials and covered the needs of industry, impact of modeling, materials by design, infrastructure stewardship, materials under extreme conditions, frontiers in neutron spectroscopy, and high throughput experiment and optimization.

The key messages are that the unique physical properties of neutrons make high intensity beams indispensable to materials discovery, characterization, and application where they complement the capabilities of electrons and photons. Their nondestructive nature, ability to penetrate real components and probe materials under working conditions, sensitivity to hydrogen and light elements, ability to observe modes and dynamics over virtually all length and time scales, and ability to highlight components in complex interacting systems using isotope substitution make them unique.

In addition, major impact and transformative capabilities can come about with the combination of high performance computing, software, new sample environments, and the promise of much higher intensities from new instrumentation and future sources, in particular the proposed Second Target Station at the Spallation Neutron Source. Such advances facilitate high throughput neutron measurements, application to small samples and open up in operando studies, 3D spatial mapping of physical composition and state in materials including dynamics, and access to new areas of application (e.g., pharmacology). Such advances include the novel opportunity to undertake concurrent spectroscopy and diffraction measurements seeing function and structure together and to make time resolved studies of materials in action.

Detailed workshop findings are listed at the end of the report. The principal outcomes and recommendations of the workshop are as follows:

Principal findings

Chemical Spectroscopy: Advances in sources, better optics, and optimized instrument design will result in a complete transformation of neutron vibrational spectroscopy and quasielastic giving access to novel science.

Materials Science and Engineering: The demand for neutron capabilities in materials science and engineering is very high and is being driven by emerging challenges in infrastructure stewardship, advanced propulsion systems, advanced materials processing, nuclear fuels and radiation tolerant materials, energy storage and energy conversion integrated systems, materials by design/Integrated Computational Materials Engineering, and materials under extreme environments.

Structural Chemistry: The field of structural chemistry makes seminal contributions to nearly every area of science. The revolutionary impact of materials by design and ability to explore systems under manifold environments and processes makes this field rich in compelling science problems for the future. The complementary properties of neutrons and x-rays make them invaluable to these investigations.

Recommendations

Chemical Spectroscopy

- High performance computing should be vigorously pursued in conjunction with neutron chemical spectroscopy, and libraries and databases are needed to provide reference spectra and models for future science.
- Develop instrumentation capable of true in situ studies of chemical reactions, materials in action, and catalytic process
- Multimodal instrumentation that combines diffraction, tomography, and inelastic methods along with other techniques for complex systems
- 3D spectroscopic, diffraction mapping, and in operando capabilities are needed.

Materials Science and Engineering

- Live data analysis that feeds directly back to data acquisition: adoption of “expert” systems to optimize experimental setup and data analysis
- Ability to easily handle unique samples (both in and out): large/heavy samples, “hot” (radioactive) samples, proprietary samples
- A multi-moderator target design (STS) will facilitate development of multimodal capabilities
- Development of high-resolution neutron microscopy, imaging, and tomography beam lines, including epithermal neutrons for resonance imaging/tomography is a priority.

Structural Chemistry

- Fast track design and construction of a high throughput powder diffractometer capable of nPDF analysis
- A very high resolution powder instrument ($\Delta d/d \sim 10^{-4}$) at Second Target Station on a moderator providing primarily ambient-moderated neutrons

- Multi modal instrumentation
 - (a) Instrument capable of measuring multiple length scales (small angle + powder diffraction and high resolution elastic + inelastic scattering on the same instrument)
 - (b) Adding other simultaneous measurements capabilities (x-ray, calorimetric, gravimetric, NMR, etc.) for complex systems and the study of irreversible processes.

An integrated and wide variety of sample environments to do in situ/in operando measurements that include but not are limited to, extreme ranges of temperature and pressure, electrochemical cells, and gas handling systems. It is critical that sample environments be integrated from day one into the design of these instruments.

5.2 JANUS: INS INSTRUMENT FOR CATALYSIS

AJ Timmy Ramirez-Cuesta (CEMD) and Georg Ehlers (QCMD)

Abstract

JANUS is a medium-high resolution, broadband, indirect geometry spectrometer coupled together with a medium resolution direct geometry inelastic spectrometer. The main science focus for JANUS is catalysis and chemistry.

Science Case

Neutrons are a very scarce resource. There are few places in the world where they can be used as a probe for inelastic neutron scattering (INS). Both direct and indirect geometry instruments have a role to play in the understanding of catalysis. The purpose of studying catalysis with neutrons is mainly to follow the dynamics of hydrogenous materials. Direct geometry instruments like SEQUOIA and ARCS could have relative good resolution at all energies and benefit from repetition rate multiplication to use multiple incident energies during a single source pulse. However, for hydrogenous materials, the spectrum should be measured at low Q, to avoid degradation of the INS signal from the contribution of vibrational overtones and combinations. If we model the spectra at a series of Q, as in Fig. 5.1, it is clear that the low angular positions, below 40°, will be of more relevance to the study of hydrogen-containing materials.[1,2] JANUS provides the extremely high count rate and high sensitivity that indirect geometry spectrometers like VISION achieve by integrating the scattered single over a rather large Q-range at the sacrifice of Q-resolution. JANUS also provides Q-resolution at low scattering angles for cases where more detailed modeling of dynamics is required. The low-scattering angle supports measurements at low-Q that is important to minimize degradation of the signal due to contributions from overtones and

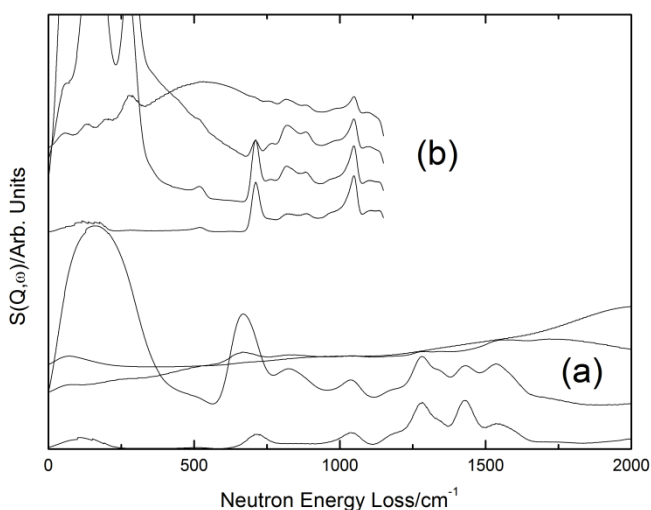


Fig. 5.1. Calculated angular dependency for polyethylene at 300K at (a) $E_{incident} = 2,300 \text{ cm}^{-1}$ and (b) $E = 1,150 \text{ cm}^{-1}$. The traces for each group are calculated at angular positions of 3, 40, 80, and 130° from the bottom up. Calculations were performed using the aClimax software.

combinations. The value in combining these two techniques into a single instrument is to enable the study of irreversible phenomena and in situ manipulation of samples.

There are three fields where JANUS would have an immediate impact: (1) catalysis, (2) proton conductors, and (3) gas separation and storage. Two additional facets will give the instrument ultimate relevance: (4) fully integrated and expanded sample environments and (5) improved connection with theoretical modeling.

1. **Catalysis:** Much of catalysis is concerned with the transfer of hydrogen between reagents and products, and JANUS is ideally suited to these types of studies. For the first time it will enable data to be collected on the same sample with sufficient resolution across the entire energy range of interest. Access to the C–H/N–H/O–H stretch region provides a very simple means of identification and is ideally suited to quantification of the species present [3]. The 0–2000 cm^{-1} region is where the details of the catalyst–adsorbate interaction can be discerned and the indirect backscattering detectors provide the good energy resolution needed for this. However, the surface species of interest are often present in low concentration, and good resolution is of no use if there is insufficient sensitivity. This problem is addressed by the indirect forward scattering which will provide at least a tenfold increase in sensitivity and possibly as much as a hundredfold increase over the backscattering detectors. The improved sensitivity will also allow industrially important non-hydrogenous adsorbates, such as CO_x , NO_x and SO_x , to be studied for the first time.
2. **Proton conductors** are heavy metal oxides that are hydrated to generate mobile hydroxyls and have considerable potential in intermediate temperature fuel cells. These materials exhibit multiple sites for incorporation of hydroxyls; thus, diffraction studies are only able to provide an average picture of the material, and the crucially important local structure around the hydroxyls is lost. Spectroscopy provides this missing local picture, and INS is particularly matched to these needs as the low energy modes that (in conjunction with first principles modeling) enable discrimination between the various possible sites [4]. These modes are often weak or invisible to optical probes. Access to the O–H stretch region is needed to quantify the species present and to discriminate between hydroxyls and water.
3. **Gas separation** is becoming an increasingly important activity with the major driver being the need to separate CO_2 from waste streams.
4. **Fully integrated and expanded sample environment capabilities.** Sample environment is a fundamental part of a neutron instrument. In catalysis, for example the rate limiting step is the time required for chemical reactions to happen. In this case, there is a need to be able to run a series of experiments simultaneously by having multiple sample assemblies. One assembly can be inserted into the beam line while others are either being dosed with gases or awaiting completion of chemical reactions off the beam line. These can be swapped in as ready.
5. **Improved connection with theory.** Computer modeling is intrinsically linked with incoherent INS spectroscopy. The techniques, methodologies, and software exist and have been proven fundamental in the interpretation of incoherent INS. It can be stated that one of the closest connections between ab-initio and experimental data is between modeling and experiments on INS.

Specific Science Examples

Hydrocarbon Chemistry on Zeolite Model Systems

Anibal Boscoboinik, Brookhaven National Laboratory

Zeolites account for the largest volume of solid catalysts used in the industry. They are especially important for chemical transformations of energy commodities, [5] rendering the studies proposed here aligned with DOE strategic directions.

Figure 5.2 (a) shows zeolite chabasite, which is composed of a three-dimensional arrangement of hexagonal prisms. The bridging hydroxyl present within the structure is emphasized in Fig. 5.2 (b). As the price of crude oil rises, the carbon-carbon bond formation using alcohols as feedstock, such as in the case of methanol to gasoline (MTG) conversion will become feasible. [6] There is therefore the urgent need to understand, in a more detailed manner, the way hydrocarbons interact with the active site of zeolite

catalysts and the nature of the active site under catalytically relevant pressures. The understanding of real catalysts in general is often complicated by their intrinsic structural complexities involving, for example, heterogeneous interfaces, surface reconstruction of nanostructures, and defects. A common strategy in surface science, to gain further mechanistic insight, is to develop “*model catalysts*,” which are inspired by the real catalysts but with simpler structures and identifiable active sites. The study of the model catalysts not only allows the understanding of the model system, but more importantly, it also provides a testbed to develop design principles that can optimize real catalysts. The synthesis of a two-dimensional version of a zeolite that has the active site exposed on a surface has recently been realized (see Fig. 5.2 [c]), [7,8] allowing now the use of surface science techniques to address the chemistry of these materials. The use of INS on 2D zeolites would allow us to follow hydrogen atoms located not only on the surface of film but also inside the cavities, and thus provide a full picture of the system.

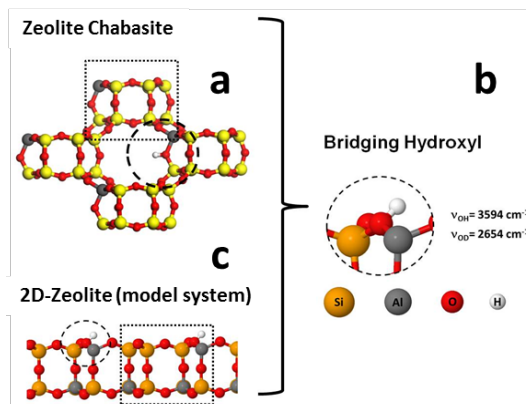


Fig. 5.2. Structure of the zeolite model system and zeolite chabasite.

The bridging hydroxyl group, common to both, is emphasized in the figure. Note that they also share the same building block, the hexagonal prism shown in the dashed rectangle, but in different special arrangements.

Fundamental investigation of the active sites on carbon-based catalysts and the reactant-surface interactions

Viviane Schwartz, Adam Rondinone, Chengdu Liang, Zili Wu, ORNL

Utilization of metal free carbon allotropes is a growing subject in heterogeneous catalysis [9]. For instance, there is a consensus in the studies of nanostructured carbon catalysts for oxidative dehydrogenation (ODH) of alkanes to olefins that the oxygen functionalities generated during synthesis and reaction are responsible for the catalytic activity of these nanostructured carbons [10]. Figure 5.4 below illustrates a calculated reaction pathway for ODH of isobutane on oxygen-functionalized graphene recently published in our group [11]. The catalytic mechanism proposed involves weakly adsorbed isobutane reducing dicarbonyls at zigzag edges (upper figure) and quinones (lower figure), and leaving

as isobutene, then O_2 in the feed weakly adsorbs and reacts with the hydrogenated functionality, leaving as H_2O_2 and regenerating the catalytic sites.

Few techniques are known that can successfully be used to characterize the structure of finely divided and highly absorbing materials such as carbon-based catalysts. It is anticipated that neutron scattering can be a powerful technique for the study of catalytic carbon-based materials. JANUS will allow identification of the highly active oxygen functionalities on carbon surfaces and consequently enable the engineering of nanocarbons for ODH of alkanes and other catalytic reactions. Furthermore, understanding how the alkane and oxygen interacts with the carbon surface functionality would unravel the reaction mechanism on such surfaces.

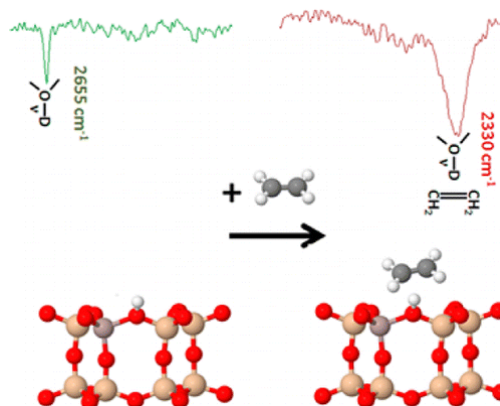


Fig. 5.3. Deuterated bridging hydroxyl before and after adsorption of ethylene in UHV.

The formation of the adduct was followed by infrared spectroscopy and the structural assignment confirmed by DFT calculations.

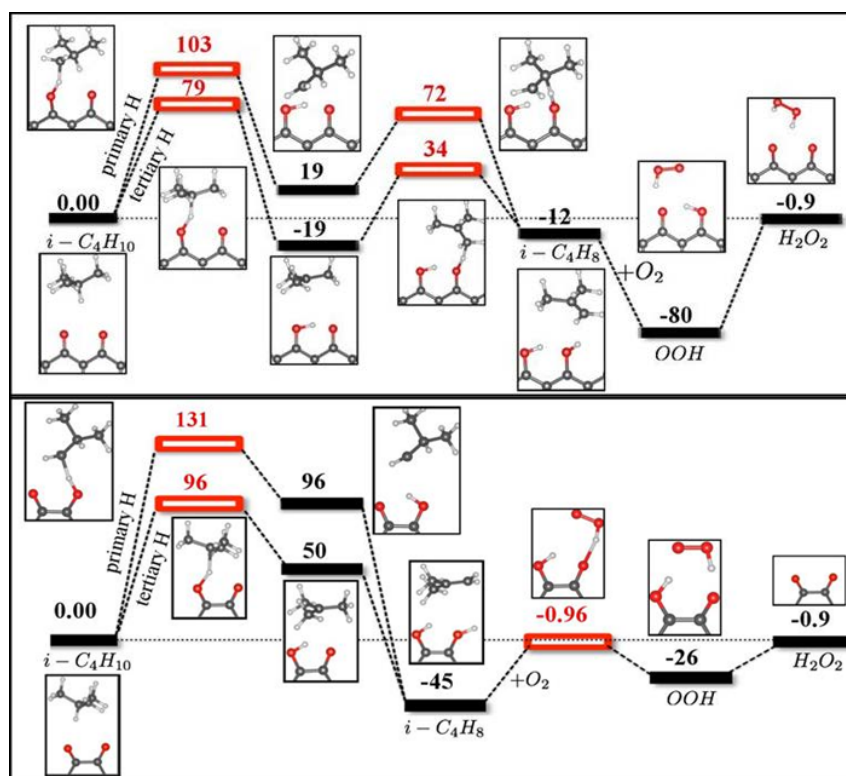


Fig. 5.4. Calculated reaction pathways for the ODH of isobutane on dicarbonyls at zigzag edges (upper) and quinones (lower) at armchair edges. Transition-state energies are shown in red. All energies are given in kJmol^{-1} . Carbon, oxygen, and hydrogen atoms are shown as gray, red, and white spheres, respectively [11].

Technical Details

JANUS can be built at a source with a low repetition rate, such as 10 Hz STS. With a frame 100 ms long, it can be positioned at 20 meters from the moderator with a direct view of the moderator and still have no frame overlap so that the energy transfer range available is from -3 meV to 500 meV including the elastic line.

Table 5.1. Key instrument parameters for JANUS

Source	STS
Moderator type	Cold, de-coupled H ₂
Energy transfer range	-3.0 meV to + 500 meV
Resolution E	$\Delta E/E = 1\%$, 150 μeV at the elastic line, Q resolution varies
Sample size range (beam size)	1 × 1 cm ²
Moderator—sample distance	40 m
Sample—detector distance	0.75–1.00 m 3 m for direct geometry
Detector type	³ He linear position sensitive

References

- [1] Ramirez-Cuesta, A. and Mitchell, P. C. "Neutrons and Neutron Spectroscopy." *Local Structural Characterisation* 173–224 (2014).
- [2] A J Ramirez-Cuesta, *Comp. Phys. Commun.* **157** 226-238 (2004).
- [3] Mitchell, P. C. H., Parker, S. F., Ramirez-Cuesta, A., & Tomkinson, J. (2005). *Vibrational Spectroscopy with Neutrons, with applications in Chemistry, Biology, Materials Science, and Catalysis. Series on Neutron Techniques and Applications*, London: World Scientific.
- [4] Colomban, P., and Tomkinson, J. (1997). "Novel forms of hydrogen in solids: the 'ionic' proton and the 'quasi-free' proton." *Solid State Ionics* **97** (1-4), 123–134. doi:10.1016/S0167-2738(97)00046-5
- [5] B. Yilmaz, U. Müller. *Top. Catal.* 2009, 52, 888–895. "Catalytic Applications of Zeolites in Chemical Industry."
- [6] U. Olsbye, S. Svelle, M. Bjørgen, P. Beato, T. V. Janssens, F. Joensen, S. Bordiga, K. P. Lillerud. *Angew. Chem. Int. Ed.* **51**, 5810 (2012). "Conversion of Methanol to Hydrocarbons: How Zeolite Cavity and Pore Size Controls Product Selectivity."
- [7] J. A. Boscoboinik, X. Yu, B. Yang, F. D. Fischer, R. Wlodarczyk, M. Sierka, S. Shaikhutdinov, J. Sauer, H.-J. Freund. "Modelling Zeolites with Metal-Supported Two-Dimensional Aluminosilicate Films." *Angew. Chem. Int. Ed.* **51**, 24, 6005 (2012).

- [8] J. A. Boscoboinik, X. Yu, E. Emmez, B. Yang, S. Shaikhutdinov, F. Fischer, J. Sauer, H.-J. Freund. "Interaction of Probe Molecules with Bridging Hydroxyls of Two-Dimensional Zeolites: A Surface Science Approach." *J. Phys. Chem. C* **117**, 13547 (2013).
- [9] B.F. Machado, P. Serp, *Catal. Sci. Technol.* **2**, 54–75 (2012).
- [10] D. S. Su, J. Zhang, B. Frank, A. Thomas, X. Wang, J. Paraknowitsch, R. Schlögl, *Chem. Sus. Chem.* **3**, 169–180 (2010).
- [11] G. K. P. Dathar, Y. T. Tsai, K. Gierszal, Y. Xu, C. D. Liang, A. J. Rondinone, S. H. Overbury, V. Schwartz, *Chem Sus Chem* **7**, 483–491 (2014).

5.3 EXTREME ENVIRONMENT MULTI-ENERGY SPECTROMETER WITH XTAL ANALYZERS (XTREME-X)

AJ Timmy Ramirez-Cuesta (CEMD), Chris Tulk (CEMD), and Bianca Haberl (CEMD), Mark Lumsden (QCMD)

Abstract

XTREME-X is an indirect geometry time-of-flight spectrometer optimized for measuring inelastic neutron scattering (INS) in a horizontal scattering geometry. The choice of horizontal geometry is a necessary consequence of the geometrical restrictions that appear when performing neutron scattering experiments under extreme conditions such as high-pressure or certain magnetic field designs. The basic concept is to maximize count rates for neutron scattering in the horizontal plane with quasi-continuous analyzer angular coverage of the scattered neutrons. High efficiency will be obtained using banks of concentric analyzers placed behind one other. Each bank analyzes a different scattered neutron energy, which is the indirect geometry spectrometer equivalent of repetition rate multiplication for direct geometry spectrometers.

Science Case

Synthesis of innovative materials to address our growing energy needs is a key objective in materials sciences. Exploiting extreme environments, notably high temperature and high pressure, has tremendous potential for the synthesis of novel materials with unique, highly useful properties [1]. For example, pressure-induced band-gap engineering may enable the formation of future photovoltaic or superconductive applications from cheap, abundant elements like silicon [2,3]. Equally, desirable mechanical properties can be engineered such as the immensely increased mechanical strength possessed by diamond and boron-nitride (both high pressure synthesized) [4,5] or the unprecedented strength-to-weight ratio exhibited by diamond nanothreads recently synthesized at ORNL [6].

Transitions under high pressure and hence potential synthesis pathways are poorly understood for the vast majority of materials. Hydrogen-rich materials and alloys represent a particular scientific challenge because they cannot be fully assessed with x-ray and optical techniques. They represent however, immense scientific and technological potential for hydrogen-storage [7], (close to) room temperature superconductivity [8,9] or photovoltaics and other thin-film applications [10]. Furthermore, even neutron diffraction techniques are not always suitable since substitution of hydrogen with deuterium is often required, thus altering the technologically relevant form of a material prior to its study. This limitation, however, does not apply to inelastic neutron scattering (INS), which can determine a hydrogen-rich material's behavior *in situ*. This has to date been hampered by the low maximum

pressure achievable (~ 1 GPa) due to large sample volumes required. The use of specialized, innovative sample environments, radical reduction of background and considerable increase in neutron flux may overcome this obstacle as we propose for XTREME-X. This project will built on existing expertise and development at SNS and will ensure that ORNL maintains its status as world-leader in high pressure neutron scattering. Therefore, five key parameters will be addressed:

1. **Optimization for measurements of small or weakly scattering samples:** The use of focusing guides and the very large neutron collecting areas that are to be available with the XTREME-X design will increase the effective flux of neutrons on the detectors. This will allow spectroscopy on samples sufficiently small to fit the extreme sample environments. Currently, no neutron spectrometers are available capable of these measurements and this instrument will thus be one-of-a-kind.
2. **Providing Q, ω resolution:** The concept behind XTREME-X preserves the information in the azimuthal angle φ . This large angular coverage of the analyzers and detectors will provide good signal while preserving Q resolution.
3. **Removal of high order reflections:** We propose to add band-pass filters for the neutrons after the analyzers. For crystals with a $E_f < 4$ meV, we will use standard Be filters (TOSCA, IRIS at ISIS and VISION at SNS). For crystals that have a $E_f > 4$ meV, we will use an innovative para-hydrogen filter that will be hundreds of times more effective than Be and can be easily removed if required.
4. **Fully integrated and expanded sample environment capabilities:** Sample environment is a fundamental part of any neutron instrument, but is particularly important for high pressure experiments, where a specialized environment “that applies” the high pressure is necessary. The choice of environment governs the sample size, but also the maximum pressure achievable: the higher the pressure, the smaller the sample. Additionally, such environments add significant background that often varies with pressure. Both these issues, size and background, are particularly significant for any INS experiment and are hence addressed in the concept for XTREME-X. Specialized, large-volume high pressure environments will be designed with reduced backgrounds and an optimized opening angle for XTREME-X. Precedent for such development has been set at the SNS recently with new high pressure environments for diffraction that quadrupled the previously accessible pressure in neutron high pressure work. This is well recognized in and beyond the neutron scattering community and the relevant paper by ORNL and Carnegie scientists [11] has been named as one of the Taylor & Francis Materials Science Top 10 for 2013. Similar improvement is anticipated for XTREME-X and will be vital to this project.
5. **Improved connection with theory.** Both high pressure and INS studies set precedent for extremely good congruency of modeling and experiment. Computer modeling is intrinsically linked with incoherent INS spectroscopy and the existing techniques, methodologies, and software have proven fundamental in the interpretation of incoherent INS data. Thus, INS represents one of the closest connections between ab-initio computed and experimental data of all neutron scattering techniques [12]. Similarly, the precise experimental control pressure allows over the interatomic distances, is replicated in computations. Hence experiments and theory usually support and strengthen each other. Albeit crucial for the understanding of high pressure INS data, this has not been implemented equally well for calculations of vibrational

density of states under elevated pressure and temperature. This will therefore be another key focus, which will make the SNS world leading not only in the recording of high pressure INS data, but also their interpretation and understanding.

Specific Science Examples

Hydrogen and Group IVa-hydrides under pressure (XTREME-X)

Hydrogen is the most abundant element in the universe and its high pressure behavior has attracted intensive theoretical and experimental interest for this reason alone. Additionally, it has been predicted that under ultra-high pressures hydrogen will transform into a metallic state that is superconducting at room temperature [8]. The nature of this metallic state is under current debate with various structures from simple close-packed monoatomic structures to graphene-like layers suggested [13]. Direct experimental proof of such metallization is however difficult and controversial due to the extreme pressures necessary. Additionally, computational predictions and theory are also hampered by the fact that even the low pressure regime poses many questions still. In particular, the influence of pressure on the ortho-para conversion (the conversion between the lowest and second-lowest rotational state of hydrogen) is not fully understood, but appears to increase dramatically above 3 GPa [14]. Understanding of these rotational states is vital since solidification, and hence metallization, require orientational ordering in the solid. INS can directly probe this conversion, but the current upper pressure limit prevents the study of the intriguing regime of pressure-enhanced conversion.

The new VISION spectrometer at SNS has opened the field for studying hydrogen in very small samples under pressure with its combination of high flux and large analyzer area (see Fig. 5.5). Under elevated pressures, however, sample size remains the issue, and the time required for such measurements is prohibitively large. The new optimized designs for XTREME-X, with focusing guide (that will increase the flux density by a factor of 100) and multiplexing of the crystal analyzers (that will increase the neutron count by a factor of 10) will yield a 3 orders of magnitude increase in signal for these restrictive sample environments. This will yield further insight into the thermodynamic functions and phase diagram of hydrogen and thus may pave the way for its metallization.

Group IVa hydrides (methane, silane, germane, stannane) have recently attracted similar interest. It has

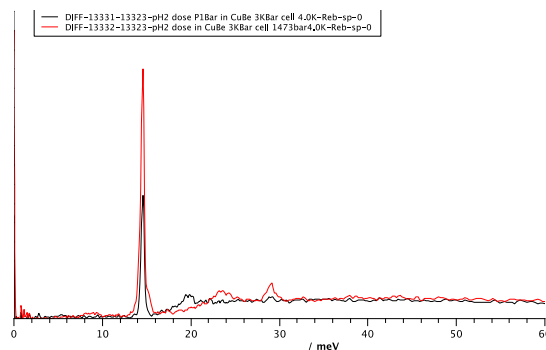


Fig. 5.5. INS of solid hydrogen dosed at 1 bar (black trace) and parahydrogen at 1.5 kbar (red trace) measured at ~5 K.

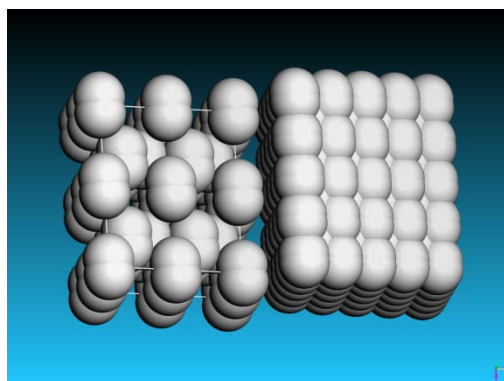


Fig. 5.6. Visual representation of the ortho hydrogen molecule in the solid at 1 bar (left) and 20 GPa (right).

The compression is in the order of 10, and the size of the spheres represents 50% of the van der Waals radius of the atoms.

been predicted that they can make the metallic state of hydrogen accessible because of “chemical precompression” [9]. These hydrides are also technologically interesting in their own right; for example, silane as adhesive coatings [15], potentially as rocket fuel [16] and as the precursor materials for the deposition of Si films used in thin-film industry, particularly in the production of low-cost solar cells [5]. Understanding its high pressure behavior may thus be crucial for the improvement of such applications.

Experimental studies remain scarce and controversial. Indeed, even behaviors at relatively low pressures (below 10 GPa) are poorly understood. For example, silane crystallizes into two different phases at 4 and 6 GPa, respectively, but their structure is unresolved [17]. Similarly, the high pressure behavior of the phases known to nucleate upon freezing has not been probed for to date. Clearly, such investigations are the key for better understanding of silane at high pressure and, thus, are necessary to facilitate synthesis of a (close to) room temperature superconductor. It is, however, impossible to study this fully with neutron diffraction because the deuterated counterpart follows a different pathway [18]. Hence INS at moderate pressures as will become accessible with XTREME-X appears the key to unlocking this topic.

INS study of amorphous ice under high pressure (XTREME-X)

The structure and phase diagram of simple water has attracted much interest for decades. While this substance is ubiquitous on our planet, many open questions remain, particularly with regard to its behavior at very high density. Furthermore, the hydrogen rich nature of ice makes it an ideal candidate for neutron scattering studies. In fact, the complete crystallographic structure of ordinary ice Ih (such as ice from a household freezer) was not fully known until neutron experiments conducted at ORNL were finally published in 1950. The most common structure of ice in the universe is most likely amorphous, not crystalline, because water is deposited onto interstellar bodies at low temperature from a low pressure gas. A variety of structural variations of amorphous ices exists, and the exact number is under debate [19]. Even the number of the more simple crystalline phases has not been fully explored. Indeed, the pressure-temperature diagram of H₂O is exceedingly rich, with more than 15 phases identified to date (Fig. 5.7). Despite the longstanding interest, many open questions about the physical details of these various ices remain. For example, the dynamic behavior ranging over the entire spectrum from low energy diffusion of hydrogen, the lattice dynamics and even the intermolecular vibrations of the crystalline ices above ~2.2 GPa remains unstudied and, as such, details of some very high pressure crystal–crystal transitions are poorly understood. Indeed, a recent structural study performed at ORNL hints that at pressures above 30 GPa, ice cannot be

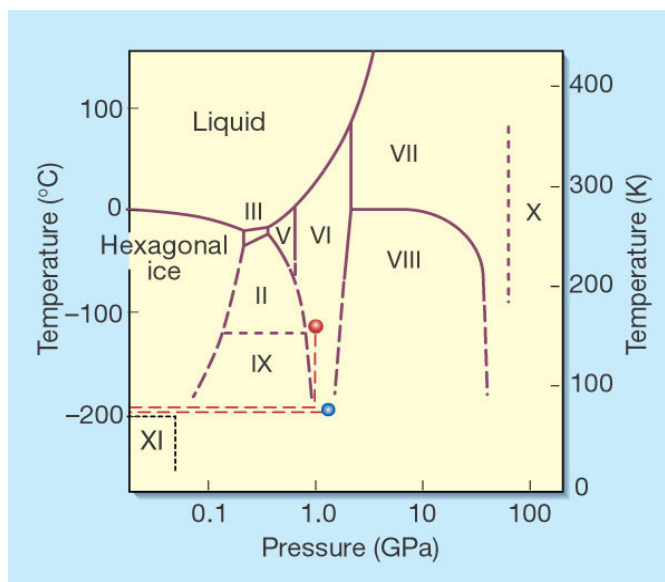


Fig. 5.7. The temperature and pressure regimes associated with most of the 13 known crystalline phases are indicated here [21].

When standard hexagonal ice at 77 K is subject to increasing pressure, so-called amorphous ice forms: at 1 GPa (blue circle), high-density amorphous ice forms; if the temperature is then raised, very-high-density amorphous ice forms (red circle).

described by a conventional network structure [20]. Matters are even more complex for amorphous ices [19,21,22]. Currently, the form of amorphous ice of most interest is synthesized by compression of “normal” ice Ih to 1 GPa at low temperature (typically 77 K). This form is known as high-density amorphous (HDA) ice [21]. Two competing theories of HDA formation have been postulated. The first suggests that the ice Ih–HDA transition results from thermodynamic melting because of large amplitude molecular vibrations; the other suggests the transition results from a mechanical instability in the water network. In situ INS observation of the presence or absence of phonon softening would solve this controversy. Temperature annealing the HDA form results in topological changes of the water network structure, and these phases are often identified as energetically distinct. As such, it is said that amorphous ice may undergo amorphous–amorphous transitions from one highly disordered metastable state to the other. However, the nature of these transformations remains controversial and poorly understood [19,22].

In situ INS could directly probe the short and intermediate range intermolecular interactions and extended lattice vibrations and give clues as to the nature of both the amorphous–amorphous transitions and the hydrogen bonding nature of the crystalline phases above 30 GPa [23]. However, the technology to reach the necessary pressures, while measuring INS data, is not currently available because of issues with sample sizes and flux. Therefore, the implementation of XTREME-X will aid in understanding the properties of the ubiquitous material water.

High pressure synthesis of novel phases from hydrogenated amorphous silicon (XTREME-X)

The elemental semiconductor Si forms the basis of our current technology and is most commonly utilized in the crystalline high-purity diamond-cubic phase and as thin films of deposited amorphous Si [10]. Interestingly, however, further structures kinetically stable at ambient conditions can be synthesized through high pressure [2,3,24]. These exotic phases possess significantly altered electronic structures [24]. This promises a host of application, but their exploitation for photovoltaics is one of the most promising goals (see Fig. 5.8) [3]. Indeed, several existing structures are predicted to be vastly improved for photovoltaics [3,25]. It would be highly advantageous if these phases could be synthesized from the cheapest Si material, deposited hydrogenated amorphous Si, as used for cheap thin-film solar cells or thin-film transistors [9], because performance of devices based on these thin films is inferior to their crystalline counterpart [9]. Because of a shortage in solar-grade Si feedstock, their improvement has regained immense interest, and clearly pressure-induced band-gap engineering could lead the way.

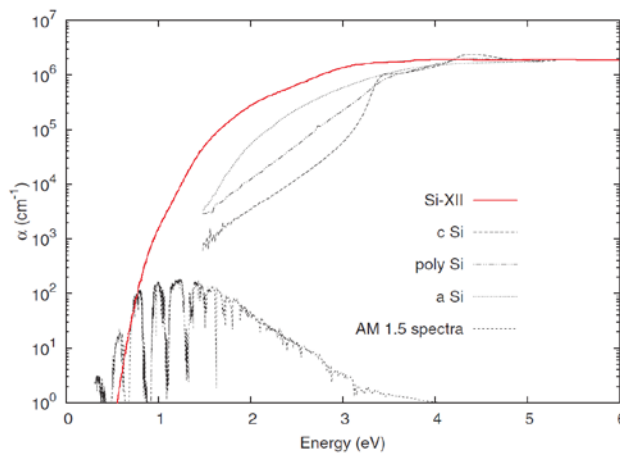


Fig. 5.8. Optical absorption α for Si-XII and Si forms used in solar cells compared with the solar spectrum irradiance under standard conditions (AM 1.5) taken from [3].

Clearly Si-XII can be expected to absorb light more efficiently than currently used forms of Si.

Clearly Si-XII can be expected to absorb light more efficiently than currently used forms of Si. Because of a shortage in solar-grade Si feedstock, their improvement has regained immense interest, and clearly pressure-induced band-gap engineering could lead the way.

The high pressure polymorphism of deposited amorphous Si is, however, poorly understood, and a variety of behaviors is reported regarding crystallization at high pressure or amorphous–amorphous

transitions [26]. In either case, no useful crystalline but amorphous material is recovered [26]. This variety is governed by the presence of H, but understanding of this is lacking due to the complexity of the present SiH and SiH₂ groups and molecular H₂ contained within nanovoids [27]. Indeed, it is even unclear if these H groups remain unaltered after decompression. Such understanding is critical for the synthesis of useful crystalline phases from these films and, thus, potential improvement of cheap solar cells.

High pressure INS can be used to study hydrogenated materials industrially used. Furthermore, it can directly determine the behavior of molecular H₂ contained within the films through the ortho-para transition. This can answer the critical question of how the molecular H₂ affects the metallization of the hydrogenated amorphous silicon at ~10 GPa. These pressures are currently unavailable but will become available through XTREME-X, thus opening the way for understanding of this technologically relevant material.

Technical Details

This instrumental concept is based on the design of the CAMEA spectrometer proposed at the European Spallation Source (ESS), although some changes have been introduced because of the differences between STS and ESS. CAMEA was originally envisaged for a long pulse source, but we believe that XTREME-X, with some modifications, is significantly better suited for a short pulse source like STS. XTREME-X can be built at a source with a low repetition rate, such as 10 Hz STS. With a frame 100 ms long, it can be positioned at 50 m from the moderator with a direct view of the moderator and still have no frame overlap so that the energy transfer range available is from -3 meV to 500 meV including the elastic line. Solid parahydrogen as a band-pass filter for the neutrons in the secondary spectrometer will remove the higher orders from the spectra. Unlike the CAMEA concept for the ESS, our implementation will provide access to the whole energy transfer range at constant resolution in terms of $\Delta E/E \sim 1.5\%$.

Table 5.2. Key instrument parameters for XTREME-X

Source	STS
Moderator type	Cold, de-coupled H ₂
Energy transfer range	-3.0 meV to +500 meV
Resolution E	$\Delta E/E=1.5\%$, 80 μeV at the elastic line, Q resolution varies
Sample size range (beam size)	1 \times 1 mm ² to 1 \times 1 cm ²
Moderator—sample distance	45 m
Sample—detector distance	0.75–3 m
Detector type	³ He linear position sensitive

References

- [1] R. J. Hemley, G. W. Crabtree, M. B. Buchanan, Phys. Today 62, 37 (2009).
- [2] B. D. Malone, J. S. Sau, M. L. Cohen, Phys. Rev. B 78, 35210 (2008).
- [3] B. D. Malone, J. S. Sau, M. L. Cohen, Phys. Rev. B 78, 161202(R) (2008).
- [4] F. P. Bundy, H. T. Hall, H. M. Strong, R. H. Wentorf, Jr. Nature 176, 51 (1955).

- [5] R. H. Wentorf, Jr. *J. Chem. Phys.* 34, 809 (1961).
- [6] T. C. Fitzgibbons, M. Guthrie, E.-s. Xu, V. H. Crespi *et al.*, *Nature Materials*, doi:10.1038/nmat4088
- [7] B. Sakintuna, F. Lamari-Darkrim, M. Hirscher, *Int. J. Hydr. Energy* 32, 1121 (2007).
- [8] N.W. Ashcroft, *Phys. Rev. Lett.* 31, 1748 (1968).
- [9] N.W. Ashcroft, *Phys. Rev. Lett.* 92, 187002 (2004).
- [10] R.A. Street, *"Hydrogenated Amorphous Silicon,"* Cambridge University Press, Cambridge (1991).
- [11] R. Boehler, M. Guthrie, J. J. Molaison, A. M. dos Santos, S. Sinogeikin, S. Machida, N. Pradhan, and, C. A. Tulk, *High Press. Res.*, DOI: 10.1080/08957959.2013.823197 (2013).
- [12] A J Ramirez-Cuesta, *Comp. Phys. Commun.* 157, 226-238 (2004).
- [13] Cohen, R. E., Naumov, I. I., and Hemley, R. J. *Proc. Nat. Acad. Sci.* 110, 13757 (2013).
- [14] J. H. Eggert, E. Karmon, R. J. Hemley, H.-K. Mao, A. F. Goncharov, *Proc. Nat. Acad. Sci.* 66, 12269 (1999).
- [15] K. L. Mittal, *"Silanes and other coupling agents" Vol. 4.* CRC Press (2007).
- [16] B. Hidding, M. Pfitzner, D. Simone, C. Bruno, *Acta Astronautica* 63, 379 (2008).
- [17] M. Hanfland, E. Proctor, C. L. Guillaume, O. Degtyareva, *et al.*, *Phys. Rev. Lett.* 106, 017006 (2011).
- [18] A. I. Prokhvatilov, N. N. Galtsov, N. A. Klimenko, *et al.*, *Low Temp. Phys.* 34, 142 (2008).
- [19] T. Loerting, K. Winkel, M. Seidl, M. Bauer, *et al.*, *Phys. Chem Chem. Phys.* 13, 8783 (2001).
- [20] M. Guthrie, R. Boehler, C.A. Tulk, J.J. Molaison, *et al.*, *Proc. Nat. Acad. Sci.* 110, 10552 (2013).
- [21] D. D. Klug, *Nature* 420 (2002) 749.
- [22] D. T. Limmer, D. Chandler, *Proc. Nat. Acad. Sci.* 111, 9413 (2014).
- [23] M. M. Koza, *Phys. Rev. B* 78, 064303 (2008).
- [24] S. Ruffell, K. Sears, A. P. Knights, J. E. Bradby, J. S. Williams, *Phys. Rev. B* 83, 75316 (2011).
- [25] S. Wippermann, M. Vörös, D. Rocca, A. Gali, G. Zimanyi, G. Galli, *Phys. Rev. Lett.* 110, 46804 (2013).
- [26] B. Haberl, M. Guthrie, D. J. Sprouster, J. S. Williams, J. E. Bradby, *J. Appl. Cryst.* 46, 758 (2013).
- [27] A. C. Wright, A. C. Hannon, R. N. Sinclair, *et al.*, *J. Phys.: Condens Matter* 19, 415109 (2007).

5.4 SPHERICAL INDIRECT INELASTIC XTAL SPECTROMETER (SPHIINXS)

AJ Timmy Ramirez-Cuesta, Ulrich Wildgruber, and YQ Cheng (CEMD)

Abstract

SPHIINXS is a high resolution, broadband, indirect geometry spectrometer designed to study small samples. It will open new areas of science for neutron scattering, including chemistry, materials sciences, biology, catalysis, and quantum condensed matter. It is also a high throughput instrument.

The newly commissioned VISION spectrometer is the world's first and only high-throughput, high-resolution broadband INS spectrometer; during commissioning, it managed to measure an INS spectrum of publication quality in 120 seconds. SPHIINXS represents the next evolution of the VISION concept: increasing the analyzer area coverage while retaining Q-resolution.

Science Case

A recent Special Issue of Chemical Physics (Vol. 427, December 2013) titled "Advances and Frontiers in Chemical Spectroscopy with Neutrons" that contains a collection of papers presented at a symposium organized at the Cosener's House in Abingdon, England, in November 2012 is the most up-to-date account of the state of the art in the use of neutron spectroscopy in chemistry. The preface states, *"These advances in instrumentation will open new fields previously unattainable. They promise to make measurements of non-hydrogen containing samples, much smaller samples, or low concentration materials for catalysis or surface species, routine. Furthermore, improvements in signal-to-noise may lift one of the primary restrictions on performing experiments only at low temperatures. The latter restriction based on the INS intensity being modulated by the Debye-Waller factor may be tractable at reasonable temperatures with good statistics."* [1] Neutron scattering, and in particular inelastic neutron scattering, is well known to be a flux limited technique; sample size is always a serious consideration that sometimes makes interesting systems and new science not feasible.

1. **Optimize for measurements on small or weakly scattering samples.** The use of focusing guides and the very large neutron collecting areas that are going to be available with the SPHIINXS design will increase the effective flux of neutrons on the detectors. It will allow the study of samples that are 20 times smaller than the smallest samples measurable today.
2. **Provide Q, ω resolution.** The designs of the current broadband inverted geometry INS spectrometers take two approaches; they integrate either along Q (like Lagrange at the ILL) or around two values of Q ($35 < \theta < 55$ and $125 < \theta < 145$) in a cylindrical arrangement around the incident beam, as is the case of TOSCA at ISIS and VISION at ORNL. The concept behind SPHIINXS preserves the information in the azimuthal angle ϕ but also in elevation θ by using an innovative arrangement of graphite crystals similar to the focusing arrangement used in VISION. This large area covered by analyzers and detectors will provide increased signal that in the case of powder samples can be integrated improving the statistics or enable the use of small samples, making SPHIINXS a high throughput instrument for hydrogenous samples.

3. **Fully integrated and expanded sample environment capabilities.** Sample environment is a fundamental part of a neutron instrument. As was the case for JANUS, optimal use of the instrument will require a means to process materials off-line and allow time for chemical reactions to occur while not wasting precious beam time.
4. **Improved connection with theory.** Computer modeling is intrinsically linked with incoherent INS spectroscopy. The techniques, methodologies, and software exist and have been proven fundamental in the interpretation of incoherent INS. It can be stated that one of the closest connections between ab-initio and experimental data is between modeling and experiments on INS.[2]

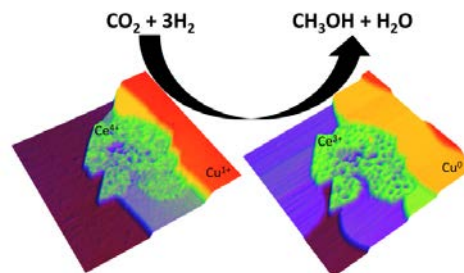


Fig. 5.9. In situ study of CO_2 hydrogenation on $\text{CeO}_x/\text{Cu}(111)$ catalysts.

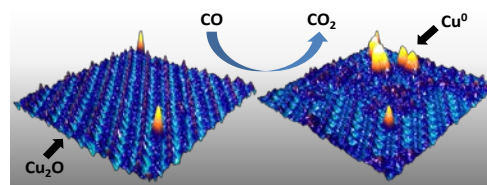


Fig. 5.10. Reduction of Cu_2O by CO .

Specific Science Examples

Methanol synthesis from the hydrogenation of CO_2

Dario Stacchiola, Brookhaven National Laboratory

The transformation of CO_2 into alcohols or other hydrocarbon compounds is challenging because of the difficulties associated with the chemical activation of CO_2 by heterogeneous catalysts. Pure metals and bimetallic systems used for this task usually have low catalytic activity. We have recently shown experimental and theoretical evidence for a completely different type of site for CO_2 activation: a copper-ceria interface that is highly efficient for the synthesis of methanol [3]. The combination of metal and oxide sites in the copper-ceria interface affords complementary chemical properties that lead to special reaction pathways for the $\text{CO}_2 \rightarrow \text{CH}_3\text{OH}$ conversion. One critical aspect that needs to be investigated is the mechanism for the supply of atomic hydrogen in the formation of methanol, and how ceria nanoparticles facilitate the dissociation of H_2 . For this study, elevated pressures of hydrogen above one atmosphere need to be used.

In the catalysis programs, we have reported the in situ study of the reduction of $\text{Cu}_2\text{O}(111)$ films by CO at pressures ~ 0.01 mbar (see Fig. 5.10). The reduction by CO can be followed spectroscopically

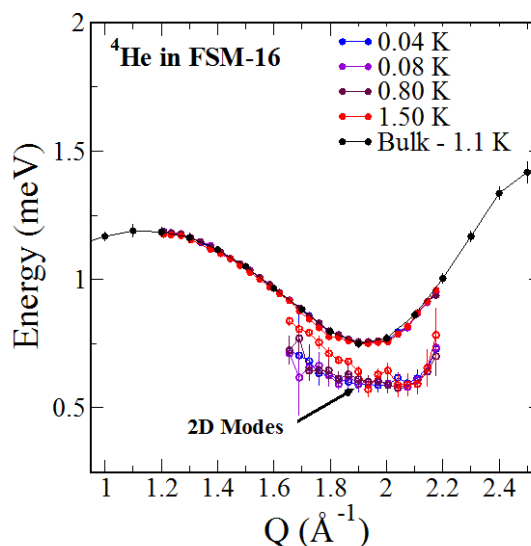


Fig. 5.11. Excitation spectra of liquid ^4He confined in silica FSM-16 (28 Å mean pore diameter) at various temperatures measured on CNCS (2). Accessing $Q > 2.5 \text{ \AA}^{-1}$ is at the expense of a coarser energy resolution, which significantly broadens the spectrum. A background consisting of the FSM16 sample and the first two solid layers has been subtracted.

by ambient pressure AP-XPS. We have carried similar experiments investigating with AP-STM the reduction of Cu_2O by hydrogen, but we cannot correlate this with spectroscopic experiments. This could be accomplished by using INS. We will extend our studies to more complex mixed-oxide and metal carbide model catalysts where we will be able to follow the removal of oxygen by hydrogen and the possible formation of carbonaceous species. This data will complement our studies by AP-STM. The systematic study of reduction on oxides and carbides will be used as the starting point for the study of the hydrogenation of CO and CO_2 on similar mixed-metal oxide and carbide model catalysts, which require higher operating pressures of >1 atm and could therefore be performed at the new INS facility.

The methanol produced by using the CO_2 captured from various sources (methane reservoirs, waste landfills, thermal power stations, etc.) can be converted to other chemicals and fuels by using zeolites.

Superfluid He

Liquid ^4He serves as the archetypical “superfluid” system, and its normal-to-superfluid transition is a continued testing ground for basic quantum mechanical principles. Confined to nanoscale materials, such as porous silica glass (Vycor or MCM-41), ^4He exhibits even more peculiar thermodynamics properties that are remarkably different than in the bulk liquid. The superfluid transition temperature T_λ shifts to lower temperatures (to values that are dependent on the type of porous media used), while the solidification pressure increases [4]. As in the bulk superfluid helium, confined ^4He atoms also undergo well-defined cooperative motions (\sim phonons) and are dominated by single-particle excitations (maxon and rotons). These single particle excitations, which have originally been shown to be a hallmark of Bose-Einstein condensate by Bogoliubov, Gavoret, and Nozieres [5], are somewhat modified in confinement by disorder. The excitation spectrum or P-R modes of ^4He at low temperatures, as well as the layer modes that propagate in the superfluid layers adjacent to the porous media walls, have been investigated by various groups in several porous media for wave vectors up to $Q = 2.15 \text{ \AA}^{-1}$ [5-12], beyond the roton wave vector of $Q_R = 1.95 \text{ \AA}^{-1}$ and for energies around the roton energy $\Delta \sim 0.740 \text{ meV}$ (see Fig. 1 from Ref.[10]). Accurate measurements of the P-R modes (energy and spectral weight) have been reported beyond Δ , and Q up to 3.5 \AA^{-1} for bulk liquid ^4He , both at saturated vapor pressure ($p \sim 0$) [12] and at $p = 20$ bars [13]. These studies point conclusively that the excitation energy never exceeds twice that of the roton and plateaus at 2Δ , because the modes decay into lower energy excitations, in agreement with theory. While there has been at least one successful attempt to clarify the high Q behavior of the modes of ^4He in porous MCM-41 on the upgraded OSIRIS instrument at ISIS [7], experimenters will continue to face challenges in tackling this issue, because of the rather weak liquid signal compared to the massive background, but also due to instrument kinematic constraints and performance. Moreover, because large samples are generally necessary to absorb enough ^4He in the pores, these measurements tend to be complicated by multiple scattering effects (e.g., “signal from ghost roton”), causing difficulties in the interpretation of the data.

A high flux instrument with excellent energy resolution, optimized to access the (Q,E) space of relevance and that can accommodate small samples, would be of high relevance to understanding the high Q evolution of the excitation spectra. Another unsettled topic of continued scientific importance that could be addressed by such an instrument is the determination of the lifetime of the roton and its evolution with temperature, both in bulk and in the confined liquid. There have been some conflicting reports on whether or not the roton lifetime is infinite or just too small to be observed by current capabilities (using a resolution down to 0.7 microeV) [13]. While the temperature dependence of the measured line width has been found [14] to be in excellent agreement with theory, the corresponding energy was found to vary significantly more slowly with temperature than expected. These observations

have since been refuted [12], but the subject remains unsatisfactorily settled and need further studies, which could take advantage of new instrumentation and higher neutron flux. Recent findings by Zsigmond et al. [15] using the IRIS instrument in a high-resolution mode, suggest that the roton does not actually disappear above the superfluid phase transition in bulk, contrary to all known reports to date. Rather, its intensity gradually diminishes and persists further into the normal phase. In light of these two selected science examples and related topics, novel neutron instruments with high-energy resolution and high flux would be an added asset for basic research in quantum fluids and solids.

Technical Details

SPHIINXS can be built at a source with a low repetition rate, such as 10 Hz STS. With a frame 100 ms long, it can be positioned at 40 m from the moderator with a direct view of the moderator and still have no frame overlap so that the energy transfer range available is from -3 meV to 500 meV including the elastic line.

The concept of SHIINXS is similar to VISION, but the practical implementation requires some research and development. In particular, it should be explored if it is possible to use solid para-hydrogen as a band-pass filter for the neutrons in the secondary spectrometer. SHIINXS will have a T0 chopper (two counter-rotating T0 choppers if allowed by the space available). A focusing arrangement of graphite crystals and a removable collimator mean that the detector can be made of relatively short position sensitive He3 tubes.

Table 5.3. Key instrument parameters for SPHIINXS

Source	STS
Moderator type	Cold, de-coupled H ₂
Energy transfer range	-3.0 meV to +500 meV
Resolution E	$\Delta E/E=1\%$, 50 μeV at the elastic line, Q resolution varies
Sample size range (beam size)	1 × 1 cm ²
Moderator—sample distance	40 m
Sample—detector distance	0.75–1 m
Detector type	³ He linear position sensitive

References

- [1] Brown, C. M., Ramirez-Cuesta, A. (Timmy) J., Johnson, M. R., and García-Sakai, V. (2013). Chemical spectroscopy using neutrons. *Chemical Physics*, 427, 1–2. doi:10.1016/j.chemphys.2013.11.009
- [2] A J Ramirez-Cuesta, *Comp. Phys. Commun.* **157**, 226-238 (2004).
- [3] J Graciani, K Mudiyansele, F Xu, AE Baber, J Evans, SD Senanayake, DJ Stacchiola, P Liu, J Hrbek, J Fernández-Sanz, JA Rodriguez, *Science* **345**, 546 (2014)
- [4] Plantevin, B. Fak, H. R. Glyde, J. Bossy, and J. R. Beamish, *Phys. Rev. B* 57, 10775 (1998).

- [5] K. Yamamoto, H. Nakashima, Y. Shibayama, and K. Shirahama, Phys. Rev. Lett. 93, 075302 (2004)
- [6] R. M. Dimeo, P. E. Sokol, C. R. Anderson, W. G. Stirling et al., Phys. Rev. Lett. 81, 5860 (1998).
- [7] R. T. Azuah, S. O. Diallo, M. A. Adams, O. Kirichek, and H. R. Glyde. Phys. Rev. B 88, 024510 (2013).
- [8] B. Fak, O. Plantevin, H.R. Glyde, and N. Mulders, Phys. Rev. Lett. 85, 3886 (2000)
- [9] J. V. Pearce, J. Bossy, H. Schober, H. R. Glyde et al., Phys. Rev. Lett. 93, 145303 (2004)
- [10] T. R. Prisk, N. C. Das, S. O. Diallo, N. Wada, S. Inagaki, and P. E. Sokol. Phys. Rev. B 88, 014521 (2013).
- [11] H. R. Glyde, M. R. Gibbs, W. G. Stirling, and M. A. Adams, Euro. Phys. Lett. 43, 422 (1998).
- [12] J. V. Pearce, R. T. Azuah, B. Fak, A. R. Sakhel, H. R. Glyde, et al., J. Phys. Condens. Mat. 13, 4421 (2001).
- [13] C. R. Anderson, K. H. Andersen, J. Bossy, and W. G. Stirling, R. M. Dimeo, P. Sokol, J.C. Cook, and D. W. Brown. Phys. Rev. 59, 13588 (1999)
- [14] K. H. Andersen, J. Bossy, J. C. Cook, O. G. Randl, and J.-L. Ragazzoni. Phys. Rev. Lett. 77, 4043 (1996).
- [15] G. Zsigmond and F. Mezei and M. T. F. Telling. Physica B: Condens. Matter. 388, 43 (2007).

5.5 MATERIALS PERFORMANCE AND PROCESSING

Andrew Payzant (CEMD)

The manufacture, properties, and performance of advanced materials are of enormous significance to society in general and to the economy of the United State in particular. Neutron scattering provides a unique understanding of the structural basis of materials properties and how advanced processing techniques can be employed to realize significant cost savings and property optimization. Examples of such neutron-based studies include imaging and tomography of functional components, small angle neutron scattering to characterize the microstructure of hard matter, and spatially-resolved neutron diffraction for study (primarily) of microstructure and mechanics in metals, alloys, and ceramics. While in some cases there are x-ray based analogs of these techniques, neutrons provide important advantages in many systems that make them either a complementary or sometimes unique characterization probe.

Instrumentation

Instrumentation presently realized at HFIR includes the CG-1D Imaging, the CG-2 GP-SANS, and the HB-2B Residual Stress instruments. The strong user demand for these instruments is such that comparable instruments have been built at all major reactor facilities around the world and, in all cases, are significantly oversubscribed. CG-1D was built as an instrument prototype to demonstrate cold neutron

imaging at ORNL, but the demand has been so strong that it has become a full-time instrument in the user program, and this demand is likely to continue even after the SNS imaging instrument VENUS is built and commissioned. CG-2 remains one of the most productive instruments in the ORNL user program and is being continuously upgraded with new sample environments, improved detector collimation, additional polarization capabilities, etc. HB-2B has seen significant investment in upgrading the motor controllers, detector electronics, and data acquisition software, after a hiatus following the termination of the EERE-funded HTML User Program, and has recently returned to operational status within the neutron scattering user program.

The SMARTS beam line at LANL (and the ENGIN-X beam line at ISIS) provided the baseline for designing the next-generation VULCAN beam line at SNS. VULCAN has realized significant success across a diverse array of advanced materials characterization studies, including in situ charge–discharge studies of full battery systems, chemistry mapping of bulk hydrogen storage materials, residual stress mapping in aerospace and other structural materials parts, and multi-axial loading studies on engineering materials. The VULCAN instrument remains unfinished, with only the ± 90 degree detector banks installed, pending the allocation of NScD resources to complete the originally planned detector coverage.

For materials science and engineering, it is clear that an investment to expand the detector coverage at VULCAN should realize gains in data rates based on two factors: (1) a greatly increased number of detected neutrons resulting from the larger total detector area, and (2) routine operation at 60 Hz compared to operation at 30 Hz (or even 20 Hz) frequently required at present to achieve adequate Q-range with the present limited 2θ coverage. A further advantage of increased detector coverage will be a greatly enhanced capability to quickly and accurately analyze microstructural preferred orientation (texture).

New Instrument concepts

Recent advances in detector technology have enabled the feasibility of dedicated neutron imaging and 3D neutron tomography instruments at neutron sources. New time-of-flight (TOF) sources open the potential for energy-resolved measurements (i.e., with Bragg edge and resonance contrast) at high data rates; also, dedicated instruments are in commissioning at J-PARC and ISIS. A prototype imaging instrument was set up at the HFIR CG-1D beam line, and this has subsequently become a heavily subscribed instrument in the neutron user program. In addition, it has provided NScD staff the opportunity to fully develop a plan for a dedicated TOF instrument (VENUS) at SNS.

A new dedicated engineering instrument (MENUS) built at either FTS or STS will greatly expand the number of users and range of experiments now possible with VULCAN and will go beyond what could be done on HIPPO at LANL. There is a clear need from the engineering materials/materials science community for “multimodal” instruments; i.e., instruments with multiple simultaneous/parallel characterization capabilities and complex sample environments. It makes sense to develop these capabilities from the ground up on a new instrument rather than by simply modifying/upgrading VULCAN.

5.6 VENUS (VERSATILE NEUTRON IMAGING INSTRUMENT AT THE SNS)

Hassina Bilheux (CEMD)

Abstract

We propose to build VENUS, a pulsed neutron imaging (NI) facility optimized for energy dependent applications at SNS. Based on the strong applicability of neutron imaging techniques, it is expected that the primary usage of VENUS will focus on US Department of Energy (DOE) Energy Efficiency and Reliable Energy (EERE) research programs. VENUS will also support Office of Science Basic Energy Sciences (BES) research programs by contributing in the fundamental scientific understanding of materials chemistry, mechanical behavior, and radiation effects on materials, physical behavior of materials, and geosciences. VENUS will also scientifically affect Office of Science Biological and Environmental Research (BER) research areas such as plant biology and physiology, biofuel and energy production, impact of climate change on the environment, and defined bio-systems. VENUS will contribute in the advances of DARPA materials science and engineering programs. It is likely that a small fraction of the research performed at VENUS will comprise archeological, biological, biomedical, forensic, and homeland security applications as well.

Energy selective techniques such as neutron scattering Bragg-features imaging for improved contrast and identification of phases in an absorption image have been demonstrated at reactor facilities and can be exploited to their full capability at a pulsed, broad-energy-band neutron source such as SNS. The high peak flux is useful for stroboscopic imaging of repetitive or cyclic motions and is synchronized to a selected neutron energy range for enhanced image contrast. The fast/epithermal flux available at SNS will provide additional possibilities for contrast extension and/or enhancement such as epithermal imaging and some resonance imaging capability. This next-generation imaging capability provides a unique approach to strain mapping of manufactured samples such as newly developed additive manufacturing technology.

VENUS uses a large wavelength spectrum, and for wavelength resolution needed for energy selective imaging (for Bragg edge measurements for example), a decoupled poisoned H₂ moderator is the right choice because it has a narrow neutron emission-time uncertainty. The Neutron Scattering Sciences Advisory Committee (NSSAC) approved VENUS at the FTS BL-10 position in November 2008.

Science Case

Based on the strong applicability of the techniques mentioned above to technological challenges, it is expected that the primary usage of VENUS will focus on engineering research, such as the following:

- **Additive manufacturing:** crystallographic plane identification, grain size and distribution, grain orientation, porosity measurements, comparison engineering and neutron data for predictive modeling, change in manufacturing process validation, etc.
- **US energy intensive industry:** aluminum/steel applications, forest products, glass industry, metal casting and petroleum refining, in situ heat treatment
- **Vehicle technology:** energy storage, carbon fiber modeling, magnetic materials, hybrid drive component castings, reducing friction, hydrocarbon spray patterns, hydrocarbon flow through surfaces

- **Industrial technology:** carbon fiber components, energy storage, magnetic materials, fluid power, compressed air systems, motor drive efficiency, combustion processes, steam systems, welding technologies
- **Building technology:** moisture transport in walls/roofs/foundations, microfractures in materials, load bearing structures, deformation of materials, efficient compressors/heat pumps, materials performance, working fluids, corrosion, material fatigue, reduced manufacturing costs, energy storage
- **Geothermal technology:** enhanced geothermal systems, fluid flow in porous and fractured media, reservoir flow, creation and production
- **Biomass research:** anatomic structure, chemical imaging, tension wood, plant growth/maturation, reactor dynamics, pre-treatment, pyrolysis

VENUS will also support **BES research programs by contributing in the fundamental scientific understanding of the following:**

- **Materials chemistry:** materials properties and chemistry, complex fluid microscale dynamics, energy storage materials, transport and chemical interaction of nanoparticles at microscale level, and associated modeling
- **Mechanical behavior and radiation effects:** mechanical behavior after radiation, failure and fatigue, fracture propagation, deformability under stress
- **Physical behavior of materials:** magnetic properties, superconducting properties
- **Geosciences:** geophysical imaging of subsurface reservoirs for hydrocarbon production and CO₂ sequestration, physical and chemical properties, fluid flow studies to understand contaminant transport, geothermal energy production, comparison neutron imaging, and modeling of geological systems

In addition, VENUS will scientifically contribute to research programs within BER such as plant biology and physiology, biofuel and energy production, impact of climate change on the environment, and defined biosystems. VENUS will also contribute in the advances of DARPA materials science and engineering programs.

It is likely that a small fraction of the research performed at VENUS will comprise archeological, biological, biomedical, forensic, and homeland security applications as well. Existing neutron imaging facilities are routinely used for some of these research areas.

Engineering applications can also benefit from a high peak flux used to achieve short time resolution at constant spatial resolution for studying kinetics or moving parts.

The following conferences and workshops were organized to engage the neutron user committee:

- IAN 2006 (Imaging And Neutrons 2006), over 220 participants

- NI@SNS 2008 (Neutron Imaging at the SNS 2008), over 100 participants with strong industry participation
- Neutron Imaging Short Source during ICNS 2009
- NeuWave-4 2011 (Neutron-Wavelength Dependent Imaging Workshop), followed by VENUS Conceptual Design Review (25 and 45 m positions)
- Neutron Imaging Session at User Meeting in 2013, followed by VENUS Conceptual Design Review (25 m position only)

Technical Description

VENUS is an instrument optimized for the measurement of microscale structures in radiography (2D) and tomography (3D) modes. Neutrons from the moderator pass an aperture of variable size, through tapered flight tubes, and through the sample at 25 m. The sample can be moved to 20 m for magnification measurements to reach spatial resolution below a few microns, using a high-resolution Wolter mirror set-up. Bandwidth choppers define the wavelength band of neutrons incident on the sample and eliminate contamination from preceding and succeeding neutron pulses. At 25 m, the sample is placed as close to the detector as possible. A T0 chopper is placed downstream of the bandwidth choppers to decrease the fast neutron flux. A removable cooled Bi filter positioned between the moderator and the aperture can be utilized to remove gammas from the beam. Both a secondary shutter (users are expected to enter the cave as often as 30–50 times a day, which would lower the lifetime of the main shutter) and a fast shutter (to limit thermal and cold neutron activation) are necessary.

The bandwidth choppers are composed of two single and one double bandwidth disks. The double bandwidth can be rephased by changing the phase of the two disks relative to one another to prevent wavelength contamination at 20 or 25 m. The layout of the VENUS front-end optics is illustrated (see Fig. 5.12). Two reviews led by HZB, FRM-II, PSI, and ESS lead neutron imaging beam line scientists have been conducted at SNS to validate the VENUS conceptual design. The VENUS expected performance is described in the table below.

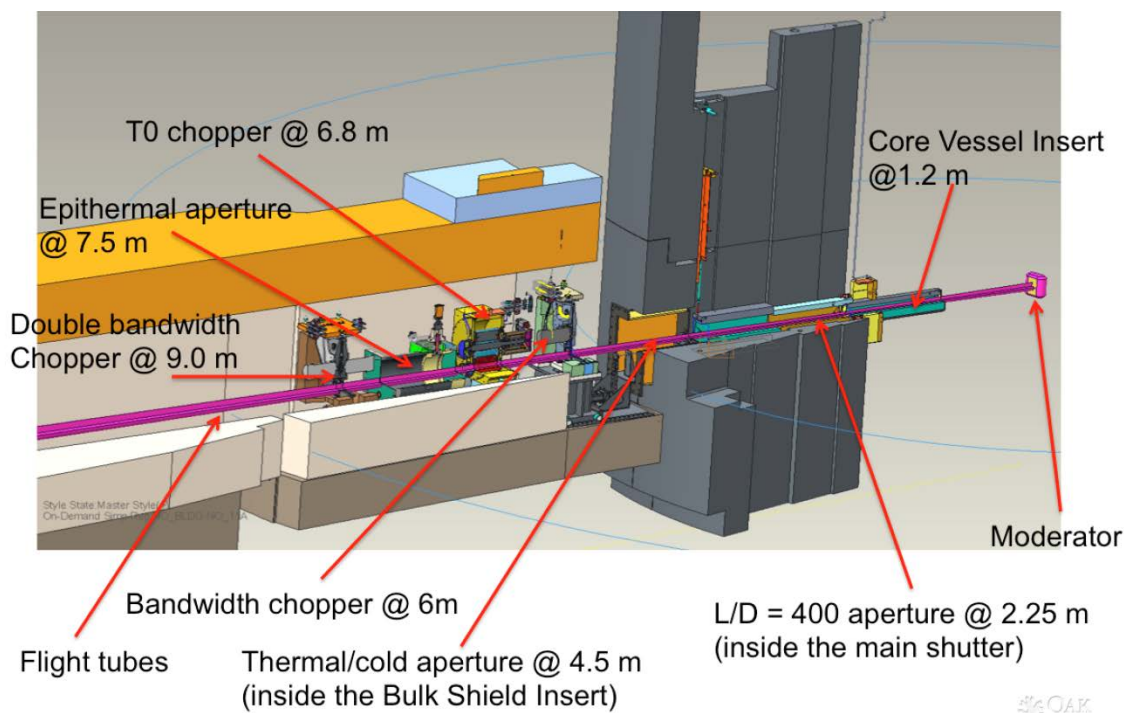


Fig. 5.12. The VENUS instrument.

Table 5.4. VENUS specific parameters

VENUS (FTS beam line 10)	
Beam Spectrum	Epithermal, thermal, cold
Moderator	H2 decoupled poisoned (sharpest pulse at SNS)
Wavelength bandwidth	~ 2.4 Å (time-of-flight mode)
Spatial resolution	< 15 microns (< a few microns with magnification)
Resolution $\Delta d/d$	0.12%
Source-to-detector distance	25 m
Sample-to-detector distance	A few mm to 10s of cm (as needed for magnification)
Detection system and resolution	Cameras (CCDs and sCMOS) and Micro-Channel Plate TOF detector (few microns spatial resolution)
Flux on sample (n/s/cm²)	1 × 10 ⁷ in TOF mode 1 × 10 ⁸ in white beam mode
Field of view	Up to 20 cm × 20 cm (full illumination), 28 cm × 28 cm maximum in 2D imaging

In summary, VENUS at 25 m:

- Is optimized so every pixel on the detector sees 9.5 cm × 9.5 cm of the moderator face (10 cm × 12 cm)
- Has a 20 cm × 20 cm Field of View (FOV) with full illumination
- Can image up to 28 cm × 28 cm maximum FOV (80% of full illumination)
- Provides three sets of apertures optimized for thermal/cold and epithermal neutrons
 - L/D = 400 aperture at 2.55 m (for thermal/cold)
 - Thermal/cold aperture at 4.5 m (L/D > 400)
 - Epithermal aperture at 7.48 m
- Does not have any guides
- Has a T0 and three bandwidth choppers
- Has a removable Bi filter
- Has a suite of off-the-shelf detectors such as CCDs, sCMOS, and MCPs

Table 5.5. Key instrument parameters for VENUS

Source	FTS
Moderator type	Cold, de-coupled H ₂
Wavelength range	0.1 to 10 Å
Resolution	$\delta d/d = 0.12\%$
Beam size	20 × 20 cm ² (full illumination) 28 × 28 cm ² (maximum)
Moderator—sample distance	20 m and 25 m (two locations)
Sample—detector distance	Variable (few mm to 10s cm)
Detector type	Cameras (CCDs and sCMOS) and Micro-Channel Plate TOF detector (few microns spatial resolution)

5.7 GRATING INTERFEROMETRY NEUTRON IMAGING (GINI)

Hassina Bilheux (CEMD) and Roger Pynn (Indiana University)

Abstract

Imaging with cold neutrons is an important part of ongoing science in engineering materials and geosciences, and an increasingly key component in plans for imaging of biological systems. We propose to build a novel time-of-flight (TOF) grating-based cold neutron imaging beam line at STS, GINI, which will utilize cold neutrons to detect small-scale structures (< 1 micron) using attenuation, differential phase, and dark field images in samples with low contrast. The advantage of building a grating-based

cold neutron imaging beam line at a pulsed source is a factor 40 gain in flux for phase imaging measurements, with appropriate TOF grating interferometers based on microfluidic physics.

A unique complementary set of data including attenuation, differential phase, and ultra-small angle scattering, will provide micrometer and sub-micrometer structural information that cannot be achieved using current conventional imaging capabilities.

Science Case

This new concept offers high spatially resolved imaging capability that will open unique new science opportunities for samples that (1) are significantly thinner (a few microns, such as biological cells) than what is currently achievable on thick (a few mm) samples, and (2) have low contrast such as in mesoporous carbon electrodes. Grating interferometry will allow phase and dark field imaging capabilities, which will provide edge enhancement and ~ 100 nm spatial resolution, respectively.

- Energy materials: Understanding energy storage device performance is limited by the inability to accurately model Li (batteries) or H (fuel cells) distribution around the boundaries of the electrodes and membranes, respectively. Currently, a large portion of the industrial battery/fuel cell research is dedicated to modeling ion transport. High spatial resolution (i.e., 1 micron) neutron computed resolution is the only tool capable of visualizing Li mass transport in 3D in battery electrodes. The Li concentration changes in both cathodes and anodes as a function of charge/discharge are essential to validate 3D modeling transport tools. Real time mapping at different C- rates will help understand the rate limitation and the origin of various polarization factors that limit the capacity utilization. The tomography analysis provides the local Li concentration at a given spatio-temporal location. This information can be utilized to feed a multi-physics based transport model that ultimately forms the basis for a predictive capability for determining the cycle life and safety of Li-ion batteries both at the cell and system level. Moreover, the edge enhancement provided by neutron phase contrast is key to determining the location of aggregates of atoms in these interface regions (fuel cell membranes). Reaching high spatial resolution will address important materials properties such as changes in morphology and due to red-ox reactions (dissolution, reduction, nucleation), and elemental 3D mapping of aggregates of atoms under both ex situ and in situ conditions.
- Porous quantification in advanced manufacturing and geological materials
- Cellular imaging of biomass and biological tissues
- Subcellular imaging of biomass and biological tissues
- H₂O/D₂O contrast variation and selective D-labeling will reveal unique information about the dynamic assembly of functioning biological membranes in living systems.
- Physics: magnetic and superconducting domain systems, bulk magnetic domain imaging, magnetization

Technical Description

Compared with thermal and epithermal neutrons, cold neutrons are ideal for complex beam line optics such as grating-based interferometry because they can be easily absorbed in the gratings. The grating method has been successfully deployed using monochromatic neutrons and x-rays but, to our knowledge, has not been attempted at neutron pulsed sources (though scientists at ISIS have shown interest in doing so). The potential advantages of doing so include the fact that neutron absorption and, in some cases scattering length density, vary with neutron wavelength and hence provide additional information about the radiographed object. In addition, use of the time-of-flight method allows individual wavelengths to be recorded and a broad wavelength band at a pulsed source may give the latter a neutron flux advantage over the use of a narrow wavelength band at a reactor source, a factor 40 improved in flux compared with reactor-based monochromatic phase imaging beam lines. Although the grating method could be used directly at a pulsed source, the visibility of the diffraction fringes produced by G1 (the phase grating) varies with neutron wavelength so some wavelengths give less information than others do. To enhance the fringe visibility, either G1 has to be vibrated during the pulse or the phase contrast that it produces must be modulated in some way. Several methods of pulsed neutrons can be used:

- a) Rock the phase grating at the rate of the TOF source, namely 60 Hz at SNS
- b) Vary d at a repetition rate of the TOF source, namely 60 Hz at SNS
- c) Use piezoelectric gratings: apply an electric field to mechanically modify the gratings
- d) Use tunable microfluidic channels

Methods (a)–(c) all suffer from the disadvantage that the phase grating has to be moved several millimeters parallel to the neutron beam while its position perpendicular to the beam is maintained with sub-micron precision. While we believe that we have identified a mechanical system that will make method (b) possible, it is, admittedly, difficult. Method (a) is inherently limited to a narrow band of neutron wavelengths. In method (d), two immiscible fluids with low and high refractive indexes for neutrons would be filled in parallel microfluidic channels (effectively a diffraction grating), and a varying electric field would be applied to change the distribution of the fluids in the channels so that its refractive index is correct at each instant during each neutron beam pulse. This method promises great success and can be implemented at GINI, after some investment in development effort of this unprecedented grating interferometry technology for both phase and dark field imaging techniques.

Preferably, the instrument should not have a guide system, thus the beam line should be close to the moderator. If guides are necessary, the use of a nanoparticle diffuser is required. A variable aperture system with L/D s from 400 to 1,000 is acceptable.

Table 5.6. GINI instrument specifications

Mode	Energy range	Field of view	Spatial resolution	Time to acquire a radiograph	Detector/capability
High-res	2 to 20 Å	1 cm × 1 cm	<1 microns	< 5 min	Gratings with MCP detectors

5.8 MATERIALS ENGINEERING BY NEUTRON SCATTERING (MENUS)

Andrew Payzant and Ke An (CEMD)

Abstract

We propose to build a new engineering and materials science beam line MENUS optimized for multimodal characterization of bulk polycrystalline materials. MENUS is proposed to cover a range of experimental space not met by existing instruments at the SNS.

The primary characterization techniques at MENUS will be spatially-resolved diffraction to enable detailed mapping of composition, strain, grain orientation, and grain size in large bulk structures and functional materials using cubic mm size diffracting “gauge” volumes as defined by slits and radial collimators with substantial diffraction detector area. In addition we propose to include transmitted-beam detectors for complimentary SANS measurement in common engineering materials, and comparable field of view imaging cameras for parallel studies of microstructural features at high spatial resolution.

Science Case

The next generation of engineering instruments at the SNS will extend the capabilities beyond what is presently found on VULCAN. What is clearly articulated by the applied/industrial research community is the need for instruments with multiple measurement capabilities at rapid data collection rates to understand phenomena critical to manufacturing and operation of new advanced materials.

1. **Critical infrastructure materials evaluation:** The nation’s bridges, railways, power transmission lines, pipelines, nuclear power plants etc., are ageing faster than they are being replaced. There is a clear and compelling need for advanced materials characterization techniques, specifically including neutron diffraction and imaging, to ensure that the computational models presently used to determine the safety of such critical engineering structure are experimentally validated, and to provide the data necessary to build such models. Any serious attempt to investigate these problems will require significantly more neutron instrument time than is possible today, and additional instruments will need to be built to meet this demand.
2. **Advanced Manufacturing:** Additive manufacturing (or 3D printing) is a rapidly growing method of making parts and assemblies out of plastic or metal directly from a CAD drawing. This method can be highly efficient, but the highly directional thermal processing has the potential to introduce significant hidden defects and residual stresses that impact the performance. Neutron imaging and residual stress mapping are necessary to provide nondestructive characterization of these phenomena at spatial resolutions on the order of tens of microns (imaging) and mm (stress).
3. **Advanced engineering materials:** Super alloys and composite materials are a rich area for this instrument to play an important role, as the ability to simultaneously determine strain partitioning in all components of the composite is essential to understanding the mechanical properties of these materials. However, in most case, the super lattice peak (100) with large lattice of around 3 Å (some cases close to 4 Å), which requires substantial neutron flux at the nominal neutron wavelength of around 4~6 Å. The proposed instrument will have to meet this criterion.

4. **Energy Materials:** The new instrument will fulfill the requirement for measuring in situ/in operando energy materials behaviors in a working device. Neutrons play a unique role of understanding of performance, degradation, and reliability of energy storage devices including Li-ion, sodium batteries, and hydrogen storage tanks thanks to deep penetration, sensitivity to light elements, and comparable spatial resolution to the full working system. The chemistry of most energy materials usually possesses large unit cells. It is expected that the new instrument will provide not only the full view of the diffraction pattern with lower Q range but also the improvement of the flux of the colder neutrons that can facilitate the in situ/in operando observation of the energy material behaviors.
5. **Magnetic field processing of alloys is another area of potential growth.** In recent years it has been shown that high temperature processing of certain alloys, especially steels, can be strongly impacted by magnetic fields such that phase transformation temperatures (e.g., austenite-martensite) can be shifted to previously inaccessible regions of the CCT/TTT diagram. For in situ characterization studies, neutrons provide significant advantages in terms of sample environment and experimental infrastructure.

For parametric studies it is essential to use combinations of sample environment, including multiaxial stress, temperature, magnetic field, electric field, controlled atmosphere, humidity, etc. In the case of temperature, it is essential to not only control temperatures over a wide range from cryogenic to high temperature, but also to enable rapid rates of heating and cooling. There is a critical need for a next-generation instrument for studies of texture and texture evolution under pressure, temperature, etc. Both bulk and localized mapping capabilities will be needed.

Specific Science Examples

Deformation mechanisms in a precipitation-strengthened ferritic superalloy

S. Huang, Y. Gao, K. An, L. Zheng, W. Wu, Z. Teng, P. K. Liaw, Acta Materialia, 2014

The strengthening precipitates exist in Fe, Ni, and Co based super alloys, and the understanding of the close misfit of the matrix and precipitate phases is critical for the super alloys' high temperature creep reliability. As an example, the ferritic superalloy, Fe-10Ni-6.5Al-10Cr-3.4Mo strengthened by ordered (Ni,Fe)Al B_2 -type precipitates, is a candidate material for ultra supercritical steam turbine applications above 923 K. Despite earlier success in improving the room temperature ductility, the creep resistance of this material at high temperatures needs to be further improved, which requires a fundamental understanding of the high-temperature deformation mechanisms at the scales of individual phases and grains. In situ neutron diffraction has been used to investigate the lattice strain evolution and the microscopic load sharing mechanisms during tensile deformation of this ferritic superalloy at elevated temperatures. As shown in Fig 5.13, separation of the adjacent peaks challenges the available engineering diffraction instrument resolution; therefore, measurement of the solo superlattice peak becomes necessary. P(100) exists at 2.9 Å, which is measured alone, and the shift information was carried on to separate the overlapping peaks (200) of each phase. The misfit of the main phase and the precipitate phase is resolved, and by combining with crystal plasticity FEM modeling, based on these interphase and intergranular load-partitioning studies, it is found that the deformation mechanisms change from dislocation slip to those related to dislocation climb, diffusional flow, and possibly grain boundary sliding, below and above 873 K, respectively. The research will aid microstructural design in enhancing creep resistance of super alloys in power plants.

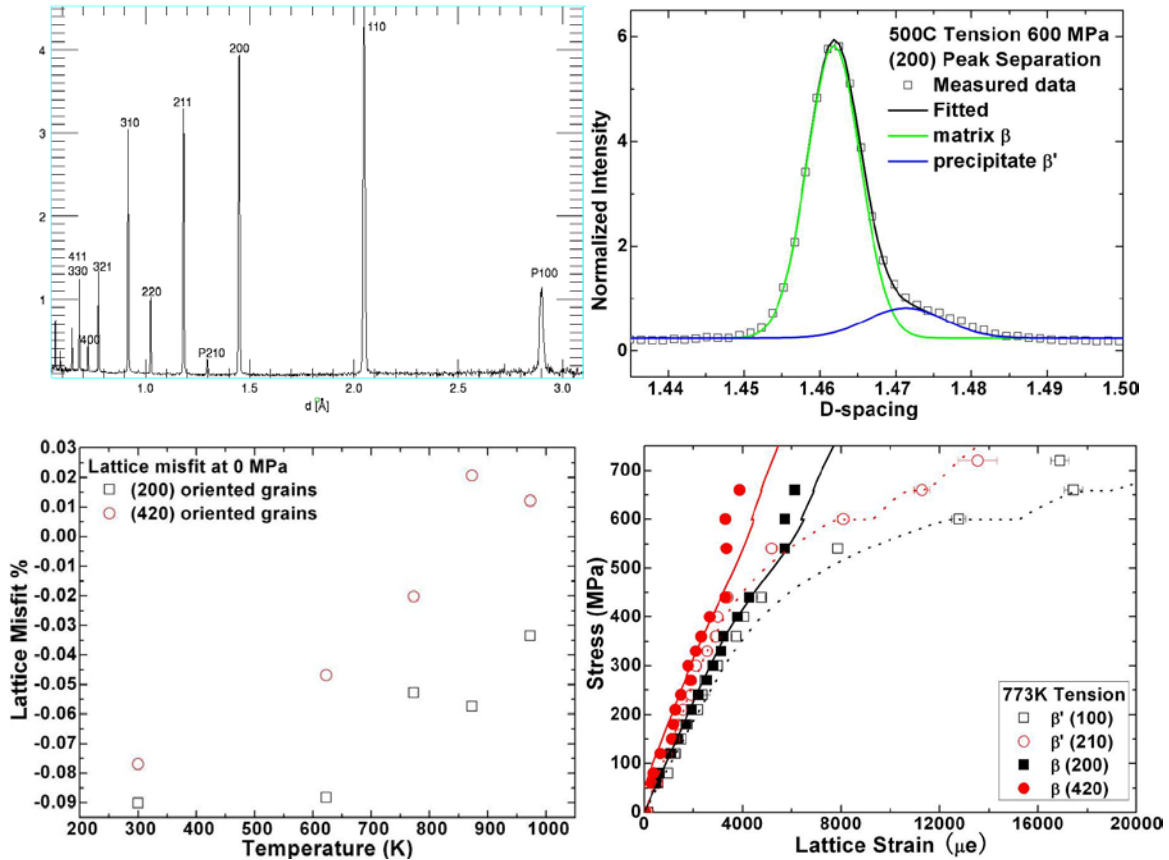


Fig. 5.13. Measurement of the superlattice peak P100 of beta prime precipitates occurring at large d and the resolved misfit in the Fe based super alloys.

The crystal plasticity finite element method modeling simulates the measured mechanical behaviors of the matrix and precipitate phases.

Energy storage material behavior in working devices

L. Cai, K. An, Z. Feng, C. Liang, S. J. Harris. Journal of power source, 2013

Electrodes behaviors in large batteries can be observed simultaneously by non-destructive neutron scattering while they are under electrochemical cycling. The kinetics of the lithium intercalation process and the degradation evolution can be revealed. A commercial large format battery (dimension $200 \times 120 \times 5$ mm) of 15Ah with the graphite anode and spinel $\text{Li}_x\text{Mn}_2\text{O}_4$ -based cathode was investigated by neutron diffraction before and after the realistic degradation cycling at 40°C . The charge state at different locations in the battery is mapped. While the fresh battery possesses homogeneous local state of charge, the degraded cell shows spatially inhomogeneous deteriorations as indicated by the non-uniform distribution of active material phase fractions (Fig. 5.14). This example shows that neutron diffraction is powerful in studying energy material behaviors in a working device non-destructively. This expands the material characterizations by neutron scattering into real world applications. Understanding of performance, reliability, and degradations in Li-ion batteries, sodium batteries, and hydrogen storage tanks will benefit from neutron scattering advantages.

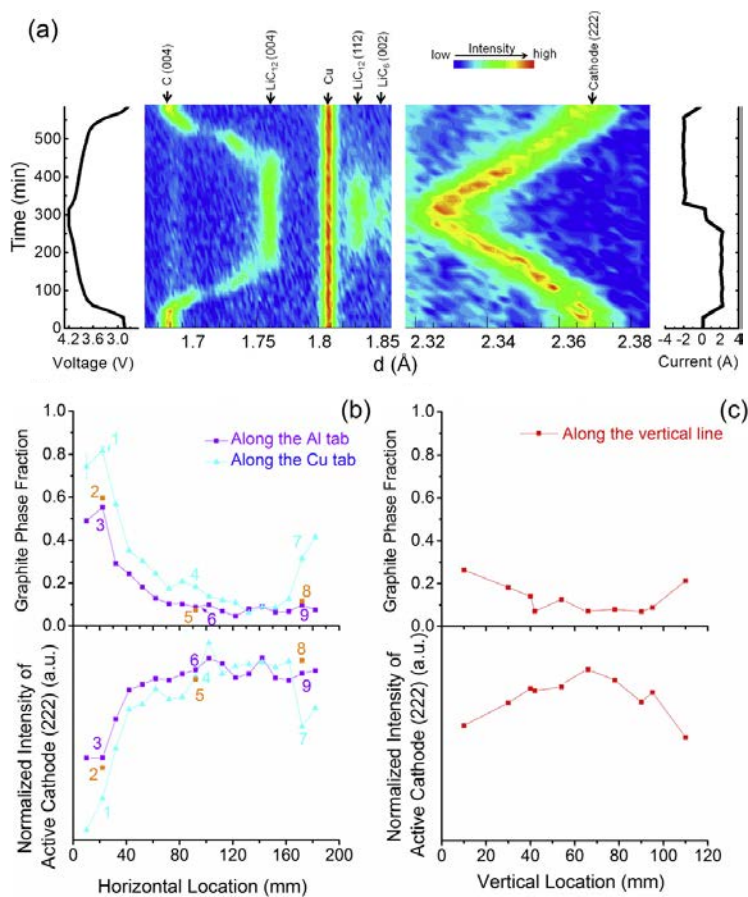


Fig. 5.14. (a) The phase evolutions of anode and cathode in a fresh large format battery. (b) and (c) The non-uniform degradation in the degraded battery from observation of the electrode activities at different locations.

Technical Details

1. Neutron Spectrum

A limitation at VULCAN is the lack of neutrons at longer wavelengths. MENUS will address this shortcoming by providing an incident beam with significant neutron flux at wavelengths up to 6 Å. These lower energy neutrons will enable studies using lower 2θ scattering angle peaks, which are needed for analysis of low symmetry materials (i.e., beyond single phase bcc/fcc/hcp engineering alloys) where key information is found in the large d-spacing diffraction peaks, for resolving superlattice lines in many advanced alloys, for resolving magnetic scattering peaks in magnetic alloys, for refining diffraction data from composite materials where the phases are otherwise difficult to resolve because of peak overlaps at small d-spacings, etc.

2. Guide Details

MENUS will use a straight guide with a T-zero chopper to eliminate the prompt pulse. The background will be reduced downstream by collimation and instrument design, whereas a curved guide as at VULCAN limits the flexibility of the instrument to select the higher energy neutrons when needed. A selection of multiple end guides will allow the beam divergence to be

optimized for high resolution diffraction, high incident flux, or transmission experiments (SANS or imaging).

3. **Sample Cave**

MENUS will require a large instrument cave with room for an array of sample environments and easy access for samples that are, in fact, large engineered systems. A major advance over VULCAN will be an ability to remove full sample environments without disturbing their operation, so that long-term characterization may be done with the sample environment running offline much of the time. An example is a long-term creep experiment, where a sample is subjected to multi-axial loading under temperature—the experiment may take several months, but neutron measurements are only needed for a few hours every few days. Robust kinematic mounts will be necessary to facilitate accurate sample positioning with minimal adjustment of sample alignment, and all electrical, utility, and data acquisition connections will stay operational at all times. Ideally, the cave will include a non-rad area so that staff can interact with the sample environment off the instrument even when other experiments are running.

4. **Detector Coverage**

MENUS will require a substantial detector coverage, which, in addition to providing more rapid data collection from the greater rate of collected neutrons, is also required to fully characterize changes in orientation texture. Based on lessons from running VULCAN, it will be essential to improve the vertical resolution to be closer to the horizontal resolution.

5. **Sample Environment**

MENUS will include dedicated multimodal sample environments unique to SNS. Examples might include: (a) a complex sample environment enabling full control of multiaxial mechanical loading of samples under high temperature and applied magnetic field in controlled atmosphere—such a capability opens up new science enquiry for magnetic shape memory materials; and (b) a fully instrumented battery charge/discharge test facility including temperature control to understand long-term degradation of energy storage devices, etc. Such an arrangement facilitates running multiple short-term and long-term experiments in parallel, thereby maximizing utilization of neutrons.

6. **Data Acquisition and Analysis Software**

MENUS will require new software tools to enable complex multimodal experimental controls and data acquisition.

7. **Radioactive sample handling capabilities**

MENUS requires integrated support for handling nuclear/rad materials. Such materials generally have complex microstructures intended to minimize the rate of microstructural damage in high radiation environments to prevent rapid reduction of key mechanical properties. A deeper understanding of microstructure and mechanical properties in these materials is essential to the development of the next generation of reactor structural materials for land-based power and

navy reactors. Relevant MENUS capabilities will include optional remote handling of hot samples and installable hot cells with kinematic mounts to maximize ALARA safety practices.

Table 5.7. Key instrument parameters for MENUS

Source	STS
Moderator type	Cold, de-coupled H ₂
Wavelength range	0.5 to 6 Å
Resolution (HiInt/HiRes)	$\Delta d/d = 0.5\%/0.2\%$
Moderator—sample distance	~60 m
Sample—detector distance	2 m
Detector type	Scintillator 2D position sensitive SANS/imaging detector

5.9 HIGHRESPD (HIGH RESOLUTION POWDER DIFFRACTION) FOR STS

Ashfia Huq (CEMD)

Abstract

Currently, the highest resolution neutron powder diffractometers in the world are HRPD at ISIS ($\Delta d/d = 0.04\%$) and SuperHRPD at J-PARC ($\Delta d/d = 0.035\%$). The history of high scientific productivity at HRPD and current synchrotron instruments where this resolution has become standard make a strong case for having an instrument of comparable performance in North America. With the higher intensity available at STS, this instrument will be able to perform high resolution powder diffraction measurement on samples that are much smaller than what is possible with the existing instruments in UK and Japan.

Science Case

1. **Ab-initio Structure Determination from Powder Diffraction (SDPD):** The collapse of information from 3D to 1D has always meant that structure solution from powder diffraction data is significantly harder than single crystal. Nevertheless, a great majority of materials are prepared and utilized as powders. With improvements in instrumentation, algorithm development and enhanced computing power, great strides have been made in ab-initio structure solution from powder diffraction. While the contrast afforded by difference in Z often makes x-ray diffraction the method of choice for structure solution, there are some cases where neutron diffraction is essential. Indexing and determination of space group is the first step in SDPD for which high resolution data is required.

The sensitivity of neutrons to light elements can play a crucial role in the determination of the correct space group, and therefore, the correct interpretation of structure-property

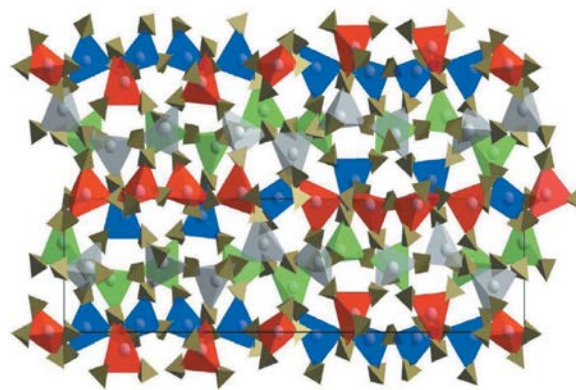


Fig. 5.15. Structure of the low-temperature Mg(BH₄)₂ phase in space group P6₁ viewed along the hexagonal a axis, showing two unit cells.

The unusually complex structure of this material with lattice parameters $a = 10.3182(1)$, $c = 36.9983(5)$ Å, and $V = 3411.3(1)$ Å³ was finally solved [1] by using a combination of high-resolution synchrotron and neutron diffraction data.

relationships. For example, the tilting of TiO_6 in perovskite or orientation of methyl group in small molecules can subtly affect the space group that is difficult to determine from x-ray data. Neutron data is used in framework structure to find light atoms such as hydrogen, CH_4 , or CO_2 inside clathrate, MOF, or zeolite structures using Fourier cycling. Neutron diffraction data can play a critical role in the structure solution of small molecule and organic inorganic hybrids, heavy metal oxides, and other, more complex compounds. As the demand for complex structure solution from powder diffraction data grows, the need to combine x-ray and neutron powder diffraction will increase. Ideally that need can be met by having access to a neutron powder instrument that has the same resolution afforded by synchrotron powder beam lines.

2. **Complexity and Subtlety:** Functional materials of scientific and technological interest, such as zeolitic solids, piezoelectrics, controlled thermal expansion materials, ionic conductors, etc., commonly display a high level of crystallographic complexity (very large unit cell volumes) and/or subtle structural distortions. In many cases, this structural complexity is integral to the useful physical properties of the materials. To properly address such problems using powder diffraction, high resolution data is needed both to resolve subtle splitting in peaks or reveal subtle features in diffraction line shapes and to resolve an adequate number of Bragg peaks at high Q, where overlap and loss of information are significant issues for large unit cells. Examples include the recent examination of phase transitions in $\text{K}_3\text{MoO}_3\text{F}_3$ where the low temperature phase is ferroelectric and the low-temperature structure of the negative thermal expansion material ZrP_2O_7 . One of the polymorphs of $\text{K}_3\text{MoO}_3\text{F}_3$, which contains polar chains, has $Z = 80$ and $V > 13,000 \text{ \AA}^3$, and the ambient-temperature pseudo-cubic ($a \sim 8.25 \text{ \AA}$) cell of ZrP_2O_7 is actually orthorhombic with $a \sim b \sim c \sim 24.75 \text{ \AA}$ [3]. To determine the complete structure of the latter material, with ~ 400 independent structural parameters, both high resolution synchrotron and neutron diffraction data (HRPD at ISIS) were combined. In the case of $\text{K}_3\text{MoO}_3\text{F}_3$, good-resolution data from POWGEN was used in combination with high resolution synchrotron data from the Advanced Photon Source [4]. POWGEN is the best instrument in the United States for this type of work but is substantially less capable than the *previous generation* instrument at ISIS.

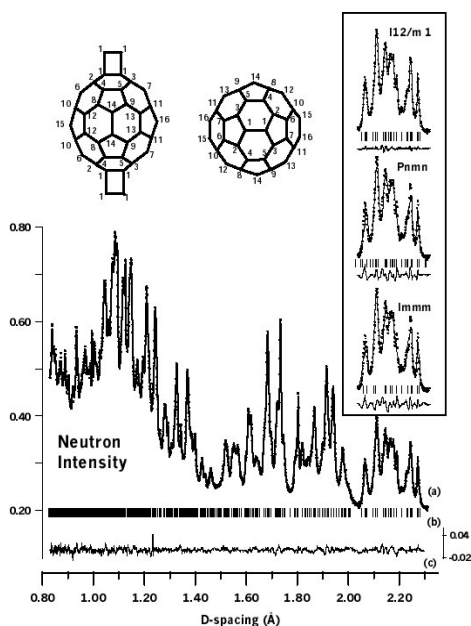


Fig. 5.16. Structure of polymer phase of alkali doped fullerene RbC_{60} .

It was not possible to determine the correct structure from high resolution synchrotron data because of the lack of sensitivity to the C atoms in the presence of Rb. High resolution data collected at HRPD at ISIS was crucial to establish the correct space group and hence the correct structure [2].

3. **Magnetism:** Neutron diffraction has been the method of choice for solving magnetic structures after the work by Wollan and Shull. Magnetic ordering phenomena and magnetic coupling to other physical properties continue to be of great scientific and technical interest. To parametrically track both the nuclear and magnetic structures using powder neutron diffraction, it is important to have access to an instrument capable of rapidly acquiring high quality data at both high and low Q. Magnetic structures can often be extremely complex; a typical example is BiFeO_3 where the structure consists of unusually long period modulation of $620 \pm 20 \text{ \AA}$. This modulation changes with temperature but remains visible nearly up to the Neel temperature. This work was only possible through the high resolution afforded by instruments like HRPD. Figure 5.17 shows data collected at HRPD in 1992 on the left, and on right is shown POWGEN data where Mn substitution was done in the Fe site. The parent compound with no doping shows the hint of the three reflections in the POWGEN instrument that is very clearly visible in the HRPD data. It was not possible with this data to understand the effect of Mn in changing the magnetic structure of this well-known multiferroic material.

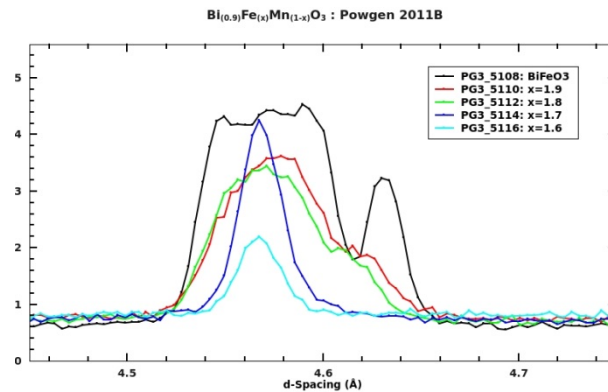


Fig. 5.17. Magnetic structure of BiFeO_3 as measured on POWGEN (right and with Mn substitution in the Fe site) and the ISIS HRPD instrument (left) [5].

Technical Details

To obtain the highest wavelength (timing) resolution, HighResPD requires a moderator that produces the sharpest neutron time pulses coupled with a long flight path. The wavelength bandwidth that can be sampled at a given operating frequency, f , of the source is $\Delta\lambda = 3956/Lf$, where L is the length of the instrument in meters and λ is in \AA . Obtaining a reasonable $\Delta\lambda$ for a long instrument requires a small f . At 120 m, the longest instrument that the SNS site allows, $\Delta\lambda$ is 3.3 \AA at the STS operating frequency of 10 Hz. The sharpest time pulses will be produced by the de-coupled moderator. To reduce the geometrical contributions to the resolution function, a premium will be placed on locating detectors at high 2θ , near backscattering conditions. The guide system will likely be straight, minimizing wavelength-dependent spatial variation of the beam across the sample. A T0 chopper will be required to suppress the initial flash of gamma and fast neutrons to reduce detector backgrounds. One or, at most, two bandwidth choppers will be required to define the wavelength range incident on the sample in any given pulse of the source.

Table 5.8. Key instrument parameters for HighResPD

Source	STS
Moderator type	Cold, de-coupled H ₂
Wavelength range	0.5 to 5 Å
Resolution	$\Delta d/d = 0.035\%$
Sample size range (beam size)	up to $1 \times 2.5 \text{ cm}^2$
Moderator—sample distance	120 m
Sample—detector distance	2–2.5 m
Detector type	³ He linear position sensitive

References

- [1] R. Cerny, Y. Filinchuk, H. Hagemann, and K. Yvon, "Magnesium borohydride: Synthesis and crystal structure," *Angew. Chem. Int. Ed.* **46**, 5765 (2007)
- [2] A. Huq, P. W. Stephens, Goetz M. Bendele, and R. M. Ibberson, "Polymeric Fullerene Chains in RbC₆₀ and KC₆₀," *Chem. Phys. Lett.* **347**, 13 (2001).
- [3] G.W. Stinton, M. R. Hampson, and J. S. O. Evans, "The 136-Atom Structure of ZrP₂O₇ and HfP₂O₇ from Powder Diffraction Data," *Inorg. Chem.* **45**, 4352-4358 (2006).
- [4] A. M. Fry and P. M. Woodward, "The structures of alpha-K₃MoO₃F₃ and alpha-Rb₃MoO₃F₃: ferroelectricity from anion ordering and non-cooperative octahedral tilting," *Crystal Growth and Design* (2013).
- [5] I. Sosnowska, M. Loewenhaupt, W. I. F. David, and R. M. Ibberson, "Investigation Of The Unusual Magnetic Spiral Arrangement In BiFeO₃," *Physica B* **180**, 117 (1992)

5.10 RAPID (RAPID ACQUISITION PARAMETRIC AND IN-SITU DIFFRACTION) FOR FTS

A. Huq and P. Whitfield (CEMD)

Abstract

Neutron powder diffraction has played a key role in the development and understanding of new, complex materials. In comparison with other major neutron centers, HFIR and SNS support a much more limited suite of powder diffraction instruments. The powder diffraction community is largely served by the SNS POWGEN and HFIR HB2A instruments, although SNAP and NOMAD at SNS also provide powder diffraction capabilities. SNAP is highly optimized for the very small samples required for extremely high pressure studies, while NOMAD is a high-intensity instrument optimized for the study of liquid and amorphous materials. NOMAD has potential for rapid parametric and small sample diffraction studies, but serving this community of powder diffraction users would displace portions of the already active community using NOMAD and would require additions/modifications that may be incompatible with the instrument's primary purpose (e.g., installation of a radial collimation). A longer-term strategy is to build an instrument optimized for the parametric studies and small samples.

Science Case

1. **Refined structures from small samples:** There is a strong scientific need for routine neutron diffraction studies of very small samples. Many materials of interest are produced using methods not amenable to the production of the gram-sized samples desirable for POWGEN. A common example would be electrochemically cycled battery materials from research-type coin cells where the electrodes may contain 10 mg of active material. POWGEN samples may require material from 20 or more cells to produce what is considered a borderline sample.

Samples that require use of particular isotopes can be prohibitively expensive to prepare in gram size quantities, and highly absorbing samples (e.g., samples containing H, Ir, Eu, etc.) also require the use of small samples. High quality structure refinements require a high signal-to-background ratio, so an instrument optimized for low background is necessary to fully capitalize on data from such small samples.

2. **High speed and parametric refinements:** The parametric approach to non-ambient studies is a powerful tool where physical models are incorporated into the analysis of a sequential series of datasets. The need for a reasonable model in such cases is offset by the ability to tease out subtle details from data otherwise too noisy by refining tens, hundreds, or thousands of datasets simultaneously. This creates an opportunity to probe on a timescale not accessible by conventional sequential refinement. Parametric refinements have been used to probe phase transitions and reactions in almost any sample environment imaginable. Physical parameters such as rate constant or order parameter actually become the refinable parameter, and the tolerances to relatively noisy data make them efficient in terms of beam time. Intermediate phases in the formation of Ti_3AlC_2 were studied using simultaneous refinement of 104, 5 min datasets from POLARIS. Sequential refinement of the data was not successful, but appropriate use of parametric constraints allowed intermediate phases to be quantified.

The Materials Genome Initiative is a multi-agency initiative designed to create a new era of policy, resources, and infrastructure that support US institutions in the effort to discover, manufacture, and deploy advanced materials twice as fast, at a fraction of the cost. The materials genome project has launched several programs where large databases of materials are being used to calculate and minimize structures of known compounds and to predict new ones using various different theoretical techniques. *Successful theory has led and will continue to lead to prediction of large numbers of unknown stable (missing) compounds. Validation through the synthesis is the challenge for experimentalists.* Figure 5.20 shows an example of one such family of compound $ZrRhBi$ that was predicted to be stable. In the exploration of this phase space of synthesis, several other compositions were discovered by using in situ synchrotron measurements. While x-rays are the perfect probe for doing this work in intermetallics, neutrons are often better suited for oxide, nitrides, and hydrides. Fast data collection is crucial to be able to measure the phase evolution as it depends on the reaction times.



Fig. 5.18. Shown at left is a coin cell where the amount of active cathode material is 0.01 g. At right is a pouch cell specially manufactured to understand the behavior of the cathode as a function of cycling using POWGEN. The active cathode material here is 1 g.

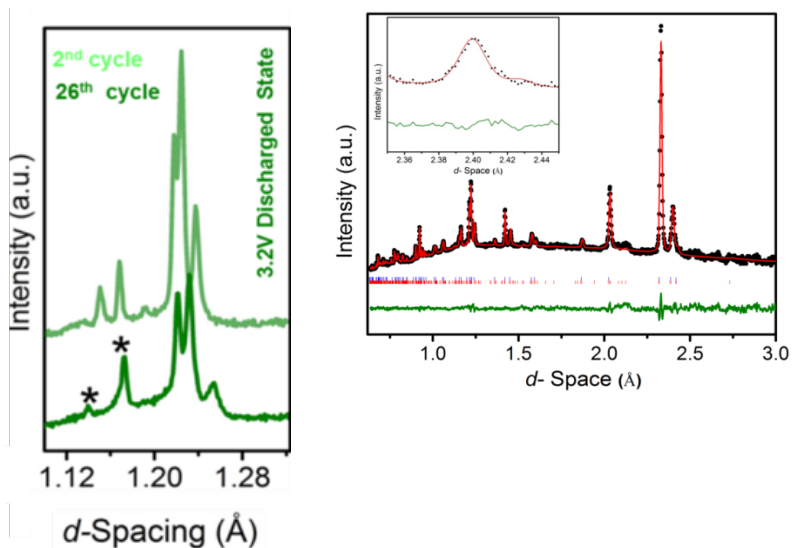


Fig. 5.19. Diffraction pattern collected at different states of cycling to establish the voltage fade mechanism in cathodes that are Li and Mn rich layered compounds.

On the right is shown the Rietveld refinement, which typically takes 4–5 hours to collect. The battery was cycled for 26 cycles, and the experiment took 4 days, even with this large sample.

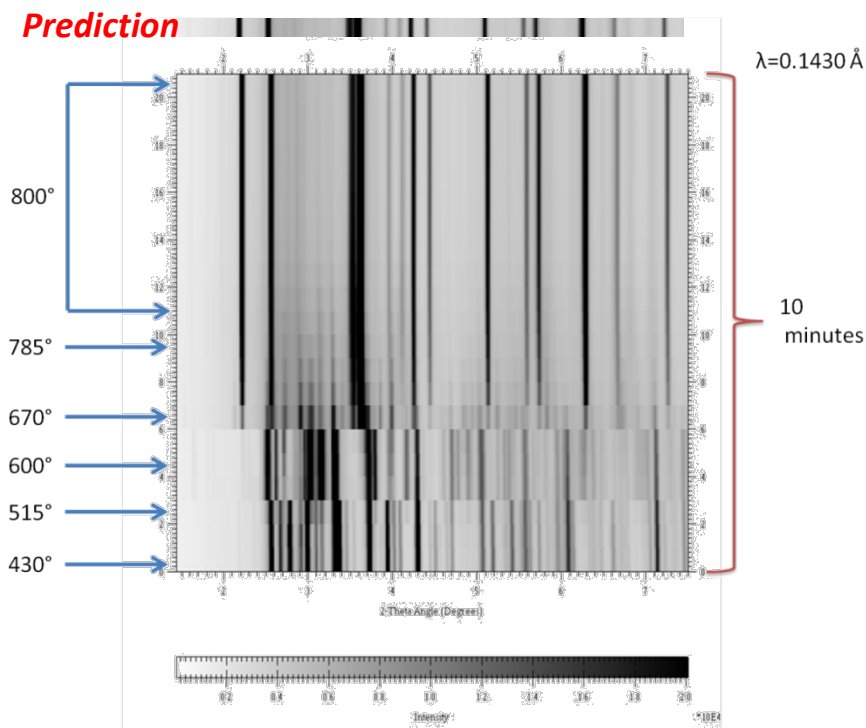


Fig. 5.20. Powder diffraction data from ZrRhBi.

3. **Stroboscopic measurements:** Where a process is rapid but reversible, a stroboscopic approach can be used to obtain data with sufficient statistics. The event-mode data collection at SNS facilitates the collection and analysis of data using this methodology. An example of such an experiment would be the use of a pulsed magnet where the data from many pulses would be required to build up a single dataset. To do this in a reasonable timeframe requires both high intensity and excellent collimation.

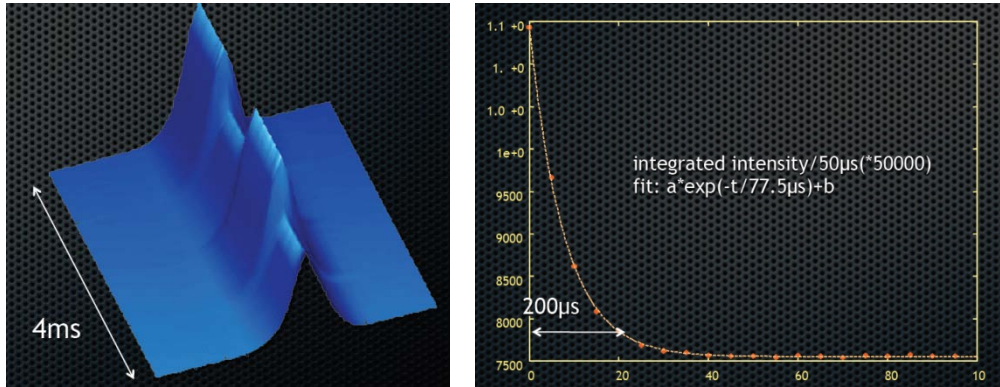


Fig. 5.21. Stroboscopic measurement done at the ILL D20 powder diffractometer to study ultrasound excited single crystals as switchable neutron mirrors.

The technique can also be used for studying electrochemistry, rapid interactions with electric and magnetic field, relaxation of laser excited states, piezoelectric materials, and more.

4. **Signal-to-noise:** Hand-in-hand with the need to reduce background is the need to reduce noise. Important details can be missed because a weak reflection is hidden by the noise. Studies relating to physisorption and magnetism can be impacted negatively in this regard. Significantly reducing the noise level requires high intensities to improve the statistics.

Technical Details

VULCAN (SNS FTS beam line 7) has demonstrated the suitability of the shallow poisoned, 300 K water moderator to produce outstanding powder diffraction measurements providing $\Delta d/d = 0.25\%$ in its high resolution (low beam divergence) mode with detectors at 90 deg 2θ . This moderator produces pulses with FWHM of 10.6 μsec at $\lambda = 1 \text{ \AA}$, which should provide better $\Delta d/d$ at higher scattering angles for an instrument with a total flight path of $\sim 35 \text{ m}$. Beam line 8 at FTS was designed to support two instrument stations and is ideal for supporting RAPID. The data collection rate of RAPID relative to POWGEN can be estimated conservatively at $\times 32$ as shown in Table 5.9.

Table 5.9. Data collection rate of RAPID relative to POWGEN

Parameter	Gain relative to POWGEN
Length (bandwidth)	$\times 2$
Detector coverage	$\times 2$
Vertical divergence	$\times 2$
Horizontal divergence	$\times 2$
Thermal moderator	$\times 2$

A 200 mg sample with simple structure currently requires approximately 6 hours of data collection on POWGEN. This data (at lower resolution) could be collected in 11 minutes on RAPID. A beam delivery system optimized for small samples can be expected to deliver even better performance. Under consideration is a controllable divergence, elliptical guide system.

Table 5.10. Key instrument parameters for RAPID

Source	FTS
Moderator type	300 K de-coupled H ₂ O
Wavelength range	0.5 to 5 Å
Resolution	$\Delta d/d = 0.2\%$
Sample size range (beam size)	1 × 1 mm ² to 1 × 1 cm ²
Moderator—sample distance	35 to 40 m
Sample—detector distance	2–2.5 m
Detector type	³ He linear position sensitive

6. ENABLING TECHNOLOGIES AND REQUIREMENTS

K. W. Herwig (ISD)

A number of technologies and methods support the neutron scattering instruments and enable their science missions. These begin with optimization of the neutron source that illuminates the neutron beam lines and continue through to the neutron detectors and their associated data acquisition systems, data storage, and systems for data reduction and analysis. A number of working groups considered key areas along this path, and summaries of their considerations and recommendations are contained in the following sections.

The **Moderators and Target Optimization** working group considered the optimization in moderator materials and geometry that might be achievable, given the operating characteristics and mission of STS. STS will be a low repetition rate source and will be optimized to provide the highest peak brightness of cold neutrons while providing simultaneous access to the broadest wavelength band.

The **Neutron Optics and Polarization** working group considered recent advances in devices, technology, and techniques that would support the science mission of the neutron scattering instruments. Many of the instrument concepts presented in the previous sections rely on key developments in these areas. The past decade has seen tremendous progress in fundamental technologies. For example, at the start of the SNS project, the highest performing guide coatings available were $m = 3.5$ (3.5 times the performance of natural nickel coatings). Today guides have been manufactured and deployed with $m = 7$, creating the opportunity to deliver neutron beams with higher angular divergence and/or extending the effectiveness of neutron guides to shorter wavelengths. Over the same period, a number of software tools for modeling neutron optics have matured to the point where quite sophisticated beam delivery systems can be designed with a high level of confidence in their ultimate performance. In addition, interest has increased in adapting the very successful polarized neutron scattering techniques available at continuous neutron sources to the more challenging environment of pulsed neutron sources and time-of-flight techniques. In particular, modification of the HFIR cold source guide system represents an opportunity to deploy the technology advances in neutron guides to deliver much higher performance to the current instruments and provide additional end stations to support several of the new instrument concepts outlined previously. A summary of initial concepts and a proposed guide configuration are given in Section 6.4.

The **Larmor Labeling Techniques** working group explored the use of polarized neutron beams to employ the neutron spin itself to encode one component of the neutron's momentum. These spin-precession techniques access the longest time and largest length scales available to neutron scattering methods that are of particular relevance to mesoscale phenomena.

The final section, **Detector Requirements**, considers the key area of neutron detectors. It discusses detector systems currently deployed at ORNL neutron sources and their limitations. Consideration is given to recent developments in alternate technologies, particularly in the use of thin boron films for large area detectors as replacements for ^3He detectors. The detector needs of the instrument concepts presented above are summarized in a table (to the extent that they are known). Recommendations for key developments and the impacted instruments conclude this section.

6.1 MODERATORS AND TARGET OPTIMIZATION

Franz Gallmeier (ISD)

Neutrons provided by the target must be conditioned by moderators before their use in scattering instruments. Tight coupling of the target and moderators has been demonstrated recently at the ISIS Target Station 2 source as an effective means to boost moderator performance. Building on this experience, screening simulations of a compact tungsten target and para-hydrogen moderators (coupled and decoupled) have demonstrated the viability of this concept for a second SNS target station [1]. For configurations with similarly sized viewed areas, STS can provide time integrated and peak brightness gains of factors of 7 and 5, respectively, for coupled hydrogen moderators compared to FTS being fed by the same intensity proton pulse. For decoupled hydrogen moderators, we have shown gains of peak brightness of a factor of 2.5 over the FTS. This concept has been extended to evaluate moderators with reduced viewed areas to increase the neutron phase space density (brightness) available to the neutron scattering instruments. Optimized moderator configurations with viewed areas reduced from $10 \times 10 \text{ cm}^2$ to $2 \times 2 \text{ cm}^2$ showed additional brightness gains of as much as factors of 3 and 2 for coupled and decoupled moderators, respectively, again based on the same proton pulse intensity. On a per proton basis, the peak brightness of STS coupled moderators can be 15 times higher than their FTS counterparts.

While neutronics simulation capabilities have proven to adequately describe and predict moderator performance in the wavelength range of interest for the current generation of scattering instruments, these simulations are based on idealistic simplified target/moderator/reflector configurations, and there is a need to add more engineering realism into the modeling. Also, optimizing the moderators to meet instrument needs rather than toward generic figures-of-merit such as peak cold flux is essential to achieve desired instrument performance gains. Although the demonstrated capabilities of para-hydrogen moderators look attractive, spectral characteristics required by the scattering instruments toward either longer and/or shorter neutron wavelengths may direct us to different moderator materials, such as hydrocarbons or ammonia, and/or to composite moderator assemblies. Solid moderators such as solid methane seem to be ruled out at the envisioned STS power level of $\sim 500 \text{ kW}$; however, there is a renewed interest in pelletized, solid moderators after the pulsed IBR-2 reactor recently demonstrated an implementation in a production facility.[2] The experience at IBR-2 indicates that a pelletized moderator could be a viable option for STS. Grooved versions of alternative moderator materials may be well worth investigating.

All preliminary simulation work has assumed that moderators would be positioned in a wing configuration fed by neutrons from a horizontal target and corresponding horizontal proton injection, as shown in Fig. 6-1.

Moderators positioned in a slab configuration especially suitable for small decoupled moderators may be an alternative to exploit the peak neutron production zone of the target.

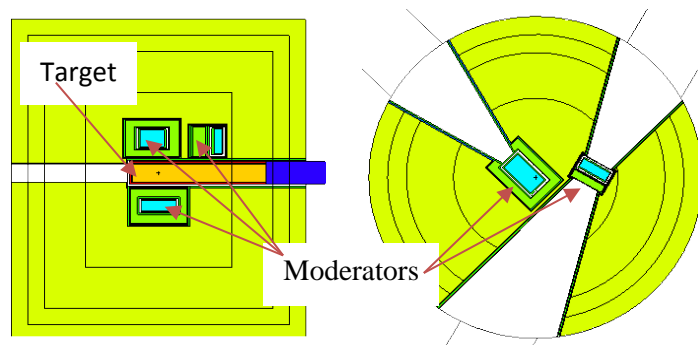


Fig. 6.1. Preliminary moderator/target geometry for STS.

Other moderator concepts that require further modeling and consideration include a Very-Cold Neutron (VCN) source such as that proposed as a complementary neutron source at Argonne National Laboratory (ANL) in 2005.[3] This option could provide higher flux of the long wavelength neutrons above 8 Å required for accessing the largest length scales and slowest dynamics.

Challenges to assess all the moderator options are being discussed. Although para-hydrogen can be produced by including a large volume catalyst into the hydrogen loop—as has been demonstrated at the Japan Proton Accelerator Research Complex (J-PARC) to a proton beam power of 300 kW[4]—it is not yet clear whether this holds to higher powers because of radiation-induced back conversion. This is of particular relevance in considering incorporation of a catalyst into the FTS hydrogen loops; it also is of concern for STS because of the higher proton energy densities per pulse. The development of online ortho-para diagnostics in the hydrogen loop is essential for answering this question.

The impact of engineering reality on the high-brightness moderator concept (small viewed areas) needs to be assessed. This is particularly important for the coupled hydrogen moderator because it has the potential for very large gains and would address the need of SNS to become competitive in the production of long-wavelength neutrons, especially in comparison to the moderator suite at J-PARC as that source matures to its planned power level of 1 MW. Evaluation includes preliminary engineering design as well as thermal hydraulic and neutron performance tests to qualify such a system for construction.

New scattering kernels must be developed to consider alternative moderator materials beyond p-H₂ (except for liquid and solid methane and mesitylene). This is particularly true of the candidate materials proposed for VCNs. These kernels are a necessary precursor to enable concept development and evaluation via Monte Carlo simulations. Of all the moderator concepts under consideration for STS, VCNs have the longest way to go to be qualified as a viable option (not only from the source perspective but also from the neutron scattering instrument point of view). Work must begin immediately if incorporation of a VCN into STS is desired.

Working Group Recommendations

1. Validate by testing high brightness (small viewed area) moderator concepts and develop engineering concepts for those.
2. Initiate kernel development and validation for a select set of new moderator materials.
3. Construct a moderator test facility at SNS to support moderator concept validation efforts.
4. Develop in situ hydrogen ortho-para diagnostics deployable in the hydrogen loops of production facilities.
5. Investigate concepts of VCNs for colder neutron beam production and how these could be implemented in STS.

References

- [1] F. X. Gallmeier. *Moderator Studies for a SNS Short-Pulse Second Target Station*, STS03-31-TR0004-R00, Oak Ridge National Laboratory, Oak Ridge, Tenn., 2013.

- [2] V. D. Anan'ev, et al. "Cold Neutron Moderator on an Upgraded IBR-2 Reactor: The first set of results." *Technical Physics* **59**, 283–286 (2014).
- [3] B. J. Micklich and J. M. Carpenter. *Proceedings of the Workshop on the Applications of a Very Cold Neutron Source*, ANL-05-42, Argonne National Laboratory, Lemont, Ill., 2005.
- [4] H. Tatsumoto, et al. "Operational Characteristics of the J-PARC Cryogenic Hydrogen System for a Spallation Neutron Source." *AIP Conference Proceedings* **1573**, 66 (2014).

6.2 NEUTRON OPTICS AND POLARIZATION

Lee Robertson (ISD)

Introduction

With the development of brighter, more compact neutron sources, one can envision a new class of advanced neutron scattering instruments that employ novel neutron optics systems to deliver the optimum neutron phase space to the sample position and from the sample position to the detectors. The use of polarized neutrons will continue to grow both as a unique probe of magnetic phenomena and in spin precession paradigms such as neutron spin echo. The enabling technologies that must be developed include focusing optics and alignment methodologies, formalisms for optimizing phase space production (moderator design) and transport, production and manipulation of spin polarized beams optimized for neutron time-of-flight applications, and improved Larmor labeling techniques for encoding the neutron energy and momentum transfer. Achieving desired instrument performance gains of a factor of 100 or greater will require co-optimization of moderator characteristics and neutron optical systems and may require instrument designs that deliver a more narrowly defined science capability rather than following a traditional path of compromising the instrument performance to maintain versatility.

Neutron Optics

To meet emerging science challenges, instrument performance gains of a factor of 100 or more relative to similar instruments on current sources are needed. The concept for STS currently under development will provide exceptionally high brilliance beams of cold neutrons that are particularly well suited for the neutron optical and polarization methods that can deliver these types of gains. In nearly every case, a full instrument optimization is necessary that begins with determination of the phase space element (both the volume and density required) that must be delivered by the optical components to support the scientific mission of the instrument. The beam line optics and source/moderator configuration that can best provide the required phase space element can then be defined. Several iterations of instrument optics design coupled to moderator geometries will probably be needed. Each moderator will be shared by multiple beam lines, and it is unlikely that each of them will have exactly the same requirement. Ultimately, a facility wide optimization must be performed that also integrates the physical constraints of the available space. One consequence may be a reduction in the total number of beam lines so that those remaining can be more highly optimized.

The source/moderator concept under development for STS will allow the entrance to the instrument optics to be placed much closer to the moderator, around 60 cm, than is feasible with current designs. This, coupled with the greater moderator brightness, will allow the optics to capture up to 10 times the available phase space as conventional beam lines (a factor of five from starting closer to the source and

a factor of two from the increased source brightness). Of course, not all the phase space density that can be captured should be transported, so various optical components must be employed to tailor the phase space element arriving at the sample to match what is required for the scientific mission of the instrument. These include straight, curved, elliptical, parabolic, ballistic, converging, and other guides; flat and focusing mirrors; curved crystal arrays; choppers; phase space transformers; virtual sources; and others. The high brilliance cold moderators of STS are exactly what is needed to get the most out of these optical components.

Incorporating modern approaches and high performance optical components: An example

Consider optimization of the recently commissioned quasi-Laue diffractometer installed at HFIR optimized for the study of macromolecular crystals, especially protein crystallography. The two main requirements of the beam line optics were the use of focusing optics to focus the beam onto small samples and an adjustable band pass wavelength filter. A crude, six dimensional phase space analysis was carried out to determine the best type of focusing optics; results indicated the best performance would be obtained using a pair of elliptical mirrors (Kirkpatrick-Baez geometry) roughly 2.5 m before the sample position and 10 m from the entrance slit. The mirrors are configured to image the opening in the entrance slit onto the sample position with a demagnification factor of 4 using no guides beyond the entrance slit. The beam is allowed to diverge past the entrance slit to a second slit at the entrance to the elliptical mirrors. The second slit is adjusted to allow through precisely the phase space element that the focusing optics can accept. The overall phase space volume arriving at the entrance to the focusing optics exhibited significant fine structure because of the optics upstream from the entrance to the IMAGINE optics. This structure in the phase space density translates into distortion of the diffraction peaks on the instrument, but the details could not be modeled because they are strongly affected by any misalignments of the upstream optics.

Thus the whole focusing optics assembly was designed so that the entire phase space volume arriving at the entrance slit to the focusing optics could be searched to locate the piece of phase space that gave the best diffraction peak shapes. This successful scheme yielded more than a factor of 2 increase in the flux on the sample over what would be delivered by a conventional setup consisting of a focusing guide covering 12.5 m from the entrance slit to the sample position and a slit in front of the sample, all without the additional distortion of phase space that the guide would introduce. The band pass filter was implemented using pairs of supermirrors with different critical angles that could be translated into the beam but that would introduce minimal phase space distortion. The reflected neutrons from the first mirror in the pair are kept so that this mirror provides the short wavelength cutoff for the bandpass filter and the transmitted neutrons through the second mirror are kept providing the long wavelength cutoff. A diagram of the instrument is shown in Fig. 6.2.

Once the concept for the focusing optics was understood, a model of the beam line was created for Monte-Carlo simulations to optimize the instrument performance. The simulations revealed that a long wavelength tail on the bandpass was leaking through the second mirror in the filter pair because of correlation in the incident angle onto the mirror with the beam divergence. The issue was resolved by adding a second long wavelength cutoff mirror inclined in the opposite direction relative to the beam divergence. This illustrates how these methods complement each other.

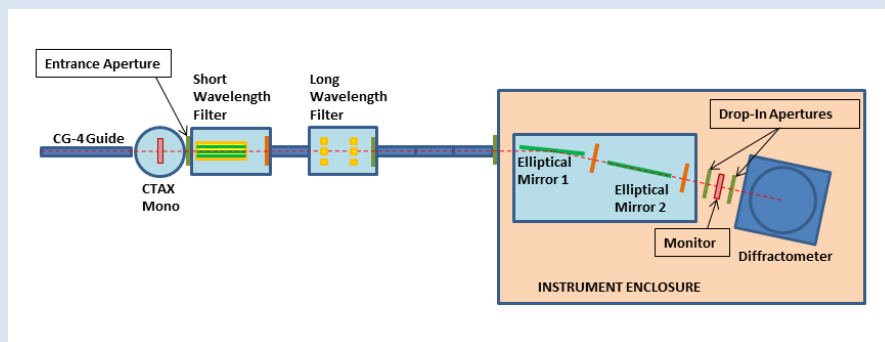


Fig. 6.2. Schematic diagram of the IMAGINE instrument.

The end of the CG-4 guide and the monochromator for the CTAX cold triple-axis instrument are shown, but the IMAGINE optics described here start at the entrance aperture. The beam line incorporates two sets of mirrors up front, the Short Wavelength Filter and the Long Wavelength Filter that together serve as a bandpass filter, and a pair of elliptical mirrors that focus the beam onto the sample position.

As an example of the practical limits to focusing a neutron beam, preliminary calculations show that a set of Kirkpatrick-Baez mirrors in the Montel geometry can produce a beam of only 1 μm (1,000 nm) in diameter with a fluence of 6×10^3 n/s/Å at 6 Å and a beam divergence of 2.0 degrees (horizontal and vertical), given the measured HFIR cold source brightness of 2.5×10^{12} n/cm²/Å/str/s. Theoretical considerations suggest an ultimate limit on the beam focus of ~ 1 nm in diameter given by the wavelength range (2 Å to 40 Å) and the nickel lattice spacing (typical of most neutron mirror materials). A more practical limit for the diameter of the beam focus of ~ 10 nm can be estimated from a 100 nm waviness in the figure of the mirrors. However, a beam focused to 1 μm would open up many new possibilities for studying biological systems, especially when combined with spin polarization analysis to suppress the high background from hydrogen incoherent scattering. It may be possible to achieve higher spatial resolutions with a combination of magnification optics and high spatial-resolution detectors. In some cases parabolic mirrors can be used to yield a very low divergence beam for use with conventional “shadow” camera geometry, but for the highest resolutions, a scheme employing coded apertures or Wolter mirrors will be required. These more sophisticated optics have the added advantage of not requiring that the sample be immediately adjacent to the detector, thus providing a much better configuration for applying polarized imaging techniques.

Finally, the STS pulse rate of 10 Hz means that repetition rate multiplication strategies can be used effectively for direct geometry inelastic spectrometers. The performance of these beam lines can be enhanced by the use of focusing elements that minimize the beam cross section at the various chopper positions, which can dramatically improve the pulse shaping of the individual sub-frames.

State of the Art Neutron Optical Components

There have been many recent advances in neutron optics such as polarizing guides, wide angle ³He polarization filters, broadband radio frequency (RF) spin flippers, Larmor labeling techniques, spin precession in magnetized thin films, Wolter optics, and high m-value supermirrors that will help realize the following required performance gains:

- **Polarizing Guides:** FeCoV/Ti and Fe/Si supermirrors with high reflectivity out to $m = 4.5$ are now available and are designed to reflect only one neutron spin state. These high quality mirrors allow polarizing benders and cavities to be designed to work at much shorter neutron wavelengths and with higher efficiency than was previously possible. The development of these mirrors has greatly expanded the range of instruments that can use polarized neutrons effectively.
- **Wide Angle ³He Polarization Filters:** These devices are used to polarize the neutron beam as well as analyze the polarization of the neutrons scattered by the sample. Recent advances in the laser systems used to optically pump the ³He nuclei have led to much higher transmission of the desired spin state together with better polarization of the neutron beam, making them useful over a wider wavelength band. These filters are the key to implementing full polarization analysis on time-of-flight (TOF) instruments.
- **Broadband RF Flippers:** RF flippers are a class of spin flippers that do not depend on the Larmor frequency of the neutrons (as do Mezei flippers, for example) and, therefore, can be used over large wavelength bands. For this reason, these devices are also the key to implementing full polarization analysis on TOF instruments.

- **Spin Precession in Magnetic Thin Films:** Another strategy for making a wavelength independent spin manipulator (nutator). Magnetized thin films are placed in the polarized beam, and the polarization direction for the beam will be rotated by an amount determined by the angle between the thin film and the neutron beam. These devices will allow us to adjust the polarization of broad bandwidth (TOF) polarized neutron beams between instrument components.
- **Larmor Labeling Techniques:** Traditional neutron scattering techniques generally require significant tradeoffs between flux and resolution, but Larmor labeling techniques (NSE, neutron resonance spin echo [NRSE], modulation of intensity emerging with zero-effort [MIEZE], spin echo resolved grazing incidence scattering [SERGIS]) offer the possibility of both high intensity and high resolution at the same time under certain conditions.
- **Wolter Optics:** A novel concept for focusing neutron optics inspired by successful use in x-ray astronomy. These devices are based on axisymmetric grazing-incidence focusing mirrors that have the potential to turn pinhole-camera-like neutron instruments into much more powerful microscopes and will have several applications for future neutron scattering instruments.
- **High Critical Angle Supermirrors:** Recent advances in neutron supermirrors are making mirrors with m-values greater than eight feasible. These new supermirrors allow greater flexibility in the volume of phase space that can be accepted by the beam line optics as well as extend the range of magnification and demagnification possible with focusing mirrors made with these coatings.

Polarized Neutrons

There are several methods for polarizing the neutron beam by filtering out one of the two spin states. The oldest is diffraction from ferromagnetic and certain antiferromagnetic (usually Heussler alloys) crystals where only one spin state is diffracted. This method is useful with monochromatic beams of both cold and thermal neutrons. Next was the development of polarizing supermirrors that only reflect one spin state and are extremely efficient broadband spin filters for cold neutrons. Their main disadvantage is that they cannot accommodate a very large beam divergence and are thus difficult to employ in wide angle scattering applications. The neutron polarization as a function of critical angle of the polarizing FeSi supermirror is shown in Fig. 6.3. At almost the same time polarized ^3He spin filters were developed that operate by absorbing one spin state and transmitting the other. They are very good at filtering large, divergent beams but require considerably more development to function efficiently over a wide wavelength band; hence, they are complementary to supermirror polarizers. Recent progress has been made in the use of sextapole magnets to deflect one spin state out of the beam. This method is also highly efficient at polarizing the beam but is only practical for very long wavelength neutrons and thus has limited applicability. Of these methods, both supermirror polarizers and ^3He spin filters will be widely used at STS.

Considerable development will be necessary because the components and techniques developed for manipulating polarized neutron beams at continuous neutron sources cannot, in general, be transferred directly to time-of-flight applications at pulsed sources. Indeed, most of the polarized neutron techniques presently available cover only a very limited wavelength band or even require monochromatic neutron beams. Such techniques and components include flippers, nutators, precession coils, and Larmor labeling.

A good example of the type of development needed is the use of focusing optics to improve the performance of a time-of-flight spin echo spectrometer. For traditional NSE, NRSE, and MIEZE, the resolution of the measured time correlation function is limited by the beam divergence because the various path lengths lead to a smearing of the path integral. However, the beam divergence can be decreased through the spin echo coils by the use of parabolic or elliptical mirrors (at the expense of expanding the beam and increasing the size of the magnet) and then re-focused on both the sample and detector. Spin echo techniques are well suited for working in the mesoscale regime, where much of the emerging science is found.

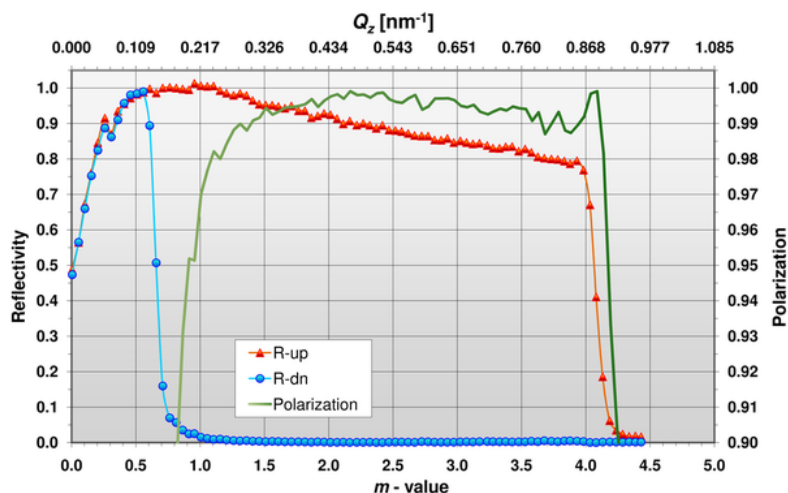


Fig. 6.3. Spin dependent reflectivity and polarization from an Fe/Si polarizing supermirror $m = 4$.

The blue line is the reflectivity for the unwanted spin state, the red line is the reflectivity for the desired spin state, and the green is the polarization of the reflected neutrons (note the expanded scale for the polarization). Both spin states are reflected below $m \sim 0.7$, and the polarization is given by $\text{Polarization} = [\text{Rup} - \text{Rdown}] / [\text{Rup} + \text{Rdown}]$. (Source: Swiss Neutronics website, <http://www.swissneutronics.ch>.)

Finally, the cold, high brilliance beams produced by STS are ideal for implementing 3D polarimetry applications where all components of the scattered polarization vector are measured in turn for three different directions of the incoming polarization vector. Determining the relationship between the directions of incident and scattered polarizations gives access to the 16 independent correlation functions involved in the most general nuclear and magnetic scattering process. In general, this allows determination of the direction of the magnetic interaction vectors of magnetic structures.

Working Group Recommendations and Observations

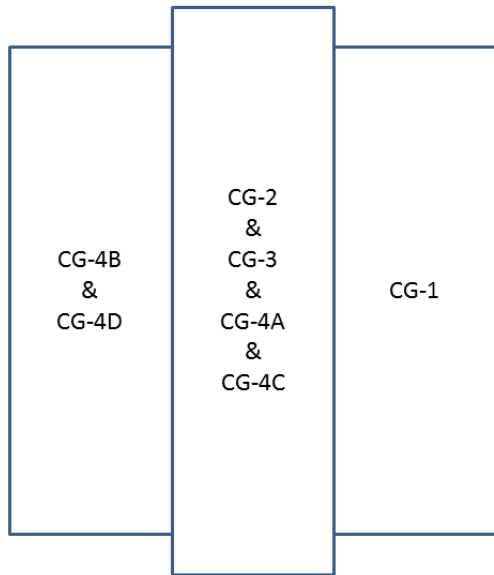
1. Initiate development of select STS instrument concepts by defining the required phase space element that must be delivered by the instrument optical components. Follow this by exploring the combination of moderator geometry, beam line optics, and engineering reality that best provides the required phase space element. This process must begin early because the instrument needs to play a significant role in the moderator/target configuration.
2. To obtain desired performance gains in targeted science capabilities, it may be necessary to trade flexibility for more optimized instrument designs. See Section 3.8, FLOODS instrument, as an example of this philosophy change.
3. There is an urgent need to develop components and techniques for manipulating polarized neutron beams that are optimized for time-of-flight neutron scattering instruments to enable effective and routine use of polarized neutrons.

- (a) Critical expertise in these areas exists outside of ORNL and outside of the United States. Collaboration with other leading neutron scattering centers and key university partners is likely to be critical to ultimate success. Establishing robust collaborations needs to be a priority.
 - (b) Access to a cold neutron beam line where components and devices can be assembled and tested as an integrated system is necessary before precious beam time is allocated on instruments that are currently in the user program. The most cost effective way to provide this is to invest in a modest test and development station on the CG-4 guide located on the HFIR cold source. Although full testing will be restricted because of the constant wavelength nature of the neutron beam, entire systems can be built up, including incident and scattered beam optics and the integrated sample environment apparatus.
4. Develop methodology for designing instrument concepts that take optimal advantage of the increased brightness of the STS moderators and for “complete” instrument optimizations that include the beam line optics, source/moderator, and secondary flight paths in the performance metric.

6.3 NEW GUIDE CONCEPT HFIR HB-4 COLD SOURCE

Lee Robertson (ISD)

Significant advancements in neutron guide technology combined with serious manufacturing defects in the current CG-4 guide leading to poor performance of that guide have prompted a new look at the



HB-4 guide system at HFIR. The current design suffers from compromises in the neutron optics that were necessary to achieve the required separation between guides, given the limited critical angles of the supermirrors available at that time. Most notably, the guides begin much too far from the cold source, and the two outer guides, CG-1 and CG-4, are over focused in the sense that they do not view the center of the HB-4 cold source. The distance between the cold source and the entrance to the guide system means that the guides are severely under illuminated, even at relatively short wavelengths; the over focusing results in a large asymmetry in the phase space element transported by these two guides, which in turn compromises the performance of the instruments they serve. The new design must address these issues as well as take advantage of the latest developments in neutron optics and beam transport.

Fig. 6.4. Entrance configuration of the new guide design proposed for the HFIR cold source.

The concept we are developing incorporates the availability of higher index supermirror guides, up to $m = 8$, and builds upon the recent successful redesigns of the H1 and H5 guide systems at ILL and the new Cryogenic Tube West (CTW) guide system at NIST. The results described here represent only a feasibility analysis of a guide configuration based on the recent work at ILL and NIST. A Monte Carlo

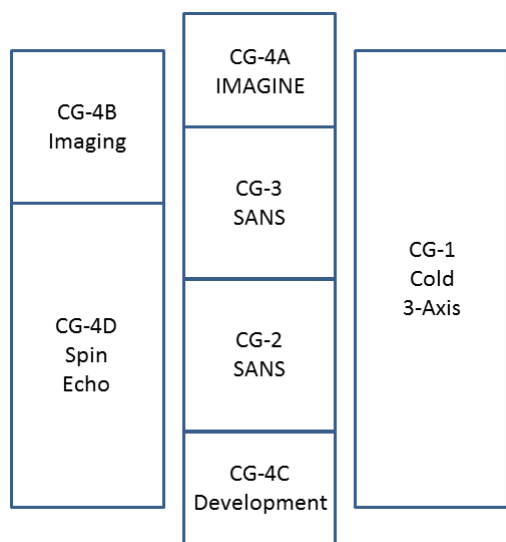


Fig. 6.5. Configuration of the new guide design proposed for the HFIR cold source at 5.2 m from the source.

The guide system begins 1.4 m closer to the cold source (2.4 m closer if the monolithic guide replacing the beam tube collimator is included). An overall layout of the guide system is shown in Fig. 6.6.

The geometry of the CG-1 guide remains largely unchanged and retains the same radius of curvature (472.7 m) and location of the guide terminus. The width of the guide is now 40 mm, and the height is 120 mm over the entire length with no septa. The guide index is 4.5, and the neutron flux at the guide exit is 9.7×10^9 n/cm²/s, compared with 4.2×10^9 n/cm²/s from an equivalent simulation of the current CG-1 configuration. If a triple-axis instrument is built on CG-1, a more complicated geometry will be used, possibly incorporating an elliptical focus and a virtual source. CG-2 and CG-3 also remain largely unchanged and benefit primarily from the guide entrance being closer to the cold source. The guide cross-sections are 40 × 40 mm, and the supermirror index is $m = 1$ for the guide and $m = 3.5$ for the deflection mirror on CG-2 and $m = 4.5$ for the two deflection mirrors on CG-3. The index of the deflection mirrors has been increased to give better performance for wavelengths below 6 Å. The neutron flux at the end of the guide (just before the velocity selector) is 5.1×10^9 n/cm²/s for CG-2 and 4.6×10^9 n/cm²/s for CG-3. The simulated fluxes for the current guides are 1.1×10^9 n/cm²/s for CG-2 and 8.4×10^8 n/cm²/s for CG-3. More detailed calculations are required to understand how these flux gains directly impact instrument performance under different collimation (resolution) requirements.

We envision that the new configuration for the CG-4 guide will have four end stations and no side ports. The same guide designations are retained, although there are more than four guides in the new guide system and CG-4A and CG-4C actually start out as part of the same guide assembly as CG-2 and CG-3 (see Figs. 6.4 and 6.5). For this study, the IMAGINE instrument currently located at the end of the CG-4 guide is moved up to the front of the Cold Neutron Guide Hall, and its optics are fed directly from the source without using a guide as shown in Fig. 6.6. The entrance to the beam line optics is 8.6 m from the cold source, and the simulated flux is 1.1×10^9 n/cm²/s compared with the simulated flux of 2×10^9 n/cm²/s at the end of the current CG-4 guide. It appears that the flux is lower, but the phase space distribution of the flux is much more favorable for the focusing optics employed on the IMAGINE beam line, so a substantial gain in useful flux is anticipated. The CG-4B guide is crudely configured to supply neutrons to a new imaging station. Much like the CG-2 and CG-3 guides, it uses a supermirror

simulation of triple axis spectrometers (McStas) simulation was carried out to determine the neutron flux and spectrum supplied to the end station of each neutron guide. In the case of CG-4A, where no guide is required, the flux is reported at the entrance to the instrument optical system. For the simulation of the new HB-4 guide system, the collimator in the HB-4 beam tube is removed. A new monolithic guide section with a metallic substrate and a single penetration is envisioned for the new guide system, but this space was left empty for the feasibility study simulations. A compound guide assembly extends from 3.8 m to 5.2 m from the face of the cold source. A cross-section of the guide assembly at the entrance is shown in Fig. 6.4, and all supermirrors' surfaces have an index of $m = 4$. A second compound guide assembly begins at 5.2 m and completes the final division of the guide cross-sections as shown in Fig. 6.5. This arrangement allows all the guides to view the center of the HB-4 cold source, and the entrance to the

guide with an index of $m = 3$ out to a deflecting mirror with an index of $m = 5$, followed by a deflecting mirror with an index of $m = 5$ at 12.8 m from the cold source and then a 12 m section of straight guide with an index of $m = 3$ and a 40×40 mm cross-section that continues on to the instrument. The simulated flux for this configuration is 1.8×10^9 n/cm²/s. The CG-4C guide is planned to feed a development beam line. It is much like the current CG-4 guide with a larger radius of curvature (78.9 m), a higher supermirror index of $m = 4$, and a cross-section of 40 mm wide by 30 mm tall, but with no septa dividing the guide vertically. The simulated flux for this guide is 2.3×10^9 n/cm²/s. Finally, the CG-4D guide is for a planned spin echo spectrometer. Again this guide is similar to the current CG-4 guide with a radius of curvature of 126 m, a supermirror index of $m = 3.5$, a cross-section of 40 mm wide by 80 mm tall, and no septa. The simulated flux for this guide is 5.9×10^9 n/cm²/s.

It should be noted that this is just a feasibility study, and no attempt was made to optimize the guide configurations. Further efforts require a determination of the optimum phase space volume that each instrument requires. After that the new guide system as a whole must be optimized to transport the desired phase space volumes as efficiently as possible.

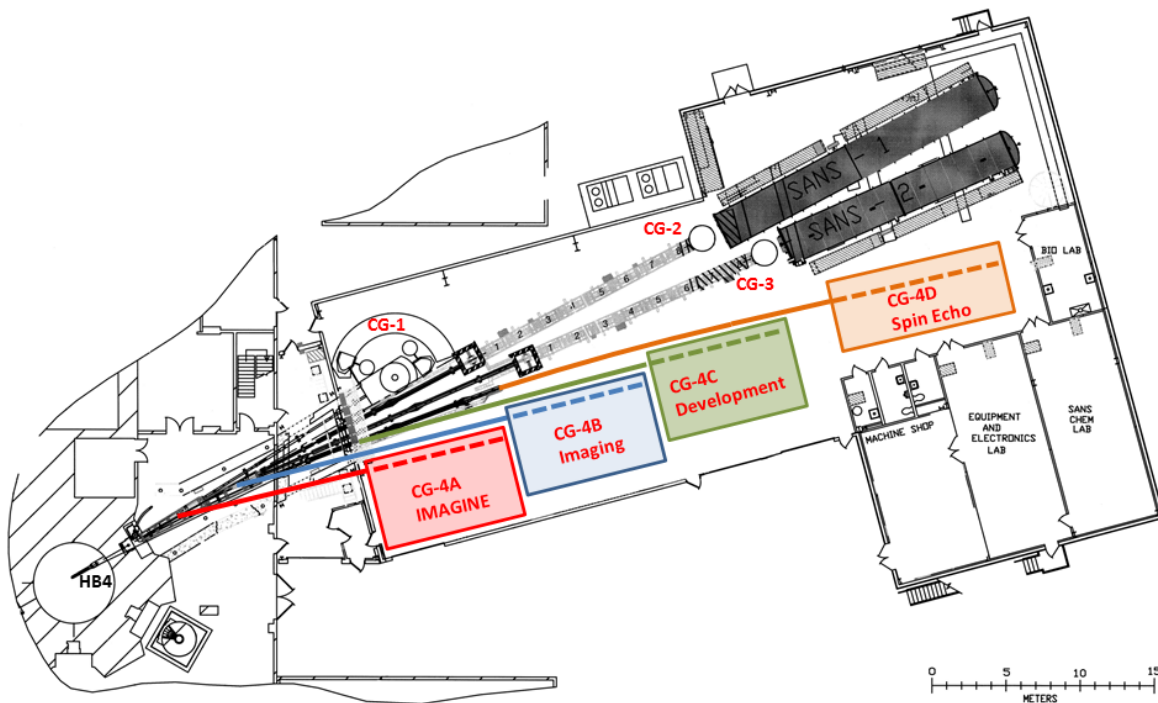


Fig. 6.6. Overall layout of the proposed new guide system with possible instrument selections indicated.

6.4 LARMOR LABELING TECHNIQUES

Roger Pynn (Indiana University) and Bill Hamilton (ISD)

Larmor labeling is a technique in which one component of the neutron's momentum is encoded into the neutron's spin state. This can be done in two ways. The most straightforward is to allow neutrons to propagate through a magnetic field within which they undergo Larmor precession. The Larmor phase that is generated in this way depends on the neutron's residence time in the magnetic field and hence on its speed and direction of travel relative to the field borders. A second method of labeling relies on Ramsey's separated field technique.[1–3] In this method, two RF pi-flippers separated by a zero-field

region produce the same effect as Larmor precession in a magnetic field. In this case, however, instead of the precession of the neutron spin in a magnetic field acting like the second hand of a “clock” that measures the neutron’s time in the field, the RF fields themselves rotate. Because all of the fields rotate in phase with each other, a neutron’s speed can be determined from the RF phases at the instant that the neutron passes each of two RF flippers separated by a known distance. In this case, the RF fields themselves become the clocks that measure each neutron’s speed. Both methods have been implemented, mainly in Europe.

In most cases (Larmor diffraction is the exception), Larmor labeling is used in conjunction with the NSE method. In this technique, the Larmor phase for each neutron is the same before and after the sample if the sample does not affect the Larmor-labeled momentum component. In this situation, the full neutron polarization is retrieved at the detector, and spin echo is achieved in exactly the same way as originally described by Hahn for nuclear spins in a solid.[4] Any change in the Larmor-labeled momentum causes a decrease in the echo polarization that can be related to the scattering properties of the sample. The real advantage of Larmor labeling techniques is that they break the dependence of the resolution (energy or momentum) of a neutron measurement on the degree of monochromatization or collimation of the neutron beam. They thus allow for a significant increase in neutron intensity relative to conventional methods while preserving high resolution. Because all of the NSE methods produce data that is effectively the Fourier transform of the scattering function along some trajectory in (Q,E) space, they may provide information that is more or less useful than conventional methods, depending on the properties of the transform and the exact measurement being performed. Because it uses resonant RF flippers, the technique based on the Ramsey method is known as NRSE rather than simply NSE.

The first instrument built to exploit Larmor labeling and the NSE technique (and still the most common use) was designed to measure the intermediate scattering function, $I(Q,t)$, for quasielastic scattering. An instrument of this type is in operation at the SNS FTS. Even though the use of a pulsed source allows the instrument to collect more information about the Q dependence of $I(Q,t)$ than an equivalent instrument at a reactor source, there are several reasons for preferring to site such an instrument at either STS or HFIR. The spin echo time that can be accessed—the “t” in $I(Q,t)$ —scales as the cube of the neutron wavelength, putting a premium on the use of the longest possible wavelength neutrons, which are produced copiously by a reactor-based cold source such as HFIR. Very relaxed monochromatization is required for this method, so a velocity selector with a 10% bandwidth at HFIR or a relatively long pulse from a fully coupled cold moderator at STS are preferred. Although at least one instrument has been built (at Laboratoire Léon Brillouin [LLB]) to exploit NRSE for measurement of $I(Q,t)$, this method has not shown itself to be superior to traditional NSE for measurement of quasielastic scattering.

A possible exception, yet to be fully explored, is the so-called MIEZE technique that uses the fact that NRSE flippers change the energies of the neutron spin components passing through them. In a conventional NSE flipper pair of either static or NRSE type, the phase or time delay initiated at the first flipper is stopped in the second. Interaction of the delayed components with a sample beyond this flipper pair must then be analyzed by a second matched flipper pair. A MIEZE spectrometer uses only one pair of flippers, with the second of the pair changing component energies by more than the first. This means that the phase difference between components continues to change—now decreasing beyond the pair and coming back into phase at a particular position downstream. This re-phasing occurs over a limited spatial region, but if the beam passes through an analyzer located after the second flipper, it can be detected by a detector with sufficiently good depth resolution. One significant advantage of this approach is that no beam handling components are required and no magnetic conditions need be maintained in the secondary arm (downstream of the analyzer and including the

sample) of the spectrometer. All of the information in a MIEZE beam is encoded before its interaction with the sample—potentially allowing much greater flexibility in environmental conditions than can be achieved with more conventional NSE techniques.

In the last 15 years, the NSE method has been used with magnetic fields whose borders are inclined with respect to the neutron beam to implement two techniques for measuring elastic scattering, SESANS and SERGIS. SESANS is used to measure bulk samples, while SERGIS is used to interrogate diffuse scattering from surfaces and interfaces. In both cases, the range of distances probed can span from ~25 nm to as much as 25 μm , significantly extending the range accessible to conventional scattering methods. SESANS has shown itself to be useful in probing scattering from strongly scattering samples because it automatically accounts for the effects of multiple scattering, which severely complicates data analysis for conventional SANS. The spin echo length probed by both SESANS and SERGIS scales as neutron wavelength squared. Early on in the development of these methods, it was thought that a large wavelength bandwidth would be beneficial because it would allow simultaneous probing of the sample over a large range of distance scales. However, it has become apparent that this is not the full story, and a narrower band width (0.2 nm to 0.8 nm, for example) is probably more useful because it provides results with comparable error bars over the entire measurement range.

Detailed McStas [5,6] calculations are probably needed to determine which of the three ORNL sources would provide optimal performance. Currently, the ISIS facility at the Rutherford Appleton Laboratory is building an instrument at its second target station (called Larmor) that will combine capabilities for SANS and SESANS on the same instrument. This seems like a good idea because it will allow both $S(Q)$ and its Fourier transform to be measured on the same sample, revealing different types of information about structural correlations. This development will need to be followed closely before a final decision is made about a user instrument for SESANS at ORNL. So far, there is only one instrument in the world—Offspec at ISIS—that has implemented SERGIS, but this technique has not yet found key areas of science where it can make unique contributions. It will be important for ORNL to gain experience with both the SESANS and SERGIS techniques using a test beam line before a dedicated user instrument is built at any source.

Unlike the techniques described so far, Larmor diffraction does not use the NSE method but rather relies on the fact that all neutrons that are Bragg scattered with the same set of Miller indices undergo the same momentum transfer. It is this momentum transfer that is encoded into the Larmor phase of neutrons in the case of Larmor diffraction. Once again, the Larmor encoding ensures that the accuracy of the measurement is not connected to the level of monochromatization and collimation of the neutron beam, which traditionally specifies the accuracy of diffraction measurements. In most Larmor diffraction experiments, the measurement involves detecting small changes in lattice parameter rather than accurate absolute values. This can be done with greater precision than can be achieved by the best x-ray instrumentation at synchrotron sources. The relative precision of the measurement in the case of Larmor diffraction is $\Delta d/d \sim 10^{-6}$, whereas high resolution x-ray powder diffraction typically achieves a value of about 10^{-4} . [7] Because the magnetic field boundaries have to be parallel to the diffracting planes to ensure the best results, Larmor diffraction can only measure Bragg peaks at a single scattering angle, almost certainly implying that such an instrument should be built at a –continuous source. Consideration could be given to installing Larmor diffraction as an “add-on” capability on a traditional diffraction instrument.

Working Group Recommendations

1. Perform detailed Monte Carlo simulations (McStas) of SESANS and SERGIS instruments as envisioned for each of the three ORNL neutron sources to determine which provides optimal performance.
2. Monitor the development and scientific impact of the ISIS Larmor instrument to evaluate the need for such an instrument at the ORNL neutron sources.
3. Develop a test beam line at the ORNL neutron sources that will enable ORNL staff to gain experience with implementing SESANS and SERGIS before a dedicated user instrument is built.
4. Ultra-high precision measurement of diffraction peaks is almost certainly best enabled at the continuous, HFIR neutron source.

References

- [1] N. F. Ramsey, "A New Molecular Beam Resonance Method," *Phys. Rev.* **76** (1949), 996.
- [2] N. F. Ramsey, "A Molecular Beam Resonance Method with Separated Oscillating Fields," *Phys. Rev.* **78** (1950), 695.
- [3] N. F. Ramsey, "Experiments with separated oscillatory fields and hydrogen masers," *Reviews of Modern Physics* **62** (1990), 541–552.
- [4] E. L. Hahn, "Spin echoes," *Physical Review* **80** (1950), 580.
- [5] K. Lefmann and K. Nielsen, "McStas, a general software package for neutron ray-tracing simulations," *Neutron News* **10** (1999), 20–23.
- [6] P. Willendrup, E. Farhi, and K. Lefmann, "McStas 1.7—a new version of the flexible Monte Carlo neutron scattering package," *Physica B: Condensed Matter* **350** (2004), E735–E737.
- [7] http://www.icdd.com/resources/axa/Vol52/v52_26.pdf.

6.5 DETECTOR REQUIREMENTS

Rick Riedel (ISD)

Abstract

The SNS second target station will complement the first target station by operating at 10 Hz rather than 60 Hz, providing a larger band width than FTS and by providing neutron beams with higher peak brightness. The higher peak brightness (as great as $\times 17$ relative to the coupled moderators on a 2 MW FTS at a neutron wavelength of 2 Å) will challenge or exceed the limits of current SNS detector and electronics technologies. A summary of current detector technologies used at SNS is followed by an estimation of STS neutron scattering instrument needs that identifies critical capability gaps. This section concludes with a set of recommendations regarding development of neutron detectors and associated electronics.

First Target Station Detectors

Instruments at FTS use one of four detector technologies: (1) linear position sensitive ^3He tubes, (2) multi-wire ^3He gas chamber, (3) Li-glass scintillator based Anger camera, and (4) LiF/ZnS wavelength shifting fiber detector. These are described below and followed by a summary of the relevant performance parameters in Table 6.1.

Table 6.1. FTS detector parameters

Technology	Resolution	Efficiency @ 2 Å	Local rate counts/cm ² /s	Full detector rate counts/s	Gamma ^a sensitivity	Magnetic field sensitivity
LPSD	5–25 mm	80–90%	10K–20K	100K	10^{-7} – 10^{-8}	None
Multi-wire	1.5–2 mm	70%	20K	20K	10^{-7} – 10^{-8}	None
Anger camera	1.2 mm	80–90%	40K	40K	10^{-5} – 10^{-6}	requires < 25 g
Wavelength shifting fiber	5 mm x 5 cm	50%	10K	10K	10^{-6} – 10^{-8}	requires < 100 g

^aGamma sensitivity is defined as the fraction of Boron energy gammas reported as counts by the detector system.

1. Linear position sensitive ^3He tubes. This detector is typically assembled into an array of individual cylindrical tubes (see Fig. 6.7) of a specific diameter (5–25 mm) and of a wide variety of lengths from 15 cm to over 300 cm. At the axis of the cylindrical steel tube is a resistive wire. When a high voltage difference is applied between the cylindrical outer wall and the center wire, amplification of the daughter products from the $^3\text{He} + n$ interaction occurs. The initially produced 40,000 electrons are amplified 10 to 100 times (close to 1 pC of charge) depending upon the high voltage applied. Higher bias voltage results in higher spatial resolution but has an associated sacrifice in the maximum count rate the tube can achieve. Assembled into an 8 detector unit (8-pack) with an associated electronics package is an ORNL (SNS) developed detector technology now licensed to GE-Reuter Stokes. Spatial resolution along the length of the tubes typically ranges from 5 mm to 25 mm with single tube count rates from 10,000 to 40,000 counts/s depending on the value of the bias voltage. Efficiency is typically > 90% at a neutron wavelength of 2 Å.
2. Multi-wire ^3He gas chamber (Fig. 6.8). This detector is similar to the cylindrical tube linear position sensitive detector (LPSD) because ^3He gas is used as the active medium for neutron detection. However, higher spatial resolution is obtained using a single chamber with multiple anode wires that are typically spaced closer than the distance between individual tube detectors. The distance between anode and cathode largely determines the count rate, which is reduced if interpolation is used to determine position (generally requiring higher gas gain). Resolutions are 1.2–2 mm, while rates vary from 50,000 counts/s (10% dead time) to 500,000 counts/s (with an amplifier per wire; i.e., MILAND). Efficiency is typically 80% at 2 Å.
3. Anger camera (Fig. 6.9). This detector is one of two scintillator based neutron detectors at SNS. The $^6\text{Li} + n$ reaction creates a scintillation flash in the glass of the order of 50 ns in length. The performance of the detector is determined to a large degree by the light output of the scintillation flash. Positional information is determined by interpolation of the light signals from multiple light sensitive elements of a photomultiplier tube. Spatial resolution of the current

modules is 1.2 mm with counts rates limited to 40,000 counts/s because of limitations in the electronic firmware. In principle, the fast scintillation of this detector should enable count rates of 10^6 counts/s. Efficiency is $> 80\%$ at 2 \AA . Gamma rejection is between 10^{-5} and 10^{-6} as determined for a ^{137}Ce source that produces gammas having a similar energy to those produced by boron neutron adsorption. This gamma energy is observed frequently at the neutron beam lines because of the high use of boron as neutron shielding.

4. LiF/ZnS scintillator wavelength shifting fiber detector (Fig. 6.10). This detector uses wavelength shifting fibers to capture scintillation light from the scintillator screen and transport the light to multiple photomultiplier tubes. An encoding scheme determines the position of the encoded event. Because the method does not use interpolation to determine position, the resolution is largely determined by the spacing of the wavelength shifting fibers. The current resolution is on the order of $5 \text{ mm} \times 5 \text{ cm}$. The active area of the detector unit is large, $1/3 \text{ m}^2$. Gamma rejection is very good, $< 10^{-7}$, due to pulse shape discrimination. However, efficiency is lower than the other detector types being on the order of 50% at 2 \AA . The count rate is limited by use of a slow scintillator to $10,000$ counts/s. Large uniformity variations would preclude its use in a single crystal instrument.

Potential Recent Technologies Demonstrated and Under Development

A number of new neutron detector technologies are under development. Of concern for the international neutron scattering community is the shortage of ^3He , and several of the technologies listed below address this, particularly for fabrication of large area detector arrays ($\sim 10\text{s of m}^2$) that require large volumes of ^3He (e.g., a 20 m^2 array of 2 cm diameter, 2 m long, 8-atmosphere ^3He tubes requires $2,515 \text{ STP l of } ^3\text{He}$). Boron-lined straw tubes and various scintillator technologies including the wavelength shifting fiber described above are likely solutions to this problem. ORNL holds in reserve sufficient ^3He to fabricate a number of large area detector arrays for critical applications such as inelastic scattering, which requires high stability detectors with very low intrinsic background and low gamma sensitivity. It is anticipated that this reserve will meet the needs of FTS and HFIR and also be sufficient for the initial instrument suite of STS. Table 6.2 summarizes the performance parameters of these detector types.

1. Boron-lined straw tubes. These are similar in appearance to LPSD tubes. Rather than ^3He , a $1\text{--}2 \text{ }\mu\text{m}$ layer of B_4C (enriched in ^{10}B) is used as a convertor material, with P10 as an amplification gas. The performance of the tubes is similar to ^3He apart from neutron counting efficiency,

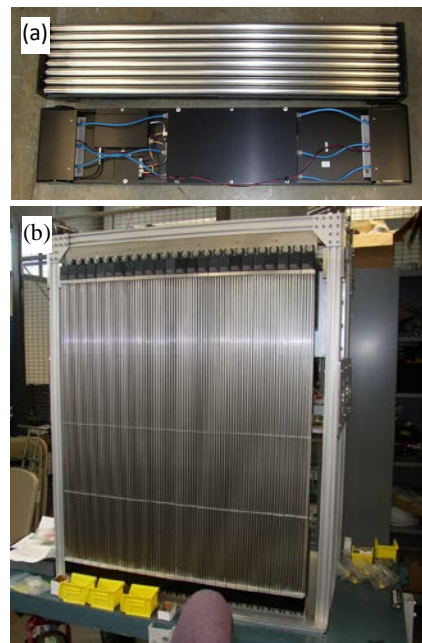


Fig. 6.7. ^3He detector arrays; (a) is a standard 8-pack showing the associated electronics package, and (b) is an assembled array of 8-pack modules.

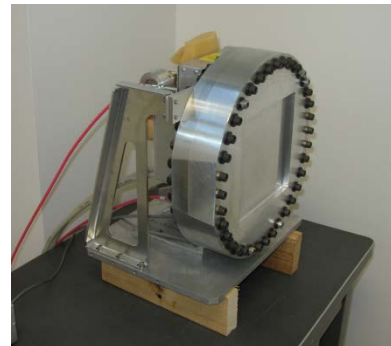


Fig. 6.8. Multi-wire ^3He gas detector.

which is limited because of restrictions on the B₄C layer thickness. To achieve higher efficiencies, numerous tubes must be placed in multiple layers. The effect of secondary scattering from such an arrangement is yet to be determined

2. Pixelated ionization mode ³He detector. This detector is similar in external appearance to the multi-wire chamber in Fig. 6.8. However the internal components are different. Because it has zero gas gain, it is a very high rate detector: > 1 M counts/s over the detector area. Spatial resolution is sacrificed to achieve this high rate. Current spatial resolution is 5 mm × 5 mm.



Fig. 6.9. Anger camera.

3. High anode count wavelength shifting fiber detector. This configuration is an improvement in the current wavelength shifting fiber technology that is achieved by use of multi-anode photomultiplier tubes (PMTs) rather than individual PMTs. More PMT elements enables a different encoding scheme, allowing much greater resolution in the y-dimension, and removes artifacts associated with the original positional encoding scheme. This detector's resolution will be approximately 5 mm × 5 mm.

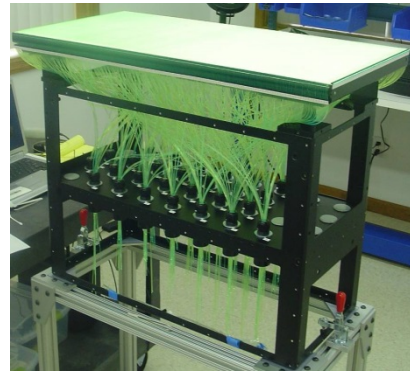


Fig. 6.10. Wavelength shifting fiber detector.

4. MILAND and Bidim multi-wire chambers (amplifier per wire). These are ³He gas proportional chambers with an internal architecture designed to increase the speed of the detector. Relatively high count rates are achieved by decreasing the ion drift distance and by using individual amplifiers per wire. Resolutions also are improved using this technique. For both the Bidim and MILAND detectors, the improvements come by adding a significant number of additional amplifiers and feed-throughs into the gas volume. Typical counting rates are 200K counts/s for the Bidim with a 2 mm × 2 mm resolution, while MILAND has a count rate of 0.5M counts/s with a resolution of 1.2 mm × 1.2 mm.

Table 6.2. New technology detector parameters

Technology	Resolution	Efficiency @ 2Å	Local Rate counts/cm ² /sec	Full Detector Ratecounts/sec	Gamma Sensitivity	Magnetic Field Sensitivity
Boron tubes	5 mm	20%	40K	500K	10 ⁻⁷ -10 ⁻⁸	None
Ionization mode	5 mm	70%	200K	1,000K	10 ⁻⁷ -10 ⁻⁸	None
Wavelength shifting fiber	5 mm	50%	10K	10K	10 ⁻⁶ -10 ⁻⁷	< 100 g
MILAND	1.2 mm	60%	100K	500K	10 ⁻⁷ -10 ⁻⁸	None

Second Target Station Parameters

The second SNS target station will be optimized for the production of cold neutrons with high peak brightness ~10–30 times greater than the current FTS. This increase in peak flux will increase the rate requirements of most detectors installed at STS by close to an order of magnitude over similar instruments located at FTS. Some instrument concepts currently under consideration for STS will exploit the high peak flux to either improve experimental resolution or examine smaller samples, lowering the detector count rate. However, when possible, these instrument concepts will likely retain the capability to operate at lower resolution or examine larger samples as well. At this stage of instrument specification, it is best to take the more conservative approach in identifying detector requirements. Many instrument concepts benefit from increased solid angle detector coverage, so seeking ways to minimize per-unit detector cost remains a consideration.

Limitations of Current Neutron Detectors

Four major limitations contribute to the need for better detectors for pulsed sources: (1) lack of high spatial resolution detectors that can be used with time-of-flight techniques; (2) detector count rate limitations; (3) lack of a magnetic field insensitive Anger camera; and (4) lack of a high brightness, high speed, low gamma sensitivity scintillator. Optimal use of FTS and STS requires the use of neutron time-of-flight techniques, and this restricts the useful detectors to those that can provide event-by-event time stamping. High-spatial-resolution detectors, such as charge-coupled device detectors and image plates that are successfully used at reactors, are integrating detectors that do not preserve sufficient timing information necessary for time-of-flight applications. Pulsed-source instruments must have a count rate capability sufficient to use the high peak instantaneous flux, which can be much higher than that found in monochromatic reactor-produced neutron beams. The FTS liquids and magnetism reflectometers are currently using detectors that are unable to meet the maximum count rates that could be employed by the instruments, requiring the routine use of attenuators or excessively narrowed neutron beams. This situation is anticipated to be even more extreme at STS for the instruments M-STAR, TLR, and mmLR. Other instruments will suffer from detector count rate limitations for at least some types of science. Medium resolution (1.0 mm) scintillator-based detectors currently have gamma-ray sensitivities $\sim 10^{-4}$, while ZnS/LiF wide area detectors have poor resolution and low count rate capabilities. Improvements in basic properties in available large area scintillators would significantly improve inelastic scattering experiments that probe the weak intensities from excitations (phonons, spin excitations, rotation, and diffusion in polymers and molecular substances, etc.) in condensed matter. Improving spatial resolution from the current state of the art ~ 1 mm to $50 \mu\text{m}$ would greatly benefit radiography, tomography, phase contrast imaging, and holography.

There are three broad areas of scientific investigation that are lacking an appropriate detector match from the current available suite of detectors:

1. Powder diffraction and crystallography applications, for example, are important innovative avenues of research in our pursuit of new superior materials and understanding of human diseases such as Alzheimer's or AIDS. New first generation scintillator-based detector technology has successfully been developed to address the ^3He shortage for a small number of instrument types and has been deployed on a modest scale at SNS. Improving the resolution by developing brighter scintillators is needed to enable new science at the single crystal and powder diffractometer beam lines.

2. Neutron reflectometry is used successfully to study nanostructures at surfaces and interfaces using existing ^3He -based detectors. The small amount of ^3He required to fulfill these requirements suggests continuing the development of ^3He based detector technologies for high rate and high dynamic range required for such applications. Detectors with such features will enable performing 3D (or complete reflectometry) experiments on nanosystems. Complete reflectometry includes TOF reflectometry, off-specular scattering, and GI-SANS geometry in “one shot.”
3. Detector technology to meet requirements for neutron imaging (tomography) will be critical in supporting materials and energy research. These detectors will require high position (micron) and timing (sub microsecond) to reach accurate combined 2D mapping from all the scattering and reaction processes occurring in a sample. The spatial and temporal resolutions of the detection system are the critical parameters defining the accuracy of neutron transmission spectroscopic measurements. No present detection system meets these specifications.

Second Target Station Instrument Detector Requirements

In this section, we list the detector requirements—including most of the important performance requirements—for a proposed suite of STS detectors. The estimates for resolutions and rates will improve as models and simulations of the instruments occur. Having these simulations occur early in the design phase will ensure that any changes in detector requirements can be incorporated into the detector design.

Table 6.3. Detector requirements for proposed instruments

Instrument	Description	Requirements (resolution, average count rate)	Coverage	Notes
DIFFRACTION				
NeSCry	Magnetic diffraction for small crystal and epitaxial materials	2 mm, 50K	5 m ²	Mag field
VERDI	Long-wavelength diffractometer for magnetic structure in powders and single crystals	1 mm, 100K	>2 π	
HighResPD	High resolution powder diffractometer	2 mm, 50K	10 m ²	
EWALD	Macromolecule single crystal diffractometer (1 mg samples)	0.5 mm, 50K	> 2 π	
DYPOL	Macromolecule dynamically polarized single crystal diffraction	0.5 mm, 100K	> 2 π	
REFLECTOMETRY				
Kinetics Liquid Reflectometer	Kinetics liquids reflectometer	1–2 mm, 0.5–1M	20 cm × 20 cm	5–10M c/s peak rate
VBPR	Small sample liquids reflectometer	1–2 mm, 500K	20 cm × 20 cm	5M c/s peak rate
M-STAR	Polarized neutron reflectometer	1–2 mm, 500K	20 cm × 100 cm	5M c/s peak, mag field, curved
M-WASABI	Polarized reflectometer combined with GI-SANS	1–2 mm, 1M	50 cm × 50 cm	10M c/sec peak rate, mag field, curved

Table 6.3. (continued)

Instrument	Description	Requirements (resolution, average count rate)	Coverage	Notes
SANS				
HiRes-SWANS	High-resolution small and wide-angle neutron scattering (molecular ordering to nanostructures)	5–7mm, 500K	1 m × 1 m	Curved?
FLOODS	Flux optimized order-disorder SANS; fast kinetics and out-of-equilibrium behavior	2.0 mm, 1M	1 m × 1 m	
INELASTIC/QUASI-ELASTIC				
CHESS	Cold neutron chopper spectrometer optimized for high flux on small samples (10 mg) and polarization	5 mm–1 cm, 20K	20 m ²	100K peak
HERTZ	Cold neutron chopper spectrometer optimized for large single crystals and polarization	5 mm–1 cm, 100K	10 m ²	500K peak
MBARS	Mica-based very high resolution backscattering spectrometer	1 cm, 20K	2 m ²	
BWAVES	Very broad dynamic range using wide-angle velocity selector as analyzer	1 cm, 100K	20 m ²	
JANUS	Hybrid spectrometer (low-Q chopper spectrometer, backscattering analyzer spectrometer)	1 cm, 20K	4 m ²	
EXTREME-X	Extreme environment/inverse geometry	1 cm, 100K	4 m ²	
SPHIINXS	Spherical indirect inelastic xtal spectrometer (70 meV elastic, 1% $\delta\omega/\omega$)	1 cm, 100K	20 m ²	
EXTREME CONDITIONS				
Zeemans	Versatile instrument designed for studies at the highest magnetic fields	1 cm, TBD		High stray fields

Note on imaging beam lines: The VENUS beam line proposed for FTS is emblematic of time-of-flight imaging. Current detectors having resolution of around 100 μm do not have time-of-flight capability, while pseudo time-of-flight capability using readout chips like TIMEPIX is limited in size to 25 mm × 25 mm because of cost of the readout chips. Two potential technologies could provide detectors having resolutions in the 100 μm range with large area. These are the Anger camera or large area micro channel plate (MCP) detectors. Both these technologies would require further development to achieve the needed resolutions. The Anger camera would require a much brighter scintillator and a sensor pixel of around 1 mm × 1 mm to achieve this resolution, while MCP would require improvements in the readout and packaging scheme.

Requirements and Recommendations

Further detector research is needed in the following broad areas:

1. All the proposed reflectometers are currently underserved by FTS technology, and existing gas detectors may not meet the needs of speed and resolution. These instruments could be served by a scintillating detector that is insensitive to magnetic fields or possibly by an ionization mode or resistive plate detector. These technologies should be explored. Also of interest for some of the reflectometers are curved detectors in one or both dimensions. *Instruments that will benefit: TLR, mmLR, M-STAR, M-WASABI, and the liquids and magnetism reflectometers at FTS.*
2. Improving the resolution of the current Anger camera to 0.5 mm would offer the ability to examine the properties of very small samples on the order of .03 mm³ or smaller. *Instruments that will benefit: EWALD, DYPOL, VERDICT.*
3. Improvement in gamma rejection capability of the Anger cameras would improve signal to noise ratio, allowing for wider studies of weak or diffuse scattering. *Instruments that will benefit: TOPAZ, MANDI, SNAP, EWALD, DYPOL.*
4. Most of the proposed inelastic instruments can use ³He technology. The challenge in this case is in possible improvements to the method of linking systems of large area detectors together. *Instruments that will benefit: CHESS, HERTZ, SPHINXS.*
5. Powder diffractometers, of which there are many, will require an encoding free detector system. The encoding causes noise artifacts in the focused diffraction pattern. A multi-anode type system with a scintillator optimized for position interpolation would allow improved resolution of the detector in both dimensions. *Instruments that will benefit: NeSCRY, HighResPD, VERDIC.*
6. A large area imaging detector with resolution in the range of 100 μm and true time-of-flight capability will be useful in transmission studies such as imaging or tomography. *Instruments that will benefit: VENUS, HFIR imaging beam line.*
7. Improvements in scintillator light yield are vital to improving the resolution and performance of the Anger camera. Although there are a number of potential candidates, a true substitute for GS20 glass does not exist. Cost effective candidates are either ceramic or glass based scintillator systems, and it is recommended that efforts be focused in these broad areas.

6.6 INVENT (INSTRUMENT WITH VERSATILE ENVIRONMENT FOR NOVEL TECHNOLOGIES)

K. W. Herwig (ISD)

Abstract

INVENT will be a flexible platform for implementing complex scientific apparatus (including pump-probe techniques and high magnetic fields) and for the development of innovative technologies and techniques that are required for the transformative instrumentation envisioned for STS. While significant development activities proceed using modest development stations at HFIR, there is a strong and recurring need for an instrument station—INVENT—that provides pulsed neutrons with time-of-

flight characteristics (moderator pulse shapes and spectral distribution) representative of FTS and STS beam lines.

Science Case

To position itself to address emerging science challenges, ORNL must take a leadership role in development and implementation of novel techniques that leverage the pulsed nature of SNS and take full advantage of the high peak flux of a short-pulse spallation source to deliver new science capabilities such as the following:

- **Dynamically Polarized Crystallography.** The incoherent contribution that often dominates the background for single-crystal diffraction of proteins essentially can be suppressed to zero for fully polarized samples, while the coherent contribution can be maximized. Development and implementation of this technique will be game changing for understanding the role of hydrogen in the function of proteins, especially when coupled to the gains expected for an STS protein crystallography instrument.
- **Measuring the magnetic spin structure tensor, $S_{\alpha,\beta}(\mathbf{Q},\omega)$.** While the use of polarized inelastic neutron scattering is routine at many reactor sources, the power of time-of-flight techniques coupled to large area detectors requires significant development. Technology development is expected to proceed through to an integrated system that includes incident beam polarization, scattered beam polarization analysis, integrated low-temperature, and 3D magnetic field sample environment capabilities.
- **Spin-precession (Larmor) techniques.** The long time- and large length-scales required for study of complex, mesoscale phenomena that include protein dynamics and the excitations associated with topological phases in quantum condensed matter can best be accessed using spin-precession techniques. Investigation of the role of time-of-flight techniques in these methods is still in its infancy.
- **Time-of-flight MIEZE (Modulated Intensity by Zero Effort).** This time-encoding of a polarized neutron beam can, in principle, be deployed on a number of neutron beam lines. Coupling a MIEZE device with a SANS beam line at FTS and/or STS will provide a means to separate truly elastic from inelastic/quasielastic scattering and thus help remove the incoherent, inelastic scattering of hydrogen, which gets redistributed across time-of-flight. The low-Q, quasielastic component accesses the length and time scales relevant for excitations and dynamics at the mesoscale.

In addition to developing new neutron scattering techniques and instrument concepts for STS, INVENT will be the beam line where new technologies are demonstrated and perfected before deployment on operating beam lines. These include specialized sample environments such as high magnetic fields (pulsed, continuous, or a combination thereof) and new detector technologies along with next generation detector electronics. The high peak brilliance anticipated at STS will place a premium on more sophisticated neutron optics designs that leverage the advanced modeling tools available and advances in neutron guide and mirror technologies. These new devices, concepts, and alignment strategies need testing before they are deployed at STS.

Technical Description

As envisioned, INVENT will be a fully capable and flexible beam line located on the cold, coupled H₂ moderator at FTS beam line 14A. Its neutron optics system will include reconfigurable guide and collimator sections and a set of neutron choppers that will allow both elastic and inelastic measurements. The instrument will include a small set of standard ³He detectors and Anger camera scintillator detectors (to provide high spatial resolution when required) that can be repositioned around a sample, device, or optical element, as required.

Table 6.4. Key instrument parameters for INVENT

Source	FTS
Moderator type	Cold, coupled H ₂ (beam line 14a)
Wavelength/energy range	1–10 Å
Resolution $\Delta E/E$	Variable: 2–6% (depending on position of detectors)
Sample size range (beam size)	Variable depending on optics selection, 10–100 mm
Moderator—sample distance	60–72 m (variable)
Sample—detector distance	1–4 m
Detector type	³ He linear position sensitive (48 tubes, 1 m long, 7 mm to 1 cm in diameter); 2 Anger camera detectors (15 × 15 cm ² with 1.5 mm spatial resolution, horizontal and vertical)

APPENDIX A. DISCUSSION ON THE RELATIVE MERITS OF A SHORT- OR LONG-PROTON PULSE SECOND TARGET STATION AT THE SPALLATION NEUTRON SOURCE

K. W. Herwig (ISD)

Introduction

The 1998 report of the Russell Subpanel [1] defining the technical specifications for the Spallation Neutron Source (SNS) at Oak Ridge National Laboratory (ORNL) included recommendations to design the facility “such that it can be operated at a significantly higher power in a later stage” and to include the “capability of additional targets.” Both of these recommendations were incorporated into the original SNS design. Subsequent conceptual design studies examined possible configurations of the second target station (STS) [2,3]. The first of these considered a target station using short proton pulses (SP) in a similar fashion to the SNS first target station (FTS) but operating at a source frequency of 10 Hz. In SP mode, the 1 msec production of the linac is compressed to ~700 ns using the accumulator ring. The second study proposed a 20 Hz, long proton pulse (LP) mode of operation where the 1 msec production of the linac would be sent directly to the neutron production target without time-compression.

Both studies emphasized optimizing the source for the production and use of long wavelength neutrons. The mission need statement for STS was recognized by the Department of Energy with approval of CD-0 in January 2009 to “provide an additional target station at ORNL optimized for cold neutron beams.” The pros and cons of the two source options were discussed at the April 2–3, 2013, meeting of the ORNL Neutron Sciences Directorate’s Neutron Advisory Board (NAB); the board’s report stated, “NAB is in favor of using the short pulse option for reference purposes during the upcoming scoping and design phases for upgrading the SNS.”

Source Frequency, Power, and Neutron Production

The STS project calls for a doubling of the proton power produced by the accelerator complex from the baseline 1.4 MW to 2.8 MW. In the simplest and likely most cost effective operating scenario, the accelerator will continue to operate at 60 Hz with proton pulses split between the two target stations. Operating STS at 20 Hz would produce approximately twice as many total neutrons as 10 Hz operation but would reduce the neutron wavelength band width, $\Delta\lambda$, available between pulses by the same factor. ($\Delta\lambda = 3956/\nu L$ where ν is the source frequency and L is the instrument length.) The final operating frequency of STS will be selected during the conceptual design phase of the project, but both the SP and LP concepts could operate effectively at a repetition rate of 10–20 Hz. A larger $\Delta\lambda$ better enables simultaneous measurements over wider length and time ranges, favoring an operating frequency toward the lower end of this range, and this consideration applies to both SP and LP operating modes.

An advantage of LP operation considered in [3] was the possibility of producing more neutrons per pulse by up to 50% by eliminating proton pulse chopping. NAB also considered a 10 Hz LP mode where 2 msec output from the linac could be sent to the neutron production target, requiring a 17% increase in the proposed average accelerator duty factor. Both of these options would require careful consideration during the STS conceptual design phase and impose higher cost and technical risk on the accelerator portion of the project. At most, an LP mode of operation would produce 1.5 to 2 times more time-averaged neutrons than SP mode per pulse. Even giving credit for a twice higher proposed LP source

repetition rate, NAB concluded “that the overall performance difference between these two types of source is unlikely to be decisive.”

Instrument optimization across ORNL neutron sources

With the addition of a second SNS target station, ORNL will be home to three neutron sources. The three ORNL facilities provide a unique opportunity to match neutron scattering techniques and instrument design to the source characteristics that deliver the best performance. ORNL will be the only laboratory in the world to provide neutron scattering capabilities optimized over such a diverse set of sources.

As shown in Fig. A.1, the High Flux Isotope Reactor (HFIR) produces the highest time-averaged flux in both the thermal and cold neutron energy regimes. Neutron scattering techniques and instruments that use a small number of resolution elements to complete a data set are

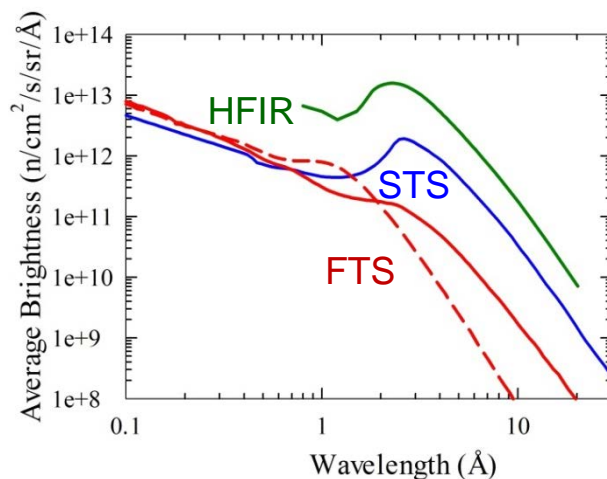


Fig. A.1. Time averaged cold source brightness for the three ORNL neutron sources.

Green: the HFIR cold source. Red: dashed, 2 MW FTS water moderator; solid, 2 MW FTS de-coupled moderator. Blue: 467 kW SP STS coupled moderator.

best optimized to HFIR, which produces the greatest time-averaged neutron flux. These instruments benefit the least from time-of-flight techniques. The SNS FTS was optimized for the production of sharp neutron pulses produced at 60 Hz with two-thirds of the instrument stations devoted to decoupled, poisoned moderators that produce the sharpest pulses. STS will be optimized for cold neutrons that are best produced in coupled moderators and operate at a lower repetition rate, providing access to the broadest length and time ranges.

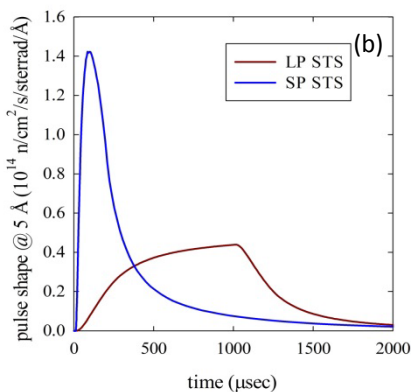
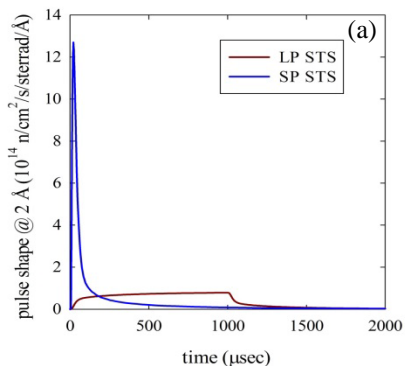


Fig. A.2. Calculated moderator pulse shapes for (a) 2 Å and (b) 5 Å neutrons at STS.

Figure A.2 shows the neutron pulse produced in a coupled moderator at LP and SP STSs for equal proton power pulses. Each pulse contains the same total number of neutrons, but the peak flux is 16 and 3.3 times higher for SP vs. LP for 2 Å and 5 Å neutrons, respectively. Instruments that benefit most from time-of-flight techniques take full advantage of the higher peak neutron production of the SP STS. As concluded in [4], “Time-of-flight instruments that depend on time-averaged moderator brightness will perform about as well on either option, while instruments that rely more on peak brightness will perform better on the SP-STS.” Furthermore, instruments that are optimized toward higher time-averaged neutron flux are likely better sited at HFIR with $\sim 10 \times$ the time

averaged cold neutron brightness of a SP STS or $\sim 5 \times$ the time averaged brightness of a 20 Hz LP STS.

At 5 MW, the baseline European Spallation Source (ESS) design would provide ~ 3 times taller and ~ 3 times broader pulses than those shown for the LP STS in Fig. A.2. The ESS neutron scattering instrument suite would significantly outperform comparable instruments on an SNS LP STS. However, by taking advantage of the existing SNS accumulator ring, an SP STS can produce comparable or significantly higher peak pulse heights benefiting large classes of neutron scattering instruments, even with an order of magnitude lower proton beam power.

References

- [1] Report of the Basic Energy Sciences Advisory Committee on Neutron Source Facility Upgrades and the Technical Specifications for the Spallation Neutron Source, http://science.energy.gov/~media/bes/besac/pdf/neutron_source_rpt.pdf (1998).
- [2] Technical Concepts for a Long-Wavelength Target Station for the Spallation Neutron Source, ANL-02/16 and ORNL/SNS-TM-2001/163, <http://www.ipd.anl.gov/anlpubs/2002/12/44951.pdf> (2002).
- [3] A Second Target Station for the Spallation Neutron Source, SNS 100000000 TR0030-R0 (2007).
- [4] Zhao, J. K., et al. "Instrument performance study on the short and long pulse options of the second Spallation Neutron Source target station." *Review of Scientific Instruments* 84, 105104 (2013).

